ALTERRA

WAGENINGEN**UR**

SWAP version 3.2
Theory description and user manual

J.G. Kroes
J.C. Van Dam
P. Groenendijk
R.F.A. Hendriks
C.M.J. Jacobs

SWAP version 3.2. Theory description and user manual

SWAP version 3.2. Theory description and user manual

J.G. Kroes
J.C. Van Dam
P. Groenendijk
R.F.A. Hendriks
C.M.J. Jacobs

ABSTRACT

Kroes, J.G., J.C. Van Dam, P. Groenendijk, R.F.A. Hendriks, C.M.J. Jacobs, 2008. *SWAP version 3.2. Theory description and user manual*. Wageningen, Alterra, Alterra Report1649, Swap32 Theory description and user manual. 262 pages.; 47 figs.; 12 tables; 39 boxes, 249 refs.

SWAP 3.2 simulates transport of water, solutes and heat in the vadose zone. It describes a domain from the top of canopy into the groundwater which may be in interaction with a surface water system. The program has been developed by Alterra and Wageningen University, and is designed to simulate transport processes at field scale and during whole growing seasons. This is a new release with special emphasis on numerical stability, macro pore flow, and options for detailed meteorological input and linkage to other models. This manual describes the theoretical background, model use, input requirements and output tables.

Keywords: agrohydrology, drainage, evaporation, irrigation, salinization, simulation model, soil water, solute transport, surface water management, transpiration, vadose zone

Contents

Preface

SWAP (Soil-Water-Atmosphere-Plant) is the successor of the agrohydrological model SWATR (Feddes et al., 1978) and some of its numerous derivatives. Earlier versions were published as SWATR(E) by Feddes et al. (1978), Belmans et al. (1983) and Wesseling et al. (1991), as SWACROP by Kabat et al. (1992) and as SWAP93 by Van den Broek et al. (1994). SWAP2.0 was published by Van Dam et al. (1997) and Kroes et al. (2001). The latest version was published as SWAP3.0.3 by Kroes and Van Dam (eds, 2003). Main differences between the current version SWAP 3.2 and the previous version are:

- Source code was restructured;
- Numerical stability has been largely improved;
- MacroPore flow is operational;
- Detailed rainfall and evapotranspiration data is optional;
- Testing has been strongly intensified;

All reports, together with the SWAP program and examples, are available through the SWAP-development group and the Internet (www.swap.alterra.nl).

The general reference to the SWAP model is Van Dam (2000).

The reference to recent advances is Van Dam et al. (2008).

The reference to numerical algorithm is Groenendijk and Kroes (in prep)

The reference to macropore flow is Hendriks et al. (in prep)

Summary

SWAP simulates transport of water, solutes and heat in the vadose zone in interaction with vegetation development. In the vertical direction the model domain reaches from a plane just above the canopy to a plane in the shallow groundwater. In this zone the transport processes are predominantly vertical, therefore SWAP is a one-dimensional, vertically directed model. In the horizontal direction, SWAP's main focus is the field scale.

The SWAP model can be downloaded from site www.swap.alterra.nl. The model input may consist of files for main input, meteorological data, crop growth and drainage. SWAP employs the TTUTIL library to read the ASCII input files in easy format. Output is generated in ASCII and binary files. The internet site contains a large number of SWAP test cases (Chapter 1).

Soil water flow is calculated with the Richards' equation. The Mualem-Van Genuchten relations, with a modification near saturation, describe the soil hydraulic functions. Scaling of main drying and main wetting curves describe hysteresis in the retention function. The bottom boundary is controlled by head, flux or the relation between flux and head. SWAP solves the Richards' equation numerically with an implicit, backward, finite difference scheme. The Newton-Raphson iterative procedure ensures mass conservation and rapid convergence (Chapter 2).

For agricultural crops and grassland, SWAP computes the interception following Von Hoyningen-Hüne and Braden. The interception concept of Gash is available for trees and forests. The Penman-Monteith equation can be used to calculate the potential evapotranspiration of uniform surfaces (wet and dry vegetation, bare soil). An alternative is providing input of reference evapotranspiration in combination with crop factors. Next the potential transpiration and evaporation fluxes of partly covered soils are derived, taking into account interception and soil cover. Actual transpiration depends on the moisture and salinity conditions in the root zone, weighted by the root density. Actual evaporation depends on the capacity of the soil to transport water to the soil surface. SWAP uses the soil hydraulic functions and semi-empirical equations to determine this transport capacity (Chapter 3).

Surface runoff will be calculated when the height of water ponding on the soil surface exceeds a critical depth. The rate of surface runoff depends on a specified resistance. Interflow may occur when the groundwater level becomes higher than the interflow drainage level.

Drainage can be calculated with the Hooghoudt or Ernst equations, with a table relating drainage flux and groundwater level, or with drainage resistances per

drainage system. In order to calculate proper residence times of solutes, the drainage fluxes are vertically distributed according to so-called discharge layers (Chapter 4).

The water balance of the surface water system can be calculated to analyse water management options. Surface water levels can be imposed, or derived by setting soil moisture criteria (groundwater level, pressure head, minimum storage) in combination with a weir (Chapter 5).

Macroporosity can be caused by shrinking and cracking of soil, by plant roots, by soil fauna, or by tillage operations. The macropore module in SWAP includes infiltration into macropores at the soil surface, rapid transport in macropores to deeper layers, lateral infiltration into and exfiltration out of the soil matrix, water storage in macropores, and rapid drainage to drainage systems. The macropores are divided in a main bypass domain (network of continuous, horizontal interconnected macropores) and an internal catchment domain (discontinuous macropores ending at different depths). The internal catchment domain causes infiltration of macropore water at different, relatively shallow depth. In addition, the macropores are divided in static and dynamic volumes. The dynamic volumes depend on shrinkage characteristics (Chapter 6).

The simple crop module prescribes crop development, independent of external stress factors. Its main function is to provide a proper upper boundary condition for soil water movement. In addition, SWAP includes the generic crop growth module WOFOST. In this module, the absorbed radiation is a function of solar radiation and crop leaf area. Next the produced carbohydrates (CH_2O) are calculated, taking into account photosynthetic leaf characteristics and possible water and/or salinity stress. The carbohydrates provide energy for living biomass (maintenance respiration) and are converted into structural material during which weight is lost as growth respiration. The material produced is partitioned among roots, leaves, stems and storage organs, using partioning factors that depend on the crop development stage. The fraction partioned to the leaves, determines leaf area development and hence the dynamics of light interception. During crop development a part of the living biomass dies due to senescence (Chapter 7).

SWAP may simulate transport of salts, pesticides and other solutes that can be described with basic physical relations: convection, diffusion, dispersion, root uptake, Freundlich adsorption and first order decomposition. In case of advanced pesticide transport, including volatilization and kinetic adsorption, SWAP can be used in combination with PEARL. In case of advanced transport of nitrogen and phosphorus, SWAP can be used in combination with ANIMO (Chapter 8).

SWAP may simulate soil temperature analytically, using an input sine function at the soil surface and the soil thermal diffusivity. In the numerical approach, SWAP takes into account the influence of soil moisture on soil heat capacity and soil thermal

conductivity. The top boundary condition can be input of air temperatures or soil surface temperatures (Chapter 9).

The snow module calculates the accumulation and melting of a snowpack when the air temperature is below a threshold value. The water balance of the snow pack includes storage, incoming snow and rain and outgoing melting and sublimation. Melting may occur due to air temperature rise or heat release from rainfall. When a snowpack is present, the soil temperature top boundary condition is adjusted in order to account for the insulating effect of the snowpack. In case of frost, reduction factors can be calculated for the hydraulic conductivity, root water uptake, drainage fluxes and bottom flux (Chapter 10).

Irrigations with fixed date, depth and quality can be specified as input. In addition, SWAP can be used to schedule irrigation. Timing criteria include allowable daily stress, allowable depletion amount and critical pressure head or water content. Depth criteria include back to field capacity and fixed depth (Chapter 11).

The appendices contain information on the parameters of the soil hydraulic functions, critical pressure heads for root water extraction, salt tolerance data, shrinkage characteristic data, numerical solution of water and heat flow, description of binary output files and list of main SWAP subroutines.

1 Model overview

1.1 Model domain and processes

SWAP simulates transport of water, solutes and heat in the vadose zone in interaction with vegetation development. The model employs the Richards equation including root water extraction to simulate soil moisture movement in variably saturated soils. Concepts are added to account for macroporous flow and water repellency. SWAP considers for solute transport the basic processes convection, dispersion, adsorption and decomposition. For more extensive studies which for instance include volatilization or nutrient transformations, SWAP generates soil water fluxes for detailed chemical transport models as PEARL for pesticides and ANIMO for nutrients. SWAP simulates soil heat flow taking into account actual heat capacities and thermal conductivities. The generic crop growth module WOFOST is incorporated to simulate leaf photosynthesis and crop growth. The soil moisture, heat and solute modules exchange status information each time step to account for all kind of interactions. Crop growth is affected by the actual soil moisture and salinity status on a daily basis. An extensive test protocol ensures the numerical code quality of SWAP.

In the vertical direction the model domain reaches from a plane just above the canopy to a plane in the shallow groundwater (Fig. 1.1).
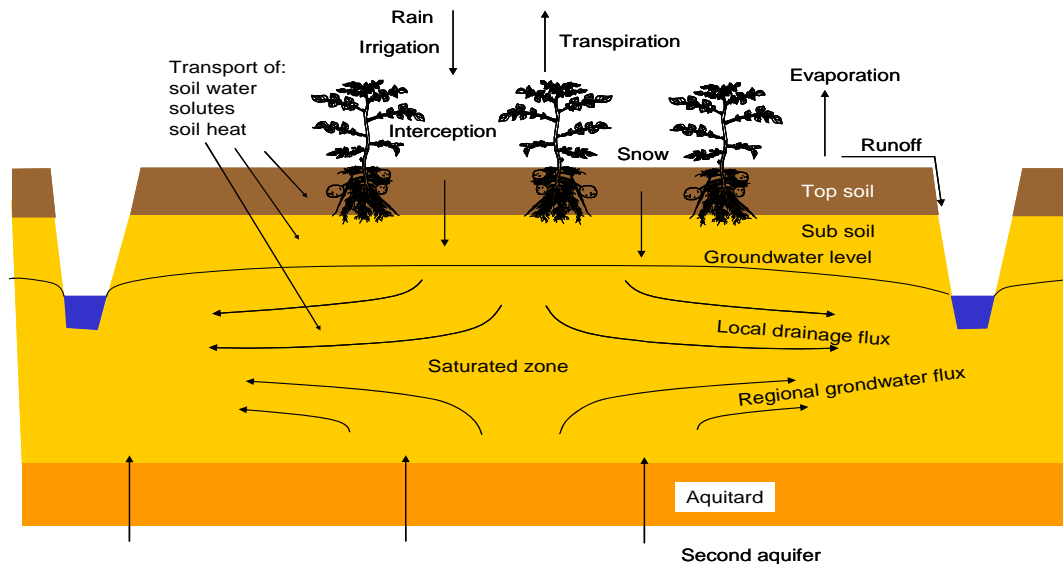
Figure 1.1 SWAP model domain and transport processes.

In this zone the transport processes are predominantly vertical, therefore SWAP is a one-dimensional, vertical directed model. The flow below the groundwater level may include

lateral drainage fluxes, provided that these fluxes can be prescribed with analytical drainage formulas. The model is very flexible with regard to input data at the top and bottom of the soil column. At the top in general daily weather conditions will suffice. For Nordic conditions a simple snow storage module has been implemented. In case of more focussed studies (e.g. runoff or diurnal transpiration fluxes) evapotranspiration and rainfall data can be specified in more detail. At the bottom various forms of head and flux based conditions are used.

In the horizontal direction, SWAP's main focus is the field scale. At this scale most transport processes can be described in a deterministic way, as a field generally can be represented by one microclimate, one vegetation type, one soil type, and one drainage condition. Also many cultivation practices occur at field scale, which means that many management options apply to this scale. Upscaling from field to regional scale for broader policy studies is possible with geographical information systems.

The smallest time steps in SWAP are in the order of seconds for fast transport processes such as intensive rain showers with runoff or flow in macroporous clay soils. These time steps are automatically increased in periods with less fluctuating flow conditions. Depending on simulation complexity, computation times for 50 year periods range from 30 to 500 seconds on ordinary personal computers.

1.2   SWAP installation

The SWAP model can be downloaded from Internet site www.swap.alterra.nl. This site contains also general information on model features, applications and test reports. Various SWAP versions are available at the Internet site, all running under MS Windows. SWAP2.0.7.d contains a graphical user interface. This manual applies to SWAP3.2. Only the most recent SWAP version is supported by the Swap team.

By running the SWAP setup file, a number of folders are created, as depicted in Figure 1.2. These folders contain:
- Swap executable
- Swap source code
- User manual (in Documents)
- Two examples (Hupsel and CranGras)
- Additional input data:

- o Daily weather data of Wageningen meteorological station of the period 1971-2000
- o Simple crop input data for grass, fodder maize, potato, sugar beet and winter wheat
- o Detailed crop input data for winter wheat, grain maize, spring barley, rice, sugar beet, potato, field bean, soy bean, winter oilseed rape and sunflower

After running the setup file, SWAP can be automatically launched for the example Hupsel.

1.3 Model input

The input data of SWAP are divided over 4 different file types:

- Main input file (*.swp)
- Meteorological file (*.yyy)
- Crop growth file (*.crp)
- Drainage file (*.dra)

Figure 1.2 Installed folders by standard SWAP setup file

Box 1.2 provides an overview of the information in these input files. The main input file and the meteorological data file are always required. Input files of crop growth and drainage are optional. The extensions of the files are fixed. An exception is the meteorological file, which has an extension equal to the last 3 digits of the year (e.g. 2008 gives .008). The names of the input files are free to choose and are specified in the main input file. As listed in Box 1.1, the main input file contains general information with regard to the simulation, meteorology, crop rotation scheme, irrigation, soil water flow, heat flow and solute transport. For meteorological data, commonly a file with daily data is used. In Chapter 3 more detailed input of evapotranspiration and rainfall fluxes will be discussed. The detailed crop growth input file is required to simulate crop development and biomass assimilation. As an alternative, the development of crop parameters as leaf area index or rooting depth can be prescribed in the simple crop growth input file. The drainage input file contains two sections. The basic drainage section provides input for drainage towards ditches and/or drains. The extended drainage section provides input for drainage including simulation of surface water levels.

SWAP uses the TTUTIL library (Kraalingen & Rappoldt, 2000) for reading input files. Box 1.3 gives an example of a part of the *.swp input file. General rules for the format of input files are:

- free format with the structure 'VariableName' = 'value' or in a table with variable names in the first line (see Box 1.3);
- order of variables is free;
- comment in lines is allowed starting with '*' or '!';
- blank lines are allowed.

In the input files, of each parameter the symbolic name, a description and an identification is given. The identification between square brackets provides information on:

- range
- unit
- data type (I = Integer, R = Real, Ax = character string of x positions)

For example: [-5000 .. 100 cm, R] means: value between -5000 and +100 with a unit in cm, given as a Real data type (which means that in the input file a dot should be added).

1.4   Model run

The most common way to run SWAP is by executing a batch file, which refers to the SWAP executable and the *.swp file. The batch file and the *.swp file need to be present in the same directory. The *.swp file contains the names and locations of other input files. Therefore, it is possible to have separate directories with meteorological, crop and drainage data.

An example of the batch file is given in Box 1.1. In this case SWAP will use Hupsel.swp as main input file. If no name is specified behind the call 'Swap.exe', SWAP will use Swap.swp as main input file. The pause statement keeps the window box with screen messages open when runtime warnings or errors might occur.

Box 1.1 Example of batch file to run SWAP with input file Hupsel.swp

```
c:\Program Files\SWAP\Swap.exe Hupsel.swp
pause
```

Box 1.2 Summary of information in input files. Optional files are denoted with #.

Main input file (*.swp)
- *General section*
  - Environment
  - Timing of simulation period
  - Timing of boundary conditions
  - Processes which should be simulated
  - Optional output files
- *Meteorology section*
  - Name of file with meteorological data
  - Rainfall intensity
- *Crop section*
  - Crop rotation scheme (calendar and files)
  - Crop data input file
  - Calculated irrigation input file
  - Crop emergence and harvest
  - Fixed irrigation parameters (Amount and quality of prescribed irrigation applications)
- *Soil water section*
  - Initial moisture condition
  - Ponding
  - Soil evaporation
  - Vertical discretization of soil profile
  - Soil hydraulic functions
  - Hysteresis of soil water retention function
  - Maximum rooting depth
  - Similar media scaling of soil hydraulic functions
  - Preferential flow due to soil volumes with immobile water
  - Preferential flow due to macro pores
  - Snow and frost
  - Numerical solution of Richards' equation
- *Lateral drainage section*
  - (optional) name of file with drainage input data
  - (optional) name of file with runon input data
- *Bottom boundary section*
  - (optional) name of file with bottom boundary conditions
  - selection out of 8 options
- *Heat flow section*
  - calculation method
- *Solute transport section*
  - Specify whether simulation includes solute transport or not
  - Top boundary and initial condition
  - Diffusion, dispersion, and solute uptake by roots
  - Adsorption
  - Decomposition
  - Transfer between mobile and immobile water volumes (if present)
  - Solute residence in the saturated zone

File with daily meteorological data (*.yyy)
  - Radiation, temperature, vapour pressure, wind speed, rainfall and/or reference evapotranspiration,
  - rainfall intensities

File with Detailed crop growth (*.crp) #
- *Crop section*
  - Crop height
  - Crop development
  - Initial values
  - Green surface area
  - Assimilation
  - Assimilates conversion into biomass
  - Maintenance respiration
  - Dry matter partitioning
  - Death rates
  - Crop water use
  - Salt stress
  - Interception
  - Root growth and density distribution
- *Calculated Irrigation section*
  - General
  - Irrigation time criteria
  - Irrigation depth criteria

File with Simple crop growth (*.crp) #
- *Crop section*
  - Crop development
  - Light extinction
  - Leaf area index or soil cover fraction
  - crop factor or crop height
  - rooting depth
  - yield response
  - soil water extraction by plant roots
  - salt stress
  - interception
  - Root density distribution and root growth
- *Calculated Irrigation section*
  - General
  - Irrigation time criteria
  - Irrigation depth criteria

File with drainage data (*.dra) #
- *Basic drainage section*
  - Table of drainage flux - groundwater level
  - Drainage formula of Hooghoudt or Ernst
  - Drainage and infiltration resistances
- *Extended drainage section*
  - Drainage characteristics
  - Surface water level of primary and/or secondary system
  - Simulation of surface water level
  - Weir characteristics

Box 1.3 Example of input according to TTUTIL in main file *.SWP.

```
* General data
  METFIL = 'Wageningen' ! File name of meteorological data without extension .YYY, [A16]
                        ! Extension equals last 3 digits of year number, e.g. 2003 has extension .003
  SWETR  = 0            ! Switch, use reference ET values of meteo file [Y=1, N=0]

* If SWETR = 0, then LAT,ALT and ALTW must have realistic values
  LAT   =   52.0        ! Latitude of meteo station, [-60..60 degrees, R, North = +]
  ALT   =   10.0        ! Altitude of meteo station, [-400..3000 m, R]
  ALTW  =    2.0        ! Altitude of wind speed measurement (10 m is default) [0..99 m, R]
*
* Use of detailed meteorological records (< 1 day)
  SWMETDETAIL = 0       ! Switch, use detailed meteor. records of both ET and rainfall [Y=1, N=0]
*
* In case of detailed meteorological weather records (SWMETDETAIL = 1):
  NMETDETAIL = 10       ! Number of weather data records per day, [1..96 -, I]
*
* In case of daily meteorological weather records (SWMETDETAIL = 0):
  SWETSINE = 0          ! Switch, distribute daily Tp and Ep according to sinus wave [Y=1, N=0]
*
*
  SWRAIN =  0           ! Switch for use of actual rainfall intensity:
                        ! SWRAIN = 0: Use daily rainfall amounts
                        ! SWRAIN = 1: Use daily rainfall amounts + mean intensity
                        ! SWRAIN = 2: Use daily rainfall amounts + duration
                        ! SWRAIN = 3: Use short time rainfall intensities, as supplied in sep. file

* If SWRAIN = 1, then specify mean rainfall intensity RAINFLUX [0.d0..1000.d0 cm/d, R]
* as function of time TIME [0..366 d, R], maximum 30 records
   TIME    RAINFLUX
    1.0         2.0
  360.0         2.0
* End of table

* If SWRAIN = 3, then specify file name of file with detailed rainfall data
  RAINFIL = 'WagRain'   ! File name of detailed rainfall data without extension .YYY, [A16]
                        ! Extension equals last 3 digits of year number, e.g. 2003 has extension .003
```

An alternative to run SWAP is by directly executing Swap.exe. In that case the main input file should be named Swap.swp, and should be located in the same folder as Swap.exe.

Three types of messages may occur:

- error messages generated by the utility library TTUTIL (Kraalingen & Rappoldt, 2000) with respect to the format of the input data
- warnings with the advise to adapt the combination of selected options because the specified combination is not feasible
- fatal errors which stop the simulation

Output files will be generated in the same directory as the main input file. Also the log file of the most recent simulation run can be found here. The Swap.log file contains a copy of the *.swp file, possible errors and warnings, and in case of a successful simulation run:

```
'Swap simulation okay!'
```

1.5 Model output

Output from SWAP is stored in general ASCII files. Some of these files are always generated, other files are optional output. Box 1.4 provides an overview of the variables that are printed in each output file. All output files have the same header with the project name, file content, file name, model version, date of generation, period of calculations and the depth of the soil profile. The output interval may range from a day to years. Some output can be generated with time intervals less than a day. We may distinguish output of state variables, incremental fluxes since the last output time, and cumulative fluxes since a specified data. The output file with final values of state variables can be used as input for a subsequent simulation period. This might be useful to derive suitable initial conditions.

In addition to the ASCII files, formatted and unformatted (binary) export files can be generated with data that cover the entire simulation period. These output files can be used as input for other models, such as the pesticide and nutrient models like PEARL (Leistra et al., 2001) and ANIMO (Groenendijk et al., 2005). A description of these files is given in 0 and 0

1.6 Example run: Hupsel catchment

The setup file contains the input for a field in the Hupsel catchment in The Netherlands. The simulation run covers the years 1980-1982. The potential evapotranspiration fluxes are calculated from daily meteorological measurements. Daily rainfall fluxes are used, as in the catchment with mild slopes and sandy soils no runoff is expected. The cropping pattern consists of maize in the summer season of 1980 and 1982. The development of these crops is prescribed. In the summer season of 1981 potatoes are grown, of which the actual growth is simulated. On 5 January 1980 a tracer is applied, which leaches in the subsequent years towards the drains. Initial soil water contents are assumed to be in hydrostatic equilibrium with a groundwater level at 75 cm depth. The sandy soil profile consists of a top- and sublayer with thicknesses of 30 and 170 cm, respectively. At the bottom of the soil profile a layer of boulder clay with low permeability prevents vertical soil water movement. Therefore at the bottom a zero flux condition is specified. Drainage fluxes are calculated for subsurface drains at 80 cm depth and with a lateral distance of 11 m. Results are shown in water balances in Box 1.5 (summary) and Box 1.6 (detail).

Box 1.4 Summary of information in output files. Optional files are denoted with #.

Short water and solute balance (*.bal)
Final and initial water and solute storage
Water balance components
Solute balance components

Extended water balance (*.blc) #
Final and initial water storage
Water balance components of sub systems

Incremental water balance (*.inc)
Gross rainfall and irrigation
Interception
Runon and runoff
Potential and actual transpiration
Potential and actual evaporation
Net drainage and bottom flux

Cumulative water balance (*.wba)
Gross and net rainfall
Runon and runoff
Potential and actual transpiration
Potential and actual evaporation
Net lateral flux (drainage)
Net bottom flux
Change water storage in profile
Groundwater level
Water balance error

Log file (SWAP.log)
Echo of input (.swp-file)*
Errors and warnings

Cumulative solute balance (*.sba) #
Flux at soil surface
Amount decomposed
Amount taken up by plant roots
Amount in soil profile
Amount in cracks
Flux at soil profile bottom
Drainage flux
Bypass flux from cracks
Amount in defined saturated aquifer
Flux from defined saturated aquifer

Soil temperatures (*.ate) #
Soil temperature of all nodes

Soil profiles (*.vap) #
Profiles of water content, pressure head, solute concentration, temperature, water flux and solute flux

Irrigation (*.irg) #
Calculated irrigation applications

Detailed crop growth (*.crp)
Development stage
Leaf area index
Crop height
Rooting dept
Cumulative relative transpiration during DVS: 0-2 and 1-2
Cumulative potential and actual weight of dry matter
Cumulative potential and actual weight of storage

Simple crop growth (*.crp)
Development stage
Leaf area index
Crop height
Rooting depth
Cumulative relative transpiration
Cumulative relative crop yield

Transpiration stress (*.str)
Potential and actual transpiration
Transpiration reduction due to wet, dry, saline and frost conditions

Extended drainage components (*.drf) #
Drainage fluxes of each level
Total drainage flux
Net runoff
Rapid drainage

Surface water management 1 (*.swb) #
Groundwater level
Weir target level
Surface water level
Storage in surface water reservoir
Sum of drainage, runoff and rapid drainage
External supply to surface water reservoir
Outflow from surface water reservoir

Surface water management 2 (*.man) #
Weir type
Groundwater level
Pressure head for target level
Total air volume in soil profile
Weir target level
Surface water level and outflow
Number of target level adjustments
Indicator weir overflow
Weir crest level

Snowpack water balance (*.snw) #
Final and initial water storage
Water balance components

Detailed waterbalance Macropores (*.bma) #
Final and initial water storage
Water balance components

Soil physical parameters (soilphysparam.csv)
For each soil layer the relation between: soil water pressure head h (cm), theta θ (cm³.cm⁻³), differential capacity C(cm⁻¹), RelSat S_e (-) and hydraulic conductivity K (cm.d¹)

Soil heat conductivity and capacity (heatparam.csv) #
For each soil layer the relation between theta, heatcapacity and heat conducitivity

Final values of state variables (*.end)
Snow and ponding layer
Soil water pressure heads
Solute concentrations
Soil temperatures

Output is requested at the end of each month for incremental and cumulative fluxes, and at the end of each year for overviews of the water and solute balance. Box 1.5 shows the water and solute balance components for the year 1980. The rainfall (66.01 cm) is divided over interception (4.52 cm), transpiration (25.82 cm), soil evaporation (14.42 cm) and drainage (21.17 cm). The soil water storage increases slightly with 0.12 cm. During the experiment a tracer application 500 mg/cm^2 has been applied. After one year, 4.3 mg/cm^2 solutes have leached towards the drains, the remaining amount (45.7 mg/cm^2) is still in the soil profile.

A more detailed overview of the water balance components is given in the Result.blc file (Box 1.6). In this output file the fluxes are presented between the subdomains plant, snow, pond layer, soil, and their environment, as depicted in Figure 1.3. Apart from the in- and outgoing fluxes, of each subdomain also the water storage and balance is depicted. For instance the ponding layer received 61.49 cm rain and 7.57 cm soil water from the first soil compartment. Of this amount 14.42 cm evaporated towards the atmosphere, and 54.69 cm infiltrated into the first soil compartment. As both the initial and final storage of the ponding layer are zero, the storage change is also zero.

Box 1.6 Example of Result.blc file for Hupsel case.

```
* Project:       Hupsel
* File content:  detailed overview of water balance components (cm)
* File name:     .\Result.blc
* Model version: Swap 3.2 (revision 10) (Date 02 May 2008)
* Generated at:  05-May-2008 15:57:05

Period            :  01-Jan-1980 until  31-Dec-1980
Depth soil profile :  200.00 cm
================================================+==================================================
INPUT                                           | OUTPUT
                 PLANT   SNOW   POND   SOIL  |                   PLANT   SNOW   POND   SOIL
================================================+==================================================
Initially Present         0.00   0.00  72.07 | Finally present           0.00   0.00  72.19
Gross Rainfall   66.01                        |
Nett Rainfall             0.00  61.49         | Nett Rainfall    61.49
Gross Irrigation  0.05                        |
Nett Irrigation                  0.05         | Nett Irrigation   0.05
                                              | Interception      4.52
Snowfall                  0.00                |
Snowmelt                         0.00         | Snowmelt                  0.00
                                              | Sublimation               0.00
                                              | Plant Transpiration                     25.82
                                              | Soil Evaporation                 14.42
Runon                            0.00         | Runoff                            0.00
Inundation                       0.00         |
Infiltr. Soil Surf.                    54.69  | Infiltr. Soil Surf.              54.69
Exfiltr. Soil Surf.              7.57         | Exfiltr. Soil Surf.                      7.57
Infiltr. subsurf.                             | Drainage
- system 1                             0.00   | - system 1                               21.17
Upward seepage                         0.00   | Downward seepage                          0.00
================================================+==================================================
Sum              66.06   0.00  69.11 126.76 | Sum               66.06   0.00  69.11 126.76
================================================+==================================================
Storage Change            0.00   0.00   0.12
Balance Deviation 0.00    0.00   0.00   0.00
==================================================================================================
```
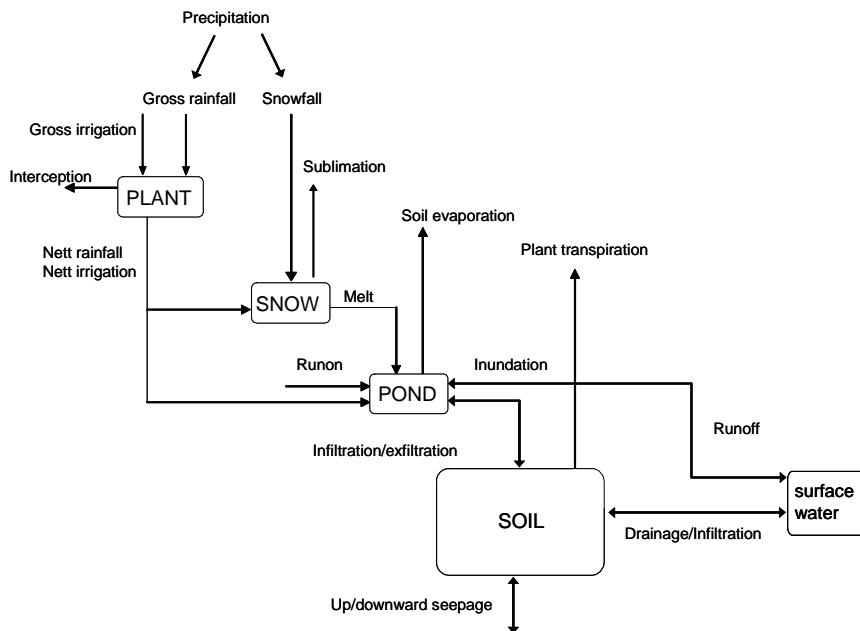
Figure 1.3 Scheme of water fluxes between the subdomains plant, snow, ponding layer, soil and surface water.

In this case also the cumulative and incremental fluxes are requested at the end of each month. Box 1.7 shows the incremental water fluxes for the same year 1980. The actual transpiration rates are close to the potential transpiration rates due to the high rain amounts in the summer season and the relatively shallow groundwater level. In May the maize is not yet covering the soil. The solar radiation fluxes are high, which cause a high potential soil evaporation rate of 11.977 cm/month. Due to the low rainfall amounts, the top soil becomes dry, and the actual soil evaporation rate is only 1.107 cm/month.

The simulated groundwater levels fluctuate between 71.6 and 112.9 cm depth.

```
Box 1.7  Example of Result.inc output file for Hupsel case.


* Project:      Hupsel
* File content: water balance increments (cm/period)
* File name:    .\Result.inc
* Model version: Swap 3.2 (revision 10) (Date 02 May 2008)
* Generated at: 05-May-2008 15:57:06
*
    Date,Day,  Dcum,   Rain,  Snow,  Irrig,  Interc,  Runon,  Runoff,  Tpot,  Tact,   Epot,  Eact, Drainage,  QBottom,    Gwl
31-Jan-1980, 31,   31,  4.690,  0.000,  0.050,  0.000,  0.000,  0.000,  0.000,  0.000,  0.563,  0.545,  2.698,  0.000,  -71.6
29-Feb-1980, 60,   60,  4.650,  0.000,  0.000,  0.000,  0.000,  0.000,  0.000,  0.000,  1.642,  1.150,  4.968,  0.000,  -74.7
31-Mar-1980, 91,   91,  5.490,  0.000,  0.000,  0.000,  0.000,  0.000,  0.000,  0.000,  3.316,  1.843,  2.430,  0.000,  -67.9
30-Apr-1980,121,  121,  4.060,  0.000,  0.000,  0.000,  0.000,  0.000,  0.000,  0.000,  6.371,  2.273,  3.085,  0.000,  -75.4
31-May-1980,152,  152,  0.930,  0.000,  0.000,  0.013,  0.000,  0.000,  0.068,  0.068, 11.977,  1.107,  0.336,  0.000,  -80.4
30-Jun-1980,182,  182,  6.620,  0.000,  0.000,  0.796,  0.000,  0.000,  3.629,  3.521,  5.680,  2.192,  0.363,  0.000,  -81.4
31-Jul-1980,213,  213, 14.570,  0.000,  0.000,  1.424,  0.000,  0.000,  7.362,  4.328,  1.056,  1.056,  6.876,  0.000,  -74.4
31-Aug-1980,244,  244,  4.640,  0.000,  0.000,  1.076,  0.000,  0.000,  9.502,  8.895,  0.757,  0.757,  0.057,  0.000, -112.9
```

1.7 Reading guide

In the next chapters we discuss subsequently:

Chapter 2. Soil water flow
Chapter 3. Evapotranspiration and rainfall interception
Chapter 4. Surface runoff, interflow and drainage
Chapter 5. Surface water system
Chapter 6. Macropore flow
Chapter 7. Crop growth
Chapter 8. Solute transport
Chapter 9. Soil heat flow
Chapter 10. Snow and frost
Chapter 11. Irrigation

The first part of each chapter describes the physical relations incorporated in SWAP. This part also describes implemented numerical procedures, if required to use SWAP in a proper way. The second part of each chapter describes the model input. If relevant, suggestions for input are included.

The appendices contain information on:
- Description of the application of the Penman Monteith method
- Description of derivation and examples of macropore equations
- Equations for the partial derivatives of F_i to pressure heads
- Equations for the implicit linearization of hydraulic conductivities
- Equations for the numerical solution of heat flow
- Tables with soil hydraulic functions: Staring Series 2001
- Tables with critical pressure heads for root water extraction
- Tables with salt tolerance data
- Tables with shrinkage characteristic data
- Tables with shrinkage characteristic data for peat soils
- List of subroutines
- List of fixed ranges of array lengths
- Listing of formatted and unformatted binary output files

2 Soil water flow

2.1 Basic equations

Gradients of the soil water potential induce soil water movement. Darcy's equation is commonly used to quantify these soil water fluxes. For one-dimensional vertical flow, Darcy's equation can be written as:

$$q = -K(h)\frac{\partial(h+z)}{\partial z}$$

(2.1)

where q is soil water flux density (positive upward) (cm d^{-1}), $K(h)$ is hydraulic conductivity (cm d^{-1}), h is soil water pressure head (cm) and z is the vertical coordinate (cm), taken positively upward.

Water balance considerations of an infinitely small soil volume result in the continuity equation for soil water:

$$\frac{\partial\theta}{\partial t} = -\frac{\partial q}{\partial z} - S_a(h) - S_d(h) - S_m(h)$$

(2.2)

where θ is volumetric water content (cm^3 cm^{-3}), t is time (d), $S_a(h)$ is soil water extraction rate by plant roots (cm^3 cm^{-3} d^{-1}), $S_d(h)$ is the extraction rate by drain discharge in the saturated zone (d^{-1}) and $S_m(h)$ is the exchange rate with macro pores (d^{-1}).

Combination of Eqs. [2.1] and [2.2] provides the general water flow equation in variably saturated soils, known as the Richards' equation:

$$\frac{\partial\theta}{\partial t} = \frac{\partial\left[K(h)\left(\frac{\partial h}{\partial z}+1\right)\right]}{\partial z} - S_a(h) - S_d(h) - S_m(h)$$

(2.3)

SWAP applies Richards' equation integrally for the unsaturated-saturated zone, including possible transient and perched groundwater levels. SWAP solves Eq. [2.3] numerically, using known relations between θ, h and K.

2.2 Soil physical relations

The Mualem-Van Genuchten function (Van Genuchten, 1980) which has been used in numerous studies and forms the basis of several national and international data-bases (e.g. Carsel and Parrish, 1988; Yates et al., 1992; Leij et al., 1996; Wösten et al., 2001) has been implemented in SWAP. The analytical $\theta(h)$ function proposed by Van Genuchten (1980) reads:

$$\theta = \theta_{res} + (\theta_{sat} - \theta_{res})\left(1 + |\alpha\,h|^n\right)^{-m}$$

(2.4)

where θ_{sat} is the saturated water content (cm^3 cm^{-3}), θ_{res} is the residual water content in the very dry range (cm^3 cm^{-3}) and α (cm^{-1}), n (-) and m (-) are empirical shape factors. Without loosing much flexibility, m can be taken equal to :

$$m = 1 - \frac{1}{n} \qquad (2.5)$$

Using the above $\theta(h)$ relation and applying the theory on unsaturated hydraulic conductivity by Mualem (1976), the following $K(\theta)$ function results:

$$K = K_{sat} S_e^{\lambda} \left[1 - \left(1 - S_e^{\frac{1}{m}} \right)^m \right]^2 \qquad (2.6)$$

where K_{sat} is the saturated conductivity (cm d^{-1}), λ is a shape parameter (-) depending on $\partial K / \partial h$, and S_e is the relative saturation defined as:

$$S_e = \frac{\theta - \theta_{res}}{\theta_{sat} - \theta_{res}} \qquad (2.7)$$

The numerical solution to the Richards' equation requires an approximation of the differential water capacity C (cm^{-1}). An expression is obtained by taking the derivative of θ to h:

$$C = \frac{\partial \theta}{\partial h} = \alpha\, m\, n\, |\alpha h|^{n-1} \left(\theta_{sat} - \theta_{res} \right) \left(1 + |\alpha h|^n \right)^{-(m+1)} \qquad (2.8)$$

A numerical approach to Eq. [2.3] yielding a steady-state solution requires an implicit treatment of the hydraulic conductivity. This implies the use of the derivative of the hydraulic conductivity to the pressure heads. Expressions are given in 0.

2.3 Modification for near saturation conditions

A modification to the Mualem-Van Genuchten function (Schaap and Van Genuchten, 2006) has been implemented in SWAP. The modification is based on the introduction of a small minimum capillary height h_e, causing a minor shift in the retention curve (Vogel et al. 2001). We follow Ippisch et al. (2006) by defining the relative water content as:

$$S_e = \begin{cases} \dfrac{1}{S_c} \left[1 + |\alpha h|^n \right]^{-m} & h < h_e \\ 1 & h \geq h_e \end{cases} \qquad (2.9)$$

where S_c is the relative saturation at the cut-off point h_e in the classical Van Genuchten model, given by:

$$S_c = \left[1 + |\alpha h_e|^n \right]^{-m} \qquad (2.10)$$

The hydraulic conductivity is then given by:

$$K = \begin{cases} K_{sat} \, (S_e)^{\lambda} \left[\dfrac{1-(1-(S_e S_c)^{1/m})^m}{1-(1-(S_c)^{1/m})^m} \right]^2 & S_e < 1 \\ \\ K_{sat} & Se \geq 1 \end{cases} \qquad (2.11)$$

This model reduces to Eq. [2.6] for $h_e = 0$. We refer to Vogel et al. (2001), Schaap and Van Genuchten (2006) and Ippisch et al. (2006) for a detailed discussion of the above equations. They showed that the modification affects the shape of the retention curve only minimally relative to the original function. However, the effects on the unsaturated hydraulic conductivity of fine-textured soils can be significant.

To prevent for numerical instabilities of the solution scheme the soil moisture retention curve between 1.05 and 0.95 times the h_e-value is approached by a cubic spline for which the parameters are chosen as such that the continuity of both the soil moisture retention curve and the differential moisture capacity function is preserved.

2.4   Hysteresis

Hysteresis refers to non-uniqueness of the θ(h) relation and is caused by variations of the pore diameter (inkbottle effect), differences in radii of advancing and receding meniscus, entrapped air, thermal gradients and swelling/shrinking processes (Hillel, 1980; Feddes et al., 1988). Gradual desorption of an initially saturated soil sample gives the main drying curve, while slow absorption of an initially dry sample results in the main wetting curve. In the field partly wetting and drying occurs in numerous cycles, resulting in so-called drying and wetting scanning curves lying between the main drying and the main wetting curves (Fig. 2.1).
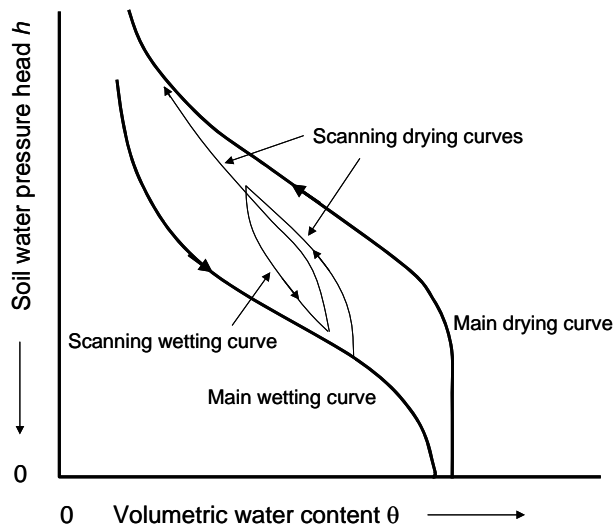
Figure 2.1 Water retention function with hysteresis, showing the main wetting, main drying and scanning curves.

In simulation practice, often only the main drying curve is used to describe the $\theta(h)$ relation. This is mainly due to the time and costs involved in measurement of the complete $\theta(h)$ relationship, including the main wetting, the main drying and the scanning curves, especially in the dry range. For instance, a generally applied soil hydraulic data base in The Netherlands, known as the Staring series (Wösten et al., 1994), contains only $\theta(h)$ data of the main drying curve. Nevertheless, it is obvious that the simulation of infiltration events with the main drying curve can be inaccurate. The scaling method of Scott et al. (1983), who derived scanning curves by rescaling the main wetting or the main drying curve to the actual water content, has been implemented into SWAP.

The main drying and main wetting curve are described analytically with the Mualem-van Genuchten parameters (α, n, θ_{res}, θ_{sat}, K_{sat}, and λ). Some of the parameters describing the main wetting and main drying curve are related. We assume θ_{res} and θ_{sat} to be equal for both curves. Usually the $K(\theta)$ function shows only minor hysteresis effects, which can be achieved by choosing for the main wetting and main drying curve a common value for n. Ultimately the two curves only differ in the parameter α, as depicted in Fig.2.1. The scanning curves are derived by linear scaling of either the main wetting or main drying curve, such that the scanning curve includes the current θ-h combination and approaches the main wetting curve in case of a wetting scanning curve and the main drying curve in case of a drying scanning curve.

The scaling principle in case of a drying scanning curve is depicted in Fig.2.2A. Based on its wetting and drying history, at a certain time and depth the soil shows an actual water content θ_{act} at the soil water pressure head h_{act}. The valid drying scanning curve should pass through the point (θ_{act}, h_{act}), and approach the main drying curve at smaller water contents.
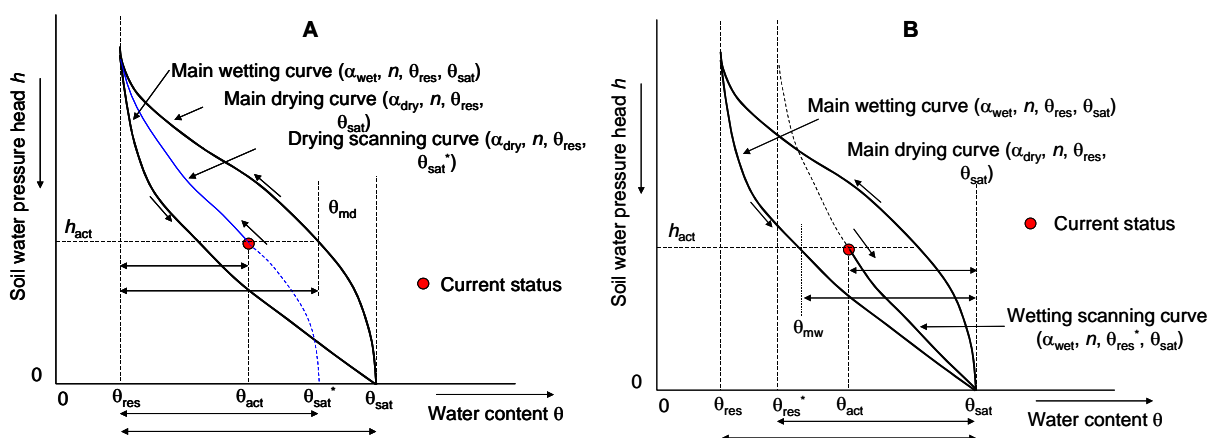
Figure 2.2 (A) Linear scaling of the main drying water retention curve in order to derive a drying scanning curve; (B) Linear scaling of the main wetting water retention curve in order to derive a drying wetting curve.

We may define θ_{md} as the water content of the main drying curve at h_{act}, and θ_{sat}^{*} as the saturated water content of the drying scanning curve. Linear scaling of the main drying curve with respect to the vertical axis $\theta = \theta_{res}$ gives (Fig.2.2A):

$$\frac{\theta_{sat}^{*} - \theta_{res}}{\theta_{sat} - \theta_{res}} = \frac{\theta_{act} - \theta_{res}}{\theta_{md} - \theta_{res}} \quad \Rightarrow \quad \theta_{sat}^{*} = \theta_{res} + \left(\theta_{sat} - \theta_{res}\right)\frac{\theta_{act} - \theta_{res}}{\theta_{md} - \theta_{res}} \qquad (2.12)$$

The only unknown in Eq. [2.13] is θ_{sat}^{*}, which can be directly solved. The drying scanning curve is described accordingly with the parameters (α_{dry}, n, θ_{res}, θ_{sat}^{*}). As long as the soil keeps drying, this drying scanning curve is valid.

The opposite occurs when the soil gets wetter. Again we start from the arbitrary actual water content θ_{act} at the soil water pressure head h_{act}, and now define θ_{mw} as the water content of the main wetting curve at h_{act}, and θ_{res}^{*} as the residual water content of the wetting scanning curve. Linear scaling of the main wetting curve with respect to the vertical axis $\theta = \theta_{sat}$ gives (Fig.2.2B):

$$\frac{\theta_{sat} - \theta_{res}^{*}}{\theta_{sat} - \theta_{res}} = \frac{\theta_{sat} - \theta_{act}}{\theta_{sat} - \theta_{mw}} \quad \Rightarrow \quad \theta_{res}^{*} = \theta_{sat} - \left(\theta_{sat} - \theta_{res}\right)\frac{\theta_{sat} - \theta_{act}}{\theta_{sat} - \theta_{mw}} \qquad (2.13)$$

From Eq.[2.14], θ_{res}^{*} can be directly solved. The wetting scanning curve is accordingly described with the parameters (α_{wet}, n, θ_{res}^{*}, θ_{sat}), and is valid as long as the soil keeps wetting. As the wetting-drying history is different at each soil depth, each node may show a different scanning curve. The unique $K(\theta)$ relation of a soil layer always follows from the parameter set (n, θ_{res}, θ_{sat}, K_{sat}, λ) according to Eq. [2.6].

2.5   Frozen soil conditions

Impacts of frozen soil moisture on soil water flow can optionally be described by a reduction of the hydraulic conductivity:

$$K^{*} = K_{min} + (K - K_{min})\cdot\max(0,\min(1,\frac{T - T_2}{T_1 - T_2})) \qquad (2.14)$$

where K^{*} is the adjusted hydraulic conductivity (cm d^{-1}), T is the soil temperature (^{o}C), T_1 and T_2 (^{o}C) are the threshold values bounding the linear reduction and K_{min} is a minimum value of the hydraulic conductivity (cm d^{-1}) which holds for temperatures less than T_2.

2.6   Lower boundary

The bottom boundary of the one-dimensional SWAP is either in the unsaturated zone or in the upper part of the saturated zone where the transition takes place to three-dimensional groundwater flow. The lower boundary conditions in SWAP can be specified, depending on the application and the relevant spatial scale.

Three general types and some special cases of lower boundary conditions are distinguished:

1) *The Dirichlet condition*

The head controlled boundary is often referred as to the Dirichlet condition and involves the imposing of a pressure head h_{bot} at the lower boundary. A special case involves the use of a recorded groundwater elevation. The pressure head at the groundwater elevation ϕ_{avg} is defined as $h=0$. This yields a linear relation between the pressure heads at the grid points above and below ϕ_{avg} :

$$h_{i+1} = -h_i \ \frac{\phi_{avg} - z_{i+1}}{z_i - \phi_{avg}} \qquad\qquad (2.15)$$

2) *The Neumann condition*

The flux is often referred as to the Neumann condition and involves prescribing a flux q_{bot} at the bottom. Since the model employs an explicit linearization scheme, the flux - groundwater level relations are treated as a Neumann condition, where the actual flux is calculated from the groundwater level of the previous time step. The relation between flux and groundwater level can be obtained from regional groundwater flow models (e.g. Van Bakel, 1986). Some special options are available to define q_{bot}:

- A *zero* bottom flux may be applied when an impervious layer exists at the bottom of the profile.
- Impose a time series of q_{bot}
- Calculate q_{bot} at the start of a time step as a function of the groundwater level ϕ_{avg} of the previous timestep, either by interpolation in a tabulated function or by using an exponential function, defined as:

$$q_{\mathrm{bot}} = a_{\mathrm{bot}} \ \exp\!\left(-b_{\mathrm{bot}} \, \phi_{\mathrm{avg}}\right) \qquad\qquad (2.16)$$

where a_{bot} (cm d^{-1}) and b_{bot} (cm^{-1}) are empirical coefficients.

- Calculate q_{bot} at the start of a time step as a function of the groundwater level ϕ_{avg} of the previous timestep, the hydraulic head in a semi-confined aquifer ϕ_{aquif} (cm), and the resistance of the semi-confining layer c_1 (d), according to:

$$q_{bot} = \frac{\phi_{aquif} - \phi_{avg}}{c_1 + \sum_{i=i_{gwl}}^{n} \frac{\Delta z_i}{k_{sat,i}}} \qquad (2.17)$$

The flow resistance in the saturated zone between the groundwater level and the lower boundary has been accounted for by summation of the flow resistances $\frac{\Delta z_i}{k_{sat,i}}$ in this zone. Some options for defining ϕ_{aquif} are available.

3) *The Cauchy condition*

The flux q at the lower boundary is defined as a function of the prevailing pressure head. This condition can be used when unsaturated flow models are combined with models for regional groundwater flow and when an implicit handling of q_{bot} in the iterative computation scheme is required. The flux through the bottom boundary is defined by the difference of the hydraulic head ($h+z$) and the hydraulic head φ (cm) of the regional groundwater outside the flow domain described by the model, divided by a flow resistance c (d).

$$q_{bot} = \frac{[h+z]_{z=bot} - \varphi}{c} \qquad (2.18)$$

4) *Special cases*

Two special cases involve the option to define a seepage face at the lower boundary and to define free drainage. The seepage face is meant to simulate moisture flow in a lysimeter which is composed of a combination the head controlled condition and the zero flux controlled condition.

$$\begin{aligned} h_{z=bot} < 0 \quad &\rightarrow \quad q_{bot} = 0 \\ h_{z=bot} \not< 0 \quad &\rightarrow \quad q_{bot} = -K_n \left[\frac{\partial(h+z)}{\partial z} \right]_{z=bot} \end{aligned} \qquad (2.19)$$

The free drainage results from the assumption that the hydraulic head gradient equals the elevation head gradient, thus: so that the magnitude of q_{bot} equals the hydraulic conductivity of the lowest compartment:

$$\left[\frac{\partial(h+z)}{\partial z} \right]_{z=bot} = 1 \quad \rightarrow \quad q_{bot} = -K_n \qquad (2.20)$$

During frost conditions, q_{bot} will be modified according to

$$q_{bot} = f_T(z) \, q_{bot} \qquad (2.21)$$

but can be reduced even to a lower value in case of the presence of frozen layers (see Chapter 10).

2.7 Numerical implementation

Accurate numerical solution of Richards' partial differential equation is difficult due to its hyperbolic nature, the strong non-linearity of the soil hydraulic functions and the rapid changing boundary conditions near the soil surface. Calculated soil water fluxes can be significantly affected by the structure of the numerical scheme, the applied time and space discretizations, and the procedure for the top boundary condition (Van Genuchten, 1982; Milly, 1985; Celia et al., 1990; Warrick, 1991; Zaidel and Russo, 1992). The numerical scheme chosen in SWAP solves the one-dimensional Richards' equation with an accurate mass balance and converges rapidly. This scheme in combination with the top boundary procedure has been shown to handle rapid soil water movement during infiltration in dry soils accurately. At the same time the scheme is computationally efficient (Van Dam and Feddes, 2000).

2.7.1 Richards' equation

The current numerical scheme of SWAP to solve Richards' equation is the implicit, backward, finite difference scheme with explicit linearization of hydraulic conductivities as described by Haverkamp et al. (1977) and Belmans et al. (1983), but with the following adaptations:

- The numerical scheme applies to both the unsaturated and saturated zone and the flow equations are solved in both zones simultaneously.
- The water storage term $\frac{\partial \theta}{\partial t}$ is evaluated instead of using an approximation for $C \frac{\partial h}{\partial t}$ where C is the water capacity (cm^{-1}).
- There are several options for calculating the internodal conductivity.

The implicit, backward, finite difference scheme of Eq. [2.23] with explicit linearization, yields the following discretization of Richards' equation:

$$\frac{\theta_i^{j+1} - \theta_i^j}{\Delta t^j} = \frac{1}{\Delta z_i} \left[K_{i-\frac{1}{2}}^{j+\kappa} \frac{h_{i-1}^{j+1} - h_i^{j+1}}{\frac{1}{2}(\Delta z_{i-1} + \Delta z_i)} + K_{i-\frac{1}{2}}^{j+\kappa} - K_{i+\frac{1}{2}}^{j+\kappa} \frac{h_i^{j+1} - h_{i+1}^{j+1}}{\frac{1}{2}(\Delta z_i + \Delta z_{i+1})} - K_{i+\frac{1}{2}}^{j+\kappa} \right]$$
$$- S_{a,i}^j - S_{d,i}^j - S_{m,i}^{j+1}$$

(2.22)

where $\Delta t^j = t^{j+1} - t^j$ and Δz_i is compartment thickness. The sink terms representing the root extraction S_a and the flow to drains S_d are evaluated at the old time level j (explicit linearization). The macro pore exchange rate S_m is evaluated at the new time level $j+1$ and the internodal conductivity $K_{i-\frac{1}{2}}^{j+\kappa}$ can be evaluated at the old time level j ($\kappa = 0$) or at the new time level $j+1$ ($\kappa = 1$). The internodal conductivity $K_{i-\frac{1}{2}}^{j+\kappa}$ can be calculated as:

Arithmic mean:
$$K_{i-\frac{1}{2}}^{j+\kappa} = \frac{1}{2}\left(K_{i-1}^{j+\kappa} + K_i^{j+\kappa} \right)$$
(2.23)

Weighted arithmic mean:
$$K_{i-\frac{1}{2}}^{j+\kappa} = \frac{\Delta z_{i-1} K_{i-1}^{j+\kappa} + \Delta z_i K_i^{j+\kappa}}{\Delta z_{i-1} + \Delta z_i}$$
(2.24)

Geometric mean:
$$K_{i-\frac{1}{2}}^{j+\kappa} = \left(K_{i-1}^{j+\kappa} \right)^{\frac{1}{2}} \left(K_i^{j+\kappa} \right)^{\frac{1}{2}}$$
(2.25)

Weighted geometric mean:
$$K_{i-\frac{1}{2}}^{j+\kappa} = \left(K_{i-1}^{j+\kappa} \right)^{\frac{\Delta z_{i-1}}{\Delta z_{i-1} + \Delta z_i}} \left(K_i^{j+\kappa} \right)^{\frac{\Delta z_i}{\Delta z_{i-1} + \Delta z_i}}$$
(2.26)

Starting in the saturated zone, the groundwater table is simply found at $h = 0$. Also perched water tables may occur above dense layers in the soil profile. Since the SWAP model attempts to describe a wide range of layered soil types combined with different types of boundary conditions, the nodal distance is made variable and should be specified by the user. Calculations using a non-weighted arithmic mean for the internodal conductivity show that for accurate infiltration and evaporation simulations, the nodal distance should be in the order of centimetres near the soil surface (Van Dam and Feddes, 2000).

2.7.2 Numerical solution

The discrete form of the Richard's equation is solved iteratively using the pressure heads as state variables. Taylor-expansion of the new moisture fraction at a new iteration level with respect to the moisture fraction at the preceding iteration step is defined by:

$$\theta_i^{j+1,p+1}(h_i^{j+1}) \approx \theta_i^{j+1,p}(h_i^{j+1,p}) + (h_i^{j+1,p+1} - h_i^{j+1,p}) \frac{\partial \theta_i^{j+1,p}}{\partial h_i^{j+1,p}} + \cdots + \cdots$$
(2.27)

Ignoring the second and higher order terms of the Taylor series yields an expression which can substitute the moisture fraction variable at the new time-level. The first order derivate of the moisture fraction to the pressure head is identical to the water capacity $C^{j+1,p}$. In fact the basis (first order approximation of the new moisture

fraction) of the method proposed by Celia et al. (1990) complies with the assumptions made in the Newton-Raphson iteration procedure. An improvement to this method is made by defining F_i based on the closure term of the water balance as a function of h_i^{j+1}:

$$
F_i = \frac{\Delta z_i}{\Delta t^j}\left(\theta_i^{j+1,p} - \theta_i^j\right) - K_{i-\frac{1}{2}}^{j+\kappa,\kappa p}\frac{h_{i-1}^{j+1,p} - h_i^{j+1,p}}{\frac{1}{2}(\Delta z_{i-1} + \Delta z_i)} - K_{i-\frac{1}{2}}^{j+\kappa,\kappa p}
$$
$$
+ K_{i+\frac{1}{2}}^{j+\kappa,\kappa p}\frac{h_i^{j+1,p} - h_{i+1}^{j+1,p}}{\frac{1}{2}(\Delta z_i + \Delta z_{i+1})} + K_{i+\frac{1}{2}}^{j+\kappa,\kappa p} + \Delta z_i S_{a,i}^{j+\kappa,p} + \Delta z_i S_{d,i}^{j} + \Delta z_i S_{m,i}^{j+1,p}
$$

(2.28)

where the superscript $p+1$ points to the solution of iteration round p. This discrete form of the Richards' equation allows for a straightforward evaluation of the storage term and is flexible with the respect to adding of h_i^{j+1}-dependent source and sink-terms. Solving the set of non-linear equations numerically implies root finding of the function $F_i \approx 0$ for $i=1..N$. The Newton Raphson-iteration scheme for the set of equations is written as follows:

$$
\begin{pmatrix} h_1^{j+1,p+1} \\ \vdots \\ h_i^{j+1,p+1} \\ \vdots \\ h_n^{j+1,p+1} \end{pmatrix} = \begin{pmatrix} h_1^{j+1,p} \\ \vdots \\ h_i^{j+1,p} \\ \vdots \\ h_n^{j+1,p} \end{pmatrix} - \begin{pmatrix} \dfrac{\partial F_1}{\partial h_1^{j+1,p}} & \dfrac{\partial F_1}{\partial h_2^{j+1,p}} & 0 & 0 & 0 \\ \dfrac{\partial F_2}{\partial h_1^{j+1,p}} & \dfrac{\partial F_2}{\partial h_2^{j+1,p}} & \cdots & 0 & 0 \\ 0 & \dfrac{\partial F_i}{\partial h_{i-1}^{j+1,p}} & \dfrac{\partial F_i}{\partial h_i^{j+1,p}} & \dfrac{\partial F_i}{\partial h_{i+1}^{j+1,p}} & 0 \\ 0 & 0 & \cdots & \dfrac{\partial F_{n-1}}{\partial h_{n-1}^{j+1,p}} & \dfrac{\partial F_{n-1}}{\partial h_n^{j+1,p}} \\ 0 & 0 & 0 & \dfrac{\partial F_n}{\partial h_{n-1}^{j+1,p}} & \dfrac{\partial F_n}{\partial h_n^{j+1,p}} \end{pmatrix}^{-1} \begin{pmatrix} F_1 \\ \vdots \\ F_i \\ \vdots \\ F_n \end{pmatrix}
$$

(2.29)

The starting values are the results of the previous iteration round, indicated by the superscript p. The solution of the second part of the right hand side is found by solving a tri-diagonal system of equations which can be solved efficiently (Press et al., 1989). The coefficients of the Jacobian are listed in 0. The contribution of the partial derivative of the macro-pore exchange to the pressure head ($\dfrac{\partial S_{m,i}^{j+1,p}}{\partial h_i^{j+1,p}}$) is discussed in Chapter 6. If the option to treat the hydraulic conductivities implicitly is used ($\kappa=1$), the contribution of the partial derivates of the internodal conductivity relation to the pressure head should also accounted. Expressions for these terms are given in 0.

Newton's method for solving nonlinear equations might wander off into the wild blue yonder if the initial guess is not sufficiently close to the root.
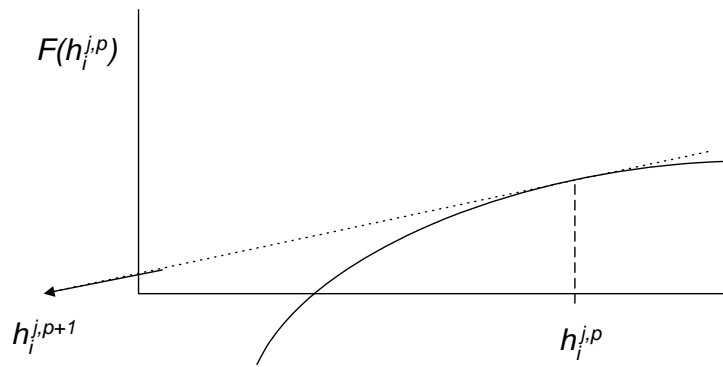
Figure 2.3 Influence of initial estimate on an intermediate solution of a first order approximation based root finding procedure.

The solution to the second part of the right hand side of Eq. [2.30] is referred to as the Newton-step $\Delta h_i^{j+1,p}$ (Eq. [2.31]).

$$
\begin{pmatrix} h_1^{j+1,p+1} \\ \vdots \\ h_i^{j+1,p+1} \\ \vdots \\ h_n^{j+1,p+1} \end{pmatrix} = \begin{pmatrix} h_1^{j+1,p} \\ \vdots \\ h_i^{j+1,p} \\ \vdots \\ h_n^{j+1,p} \end{pmatrix} + \lambda \begin{pmatrix} \Delta h_1^{j+1,p} \\ \vdots \\ \Delta h_i^{j+1,p} \\ \vdots \\ \Delta h_n^{j+1,p} \end{pmatrix}
\qquad (2.30)
$$

We always first try the full Newton step and we check at each iteration that the proposed step reduces $\frac{1}{2}\sum_{i=1}^{n} F_i^2$. If not, we backtrack along the Newton direction until we have an acceptable step. The aim is to find λ which results in a decrease of $\frac{1}{2}\sum_{i=1}^{n}\left[F_i(h_i^{j+1,p} + \lambda \Delta h_i^{j+1,p})\right]^2$. The first estimate of λ amounts to 1. If it is decided that a second estimate is needed, λ is set to 1/3. The third estimate amounts to 1/9. Thereafter, no further reduction of λ is applied but a new Newton -iteration step is performed.

In SWAP the main convergence criterium in the unsaturated zone is based on the water closure term of the water balance F. If $|F_i|$ is less than a user defined criterion for all compartments, it is decided that the iteration cycle has resulted into a sufficiently accurate solution.

2.7.3 Numerical implementation of boundary conditions

2.7.3.1 Top boundary condition

Appropriate criteria for the procedure with respect to the top boundary condition are important for accurate simulation of rapidly changing soil water fluxes near the soil surface. This is for instance the case with infiltration/runoff events during intensive rain showers or when the soil occasionally gets flooded in areas with shallow groundwater tables. At moderate weather and soil wetness conditions the soil top boundary condition will be flux-controlled. In either very wet or very dry conditions the prevailing water pressure head at the soil surface starts to govern the boundary condition.

In case of a *Flux controlled top boundary* the term $-K_{i-\frac{1}{2}}^{j+\kappa,\kappa\,p}\left(\dfrac{h_{i-1}^{j+1,p}-h_i^{j+1,p}}{\frac{1}{2}(\Delta z_{i-1}+\Delta z_i)}+1\right)$ is replaced by the flux through the soil surface q_{top} (cm d^{-1}) which yields the following expression*:*

$$F_1 = \frac{\Delta z_1}{\Delta t^j}\left(\theta_1^{j+1}-\theta_1^j\right)+q_{top}+K_{1\frac{1}{2}}^{j+\kappa}\frac{h_1^{j+1}-h_2^{j+1}}{\frac{1}{2}(\Delta z_1+\Delta z_2)}+K_{1\frac{1}{2}}^{j+\kappa}+\Delta z_1 S_{a,1}^{j+\kappa}+\Delta z_1 S_{d,1}^{j}+\Delta z_1 S_{m,1}^{j+1} \quad (2.31)$$

where q_{top} is calculated from external driving factors as net precipitation (q_{prec}), irrigation (q_{irri}), melt of a snow pack (q_{melt}) runon originating from adjacent fields (q_{runon}) and inundation from adjacent water courses (q_{inun})

$$q_{top} = -q_{prec}-q_{irri}-q_{melt}-q_{runon}-q_{inun} \qquad (2.32)$$

In case of a *Head controlled top boundary* the term $-K_{i-\frac{1}{2}}^{j+\kappa,\kappa\,p}\left(\dfrac{h_{i-1}^{j+1,p}-h_i^{j+1,p}}{\frac{1}{2}(\Delta z_{i-1}+\Delta z_i)}+1\right)$ is replaced by $-K_{\frac{1}{2}}^{j+1}\left(\dfrac{h_0^{j+1}-h_1^{j+1}}{\frac{1}{2}(\Delta z_1)}+1\right)$, where h_0^{j+1} is the pressure head at the soil surface at the new time level. The internodal conductivity $K_{\frac{1}{2}}^{j+1}$ is always treated implicitly.

Within each iteration round and also within each backtracking sub-cycle it is tested whether the combination of q_{top} and h_1^{j+1} would lead to $h_1^{j+1}-\frac{1}{2}(\Delta z_1)\left(\dfrac{q_{top}}{K_{\frac{1}{2}}^{j+1}}+1\right)>0$. In such a case it is decided that the head boundary condition holds and the water balance of the so-called ponding layer is calculated which includes the surface runoff flux and

the ponding depth at time level $j+1$. The value of h_0^{j+1} is set to the ponding depth at time level $j+1$. The water balance of the ponding layer reads as:

$$\frac{h_0^{j+1} - h_0^{j}}{\Delta t} = -K_{\frac{1}{2}}^{j+1}\left(\frac{h_0^{j+1} - h_1^{j+1}}{\frac{1}{2}(\Delta z_1)} + 1 \right) + q_{prec} + q_{irri} + q_{melt} + q_{runon} + q_{inun} - q_{e,pond} - q_{runoff} - I_{ru}$$

(2.33)

Where I_{ru} is the runoff into the macropores (section 6.1.2).

The surface runoff flux q_{runoff} is defined as a function of the ponding height:

$$
\begin{aligned}
h_0^{j+1} &\leq h_{0,threshold} & q_{runoff} &= 0 \\
h_0^{j+1} &> h_{0,threshold} & q_{runoff} &= \alpha\left(h_0^{j+1} - h_{0,threshold}\right)^{\beta}
\end{aligned}
$$

(2.34)

Where α and β are coefficients of the surface runoff equation employed by the SWAP model (see Section 4.1). Substitution of surface runoff expression into water balance equation for the ponding layer yields the relation which is solved in the iteration procedure:

$$h_0^{j+1}\left(\frac{1}{\Delta t} + \frac{K_{\frac{1}{2}}^{j+1}}{\frac{1}{2}(\Delta z_1)} \right) + \alpha\left(h_0^{j+1} - h_{0,threshold}\right)^{\beta} =$$

(2.35)

$$\frac{h_0^{j}}{\Delta t} + \frac{K_{\frac{1}{2}}^{j+1}}{\frac{1}{2}(\Delta z_1)}h_1^{j+1} - K_{\frac{1}{2}}^{j+1} + q_{prec} + q_{melt} + q_{runon} - q_{e,pond} - I_{ru}$$

which is solved in the iteration procedure.

2.7.3.2 Bottom boundary condition

The SWAP model provides a number of options to describe the relation between saturated shallow soil layers with deep groundwater (see Chapter 5). Beside handling the flux controlled boundary condition and head controlled boundary condition, the model has additional capabilities to combine these basic types of conditions. Additional options comprise the handling of:
- Predefined groundwater levels
- Cauchy relation for the bottom boundary
- Free drainage
- Free outflow

Flux controlled bottom boundary

For $i=n$, the $K_{i+\frac{1}{2}}^{j+\kappa,\kappa p}\left(\dfrac{h_i^{j+1,p} - h_{i+1}^{j+1,p}}{\frac{1}{2}(\Delta z_i + \Delta z_{i+1})} + 1\right)$-term in Eq. [2.29] is replaced by $-q_{bot}$, which

yields:

$$F_n = \frac{\Delta z_n}{\Delta t^j}\left(\theta_n^{j+1} - \theta_n^j\right) - K_{n-\frac{1}{2}}^{j+\kappa}\left(\frac{h_{n-1}^{j+1} - h_n^{j+1}}{\frac{1}{2}(\Delta z_{n-1} + \Delta z_n)} + 1\right) - q_{bot} + \Delta z_n\left(S_{a,n}^{j+\kappa} + S_{d,n}^j + S_{m,n}^{j+1}\right) \quad (2.36)$$

Beside the flux boundary condition, the SWAP model has options to handle groundwater level dependent bottom fluxes. The flux can be formulated as an exponential function of groundwater level, or as the difference between groundwater level and hydraulic head in deep groundwater outside the flow domain divided by a flow resistance. Such a flux is calculated explicitly at the start of the current time step and is treated as a flux condition in the numerical scheme.

Head controlled bottom boundary

For $i=n$, Δz_{i+1} is set to zero and $h_{i+1}^{j+1,p} = h_{bot}$, which leads to the following expression:

$$F_n = \frac{\Delta z_n}{\Delta t^j}\left(\theta_n^{j+1} - \theta_n^j\right) - K_{n-\frac{1}{2}}^{j+\kappa}\left(\frac{h_{n-1}^{j+1} - h_n^{j+1}}{\frac{1}{2}(\Delta z_{n-1} + \Delta z_n)} + 1\right) + K_{n+\frac{1}{2}}^{j+\kappa}\left(\frac{h_n^{j+1} - h_{bot}}{\frac{1}{2}\Delta z_n} + 1\right)$$
$$+ \Delta z_n\left(S_{a,n}^{j+\kappa} + S_{d,n}^j + S_{m,n}^{j+1}\right) \quad (2.37)$$

Predefined groundwater levels

First, the lowest partially unsaturated compartment is searched for and is called n^*. The set of n^* non-linear equations for $F(h)$ is then solved for the unsaturated compartments. The bottom boundary condition for this set of equations is defined by:

$$F_{n^*} = \frac{\Delta z_{n^*}}{\Delta t^j}\left(\theta_{n^*}^{j+1} - \theta_{n^*}^j\right) - K_{n^*-\frac{1}{2}}^{j+\kappa}\left(\frac{h_{n^*-1}^{j+1} - h_{n^*}^{j+1}}{\frac{1}{2}(\Delta z_{n^*-1} + \Delta z_{n^*})} + 1\right) + K_{n^*+\frac{1}{2}}^{j+\kappa}\left(\frac{h_{n^*}^{j+1} - h_{n^*+1}^{j+1}}{\frac{1}{2}(\Delta z_{n^*} + \Delta z_{n^*+1})} + 1\right)$$
$$+ \Delta z_n\left(S_{a,n^*}^{j+\kappa} + S_{d,n^*}^j + S_{m,n^*}^{j+1}\right) \quad (2.38)$$

The groundwater level is situated between the nodal points n^* and n^*+1. The pressure head of nodal point n^*+1 is approximated $h_{n^*}^{j+1}$ by:

$$h_{n^*+1}^{j+1} = -h_{n^*}^{j+1}\ \frac{gwl - z_{n^*+1}}{z_{n^*} - gwl} \quad (2.39)$$

where z_{n^*} is the height of the node in compartment n^* and *gwl* is the groundwater level. Substitution into Eq. [2.30] yields:

$$F_{n^*} = \frac{\Delta z_{n^*}}{\Delta t^j}\left(\theta_{n^*}^{j+1} - \theta_{n^*}^j\right) - K_{n^*-\frac{1}{2}}^{j+\kappa}\left(\frac{h_{n^*-1}^{j+1} - h_{n^*}^{j+1}}{\frac{1}{2}(\Delta z_{n^*-1} + \Delta z_{n^*})} + 1\right) + K_{n^*+\frac{1}{2}}^{j+\kappa}\left(\frac{h_{n^*}^{j+1}\left(\dfrac{z_{n^*} - z_{n^*+1}}{z_{n^*} - gwl}\right)}{\frac{1}{2}(\Delta z_{n^*} + \Delta z_{n^*+1})} + 1\right)$$

$$+ \Delta z_n\left(S_{a,n^*}^{j+\kappa} + S_{d,n^*}^j + S_{m,n^*}^{j+1}\right) \qquad (2.40)$$

After iteratively solving the set of equations for $i \le n^*$, the pressure head profile of the compartments $i > n^*$ can be calculated from the pressure head of the two adjacent upward nodes.

$$h_{i+1}^{j+1} = h_i^{j+1}\left(1 + \frac{K_{i-\frac{1}{2}}^{j+\kappa}(\Delta z_i + \Delta z_{i+1})}{K_{i+\frac{1}{2}}^{j+\kappa}(\Delta z_{i-1} + \Delta z_i)}\right) - h_{i-1}^{j+1}\frac{K_{i-\frac{1}{2}}^{j+\kappa}(\Delta z_i + \Delta z_{i+1})}{K_{i+\frac{1}{2}}^{j+\kappa}(\Delta z_{i-1} + \Delta z_i)} + \frac{1}{2}(\Delta z_i + \Delta z_{i+1})(1 - \frac{K_{i-\frac{1}{2}}^{j+\kappa}}{K_{i+\frac{1}{2}}^{j+\kappa}})$$

$$+ \frac{\frac{1}{2}(\Delta z_i + \Delta z_{i+1})}{K_{i+\frac{1}{2}}^{j+\kappa}}\left(\frac{\Delta z_i}{\Delta t^j}\left(\theta_{sat,i} - \theta_i^j\right) + \Delta z_i\left(S_{a,i}^{j+\kappa} + S_{d,i}^j + S_{m,i}^{j+1}\right)\right) \qquad (2.41)$$

Cauchy relation for the bottom boundary
The flux through the bottom boundary is defined by the difference the hydraulic head at the lower boundary and the hydraulic head φ (cm) of the regional groundwater specified by the user, divided by a flow resistance c (d). The hydraulic head at the lower boundary is approximated by the pressure head of the lowest nodal point plus the elevation head of node n.

$$q_{bot} = \frac{h_n^{j+1} + z_n - \varphi}{\dfrac{\frac{1}{2}\Delta z_n}{K_{n+\frac{1}{2}}^{j+\kappa}} + c} \qquad (2.42)$$

Substitution into Eq. [2.30] yields:

$$F_n = \frac{\Delta z_n}{\Delta t^j}\left(\theta_n^{j+1} - \theta_n^j\right) - K_{n-\frac{1}{2}}^{j+\kappa}\left(\frac{h_{n-1}^{j+1} - h_n^{j+1}}{\frac{1}{2}(\Delta z_{n-1} + \Delta z_n)} + 1\right) + K_{n+\frac{1}{2}}^{j+\kappa}\frac{h_n^{j+1} - (\varphi - z_n)}{\frac{1}{2}\Delta z_n + cK_{n+\frac{1}{2}}^{j+\kappa}}$$

$$+ \Delta z_n\left(S_{a,n}^{j+\kappa} + S_{d,n}^j + S_{m,n}^{j+1}\right) \qquad (2.43)$$

Seepage face
The seepage face option is used to simulate the soil moisture flow in a lysimeter with an open outlet at the bottom. No outflow occurs when the bottom soil layer is still unsaturated. Since the flow resistance of the outlet is negligible small, no positive pressure head values will be build up at the bottom when the soil water percolates at the bottom. Within the iteration cycle for solving the numerical expression of the

Richards' equation, it is checked whether the flux or the head controlled boundary condition prevails. When $h_n^{j+1} + \frac{1}{2}\Delta z_n < 0$ the bottom flux q_{bot} is set to zero, but when $h_n^{j+1} + \frac{1}{2}\Delta z_n$ tends to take values larger than zero, the pressure at the bottom is set to zero ($h_{bot} = 0$). The numerical implementation is as follows:

$$h_n^{j+1} + \tfrac{1}{2}\Delta z_n < 0 \rightarrow \begin{aligned} F_n &= \frac{\Delta z_n}{\Delta t^j}\left(\theta_n^{j+1} - \theta_n^j\right) - K_{n-\frac{1}{2}}^{j+\kappa}\left(\frac{h_{n-1}^{j+1} - h_n^{j+1}}{\frac{1}{2}(\Delta z_{n-1} + \Delta z_n)} + 1\right) \\ &\quad + \Delta z_n\left(S_{a,n}^{j+\kappa} + S_{d,n}^j + S_{m,n}^{j+1}\right) \end{aligned} \qquad (2.44)$$

$$h_n^{j+1} + \tfrac{1}{2}\Delta z_n \not< 0 \rightarrow \begin{aligned} F_n &= \frac{\Delta z_n}{\Delta t^j}\left(\theta_n^{j+1} - \theta_n^j\right) - K_{n-\frac{1}{2}}^{j+\kappa}\left(\frac{h_{n-1}^{j+1} - h_n^{j+1}}{\frac{1}{2}(\Delta z_{n-1} + \Delta z_n)} + 1\right) \\ &\quad + K_{n+\frac{1}{2}}^{j+\kappa}\left(\frac{h_n^{j+1}}{\frac{1}{2}\Delta z_n} + 1\right) + \Delta z_n\left(S_{a,n}^{j+\kappa} + S_{d,n}^j + S_{m,n}^{j+1}\right) \end{aligned} \qquad (2.45)$$

Free drainage
The free drainage option is applied for soil profiles with deep groundwater levels. The bottom flux is only provoked by gravity flow and the head pressure gradient equals zero:

$$q_{bot} = -K_{n+\frac{1}{2}}^{j+1}\left(\left(\frac{\partial h}{\partial z}\right)_{n+\frac{1}{2}} + 1\right) \quad \rightarrow \quad q_{bot} = -K_{n+\frac{1}{2}}^{j+1} \qquad (2.46)$$

Substitution into Eq.[2.30] yields:

$$\begin{aligned} F_n &= \frac{\Delta z_n}{\Delta t^j}\left(\theta_n^{j+1} - \theta_n^j\right) - K_{n-\frac{1}{2}}^{j+\kappa}\left(\frac{h_{n-1}^{j+1} - h_n^{j+1}}{\frac{1}{2}(\Delta z_{n-1} + \Delta z_n)} + 1\right) + K_{n+\frac{1}{2}}^{j+1} \\ &\quad + \Delta z_n\left(S_{a,n}^{j+\kappa} + S_{d,n}^j + S_{m,n}^{j+1}\right) \end{aligned} \qquad (2.47)$$

2.8   User instructions

2.8.1   General

Box 2.1 shows the general input with regard to soil water flow. The initial soil moisture condition (Part 1) is defined by the soil water pressure head. Initial values can by specified as function of soil depth with linear interpolation between depths or can be calculated assuming hydrostatic equilibrium with a groundwater level. A third option is to use the output of an earlier SWAP simulation. This option is very useful when no data are available of the initial soil moisture condition.

Part 4 describes the vertical discretization of the soil profile. In addition to the natural soil layers with different hydraulic functions, the thicknesses of the calculation compartments should be defined. For correct simulation of infiltration and evaporation fluxes near the soil surface, the compartment thickness near the soil surface should be ≤ 1 cm. Deeper in the soil profile, where the soil water flow is less dynamic, the compartment thicknesses may increase to 10 cm. Subsequently in part 5 the hydraulic parameters of each distinct soil layer are defined, which describe the water retention and hydraulic conductivity functions. Caution should be exercised with the use of the air-entry-value concept h_e. The effects of even a small value of $|h_e|$ on the unsaturated hydraulic conductivity of fine-textured soils can be significant. The introduction of the air-entry-value concept requires the re-fitting of the other parameters of the classical Mulaem-Van Genuchten model on the original experimental data.

In part 6 the inclusion of hysteresis in the water retention function can be selected. In case of hysteresis, the parameter ALFAW of the wetting curve (part 5) should be properly defined. Whether the initial condition is wetting or drying, may have a large effect on the water balance. In general the simulations are not sensitive to the minimum head difference to change from wetting to drying scanning curves and vice versa (TAU). The parameter TAU is usually set equal to 0.2 cm.

In part 11 various parameters are defined that may affect the numerical solution of the Richards' equation. In general, the default values will garantuee an accurate numerical solution of the highly non-linear Richards' equation. In extreme cases different input values might be required. The user should specify a minimum and a maximum time step, Δt_{min} and Δt_{max} (d). SWAP will determine the optimal time step which minimizes the computational effort of a simulation while the numerical solution still meets the convergence criterion. For this purpose, SWAP employes the

number of iterations needed to reach convergence, N_{it}, in the following way (Kool and Van Genuchten, 1991):

- $N_{it} < 3$: multiply time step with a factor 2
- $3 \leq N_{it} \leq Max_{it}$: keep time step the same
- $N_{it} > Max_{it}$: divide time step by a factor 2

where Max_{it} is a user defined maximum number of iterations allowed. The maximum number of back-track cycles should also be specified by the user. A common value for this maximum is 3.

Routinely, SWAP uses three convergence criteria:

- the maximum difference of nodal water contents between iterations
- the maximum difference of groundwater level fluctuations between iterations
- the water balance error of a possible ponding layer

For the initial time step, SWAP will take $\Delta t = \sqrt{\Delta t_{min} \Delta t_{max}}$. Depending on N_{it}, the time step will be decreased, maintained or increased for the following timesteps. The timestep is always confined to the range $\Delta t_{min} \leq \Delta t \leq \Delta t_{max}$. When the actual time step in a certain part if the simulation period is at its minimum size ($\Delta t = \Delta t_{min}$), the maximum number of iterations allowed is set to $2 * Max_{it}$.

In the numerical solution section also a choice can be made with respect to spatial averaging of hydraulic conductivity and explicit/implicit use of hydraulic conductivity in the numerical solution. Haverkamp and Vauclin (1979), Belmans et al. (1983) and Hornung and Messing (1983) proposed to use the geometric mean. In their simulations the geometric mean increased the accuracy of calculated fluxes and caused the fluxes to be less sensitive to changes in nodal distance. However, the geometric mean has serious disadvantages too (Warrick, 1991). When simulating infiltration in dry soils or high evaporation from wet soils, the geometric mean severely underestimates the water fluxes. Other researchers proposed to use the harmonic mean of K or various kind of weighted averages (Ross, 1990; Warrick, 1991; Zaidel and Russo, 1992; Desbarats, 1995). Van Dam and Feddes (2000) show that, although arithmetic averages at larger nodal distances overestimate the soil water fluxes in case of infiltration and evaporation events, at nodal distances in the order of 1 cm non-weighted arithmetic averages are more close to the theoretically correct solution than geometric averages. Also they show that the remaining inaccuracy between calculated and theoretically correct fluxes, is relatively small compared to effects of soil spatial variability and hysteresis. Therefore the SWAP development team has a preference for applying weighted arithmetic averages of K, which is in line with commonly applied finite element models (Kool and Van Genuchten, 1991; Šimůnek et al., 1992). Therefore default choices are weighted arithmetic mean (SWKMEAN = 2) and explicit solution (SWKIMPL = 0).

*Box 2.1 Information on soil water flow in main file *.swp*

```
***********************************************************************************
* Part 1: Initial soil moisture condition

 SWINCO = 2 ! Switch, type of initial soil moisture condition:
             ! 1 = pressure head as function of depth is input
             ! 2 = pressure head of each compartment is in hydrostatic equilibrium
             !     with initial groundwater level
             ! 3 = read final pressure heads from output of previous Swap simulation

* If SWINCO = 1, specify (maximum MACP):
* ZI = soil depth, [-10000..0 cm, R]
* H  = initial soil water pressure head, [-1.d10..1.d4 cm, R]

      ZI         H
    -0.5      -93.0
  -195.0      120.0
* End of table

* If SWINCO = 2, specify:
  GWLI   = -75.0  ! Initial groundwater level, [-10000..100 cm, R]

* If SWINCO = 3, specify:
  INIFIL = 'result.end'   ! name of final with extension .END [a200]
***********************************************************************************

***********************************************************************************
* Part 4: Vertical discretization of soil profile

* Specify the following data (maximum MACP lines):
* ISOILLAY = number of soil layer, start with 1 at soil surface, [1..MAHO, I]
* ISUBLAY  = number of sub layer, start with 1 at soil surface, [1..MACP, I]
* HSUBLAY  = height of sub layer, [0.0..1000.0 cm, R]
* HCOMP    = height of compartments in this layer, [0.0..1000.0 cm, R]
* NCOMP    = number of compartments in this layer (= HSUBLAY/HCOMP), [1..MACP, I]

 ISOILLAY ISUBLAY  HSUBLAY    HCOMP    NCOMP
    1       1        10.0      1.0      10
    1       2        20.0      5.0       4
    2       3        30.0      5.0       6
    2       4       140.0     10.0      14
* end of table
***********************************************************************************

***********************************************************************************
* Part 5: Soil hydraulic functions

* Specify for each soil layer (maximum MAHO):
* ISOILLAY1 = number of soil layer, as defined in part 4 [1..MAHO, I]
* ORES    = Residual water content, [0..0.4 cm3/cm3, R]
* OSAT    = Saturated water content, [0..0.95 cm3/cm3, R]
* ALFA    = Shape parameter alfa of main drying curve, [0.0001..1 /cm, R]
* NPAR    = Shape parameter n, [1..4 -, R]
* KSAT    = Saturated vertical hydraulic conductivity, [1.d-5..1000 cm/d, R]
* LEXP    = Exponent in hydraulic conductivity function, [-25..25 -, R]
* ALFAW   = Alfa parameter of main wetting curve in case of hysteresis, [0.0001..1 /cm, R]
* H_ENPR = Air entry pressure head [-40.0..0.0 cm, R]

  ISOILLAY1   ORES    OSAT     ALFA    NPAR     KSAT      LEXP    ALFAW H_ENPR
      1       0.01    0.43   0.0227   1.548     9.65    -0.983   0.0454 0.0
      2       0.02    0.38   0.0214   2.075    15.56     0.039   0.0428 0.0
* --- end of table

***********************************************************************************

***********************************************************************************
* Part 6: Hysteresis of soil water retention function

* Switch for hysteresis:
  SWHYST = 0   ! 0 = no hysteresis
               ! 1 = hysteresis, initial condition wetting
               ! 2 = hysteresis, initial condition drying

* If SWHYST = 1 or 2, specify:
  TAU = 0.2    ! Minimum pressure head difference to change wetting-drying, [0..1 cm, R]
***********************************************************************************
```

```
*******************************************************************************
* Part 11 Numerical solution of Richards' equation

  DTMIN      = 1.0d-6      ! Minimum timestep, [1.d-7..0.01 d, R]
  DTMAX      = 0.2         ! Maximum timestep, [ 0.01..0.5 d, R]
  GWLCONV    = 100.0       ! Maximum dif. groundwater level between iterations, [1.d-5..1000 cm, R]
  CritDevPondDt = 1.0d-4   ! Maximum water balance error of ponding layer, [1.0d-6..0.1 cm, R]
  MaxIt      = 30          ! Maximum number of iteration cycles, [5..100 -, I]
  MaxBackTr = 3            ! Max. number of back track cycles within an iteration cycle, [1..10 -,I]

* Switch for mean of hydraulic conductivity, [1..4 -, I]:
* 1 = unweighted  arithmic mean; 2 = weighted  arithmic mean
* 3 = unweighted geometric mean; 4 = weighted geometric mean
  SWkmean = 2

* Switch for explicit/implicit solution Richards equation with hydr. conductivity, [1..2 -, I]:
  SWkImpl = 0   ! 0 = explicit solution
                ! 1 = implicit solution
*******************************************************************************
```

2.8.2   Bottom boundary conditions

SWAP offers a number of options to prescribe the lower boundary condition, each having their typical scale of application (Table 2.1, Box 2.2).

Table 2.1. Options for the lower boundary condition

Lower boundary condition (input switch SwBotB)	Description	Type of condition	Typical scale of application
1	Prescribe groundwater level	Dirichlet	Field
2	Prescribe bottom flux (q_{bot})	Neumann	region
3	Calculate bottom flux from hydraulic head of deep aquifer	Cauchy	region
4	Calculate bottom flux as function of groundwater level	Cauchy	region
5	Prescribe soil water pressure head of bottom compartment	Dirichlet	field
6	Bottom flux equals zero	Neumann	Field / region
7	Free drainage of soil profile	Neumann	field
8	Free outflow at soil-air interface	Neumann / Dirichlet	field

In case of options 1, 2, 3, 5 and 6, in addition to the flux across the bottom of the modelled soil profile *(q_{bot})*, a drainage flux *(q_{drain})* can be defined (Chapter 4). In case of option 4 the lower boundary includes drainage to local ditches or drains so q_{drain} should not be defined separately. In case of options 7 and 8, the simulated soil profile

is unsaturated, so lateral drainage will not occur. We will discuss the 8 available bottom boundary conditions sequentially.

1. Prescribed groundwater levels

In this case a field-averaged groundwater level (φ_{avg}) is given as a function of time (Box 2.2). SWAP will linearly interpolate between the days at which the groundwater levels are specified. The main advantage of this boundary condition is the easy recording of the phreatic surface in case of a present groundwater table. A drawback is that at shallow groundwater tables the simulated phreatic surface fluctuations are very sensitive to the soil hydraulic functions and the top boundary condition. If the top and bottom boundary condition not properly match, or the soil hydraulic functions deviate from reality, strong fluctuations of water fluxes across the lower boundary may result. Especially when the output of SWAP is used as input in water quality calculations, it is recommended to use another type of lower boundary condition. The option of prescribed groundwater levels is disabled for macropore flow simulations.

2. Prescribed bottom flux

In this case the bottom flux (q_{bot}) might be given as function of time with linear interpolation between the data pairs, or as a sine function (Box 2.2). This option has a similar disadvantage as the previously described option with the prescribed groundwater level at the field scale. When a mismatch occurs between boundary conditions (e.g. drainage + leakage to deep aquifer exceeds net precipitation excess) the result may be a continuously declining or increasing groundwater level. In particular in cases where the output of SWAP is used as input in water quality calculations, it is recommended to use another type of lower boundary condition.

3. Calculate the bottom flux from the hydraulic head of a deep aquifer

To illustrate this option figure 2.4 shows a soil profile which is drained by ditches and which receives a seepage flux from a semi-confined aquifer. SWAP makes a distinction between q_{drain}, the local drainage flux to ditches and drains (see Chapter 4), and q_{bot} the bottom flux due to regional groundwater flow.
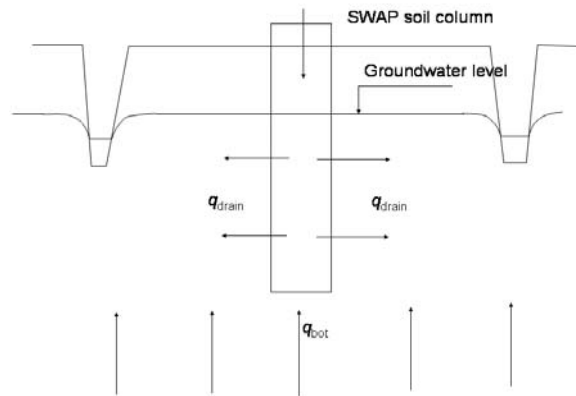
Figure 2.4 Pseudo two-dimensional Cauchy lower boundary conditions, in case of drainage to ditches and seepage from a deep aquifer

The bottom flux q_{bot} depends on the average groundwater level φ_{avg} (cm), the hydraulic head in the semi-confined aquifer ϕ_{aquif} (cm), and the resistance of the semi-confining layer c_1 (d):

$$q_{bot} = \frac{\phi_{aquif} - \phi_{avg}}{c_1 + \sum_{i=i_{gwl}}^{n} \frac{\Delta z_i}{k_{sat,i}}} \qquad (2.48)$$

where the subscript i_{gwl} points to the compartment number in which the groundwater level is located. The vertical resistance between the bottom of the model and the groundwater level is taken into account by adding it to the aquitard resistance c_1. The hydraulic head ϕ_{aquif} is prescribed using a sinusoidal wave:

$$\phi_{aquif} = \phi_{aquif,m} + \phi_{aquif,a} \cos\left(\frac{2\pi}{\phi_{aquif,p}} \left(t - t_{max} \right) \right) \qquad (2.49)$$

where $\phi_{aquif,m}$, $\phi_{aquif,a}$, and $\phi_{aquif,p}$ are the mean (cm), amplitude (cm) and period (d) of the hydraulic head sinus wave in the semi-confined aquifer, and t_{max} is a time (d) at which ϕ_{aquif} reaches its maximum.

The SWAP model comprises option for the implicit treatment of pressure head in lowest compartment by substitution of ϕ_{avg} by $h_n^{j+1} + z_n$ and considering the vertical resistance within the model domain only between the lowest node and the lower boundary. Another option involves the possibility to specify a groundwater flux additional to q_{bot} to facilitate the coupling of the SWAP model to a regional groundwater model.

4. Calculate bottom flux as a function of groundwater level

The relation between q_{bot} and φ_{avg} can be given as an exponential relation or as a table (Box 2.2). The exponential relationship is formulated as:

$$q_{bot} = a_{qbot} \exp\left(b_{qbot} \left| \phi_{avg} \right|\right) \qquad (2.50)$$

where a_{qbot} (cm d^{-1}) and b_{qbot} (cm^{-1}) are empirical coefficients. This kind of exponential relationships was derived for deep sandy areas in The Eastern part of The Netherlands (Massop and De Wit, 1994).

Special care should be taken with respect to the distinction between drainage and bottom boundary flux. The relationship that may be used to compute drainage (Chapter 4) can conflict with the relation for q_{bot}. It may then be appropriate to apply another type of boundary condition.

When the relation between q_{bot} and φ_{avg} is given as a table q_{bot} results from an interpolation between groundwater level and bottom flux listed in the table, using the simulated groundwater level (φ_{gwl}).

5. Prescribed soil water pressure heads at the bottom of the model

In this case values of h_{bot} are given as input to the model. For days with unknown values a linear interpolation is carried out between the days with known values.

6. Zero flux at the bottom of the model domain

A bottom flux (q_{bot}) of zero may be applied when an impervious layer exists at the bottom of the profile. This option is implemented with a simple switch, which forces q_{bot} to zero.

7. Free drainage

In the case where free drainage is taken to be the bottom boundary condition, the gradient of hydraulic head H is assumed to be equal to one at the bottom boundary, which sets q_{bot} equal to the hydraulic conductivity of the lowest compartment:

$$\frac{\partial H}{\partial z} = 1 \qquad \text{thus:} \quad q_{bot} = -K_n \qquad (2.51)$$

8. Free outflow

In this case, drainage will only occur if the pressure head in the bottom compartment (h_n) becomes greater than zero. During drainage and after a drainage event, h_n is set equal to zero and q_{bot} is calculated by solving the Richards' equation. This option is commonly applied for lysimeters, where outflow only occurs when the lowest part of the lysimeter becomes saturated. In the field this condition is appropriate when the soil profile is drained by a coarse gravel layer. Lysimeters with groundwater table

controlling provisions can be better simulated imposing a zero bottom flux condition (SWBOTB=6), combined with a single drainage system, where the drainage resistance is low.

```
Box 2.2 Bottom boundary section in main input file *.swp

**********************************************************************************
* If SWBBCFILE = 0, select one of the following options:
                ! 1  Prescribe groundwater level
                ! 2  Prescribe bottom flux
                ! 3  Calculate bottom flux from hydraulic head of deep aquifer
                ! 4  Calculate bottom flux as function of groundwater level
                ! 5  Prescribe soil water pressure head of bottom compartment
                ! 6  Bottom flux equals zero
                ! 7  Free drainage of soil profile
                ! 8  Free outflow at soil-air interface

 SWBOTB = 6   ! Switch for bottom boundary [1..8,-,I]

* Options 6,7 and 8 require no additional bottom input data
**********************************************************************************


**********************************************************************************
* SWBOTB = 1  Prescribe groundwater level

* specify DATE [dd-mmm-yyyy] and groundwater level [cm, -10000..1000, R]

        DATE1    GWLEVEL           ! (max. MABBC records)
  01-jan-1981    -95.0
  31-dec-1983    -95.0
* End of table
**********************************************************************************


**********************************************************************************
* SWBOTB = 2   Prescribe bottom flux

* Specify whether a sine or a table are used to prescribe the bottom flux:
  SW2   = 2     ! 1 = sine function; 2 = table

* In case of sine function (SW2 = 1), specify:
  SINAVE = 0.1   ! Average value of bottom flux, [-10..10 cm/d, R, + = upwards]
  SINAMP = 0.05  ! Amplitude of bottom flux sine function, [-10..10 cm/d, R]
  SINMAX = 91.0  ! Time of the year with maximum bottom flux, [1..366 d, R]

* In case of table (SW2 = 2), specify date [dd-mmm-yyyy] and bottom flux QBOT2
* [-100..100 cm/d, R, positive = upwards]:
        DATE2    QBOT2             ! (maximum MABBC records)
  01-jan-1980      0.1
  30-jun-1980      0.2
  23-dec-1980      0.15
* End of table
**********************************************************************************


**********************************************************************************
* SWBOTB = 3  Calculate bottom flux by using a Cauchy-relation from hydraulic head in deep aquifer

* Switch for implicit treatment of pressure head in lowest compartment while applying a Cauchy
* boundary condition: 0 = explicit, 1 = implicit
  SWBOTB3IMPL = 0           ! Switch for implicit/explicit [0,1, - , I]

* Specify:
  SHAPE  =   0.79 ! Shape factor to derive average groundwater level, [0.0..1.0 -, R]
  HDRAIN = -110.0 ! Mean drain base to correct for average groundwater level, [-10000..0 cm, R]
  RIMLAY =  500.0 ! Vertical resistance of aquitard, [0..10000 d, R]

* Specify prescribe hydraulic head of the deep aquifer by either a sine function or as a
* tabulated time series:
  SW3   = 1        ! 1 = sine function;  2 = table

* In case of sine function (SW3  = 1), specify:
  AQAVE  = -140.0 ! Average hydraulic head in underlaying aquifer, [-10000..1000 cm, R]
  AQAMP  =   20.0 ! Amplitude hydraulic head sinus wave, [0..1000 cm, R]
  AQTMAX =  120.0 ! First time of the year with maximum hydraulic head, [1..366 d, R]
  AQPER  =  365.0 ! Period hydraulic head sinus wave, [1..366 d, I]
```

```
* In case of table (SW3  = 2), specify date [dd-mmm-yyyy] and average hydraulic head
* HAQUIF in underlaying aquifer [-10000..1000 cm, R]:

        DATE3   HAQUIF              ! (maximum MABBC records)
  01-jan-1980     -95.0
  30-jun-1980    -110.0
  23-dec-1980     -70.0
* End of table

* Specify an additional bottom flux to be added to the Cauchy relation by a tabulated time series:
* (this option is only meant to facilitate the coupling of the SWAP model to a regional
* groundwater model)
  SW4   = 0          ! 0 = no extra flux; 1 = include extra flux

* If SW4 = 1, specify date [dd-mmm-yyyy] and bottom flux QBOT4 [-100..100 cm/d, R,
* positive = upwards]:

        DATE4    QBOT4              ! (maximum MABBC records)
  01-jan-1980      1.0
  30-jun-1980     -0.15
  23-dec-1980      1.2
* End of table
********************************************************************************


********************************************************************************
* SWBOTB = 4       Calculate bottom flux as function of groundwater level

* Specify whether an exponential relation or a table is used to calculate the bottom flux
* from the groundwater level:
  SWQHBOT = 2        ! 1 = exponential relation;  2 = table

* In case of an exponential relation (SWQHBOT  = 1),
* specify coefficients of relation qbot = A exp (B*abs(groundwater level))
  COFQHA =  0.1  ! Coefficient A, [-100..100 cm/d, R]
  COFQHB =  0.5  ! Coefficient B  [-1..1 /cm, R]

* In case of a table (SWQHBOT  = 2),
* specify groundwaterlevel Htab [-10000..1000, cm, R]  and bottom flux QTAB [-100..100 cm/d, R]
* Htab is negative below the soil surface, Qtab is negative when flux is downward.
  HTAB   QTAB
  -0.1   -0.35
  -70.0  -0.05
 -125.0  -0.01
********************************************************************************


********************************************************************************
* SWBOTB = 5       Prescribe soil water pressure head of bottom compartment

* Specify DATE [dd-mmm-yyyy] and bottom compartment pressure head HBOT5 [-1.d10..1000 cm, R]:

        DATE5    HBOT5              ! (maximum MABBC records)
  01-jan-1980     -95.0
  30-jun-1980    -110.0
  23-dec-1980     -70.0
* End of table
********************************************************************************
```

3 Evapotranspiration and rainfall interception

3.1 Introduction

In contrast to rainfall, measurement of reliable evapotranspiration fluxes is far from trivial and strongly varies with the local hydrological conditions. Therefore SWAP simulates evapotranspiration fluxes from basic weather data or reference crop evapotranspiration data, as discussed in this chapter.

Rainfall and irrigation minus the sum of transpiration, evaporation and interception determine the amount of infiltration in the soil (Fig. 3.1) and groundwater fluxes. In general the sums of rainfall+irrigation and transpiration+evaporation+interception are large compared to their difference, which equals the infiltration. This means that relative errors in these sums will magnify in relative errors in the infiltration and groundwater fluxes. Therefore, reliable soil water and groundwater fluxes require accurate simulation of evapotranspiration and interception fluxes.
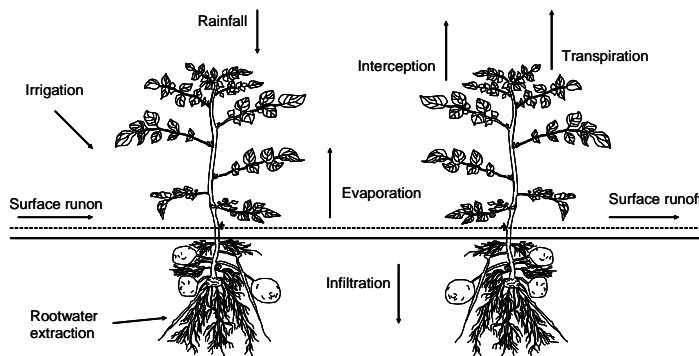
Figure 3.1 Water fluxes near the soil surface.

In general the daily water fluxes passing through a canopy are large compared to the amounts of water stored in the canopy itself. Therefore we will assume that root water extraction in the soil is equal to plant transpi-ration. While root water extraction may occur throughout the root zone, soil evaporation occurs at the interface soil-atmosphere. The consequence is that during drying conditions, evaporation fluxes decline much more rapidly than transpiration fluxes. Water harvesting, by leaving fields fallow during one or several seasons, uses this phenomenon. Because of the different physical behaviour of transpiration and evaporation, SWAP will consider evaporation and transpiration separately.

In this chapter we will first discuss the rainfall interception as used for low vegetation and forests. Next we discuss the simulation of potential evapotranspiration and its distribution into potential transpiration and evaporation for partly covered soils. Then we will discuss the reduction of transpiration for wet, dry and saline soil conditions, and the reduction of evaporation for dry top soils. In the last part the related model input is described.

3.2 Rainfall interception

Two methods are available in SWAP to simulate rainfall interception, one for agricultural crops and one for trees and forests.

3.2.1 Agricultural crops

For agricultural crops and for grassland, SWAP computes the interception following Von Hoyningen-Hüne (1983) and Braden (1985). They proposed the following general formula for canopy interception (Fig. 3.2):

$$P_i = a \cdot LAI \left(1 - \frac{1}{1 + \dfrac{b \cdot P_{gross}}{a \cdot LAI}} \right) \qquad (2.52)$$

where P_i is intercepted precipitation (cm d^{-1}), LAI is leaf area index, P_{gross} is gross precipitation (cm d^{-1}), a is an empirical coefficient (cm d^{-1}) and b represents the soil cover fraction (-). For increasing amounts of precipitation, the amount of intercepted precipitation asymptotically reaches the saturation amount $aLAI$. In principle a must be determined experimentally and should be specified in the input file. In case of ordinary agricultural crops we may assume $a = 0.025$ cm d^{-1}. The coefficient b denotes the soil cover fraction and is estimated by SWAP as $b = LAI / 3$.

In case irrigation water is applied with sprinklers, SWAP will simulate separately interception of rainfall and irrigation. This is required because the solute concentration of both water sources may be different. Observed rainfall P_{gross} minus intercepted rainfall P_i is called net rainfall P_{net}. Likewise, applied irrigation depth I_{gross} minus intercepted irrigation water is called net irrigation depth I_{net}.

The method of Von Hoyningen-Hüne and Braden is based on daily precipitation values. Although rainfall may be specified in smaller time steps, the interception will be based on daily amounts.

3.2.2 Forests

An important drawback of the method of Von Hoyningen-Hüne and Braden is that the effect of rain duration and evaporation during the rain event is not accounted for. In case of interception by trees and forests the effect of evaporation during rainfall can not be neglected. Gash (1979, 1985) formulated a physically based and widely used interception formula for forests. He considered rainfall to occur as a series of discrete events, each comprising a period of wetting up, a period of saturation and a period of drying out after the rainfall. The canopy is assumed to have sufficient time
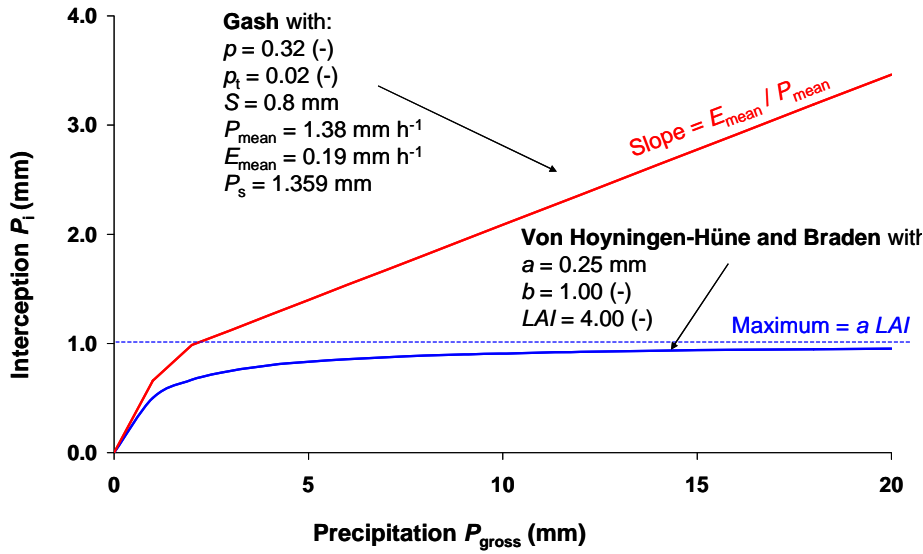
Figure 3.2 Interception for agricultural crops (Von Hoyningen-Hüne, 1983; Braden, 1985) and forests (Gash, 1979; 1985).

to dry out between storms. During wetting up, the increase of intercepted amount is described by:

$$\frac{\partial P_i}{\partial t} = \left(1 - p - p_t\right)P_{mean} - \frac{P_i}{S}E_{mean} \tag{2.53}$$

where p is a free throughfall coefficient (-), p_t is the proportion of rainfall diverted to stemflow (-), P_{mean} is the mean rainfall rate (mm h^{-1}), E_{mean} is the mean evaporation rate of intercepted water when the canopy is saturated (mm h^{-1}) and S is the maximum storage of intercepted water in the canopy (mm). Integration of Eq. [3.2] yields the amount of rainfall which saturates the canopy, P_s (mm):

$$P_s = -\frac{P_{mean}S}{E_{mean}}\ln\left(1 - \frac{E_{mean}}{P_{mean}\left(1 - p - p_t\right)}\right) \quad \text{with} \quad 1 - \frac{E_{mean}}{P_{mean}\left(1 - p - p_t\right)} \geq 0 \tag{2.54}$$

For small storms ($P_{gross} < P_s$) the interception can be calculated from:

$$P_i = \left(1 - p - p_t\right)P_{gross} \tag{2.55}$$

For large storms ($P_{gross} > P_s$) the interception according to Gash (1979) follows from:

$$P_i = \left(1 - p - p_t\right)P_s + \frac{E_{mean}}{P_{mean}}\left(P_{gross} - P_s\right) \tag{2.56}$$

Figure 3.2 shows the relation of Gash for typical values of a pine forest as function of rainfall amounts. The slope $\partial P_i / \partial P_{gross}$ before saturation of the canopy equals $\left(1 - p - p_t\right)$, after saturation of the canopy this slope equals E_{mean} / P_{mean}.

SWAP uses mean intensities of rainfall and evaporation rate to calculate the amount of rainfall which saturates the canopy, according to Eq. [3.3]. Next, depending on the total amount of rainfall during a day, the amount of interception is calculated according to either Eq. [3.4] or Eq. [3.5].

3.3 Potential evapotranspiration of uniform surfaces

Evapotranspiration refers to both *transpiration* of the plants and *evaporation* from the soil or of water intercepted by vegetation or ponding on the soil surface. The addition 'potential' refers to non-limiting water supply from the soil. The potential evapotranspiration flux is therefore only determined by atmospheric conditions and plant characteristics. In SWAP we assume the atmospheric conditions to be external conditions, which are representative for the area for which the simulations are performed.

Starting point in the calculations is the determination of the potential evapotranspiration of different uniform surfaces. The model offers two methods to calculate this potential evapotranspiration (see Fig. 3.3): the Penman Monteith method and the reference evapotranspiration method. The last method may be combined with the use of crop factors.
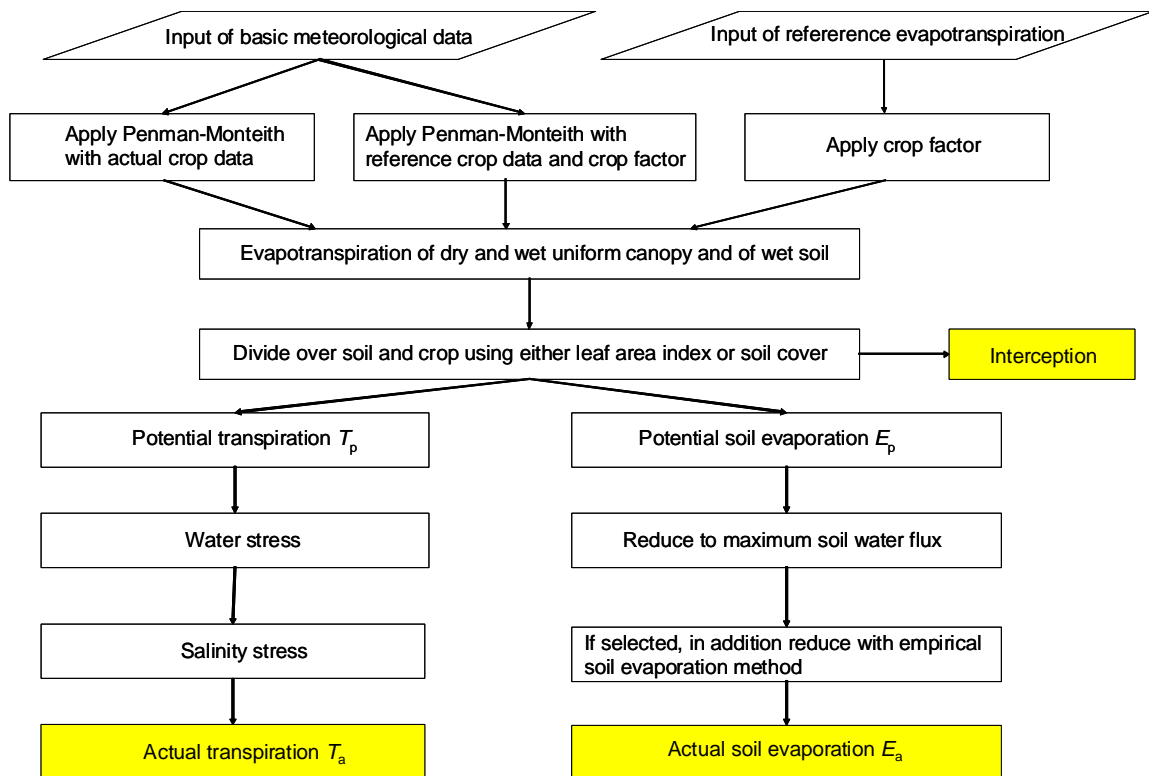
Figure 3.3 Method used in SWAP to derive actual transpiration and soil evaporation of partly covered soils from basic input data.

3.3.1 Penman Monteith method

Using similar physics as Penman (1948), Monteith (1965) derived an equation that describes the evapotranspiration from a dry, extensive, horizontally-uniform vegetated surface, which is optimally supplied with water. This equation is known as the Penman-Monteith equation. Jensen et al. (1990) analyzed the performance of 20 different evapotranspiration formula against lysimeter data for 11 stations around the world under different climatic conditions. The Penman-Monteith formula ranked as the best for all climatic conditions. Therefore this equation has become an international standard for calculation of potential evapotranspiration (Allen et al., 1998), and is applied by SWAP.

For a closed canopy with insignificant evaporation from the soil the Penman-Monteith equation can be written as (Monteith, 1965, 1981):

$$ET_p = \frac{\dfrac{\Delta_v}{\lambda_w}(R_n - G) + \dfrac{p_1 \rho_{air} C_{air}}{\lambda_w} \dfrac{e_{sat} - e_a}{r_{air}}}{\Delta_v + \gamma_{air}\left(1 + \dfrac{r_{crop}}{r_{air}}\right)} \qquad (2.57)$$

where ET is the transpiration rate of the canopy (mm d^{-1}), Δ_v is the slope of the vapour pressure curve (kPa °C^{-1}), λ_w is the latent heat of vaporization (J kg^{-1}), R_n is the net radiation flux at the canopy surface (J m^{-2} d^{-1}), G is the soil heat flux (J m^{-2} d^{-1}), p_1 accounts for unit conversion (=86400 s d^{-1}), ρ_{air} is the air density (kg m^{-3}), C_{air} is the heat capacity of moist air (J kg^{-1} °C^{-1}), e_{sat} is the saturation vapour pressure (kPa), e_a is the actual vapour pressure (kPa), γ_{air} is the psychrometric constant (kPa °C^{-1}), r_{crop} is the crop resistance (s m^{-1}) and r_{air} is the aerodynamic resistance (s m^{-1}).

The FAO has proposed a clearly defined and well established methodology to apply the Penman-Monteith equation for evapotranspiration estimates at a daily time scale using routinely measured weather data (Allen et al., 1998). The required weather data include daily values of air temperature (preferably the minimum as well as the maximum value), global radiation, wind speed and relative humidity. The FAO methodology is applied in SWAP and the basic equations are listed in 0.

In general the parameter r_{crop} is used to calculate ET_p from a mixture of vegetation and bare soil, in which case this parameter is called the surface resistance r_s. In SWAP we will always apply the Penman-Monteith method to either vegetations fully covering the soil or bare soils. Therefore we replace r_s by r_{crop} (at bare soils r_{crop} is absent and equals zero). SWAP calculates three quantities for three uniform surfaces:

- ET_{w0} (cm d^{-1}), evapotranspiration rate from a wet canopy, completely covering the soil;
- ET_{p0} (cm d^{-1}), evapotranspiration rate from a dry canopy, completely covering the soil;
- E_{p0} (cm d^{-1}), evaporation rate from a wet, bare soil.

These ET-quantities are obtained by varying the values for crop resistance (r_{crop}), crop height (h_{crop}) and reflection coefficient (α_r) for the three uniform surfaces as listed in Table 3.1. For a dry crop completely covering the soil with optimal water supply in the soil r_{crop} is minimal and varies between 30 s m^{-1} for arable crop to 150 s m^{-1} for trees in a forest (Allen et al., 1986, 1989). This value is input, as is the crop height. For a wet, bare soil SWAP will assume $r_{crop} = 0$ and 'crop height' $h_{crop} = 0.1$ cm.

As Fig. 3.3 shows, the Penman-Monteith method can be applied for the reference grass, in combination with crop factors. This method has been extensively discussed by Allen et al., (1998). In that case SWAP will set $r_{crop} = 70$ s m^{-1}, $h_{crop} = 12$ cm and $\alpha_r = 0.23$, as generally defined for the reference grass. Table 3.2 shows how the crop factors relate ET_{w0} and ET_{p0} to the corresponding values for grass. The crop factors belong to a certain crop and depend on its development stage. In case of bare soils the 'crop factor' has just one value, and is called soil factor. The use of a soil factor is optional. Without soil factor SWAP will directly calculate E_{p0} with the Penman-Monteith method. With soil factor SWAP wil relate E_{p0} to the reference evapotranspiration rate calculated with Penman-Monteith for grass, $ET_{p0,grass}$ (see Table 3.2).

Table 3.1 Three uniform surfaces and its corresponding potential evapotranspiration ET_p : parameter settings for the method Penman-Monteith

Description of uniform surface	ET_p	r_{crop} (s m^{-1})	h_{crop} (cm)	α_r (-)
wet canopy, completely covering the soil	ET_{w0}	0.0	input	input
dry canopy completely covering the soil	ET_{p0}	input	input	input
wet, bare soil	E_{p0}	0.0	0.1	0.15

Table 3.2 Options in SWAP to derive potential evapotranspiration rates for uniform surfaces

Uniform surface		Input ET_{ref}	Input basic weather data, use PM	
			Reference grass	Actual crop
Wet canopy		$ET_{w0} = k_c\,ET_{ref}$	$ET_{w0} = k_c\,ET_{w0,grass}$	ET_{w0}
Dry canopy		$ET_{p0} = k_c\,ET_{ref}$	$ET_{p0} = k_c\,ET_{p0,grass}$	ET_{p0}
Bare soil	Use soil factor	$E_{p0} = k_{soil}\,ET_{ref}$	$E_{p0} = k_{soil}\,ET_{p0,grass}$	$E_{p0} = k_{soil}\,ET_{p0}$
	No soil factor	$E_{p0} = ET_{ref}$	E_{p0}	E_{p0}

3.3.2 Reference evapotranspiration and crop factors

Application of the Penman-Monteith equation requires daily values of air temperature, net radiation, wind speed and air humidity, which data might not be available. Also in some studies other methods than Penman-Monteith might be more appropriate. For instance in The Netherlands the Makkink equation is widely used (Makkink, 1957; Feddes, 1987). Therefore SWAP allows the use of a reference evapotranspiration rate ET_{ref} (cm d^{-1}), see Fig. 3.3. In that case the potential evapotranspiration rate for the dry canopy ET_{p0} is calculated by:

$$ET_{p0} = k_c\, ET_{ref} \qquad\qquad (2.58)$$

where k_c is the so called crop factor, which depends on the crop type and the method employed to obtain ET_{ref}. In a similar way the potential evapotranspiration rate for the wet canopy ET_{w0} is derived:

$$ET_{w0} = k_c\, ET_{ref} \qquad\qquad (2.59)$$

The evaporation rate of a wet, bare soil, can be derived with a soil factor k_{soil} :

$$E_{p0} = k_{soil}\, ET_{ref} \qquad\qquad (2.60)$$

Without soil factor, E_{p0} is set equal to ET_{ref}. Table 3.2 provides an overview of the SWAP options when ET_{ref} and crop factors are used.

The reference evapotranspiration rate can be determined in several ways, such as pan evaporation, the Penman open water evaporation (Penman, 1948), the FAO modified Penman equation (Doorenbos and Pruitt, 1977), the Penman-Monteith equation applied for a reference crop (Allen et al., 1998), Priestly-Taylor (1972), Makkink (Makkink, 1957; Feddes, 1987) or Hargreaves et al. (1985). In case of Priestly-Taylor and Makkink, only air temperature and solar radiation data are required. Hargreaves requires solely air temperature data.

In SWAP the crop factors are used to convert the evapotranspiration rate of a reference crop fully covering the soil to the potential evapotranspiration rate of the actual crop fully covering the soil (Fig. 3.3). This is different from programs like CROPWAT (Smith, 1992) and CRIWAR (Bos et al., 1996), which use crop factors that depend on the crop development stage and soil cover. Because the soil has generally a dry top layer, soil evaporation is usually below the potential evaporation rate. Hence, these crop factors semi-empirically combine the effect of an incomplete soil cover and reduced soil evaporation. Instead SWAP uses the crop factor to relate uniform, cropped surfaces. Therefore crop factors in SWAP can be larger than those in CROPWAT and CRIWAR.

3.4 Potential transpiration and evaporation fluxes of partly covered soils

Until now we considered fluxes of uniform surfaces: either a wet (ET_{w0}) or dry (ET_{p0}) canopy and a wet soil (E_{p0}). In order to partition these fluxes into potential transpiration rate and potential soil evaporation rate, SWAP uses either the leaf area index, LAI (m^2 m^{-2}) or the soil cover fraction, SC (-). This will be discussed in the next sections.

3.4.1 Use of leaf area index

The potential evaporation rate of a soil under a standing crop is derived from the Penman- Monteith equation by neglecting the aerodynamic term. The aerodynamic term will be small because the wind velocity near the soil surface is relatively small, which makes the aerodynamic resistance r_{air} very large (Ritchie, 1972). Thus, the only source for soil evaporation is net radiation that reaches the soil surface. Assuming that the net radiation inside the canopy decreases according to an exponential function, and that the soil heat flux can be neglected, we can derive (Goudriaan, 1977; Belmans, 1983):

$$E_p = E_{p0}\, e^{-\kappa_{gr}\, LAI} \tag{2.61}$$

where κ_{gr} (-) is the extinction coefficient for solar radiation. Ritchie (1972) and Feddes (1978) used $\kappa_{gr} = 0.39$ for common crops. More recent approaches estimate κ_{gr} as the product of the extinction coefficient for diffuse visible light, κ_{df} (-), which varies with crop type from 0.4 to 1.1, and the extinction coefficient for direct visible light, κ_{dir} (-):

$$\kappa_{gr} = \kappa_{df}\, \kappa_{dir} \tag{2.62}$$

SWAP assumes that the evaporation rate of the water intercepted by the vegetation is equal to ET_{w0}, independent of the soil cover fraction. Then the fraction of the day that the crop is wet, W_{frac} (-), follows from the ratio of the daily amount of intercepted precipitation P_i (Section. 3.2) and ET_{w0}:

$$W_{frac} = \frac{P_i}{ET_{w0}} \qquad \text{with} \qquad W_{frac} \leq 1.0 \tag{2.63}$$

During evaporation of intercepted water, the transpiration rate is assumed to be negligible. After the canopy has become dry, the transpiration starts again at a rate of ET_{p0}. SWAP calculates a daily average of the potential transpiration rate, T_p (cm d^{-1}), taking into account the fraction of the day W_{frac} during which the intercepted water evaporates as well as the potential soil evaporation rate E_p:

$$T_p = \left(1.0 - W_{frac}\right) ET_{p0} - E_p \qquad \text{with} \qquad T_p \geq 0 \tag{2.64}$$

3.4.2 Use of soil cover fraction

Not always the LAI as function of crop development is available. In that case SWAP allows to use soil cover fraction. Taking into account the fraction of the day that the crop is wet (Eq. (2.63)), the potential soil transpiration rate T_p follows in that case from:

$$T_p = \left(1.0 - W_{frac}\right) SC \; ET_{p0} \tag{2.65}$$

The potential soil evaporation rate is calculated as:

$$E_p = \left(1.0 - SC\right)\left(1 - W_{frac}\right) E_{p0} \tag{2.66}$$

3.5 Actual plant transpiration

Potential and even actual evapotranspiration estimates are possible with the Penman-Monteith equation, through the introduction of canopy and air resistances to water vapour diffusion. This direct, or one-step, approach requires canopy and air resistances, which are not yet available for many crops. Therefore, at present SWAP follows a two-step approach. The first step is calculation of potential evapotranspiration, using the minimum value of the canopy resistance and the actual air resistance, as shown in Section 3.3. In the second step actual evapotranspiration is calculated taking into account reduction of root water uptake due to water and/or salinity stress (this section) and reduction of soil evaporation due to drying of the top soil (next section), see Fig. 3.3.

The maximum possible root water extraction rate, integrated over the rooting depth, is equal to T_p (cm d^{-1}), which is governed by atmospheric conditions and plant characteristics. Taking into account the root length density distribution (Bouten, 1992), the potential root water extraction rate at a certain depth, $S_p(z)$ (d^{-1}) is calculated by:

$$S_p(z) = \frac{\ell_{root}(z)}{\int_{-D_{root}}^{0} \ell_{root}(z)\,dz} T_p \tag{2.67}$$

where D_{root} is the root layer thickness (cm).
Stresses due to dry or wet conditions and/or high salinity concentrations may reduce $S_p(z)$. The water stress in SWAP is described by the function proposed by Feddes et al. (1978), which is depicted in Fig. 3.4. In the range $h_3 < h < h_2$ root water uptake is optimal. Below h_3 root water uptake linearly declines due to drought until zero at h_4 (wilting point). Above h_2 root water uptake linearly declines due to insufficient aeration until zero at h_1. The critical pressure head h_3 increases for higher potential transpiration rates T_p.
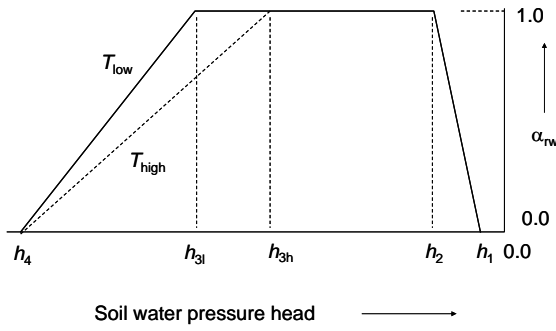
Figure 3.4 Reduction coefficient for root water uptake, α_{rw}, as function of soil water pressure head h and potential transpiration rate T_p (after Feddes et al., 1978).
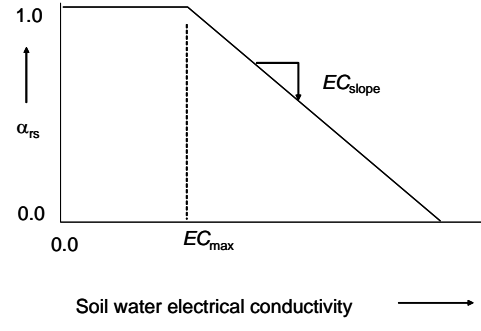
Figure 3.5 Reduction coefficient for root water uptake, α_{rs}, as function of soil water electrical conductivity EC (after Maas and Hoffman, 1977).

SWAP uses the response function of Maas and Hoffman (1977) for salinity stress (Fig. 3.5). Below salinity concentrations of EC_{max} (dS/m) no salinity stress is assumed. At salinity levels above EC_{max} the root water uptake declines at a rate of EC_{slope} (m/dS).

In case of both water and salt stress, Skaggs et al. (2006) argue that we may multiply the stress factors for water and salt stress. In SWAP we follow this multiplication approach and calculate the actual root water flux, $S_a(z)$ (d^{-1}), by:

$$S_a(z) = \alpha_{rd}\alpha_{rw}\alpha_{rs}\alpha_{rf}\, S_p(z) \qquad (2.68)$$

where α_{rd} (-), α_{rw} (-), α_{rs} (-) and α_{rf} (-) are the reduction factors due to wet conditions ($h>h_2$) , drought stress ($h<h_3$), salinity stress and frozen soil conditions (Par. 10.2).

Integration of $S_a(z)$ over the root layer yields the actual transpiration rate T_a (cm d^{-1}):

$$T_a = \int_{-D_{root}}^{0} S_a(z)\partial z \qquad (2.69)$$

Splitting up the total transpiration reduction into individual contributions is performed by multiplying $(S_p(z)-S_a(z))$ by the proportion of the logarithmic value of each of the reduction factors ($\log(\alpha_j)\Big/\sum_{i=1}\log(\alpha_i)$).

3.6   Actual soil evaporation

At a wet soil, soil evaporation equals its potential rate E_p. This is also the case at ponded conditions, during which SWAP will increase E_p to the evaporation rate of intercepted water. When the soil becomes drier, the soil hydraulic conductivity decreases, which may reduce E_p to evaporation rate, E_a (cm d^{-1}). In SWAP the maximum evaporation rate that the top soil can sustain, E_{max} (cm d^{-1}), is calculated according to Darcy's law:

$$E_{\max} = K_{\frac{1}{2}} \left(\frac{h_{\text{atm}} - h_1 - z_1}{z_1} \right) \qquad (2.70)$$

where $K_{\frac{1}{2}}$ is the average hydraulic conductivity (cm d^{-1}) between the soil surface and the first node, h_{atm} is the soil water pressure head (cm) in equilibrium with the air relative humidity, h_1 is the soil water pressure head (cm) of the first node, and z_1 is the soil depth (cm) at the first node. Equation (2.70) excludes water flow due to thermal differences in the top soil and due to vapour flow, as on daily basis the concerned flow amounts are probably negligible compared to isothermal, liquid water flow (Koorevaar et al., 1983; Ten Berge, 1986; Jury et al., 1991). Note that the value of $E_{\max}$ in Eq. (2.70) depends on the thickness of the top soil compartments. Increase of compartment thickness, generally results in smaller values for $E_{\max}$ due to smaller hydraulic head gradients. For accurate simulations at extreme hydrological conditions, the thickness of the top compartments should not be more than 1 cm (see Chapter 2).

There is one serious limitation of the $E_{\max}$ procedure as described above. $E_{\max}$ is governed by the soil hydraulic functions $\theta(h)$ and $K(\theta)$. It is still not clear to which extent the soil hydraulic functions, that usually represent a top layer of a few decimeters, are valid for the top few centimeters of a soil, which are subject to splashing rain, dry crust formation, root extension and various cultivation practices. Therefore also empirical evaporation functions may be used, which require calibration of their parameters for the local climate, soil, cultivation and drainage situation. SWAP has the option to choose the empirical evaporation functions of Black (1969) or Boesten and Stroosnijder (1986).

Reduction of soil evaporation according to Black
Black (1969) calculated the cumulative actual evaporation during a drying cycle, ΣE_a (cm) as:

$$\sum E_a = \beta_1 t_{\text{dry}}^{\frac{1}{2}} \qquad (2.71)$$

where β_1 is a soil specific parameter (cm d$^{-0.5}$), characterizing the evaporation process and t_{dry} is the time (d) after a significant amount of rainfall, $P_{\min}$. SWAP resets t_{dry} to zero if the net precipitation P_{net} exceeds $P_{\min}$.

Reduction of soil evaporation according to Boesten/Stroosnijder
In order to take account for the dependence of the Black-parameter β_1 on E_p, Boesten and Stroosnijder (1986) proposed to use the sum of potential evaporation, ΣE_p (cm), as time variable:

$$\sum E_{\mathrm{a}} = \sum E_{\mathrm{p}} \qquad \text{for} \qquad \sum E_{\mathrm{p}} \le \beta_2^2$$
$$\sum E_{\mathrm{a}} = \beta_2 \left(\sum E_{\mathrm{p}} \right)^{\frac{1}{2}} \qquad \text{for} \qquad \sum E_{\mathrm{p}} > \beta_2^2 \qquad \qquad (2.72)$$

where β_2 is a soil parameter (cm$^{\frac{1}{2}}$), which should be determined experimentally. The parameter β_2 determines the length of the potential evaporation period, as well as the slope of the ΣE_{a} versus $(\Sigma E_{\mathrm{p}})^{\frac{1}{2}}$ relationship in the soil limiting stage.

Boesten and Stroosnijder suggest the following procedure with respect to updates of ΣE_{p}. On days with no excess in rainfall ($P_{\mathrm{net}} < E_{\mathrm{p}}$), ΣE_{p} follows from Eq. (2.72), that is:

$$\left(\sum E_{\mathrm{p}} \right)^{j} = \left(\sum E_{\mathrm{p}} \right)^{j-1} + \left(E_{\mathrm{p}} - P_{\mathrm{net}} \right)^{j} \qquad \qquad (2.73)$$

in which superscript j is the day number. $(\Sigma E_{\mathrm{a}})^{j}$ is calculated from $(\Sigma E_{\mathrm{p}})^{j}$ with Eq. (2.72) and E_{a} is calculated with

$$E_{\mathrm{a}}^{j} = P_{\mathrm{net}}^{j} + \left(\sum E_{\mathrm{a}} \right)^{j} - \left(\sum E_{\mathrm{a}} \right)^{j-1} \qquad \qquad (2.74)$$

On days of excess in rainfall ($P_{\mathrm{net}} > E_{\mathrm{p}}$)

$$E_{\mathrm{a}}^{j} = E_{\mathrm{p}}^{j} \qquad \qquad (2.75)$$

and the excess rainfall is subtracted from ΣE_{a}

$$\left(\sum E_{\mathrm{a}} \right)^{j} = \left(\sum E_{\mathrm{a}} \right)^{j-1} - \left(P_{\mathrm{net}} - E_{\mathrm{p}} \right)^{j} \qquad \qquad (2.76)$$

Next $(\Sigma E_{\mathrm{p}})^{j}$ is calculated from $(\Sigma E_{\mathrm{a}})^{j}$ with Eq. (2.72). If the daily rainfall excess is larger than $(\Sigma E_{\mathrm{p}})^{j-1}$, then both $(\Sigma E_{\mathrm{a}})^{j}$ and $(\Sigma E_{\mathrm{p}})^{j}$ are set to zero.

SWAP will determine E_{a} by taking the minimum value of E_{p}, E_{max} and, if selected by the user, one of the empirical functions.

3.7   User instructions

3.7.1   General information

Box 3.1 lists the general input data with respect to evapotranspiration. The name of the meteorological files is generic, and the extension denotes the year. A main choice is whether pre-calculated ET_{ref} are used (SWETR = 1) or basic data on solar radiation, air temperature, air humidity and wind speed. These basic weather data may be specified daily or with shorter, constant time intervals (SWMETDETAIL = 1). In case of daily meteorological weather records, SWAP may distribute the evapotranspiration fluxes uniform over the day (default) or sinusoïdal during daylight

(SWETSINE = 1). As listed in Box 3.1, the rainfall input may range from daily amounts to short time rainfall amounts.

```
Box 3.1 General information on meteorological input in main file *.SWP.

*** METEOROLOGY SECTION ***

**********************************************************************************
* General data

  METFIL = 'Wageningen' ! File name of meteorological data without extension .YYY, [A16]
                        ! Extension equals last 3 digits of year number, e.g. 2003 has extension .003
  SWETR  =  0           ! Switch, use reference ET values of meteo file [Y=1, N=0]

* If SWETR = 0, then LAT,ALT and ALTW must have realistic values
  LAT    =   52.0       ! Latitude of meteo station, [-60..60 degrees, R, North = +]
  ALT    =   10.0       ! Altitude of meteo station, [-400..3000 m, R]
  ALTW   =    2.0       ! Altitude of wind speed measurement [0..99 m, R]
*
* Use of detailed meteorological records (shorter time interval than one day)
  SWMETDETAIL = 0       ! Switch, use detailed meteorological records of both ET and rainfall [Y=1, N=0]
*
* In case of detailed meteorological weather records (SWMETDETAIL = 1):
  NMETDETAIL = 10       ! Number of weather data records per day, [1..96 -, I]
*
* In case of daily meteorological weather records (SWMETDETAIL = 0):
  SWETSINE = 0          ! Switch, distribute daily Tp and Ep according to sinus wave [Y=1, N=0]
*
  SWRAIN =  0           ! Switch for use of actual rainfall intensity:
                        ! SWRAIN = 0: Use daily rainfall amounts
                        ! SWRAIN = 1: Use daily rainfall amounts + mean intensity
                        ! SWRAIN = 2: Use daily rainfall amounts + duration
                        ! SWRAIN = 3: Use actual rainfall amounts and times, as supplied in separate file

* If SWRAIN = 1, then specify mean rainfall intensity RAINFLUX [0.d0..1000.d0 cm/d, R]
* as function of time TIME [0..366 d, R], maximum 30 records
   TIME    RAINFLUX
    1.0        2.0
  360.0        2.0
* End of table

* If SWRAIN = 3, then specify file name of file with detailed rainfall data
  RAINFIL = 'WagRain'   ! File name of detailed rainfall data without extension .YYY, [A16]
                        ! Extension equals last 3 digits of year number, e.g. 2003 has extension .003
```

For many applications daily input of solar radiation, air temperature, air humidity and wind speed is preferred. In that case SWAP applies the Penman-Monteith method to determine ET_p. If some of these data are missing or unreliable, alternative methods to determine ET_{ref} in combination with crop factors are advised.

Input of daily rainfall amounts will suffice for most applications. However when surface runoff is expected, daily rainfall amounts may underestimate the amount of surface runoff. In such situations real rainfall intensities should be used.

3.7.2 Weather data

In case of daily weather records, the data should be specified as listed in Box 3.2. Missing data are given the number -99.9. When SWAP should use Penman Monteith (SWETR = 0, Box 3.1), data on solar radiation, air temperature (min and max), air humidity and wind speed are required. When SWAP should simulate detailed crop

growth (Chapter 7), data on solar radiation and air temperature (min and max) are required. For rainfall, either daily amounts (SWRAIN = 0, Box 3.1) or daily amounts plus duration (SWRAIN = 0, Box 3.1) should be specified.

Box 3.2 Daily basic weather data.

```
********************************************************************************************************
* Filename: Wageningen.003
* Contents: Daily meteorological data of Wageningen weather station
********************************************************************************************************
* Comment area:
*
* Use of basic weather data for Penman-Monteith method. Including rainfall duration. Missing data -99.9
********************************************************************************************************
    Station        DD     MM     YYYY     RAD      Tmin    Tmax    HUM     WIND    RAIN    ETref    WET
*                  nr     nr      nr     kJ/m2      C       C      kPa     m/s     mm       mm       d
********************************************************************************************************
'Wageningen'        1      1     2003    2540.0    -1.2    1.4     0.62    3.5     6.2     -99.9   0.1550
'Wageningen'        2      1     2003    3520.0    -6.5    1.4     0.53    1.7     0.0     -99.9   0.0000
'Wageningen'        3      1     2003    1510.0    -8.2    0.1     0.49    2.2     0.2     -99.9   0.0050
'Wageningen'        4      1     2003     740.0    -0.3    3.5     0.66    4.5     7.0     -99.9   0.1750
'Wageningen'        5      1     2003     990.0     2.8    5.1     0.78    3.0     2.2     -99.9   0.0550
'Wageningen'        6      1     2003    1090.0     3.8    6.0     0.82    2.7     8.7     -99.9   0.2175
'Wageningen'        7      1     2003    1720.0     1.4    5.5     0.76    1.5     0.3     -99.9   0.0075
'Wageningen'        8      1     2003     500.0     0.2    3.5     0.66    2.5     0.0     -99.9   0.0000
'Wageningen'        9      1     2003    1500.0    -0.1    1.3     0.59    2.2     0.0     -99.9   0.0000
'Wageningen'       10      1     2003     660.0    -1.6    0.5     0.49    2.5     0.0     -99.9   0.0000
'Wageningen'       11      1     2003    1080.0    -5.9   -1.2     0.39    2.7     0.0     -99.9   0.0000
```

Alternatively weather records can be specified with short, constant time intervals (> 15 minutes) according to the format listed in Box 3.3. Radiation and rainfall denote cumulative amounts during the time interval. Air temperature, humidity and wind speed denote average values during the time interval.

A third combination is daily evapotranspiration data and detailed rainfall data. In this case evapotranspiration data are input according to Box 3.2, while the rainfall data are input according to Box 3.4. The rainfall data follow the format of a tipping bucket measurement device. The rainfall amount refers to the amount fallen in the previous period.

```
***************************************************************************
* Filename: Raindetail.003
* Contents: Detailed meteorological data of Wageningen weather station
***************************************************************************
* Comment area:
*
* Each day 10 weather records, as specified in general input file
***************************************************************************
   Date      Record     Rad      Temp      Hum     Wind     Rain
*              nr      kJ/m2      'C       kPa      m/s      mm
***************************************************************************
 01-may-2003    1       0.0      10.0      0.75     0.5      0.0
 01-may-2003    2       3.0      10.0      0.76     0.4      0.1
 01-may-2003    3    1347.0       9.0      0.76     0.6      1.2
 01-may-2003    4    3622.0       8.5      0.74     1.2      4.7
 01-may-2003    5    5029.0      10.5      0.78     2.4      0.0
 01-may-2003    6    5029.0      15.3      0.85     4.0      0.0
 01-may-2003    7    3622.0      14.0      0.84     3.5      0.0
 01-may-2003    8    1347.0      13.5      0.82     2.0      0.0
 01-may-2003    9       3.0      11.8      0.75     1.1      0.0
 01-may-2003   10       0.0      10.5      0.73     0.7      0.0
 02-may-2003    1       0.0       9.8      0.71     0.4      0.0
 02-may-2003    2       8.0       9.0      0.69     0.3      0.0
 02-may-2003    3    2046.0       8.5      0.68     0.5      0.0
 02-may-2003    4    5429.0      12.0      0.76     1.2      0.0
 02-may-2003    5    7520.0      14.5      0.82     2.5      0.0
```

Box 3.4 Detailed rainfall data.

```
*************************************************************
* Filename: Raindetail.003
* Contents: Detailed rainfall data of Wageningen weather station
*************************************************************
* Comment area:
*
* Amount refers to the rainfall amount in the previous period
* (like  a tipping bucket rainfall measurement device)
*************************************************************
  Station      Day  Month Year     Time    Amount
*               nr    nr    nr       d       mm
*************************************************************
 'Wageningen'    1    1   2003     0.00      0.0
 'Wageningen'    1    1   2003     0.43      2.0
 'Wageningen'    1    1   2003     0.50      4.2
 'Wageningen'    3    1   2003     0.35      0.0
 'Wageningen'    3    1   2003     0.37      0.2
 'Wageningen'    4    1   2003     0.10      1.2
 'Wageningen'    4    1   2003     0.15      2.0
 'Wageningen'    4    1   2003     0.18      0.3
 'Wageningen'    4    1   2003     0.26      3.4
```

3.7.3 Soil data

Box 3.5 lists the soil data which are required to determine the actual evaporation at the soil surface. The soil factor CFBS can be used to transform reference crop evapotranspiration into potential soil evaporation (see Section 3.3.2 and Table 3.2). When the Penman-Monteith equation is applied (SWETR = 0 in Box 3.1), SWAP will calculate directly potential soil evaporation by setting $r_{crop} = 0$, $h_{crop} = 0.1$ cm and $\alpha_r = 0.15$. In that case soil factor CFBS is not needed.

Three options are offered to reduce soil evaporation according to the maximum water flux which can be delivered by the soil. Applying straight soil physically theory, the first option would suffice. However, as discussed in section 3.6 this method in generally results in overestimation of the actual soil evaporation. Therefore we

recommend to use the combination of reduction to maximum Darcy flux and reduction with either the Black or Boesten/Stroosnijder method (SWREDU = 1 or 2). Default soil evaporation coefficient for Black equals 0.35 cm $d^{-0.5}$, and for Boesten/Stroosnijder 0.54 cm$^{-0.5}$.

```
Box 3.5 Soil data to derive actual soil evaporation in main file *.SWP

**********************************************************************************
* Part 3: Soil evaporation
*
  SWCFBS = 0   ! Switch for use of  a soil factor to derive soil evaporation [Y=1, N=0]
               ! 0 = CFBS is not used
               ! 1 = CFBS used to calculate potential evaporation from reference ET

* If SWCFBS = 1, specify soil factor CFBS:
  CFBS   = 1.0 ! Soil factor for potential soil evaporation, [0.5..1.5 -, R]

  SWREDU = 1   ! Switch, method for reduction of potential soil evaporation:
               ! 0 = reduction to maximum Darcy flux
               ! 1 = reduction to maximum Darcy flux and to maximum Black (1969)
               ! 2 = reduction to maximum Darcy flux and to maximum Bo/Str. (1986)

 COFRED = 0.35 ! Soil evaporation coefficient of Black, [0..1 cm/d1/2, R],
               ! or Boesten/Stroosnijder, [0..1 cm1/2, R]

 RSIGNI =  0.5 ! Minimum rainfall to reset method of Black [0..1 cm/d, R]
**********************************************************************************
```

4   Surface runoff, interflow and drainage

The interaction between soil water and surface water is of importance in lowland areas. Dependent on the specific setting in the landscape of the field studied, different types of pathways and interconnections may play a role.

Surface runoff that occurs when the rainfall rate exceeds the infiltration rate is called *Horton overland flow*. A second form of runoff occurs after the water storage volume of a soil has been exceeded, which means that the groundwater table has reached the soil surface. This runoff is commonly called the *Dunne overland flow*. It occurs in areas with a shallow groundwater table and light rainfall of long duration.

Interflow can be defined as the near-surface flow of water within the soil profile resulting in seepage to a stream channel within the time frame of a storm hydrograph. Interflow involves both unsaturated and saturated flows, the latter being in zones of limited vertical extent caused by soil horizons impeding vertical percolation. The mechanisms by which subsurface flow enters streams quickly enough to contribute to streamflow responses to individual rainstorms are summarized in various publications (Beven 1989).

Infiltration excess moves slowly downwards and once it has reached the saturated zone, it is called ground water. Ground water moves downward and laterally through the subsurface and eventually discharges through tile drains, field ditches or other open conduits. A tile drain is a perforated conduit, such as tile, pipe or tubing, installed below the ground surface to intercept and convey drainage water.

The SWAP model can take account for the different types of interconnections between soil moisture/groundwater and surface water by offering options for describing surface runoff as a non-linear function of water storage on the field, interflow as a non-linear function of the groundwater elevation when it has reached the near-surface zone and the discharge to a series of drainage systems. Options to simulate dynamically the levels in surface water systems provide the possibility to describe the feedback and the close interconnection between groundwater and surface water in stream valleys and polders.

4.1 Surface runoff

Surface runoff is one of the terms in the water balance of the ponding reservoir. The ponding reservoir stores a certain amount of excess water on top of the soil surface (Fig.4.1).
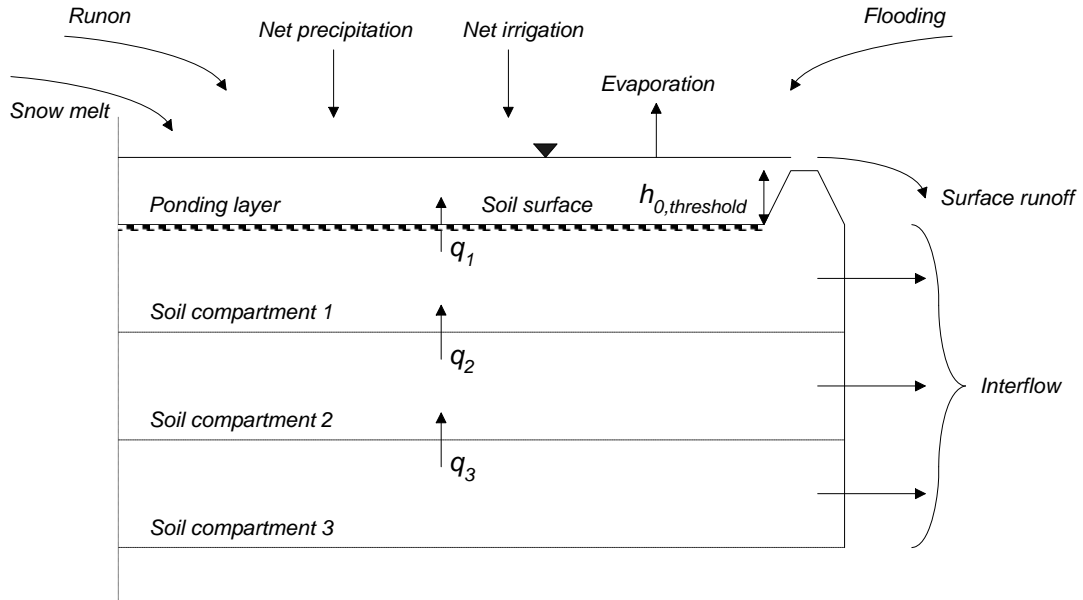
Figure 4.1 Schematic representation of the near surface flux to a surface water system and the water balance of the ponding layer.

The water balance of the ponding reservoir is governed by:

$$\frac{\Delta h_0}{\Delta t} = q_{\mathrm{prec}} + q_{\mathrm{irri}} + q_{\mathrm{melt}} + q_{\mathrm{runon}} + q_{\mathrm{inun}} + q_1 - q_{\mathrm{e,pond}} - q_{\mathrm{runoff}} - I_{ru} \qquad (4.1)$$

where Δh_0 is the storage change of the ponding reservoir (cm d^{-1}), q_{prec} is the precipitation flux subtracted with interception, (cm d^{-1}), q_{irri} is the irrigation flux subtracted with interception (cm d^{-1}), q_1 is the flux from the first model compartment to the ponding layer (cm d^{-1}), q_{melt} is snowmelt (cm d^{-1}), q_{runon} is the runon flux of water which enters the field from an upstream adjacent field (cm d^{-1}), q_{inun} is the inundation or flooding from surface water to the field (cm d^{-1}), q_{runoff} is surface runoff flux (cm d^{-1}) and $q_{e,pond}$ is the evaporation flux of the open water stored on the soil surface (cm d^{-1}) and I_{ru} is the runoff into the macropores (cm d^{-1}, see section 6.1.2)

Surface runoff occurs when the water storage in the ponding layer exceeds the critical depth of $h_{0,\mathrm{threshold}}$ (cm):

$$q_{\text{runoff}} = \frac{1}{\gamma} \left(\max(0, (h_0 - h_{0,\text{threshold}})) \right)^{\beta} \tag{4.2}$$

where h_0 is the ponding depth of water (cm) on the soil surface, γ is a resistance parameter (cm$^{\beta-1}$ d) and β is an exponent (-) in the empirical relation. Inundation of the field from an adjacent water course can be simulated when the surface water level exceeds both h_0 and $h_{0,\text{threshold}}$. This option is only available when the so-called extended drainage option is chosen (see Chapter 5).

4.2 Interflow

In some applications one may wish to describe an interflow system, which has a rapid discharge with short residence times of the water in the soil system. If the groundwater level is higher than the reference level $\varphi_{\text{drain,n}}$, the interflow flux is optionally calculated as:

$$q_{\text{drain,n}} = \frac{\varphi_{\text{gwl}} - \varphi_{\text{drain,n}}}{\max(\gamma_{\min}, 1 \cdot \varphi_{\text{gwl}} - \gamma_{\text{ref}})} \tag{4.3}$$

or as:

$$q_{\text{drain,n}} = A_{\text{interflow}} (\varphi_{\text{gwl}} - \varphi_{\text{drain,n}})^{B_{\text{interflow}}} \tag{4.4}$$

Where $q_{\text{drain,n}}$ is the interflow flux (cm d^{-1}), $\gamma_{\min}$ and γ_{ref} are the minimum and the reference resistance related to the interflow process, "1" is a factor that expresses the unit conversion and is equal to 1 (d cm^{-1}) in this case. $A_{\text{interflow}}$ is a conductance parameter (cm^{1-B} d^{-1}) and $B_{\text{interflow}}$ is an exponent (-) in the empirical relation. The subscript n points to the rule that in the SWAP model interflow is always assigned to the highest order of distinguished drainage systems.

4.3 Drain discharge

Although the entity for which the SWAP model operates is at field scale, the model is used both for field studies and for regional studies. The different spatial scales of operation are expressed among other things by the type of drainage relation and its associated parameters chosen. For the purpose of a drainage system at field scale, one may use one of the classical drainage equations, but for simulation of water discharge in the spatial entity of a sub-catchment, the use of a multiple drainage system formulation is more convenient. Table 4.1 provides a brief overview of the drainage options available in the SWAP model. Additionally, options are available to take account for the influence of surface water management strategies on soil water flow and drain discharge. The background and the implementation of this option is presented in Chapter 5.

Table 4.1 Options to simulate drain discharge at field scale and at regional scale

Scale of application	No of systems	Drainage flux relation	Drainage level
Field	Single drainage system	Hooghoudt or Ernst equation	Specified in model input
		Tabulated input	Implicitly included in tabulated input
Regional	Single drainage system	Tabulated input	Implicitly included in tabulated input
	Multiple drainage system	Drainage resistance per sub-system	Specified in model input per drainage system
		Drainage resistance per sub-system dependent on wetted perimeter of drains	Specified in model input per drainage system / Simulated (see Chapter 5)

The options provided by the SWAP model are limited to lowland conditions. Subsurface groundwater flow and drainage response of sloping fields can better be described by 2D or 3D models or Boussinesq-equation based models. Another limitation of the drainage equations involves the steady-state assumption. Hysteresis phenomena in the groundwater – discharge relation as they can be observed in experimental data are attributed to the different possible shapes of the groundwater elevation surface pertaining to one groundwater level value. Although there are possibilities to conceptualize the 2D groundwater depth discharge relation for nonsteady-state conditions (Kraijenhoff van de Leur, 1957, Wesseling and Wesseling, 1984), such relation is not implemented. These relations consider only one over-all value for the storage coefficient and neglect the influence of the pressure head variations in space and time on the storativity. If such phenomena are of interest for drainage flow simulations, the reader is referred to 2D and 3D models as MODFLOW-VSF (Thoms et al., 2006), SUTRA (Voss and Provost, 2002), FEMWATER (Lin et al., 1997), and HYDRUS (Šimůnek et al., 2007)

The drainage flux are incorporated in the numerical solution to the Richards' equations (see Chapter 2) by specifying it as a sink term. The drainage relations presented in Section 4.3 are conceptualizations of 2D and 3D saturated groundwater flow to surface water systems and are based on the head difference between groundwater elevation and drainage level. Assignment of drainage sink term values in the Richards' equation involves a conceptualization of the 2D and 3D flow field, which is briefly explained in chapter 4.4. Optionally, to provide possibilities to compare the SWAP model with other 1D soil moisture models as HYDRUS1D

(Šimůnek et al., 1998), the drain flux can be described as a vertical flow in the model, which leaves the flow domain at the bottom.

It should be noticed that the calculation of drainage resistance should be attuned to the definition of the groundwater elevation as one of the driving forces of groundwater discharge and to the lower boundary condition one wants to impose. The general formulation of the drainage equation:

$$q_{\text{drain}} = \frac{(\varphi_{\text{gwl}} \text{ or } \varphi_{\text{avg}}) - \varphi_{\text{drain}}}{\gamma_{\text{drain}}} \qquad (4.5)$$

where:

φ_{gwl} phreatic groundwater level midway between the drains or ditches (cm)

φ_{avg} averaged phreatic groundwater level midway between the drains or ditches (cm)

φ_{drain} drainage level (cm)

γ_{drain} drainage resistance (d)

Drainage relations are generally derived from the groundwater elevation as a function of distance. An example is given in Figure 4.2.
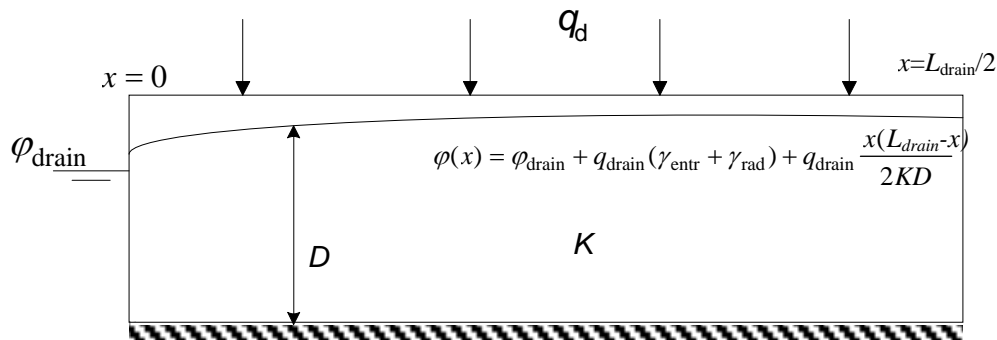
Figure 4.2 Groundwater elevation as a function of distance as the basis for drainage equations

For drainage design purposes, one may be interested in the maximum groundwater elevation (φ_{gwl}), but for the analysis of regional water management, the average groundwater elevation (φ_{avg}) is often a key variable to be studied. The different backgrounds reveals itself in the manner the drainage flux is calculated. For field applications, the relation between the drainage flux and the groundwater elevation can be expressed by the Ernst equation, modified with respect to the introduction of an additional entrance resistance :

$$\varphi_{\text{gwl}} = \varphi_{\text{drain}} + q_{\text{drain}} \left(\gamma_{\text{entr}} + \gamma_{\text{rad}} + \frac{L_{\text{drain}}^2}{8KD} \right) \quad \rightarrow \quad q_{\text{drain}} = \frac{\varphi_{\text{gwl}} - \varphi_{\text{drain}}}{\gamma_{\text{entr}} + \gamma_{\text{rad}} + \dfrac{L_{\text{drain}}^2}{8KD}} \tag{4.6}$$

and for regional applications:

$$\varphi_{\text{avg}} = \varphi_{\text{drain}} + q_{\text{drain}} \left(\gamma_{\text{entr}} + \gamma_{\text{rad}} + \frac{L_{\text{drain}}^2}{12KD} \right) \quad \rightarrow \quad q_{\text{drain}} = \frac{\varphi_{\text{avg}} - \varphi_{\text{drain}}}{\gamma_{\text{entr}} + \gamma_{\text{rad}} + \dfrac{L_{\text{drain}}^2}{12KD}} \tag{4.7}$$

By comparing Eq. [4.5] with Eq. [4.6] it can be seen that the two definitions of γ_{drain} in the equations differ by the so-called shape factor. The shape factor α is the ratio between the mean and the maximum groundwater level elevation above the drainage base.

$$\alpha = \frac{\varphi_{\text{avg}} - \varphi_{\text{drain}}}{\varphi_{\text{gwl}} - \varphi_{\text{drain}}} \tag{4.8}$$

The shape factor depends on the vertical, horizontal, radial and entrance resistances of the drainage system (Ernst, 1978). For regional situations, where the 'horizontal' resistance to flow plays an important role, the shape factor is relatively small (≈ 0.7). The smaller the horizontal resistance becomes, the more 'rectangular' shaped the water table: in the most extreme case with all the resistance concentrated in the direct vicinity of the channel, the water table is level, except for the abrupt decrease towards the drainage base. In that case the shape factor approaches to unity.
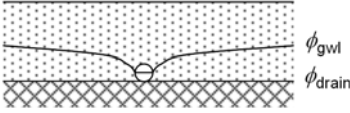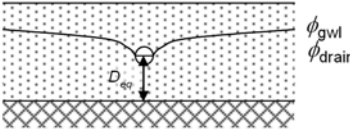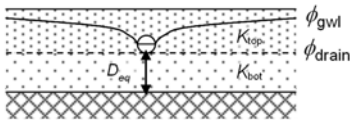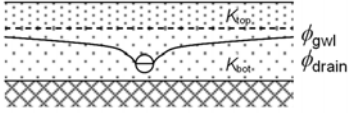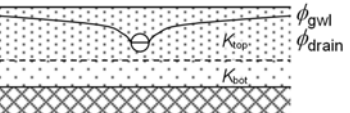
It should be noted that the parameters chosen to describe the relation between discharge and groundwater elevation should be attuned to the hydrological schematization. The combination of a Cauchy condition for the bottom boundary with a drainage relation for the lateral boundary may require an other formula (De Lange, 1999) than the one usually applied for drainage combined with a flux bottom boundary condition. Also the coupling of the SWAP model to a regional groundwater model by exchanging information concerning fluxes and hydraulic heads at the bottom of the schematization may require alternative formulations for the drainage equation to be used.

The influence of frost at a certain depth can optionally be accounted for by the reduction of prevailing drainage fluxes at that depth similar to the reduction of hydraulic conductivities (see Chapter 2).

4.3.1 Field scale drainage relation according to Hooghoudt and Ernst

The drainage equations of Hooghoudt and Ernst allow the evaluation of drainage design and are based on the drainage flux as a function the head difference the maximum groundwater elevation midway between the drains and the drainage level. Depending on position of the groundwater level, the drainage level and the possibility for water supply in the surface water system, the channels will act as either drainage or sub-irrigation media. The theory behind the field drainage equations used for drainage design purposes is summarized by Ritzema (1994). Five typical drainage situations are distinguished (Table 4.2). For each of these situations the drainage resistance γ_{drain} (d) can be defined.

Table 4.2 Five field drainage situations considered in SWAP (after Ritzema, 1994)

Case	Schematization	Soil profile	Drain position	Theory
1	ϕ_{gwl} ϕ_{drain}	Homogeneous	On top of impervious layer	Hooghoudt, Donnan
2	ϕ_{gwl} ϕ_{drain} D_{eq}	Homogeneous	Above impervious layer	Hooghoudt with equivalent depth
3	ϕ_{gwl} ϕ_{drain} K_{top} D_{eq} K_{bot}	Two layers	At interface of two soil layers	Hooghoudt
4	K_{top} ϕ_{gwl} ϕ_{drain} K_{bot}	Two layers ($K_{top} << K_{bot}$)	In bottom layer	Ernst
5	ϕ_{gwl} ϕ_{drain} K_{top} K_{bot}	Two layers ($K_{top} >> K_{bot}$)	In top layer	Ernst

Case 1: Homogeneous profile, drain on top of impervious layer

The drainage resistance is calculated as:

$$\gamma_{drain} = \frac{L_{drain}^2}{4K_{hprof}(\varphi_{gwl} - \varphi_{drain})} + \gamma_{entr} \qquad (4.9)$$

with K_{hprof} the horizontal saturated hydraulic conductivity above the drainage basis (cm d^{-1}), L_{drain} the drain spacing (cm) and γ_{entr} the entrance resistance into the drains and/or ditches (d). The value for γ_{entr} can be obtained, analogous to the resistance value of an aquitard, by dividing the 'thickness' of the channel walls with the permeability. If this permeability does not differ substantially from the conductivity in the surrounding subsoil, the numerical value of the entry resistance will become relatively minor.

Case 2: Homogeneous profile, drain above impervious layer

This drainage situation has been originally described by Hooghoudt (1940). An extension for the entrance resistance has been added later on. The drainage resistance follows from:

$$\gamma_{drain} = \frac{L_{drain}^2}{8 K_{hprof} D_{eq} + 4 K_{hprof} (\varphi_{gwl} - \varphi_{drain})} + \gamma_{entr} \qquad (4.10)$$

where D_{eq} is the equivalent depth (cm) that accounts for the extra head loss near the drains caused by converging flow lines (Hooghoudt, 1940). The numerical solution of Van der Molen and Wesseling (1991) is employed to obtain an estimate for D_{eq}. A characteristic dimensionless length scale x is used:

$$x = 2\pi \frac{\varphi_{drain} - z_{imp}}{L_{drain}} \qquad (4.11)$$

where z_{imp} is the level of the impervious layer. The equivalent depth D_{eq} is approximated for three ranges of x as:

If $x < 10^{-6}$:
$$D_{eq} = \varphi_{drain} - z_{imp} \qquad (4.12)$$

If $10^{-6} < x < 0.5$:
$$D_{eq} = \frac{L_{drain}}{\dfrac{8}{\pi} \ln\left(\dfrac{\varphi_{drain} - z_{imp}}{\pi\, r_{drain}}\right) + \dfrac{L_{drain}}{\varphi_{drain} - z_{imp}}} \qquad (4.13)$$

If $x > 0.5$:
$$D_{eq} = \frac{L_{drain}}{\dfrac{8}{\pi}\left(\ln\left(\dfrac{L_{drain}}{\pi\, r_{drain}}\right) + \sum_{k=1,3,5,\dots}^{\infty} \dfrac{4 e^{-2kx}}{k(1 - e^{-2kx})} \right)} \qquad (4.14)$$

Case 3: Heterogeneous soil profile, drain at interface between both soil layers

The drainage resistance follows from:

$$\gamma_{drain} = \frac{L_{drain}^2}{8 K_{hbot} D_{eq} + 4 K_{htop} (\varphi_{gwl} - \varphi_{drain})} + \gamma_{entr} \qquad (4.15)$$

with K_{htop} and K_{hbot} the horizontal saturated hydraulic conductivity (cm d^{-1}) of upper and lower soil layer, respectively. The equivalent depth D_{eq} is calculated using Eq. [4.11] to Eq. [4.13].

Case 4: Heterogeneous soil profile, drain in bottom layer

The drainage resistance is calculated according to Ernst (1956) with later extensions for the entrance resistance as:

$$\gamma_{drain} = \gamma_{ver} + \gamma_{hor} + \gamma_{rad} + \gamma_{entr} \tag{4.16}$$

where γ_{ver}, γ_{hor}, γ_{rad} and γ_{entr} are the vertical, horizontal, radial and entrance resistance (d^{-1}), respectively. The vertical resistance is calculated by:

$$\gamma_{ver} = \frac{\varphi_{gwl} - z_{int}}{K_{vtop}} + \frac{z_{int} - \varphi_{drain}}{K_{vbot}} \quad \textbf{Fout! Bladwijzer niet gedefinieerd.} \tag{4.17}$$

with z_{int} the level of the transition (cm) between the upper and lower soil layer, and K_{vtop} and K_{vbot} the vertical saturated hydraulic conductivity (cm d^{-1}) of the upper and lower soil layer, respectively. The horizontal resistance is calculated as:

$$\gamma_{hor} = \frac{L_{drain}^2}{8 K_{hbot} D_{bot}} \quad \textbf{Fout! Bladwijzer niet gedefinieerd.} \tag{4.18}$$

with D_{bot} the depth of the contributing layer below the drain level (cm), which is calculated as the minimum of (ϕ_{drain} - z_{imp}) and ¼ L_{drain}. The radial resistance is calculated using:

$$\gamma_{rad} = \frac{L_{drain}}{\pi \sqrt{K_{hbot} K_{vbot}}} \ln\left(\frac{D_{bot}}{u_{drain}}\right) \tag{4.19}$$

with u_{drain} the wet perimeter (cm) of the drain.

Case 5: Heterogeneous soil profile, drain in top layer

Again the approach of Ernst (1956),with later extensions for the entrance resistance, is applied. The resistances are calculated as:

$$\gamma_{ver} = \frac{\varphi_{gwl} - \varphi_{drain}}{K_{vtop}} \tag{4.20}$$

$$\gamma_{hor} = \frac{L_{drain}^2}{8 K_{htop} D_{top} + 8 K_{hbot} D_{bot}} \tag{4.21}$$

$$\gamma_{rad} = \frac{L_{drain}}{\pi \sqrt{K_{hbot} K_{vbot}}} \ln\left(g_{drain} \frac{\varphi_{drain} - z_{int}}{u_{drain}}\right) \tag{4.22}$$

with D_{top} equal to $(\varphi_{drain} - z_{int})$ and g_{drain} is the drain geometry factor, to be specified in the input. The value of g_{drain} in Eq.[4.21] depends on the ratio of the hydraulic conductivity of the bottom (K_{hbot}) and the top (K_{htot}) layer. Ernst (1962) distinguished the following situations:

$K_{hbot}/K_{htop} < 0.1$:   the bottom layer can be considered impervious and the case is reduced to a homogeneous soil profile and $g_{drain} = 1$

$0.1 < K_{hbot}/K_{htop} < 50$: g_{drain} depends on the ratios K_{hbot}/K_{htop} and D_{bot}/D_{top}, as given in *Table*

$K_{hbot}/K_{htop} > 50$ $g_{drain} = 4$

Table 4.3 The geometry factor g_{drain} (-), as obtained by the relaxation method (after Ernst, 1962).

K_{hbot}/K_{htop}	D_{bot}/D_{top}						
	1	2	4	8	16	32	1
1	2.0	3.0	5.0	9.0	15.0	30.0	2.0
2	2.4	3.2	4.6	6.2	8.0	10.0	2.4
3	2.6	3.3	4.5	5.5	6.8	8.0	2.6
5	2.8	3.5	4.4	4.8	5.6	6.2	2.8
10	3.2	3.6	4.2	4.5	4.8	5.0	3.2
20	3.6	3.7	4.0	4.2	4.4	4.6	3.6
50	3.8	4.0	4.0	4.0	4.2	4.6	3.8

4.3.2 Field scale drainage relation defined by a tabulated function

The SWAP model provides an option to specify a tabulated drainage flux relationship as a function of the groundwater level. When this option is chosen, one should specify a number of (φ_{gwl}, q_{drain}) data-pairs. For a linear relation only two data-pairs suffices, but a non-linear relation requires more data-pairs. A non-linear relation can be either the result of:
- describing the drainage flux by the Hooghoudt equation;
- an analysis of the flux relation in a stratified profile by means of a numerical model
- an analysis of measured field data.

The general shape of such a relation is given in Fig. 4.3. Specifying a non-linear relation by means of a tabulated function involves a linearization, since flux values are derived by linear interpolation. Specifying more data pairs can reduce the inaccuracy which results from this type of linearization.
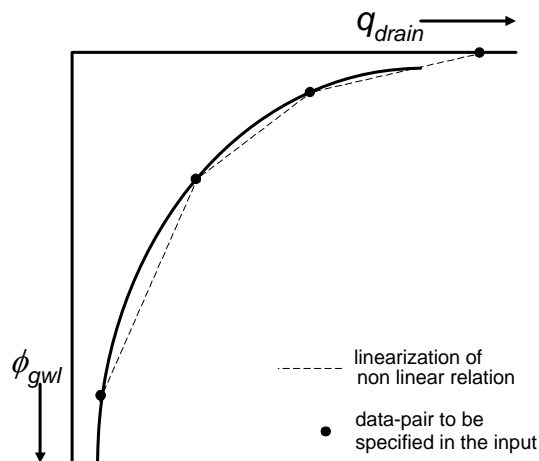
Fig.4.3 Linearization of a non-linear drainage flux relation

4.3.3 General aspects of regional scale drainage

Schematization

The groundwater-surface water system is described at the scale of a horizontal sub-region. A network of drainage devices consists of a hierarchical system of different order and incision depth, but only a single representative groundwater level is simulated for a sub-region, which is 'stretched' over a scale that in reality involves a variety of groundwater levels. In the following, due consideration will be given to the schematization of the surface water system, the simulation of drainage/sub-irrigation fluxes, and the handling of an open surface water level.

The regional surface water system consists of a hierarchical system of different order drainage devices (Fig. 4.4), each with its own with bed level, bed width, side-slope, and spacing conveyance capacity. The drainage devices can be connected to each other in different ways. In the man-made the ditches of the network systems act as perennial streams, connected to larger canals with a nearly equal surface water level. In the alluvial sandy areas of the Netherlands, the smaller streams may have intermittent character which only discharge water in periods with rainwater excess.
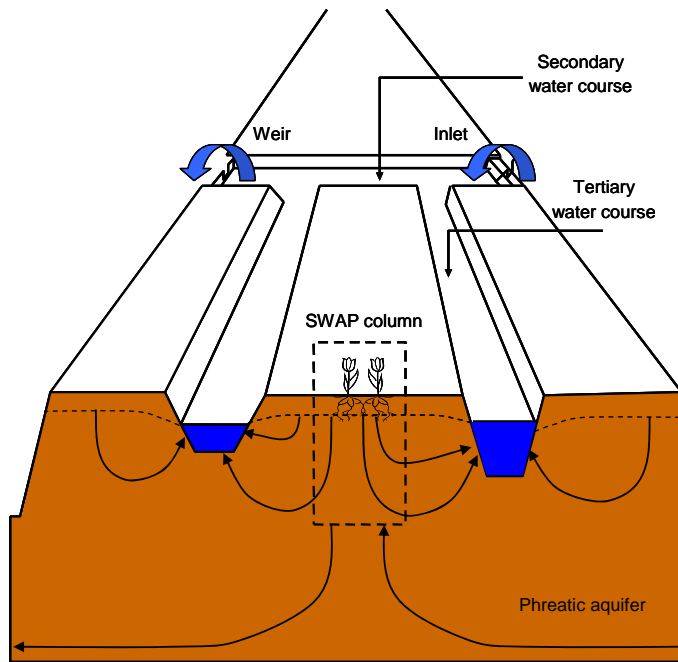
Figure 4.4 Schematization of surface water system in a control unit.

It should be noted that contrary to the classification notation used in geo-morphological sciences, in this report the stream and canal order is dictated by the level of the stream bed or water level (drainage level) compared to the land surface level: the deeper the drainage level, the lower classification index.

The representative distance between drain devices $L_{drain,i}$ (m) is derived by dividing the area of the subregion A_{reg} (m^2) by the total length of the ith order channels, $l_{drain,i}$ (m):

$$L_{drain,i} = \frac{A_{reg}}{l_{drain,i}} \qquad (4.23)$$

In the surface water model, we assume that the different channels orders are connected in a dendritic manner. Together they form a surface water 'control unit' with a single outlet (indicated by the weir in Fig. 4.4) and, if present, a single inlet. The surface water level at the outlet is assumed to be omnipresent in the subregion. Friction losses are neglected and thus the slope of the surface water level is assumed to be zero. This means that in all parts of the subregion the surface water level has the same depth below soil surface.

In the so-called 'multi-level' drainage or sub-irrigation approach employed by the SWAP model, it is possible that more than one type of surface water channel become active simultaneously. In the following, we will refer to channels in terms of their

'order' if their role as part of the surface water system is being considered. When considering their drainage characteristics we will refer to them in terms of their 'level'.

The SWAP model has the option for specifying resistances for calculating the sub-irrigation flux that differ from the resistance values used for drainage. An additional model option involves the limitation of the sub-irrigation rate by defining the groundwater level φ_{avg}^{min} at which the maximum sub-irrigation rate is reached. Such a limitation is needed because the sub-irrigation rate does not increase infinitely when the groundwater level lowers.
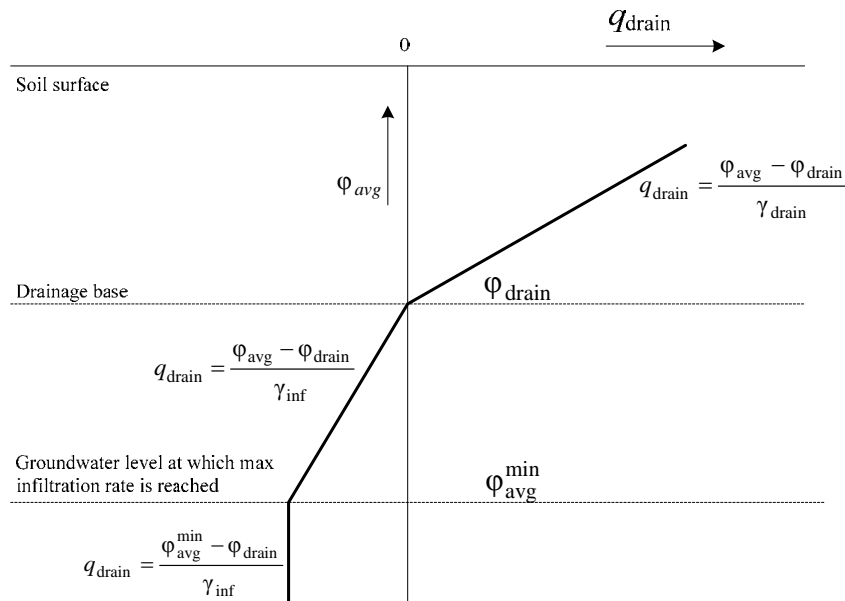
Figure 4.5 Lineair relationships between drainage ($q_{drain} > 0$) and infiltration ($q_{drain} < 0$) flux and mean groundwater level ϕ_{avg}

4.3.4   Regional scale drainage relation defined by a tabulated function

An example of a non-linear relation between discharge and groundwater elevation resulting from an analysis of observed field data is presented in Fig. 4.6 (Massop and De Wit, 1994). It can be seen from this figure that the non-linear relation may be linearized to a piece-wise linear relation in which each part of this relation corresponds to a certain type of drainage system. From Figure 4.6 one can infer that the drainage base of the larger channels is roughly at $z = -120$ cm, as no discharges were measured below that level. The schematized $q_{drain}(\phi_{avg})$-relationship has transition points at mean groundwater levels of 80 and 55 cm below soil surface. These transition points

correspond to the 'representative' bed levels of the second and third order channels. These levels could be imposed to the SWAP model as drainage levels.
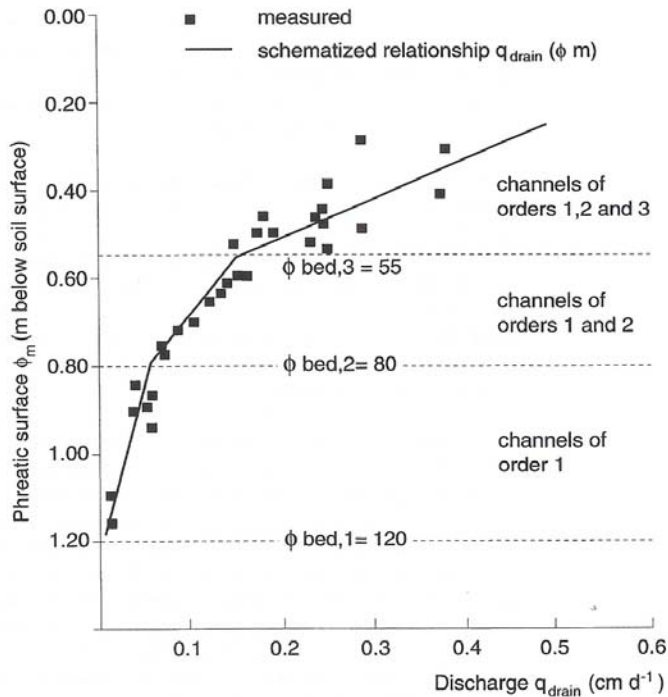
Figure 4.6 Discharge q_{drain} as function of mean phreatic surface φ_{avg} in the Beltrum area (Massop and de Wit, 1994)

4.3.5 Multi-level drainage with fixed resistances and imposed drainage levels

Prior to any calculation of the drainage/sub-irrigation rate, we determine whether the flow situation involves drainage, sub-irrigation, or neither. No drainage or sub-irrigation will occur if both the groundwater level and surface water level are below the drainage base.

Drainage will only occur if the following two conditions are met:
- the groundwater level is higher than the channel bed level;
- the groundwater level is higher than the surface water level.

Sub-irrigation can only occur if the following two conditions are met:
- the surface water level is higher than the channel bed level;
- the surface water level is higher than the groundwater level.

In both cases we take for the drainage base, ϕ_{drain} (cm), either the surface water level, ϕ_{sur} (cm), or the channel bed level, z_{bed} (cm), whichever is higher:

$$\varphi_{\text{drain}} = \max(\varphi_{sur}, z_{\text{bed}})$$ *(4.1)*

The variable φ is defined positive upward, with zero at the soil surface.

The drainage/infiltration flux $q_{\text{drain,i}}$ (cm d^{-1}) to/from each surface water system i is calculated from the linear relation:

$$q_{\text{drain,i}} = \frac{\varphi_{\text{avg}} - \varphi_{\text{drain,i}}}{\gamma_{\text{drain,i}}}$$ *(4.2)*

Where $\varphi_{\text{drain,i}}$ is the drainage base is equal to the surface water level of system i (cm below the soil surface) and $\gamma_{\text{drain,i}}$ is the drainage resistance of system i (d). Similar to the case of single-level drainage, a drainage level is only 'active' if either the groundwater level or the surface water level is higher than the channel bed level. The drainage base is determined separately for each of the drainage levels. In computing the total flux q_{drain}^{tot} to/from surface water, the contributions of the different channel orders are simply added:

$$q_{\text{drain}}^{\text{tot}} = \sum_{i=1}^{n} q_{\text{drain,i}}$$ *(4.3)*

4.3.6 Multi-level drainage with surface water dependent resistances and simulated drainage levels

In most applications, the control unit involves the primary watercourse; the largest canals with the deepest channels beds. An option is available to specify that the primary watercourse, e.g., a large river, functions separately from the other watercourses within the sub-regional surface water system. In that case the primary water courses have their own surface water level which should be specified in the input. In the real situation there may be some interaction between the primary water course and the control unit: for instance a pumping station for removal of drainage water, and/or an inlet for letting in external surface water supply (Figure 4.4). The hydraulics of such structures are not included in the model. Conveyance processes within the surface water devices are not described.

Contrary to the model option described in Par 4.3.5, the influence of the surface water level on drainage resistances can be accounted for by distinguishing two parts of the resistance: 1) a part independent of the surface water level and 2) a part that is adjusted by the level. For the drainage case:

$$\gamma_{\text{drain,i}} = \gamma^0_{\text{drain,i}} + \gamma^*_{\text{entr,i}} \frac{L_{\text{drain,i}}}{u_{\text{drain,i}}} \qquad (4.4)$$

And for the sub-infiltration case:

$$\gamma_{\text{infil,i}} = \gamma^0_{\text{infil,i}} + \gamma^*_{\text{exit,i}} \frac{L_{\text{drain,i}}}{u_{\text{drain,i}}} \qquad (4.5)$$

Where $\gamma^0_{\text{drain,i}}$ and $\gamma^0_{\text{infil,i}}$ are the level independent parts of the drainage and infiltration resistance and resp. $\gamma^*_{\text{entr,i}}$ and $\gamma^*_{\text{exit,i}}$ are the entrance and exit resistance factor per unit drain distance ($L_{\text{drain,i}}$) and divided by the wetted perimeter ($u_{\text{drain,i}}$). The radial resistance has been lumped with the entrance or exit resistance. By assuming a trapezoidal cross section of the water courses, the wetted perimeter can be calculated as:

$$u_{drain,i} = w_{bed,i} + \max\left(0, 2 \cdot (\varphi_{sur} - z_{\text{bed,i}})\sqrt{1 + \frac{1}{\alpha^2_{\text{sl,i}}}}\right) \qquad (4.6)$$

Where $w_{bed,i}$ is the channel bed width (cm) and $\alpha_{\text{sl,i}}$ (-) is the slope of the channel bank.

Another feature of this model option includes the ability to simulate the flooding of the field when the surface water level higher appears to be higher than both the ponding sill and the ponding level or groundwater level (Fig. 4.7)
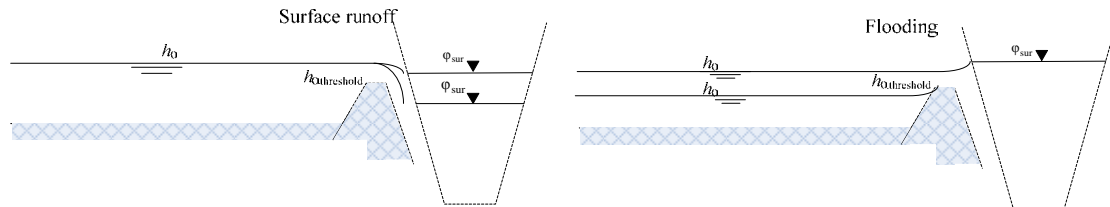
Figure 4.7 In-between position of groundwater/ponding level h_0 and surface waterlevel φ_{sur} in case of surface runoff (left) and flooding (right)

The model concept for flooding does not take account for the resistance of water flowing on the field surface and an immediate equilibrium between the ponding level and the surface water level is assumed when flooding occurs.

4.4 Distribution with depth of drainage fluxes

4.4.1 Implicit approach of travel times

In this section, the concept for the distribution drainage fluxes with depth as one of the sink terms in the SWAP model is described. Although the concept discussed here is valid for a region having any number of drainage levels, only three drainage systems are considered for reasons of convenience.

One-dimensional leaching models generally represent a vertical soil column. Within the unsaturated zone, solutes are transported by vertical water flows, whereas in the saturated zone the drainage discharge can have a three dimensional flow pattern. Van Ommen (1986) has shown that for a simple single-level drainage system, the travel time distribution is independent from the size and the shape of the recharge area. Under these assumptions, the average concentration in drainage water can mathematically be described by the linear behaviour of a single reservoir. But, the non-homogeneous distribution of exfiltration points, the variety of hydraulic properties and the influence of stratified soil chemical characteristics necessitates to distinguish between the different soil layers.

The distribution of drainage fluxes with depth is used to describe the travel time distribution of drainage water in an implicit manner. Drainage fluxes are treated as lateral sink terms of the water balance in the SWAP model. The vertical flux q_y in the saturated zone of the SWAP model relates to the distribution of lateral drainage rate sink terms according to:

$$\frac{dq_y}{dy} = -\frac{q_{drain}}{D} \tag{4.7}$$

where D is the depth of the zone for which q_{drain} has a certain value. Assume that a fluid particle is at the depth of y_0 at time t_0. The time it takes for this particle to reach a depth y is given by:

$$t - t_0 = \int_{y_0}^{y} \frac{\varepsilon \, dy}{q_y(y)} \tag{4.8}$$

The travel time relation is governed by the vertical flux as a function of depth and the porosity. It can be seen from Eq. [4.26] that the vertical flux coheres with the drainage flux.

4.4.2 Discharge layers

The concept of the distribution of the drainage flux with depth for a single level drainage system can be very simple. The Dupuit-Forcheimer assumption involves disregarding the head loss due to radial flow and vertical flow in the largest part of the flow domain. Based on this rule, the groundwater movement towards drains in a non-stratified aquifer is considered as an uni-directional flow and the drainage flux is distributed uniformly with depth.

The distribution with depth for a multi-level drainage system should ideally be based on the 3-D flow paths of water parcels migrating to drains. But since such type of information is not available in the 1-D vertical model, additional assumptions have to be made. The concept of discharge layers has been introduced, representing the flow systems associated with each of the drains. Although the verification of the concept by comparing the depth of discharge layers with the streamline patterns generated by 2D models do not always agree, the concept enables the accounting of the different types of water courses and the stratification of hydraulic properties in the implicit travel time approach.

The discharge layers are considered as horizontal layers. Each layer occupies a certain part of the groundwater volume. The ratio between the occupied flow volumes V_i is derived from the proportionality between flow volumes and volumetric discharge rates:

$$\frac{V_i}{V_{i-1}} = \frac{Q_{\text{drain,i}}}{Q_{\text{drain,i-1}}}$$ *(4.9)*

The volumetric flux $Q_{\text{drain,i}}$ to drainage system i, is calculated as:

$$Q_{\text{drain,i}} = L_{\text{drain,i}}\ q_{\text{drain,i}}$$ *(4.10)*
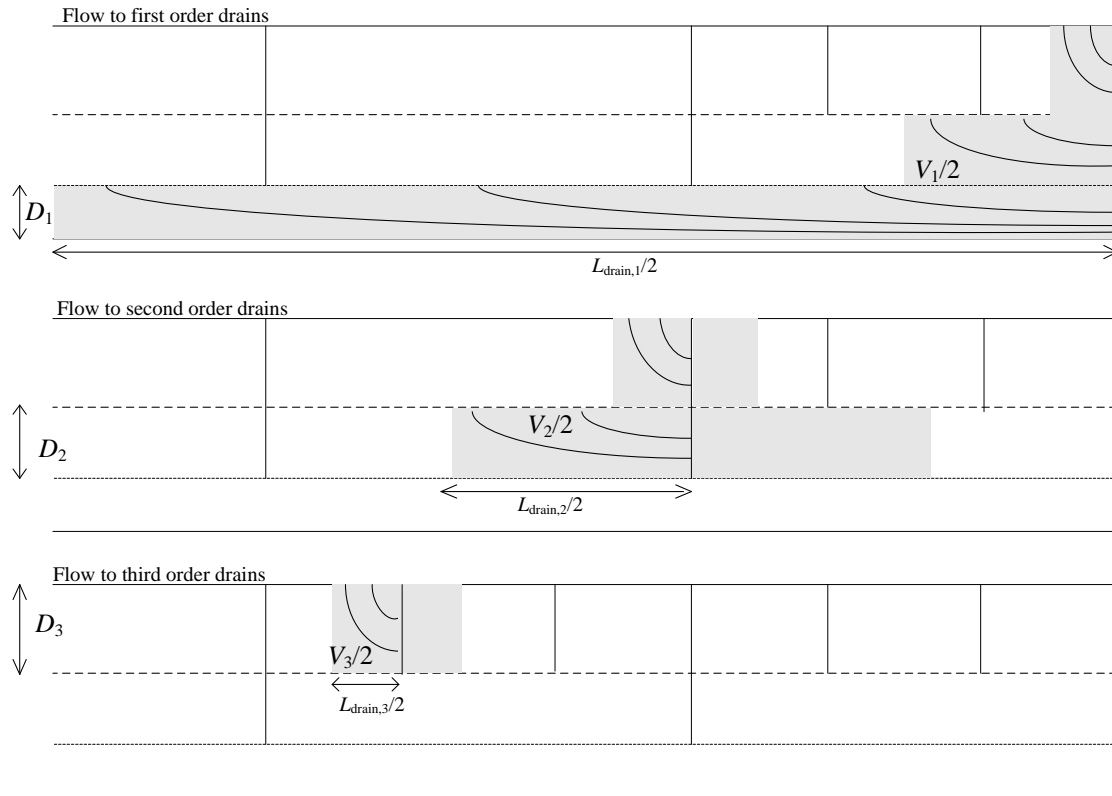
Figure 4.7 Schematization of regional groundwater flow to drains of three different orders

First order drains act also as field ditches and trenches and next higher drains act partly as third order drains. In the SWAP-model the lumped discharge flux per drainage system is computed from the relation between groundwater elevation and drainage resistance. Figure 4.7 shows the schematization of the regional groundwater flow, including the occupied flow volumes for the nested drain systems. The volume V_i consists of summed rectangles L_iD_i of superposed drains, where D_i is the thickness (cm) of discharge layer i.

The flow volume V_i assigned to drains of order 1, 2 and 3 is related to drain distances L_i and thickness D_i of discharge layers as follows:

$$V_1 = L_1D_1 + L_2D_2 + L_3D_3 \qquad (4.11)$$

$$V_2 = L_2D_2 + L_3D_3 \qquad (4.12)$$

$$V_3 = L_3D_3 \qquad (4.13)$$

Rewriting Eq. 4.30 to 4.32 and substituting Eq. 4.28 and Eq. 4.29 yields an expression which relates the proportions of the discharge layer to the discharge flow rates:

$$L_1 D_1 : L_2 D_2 : L_3 D_3 =$$
$$(q_{\mathrm{drain},1} L_{\mathrm{drain},1} - q_{\mathrm{drain},2} L_{\mathrm{drain},2}) : (q_{\mathrm{drain},2} L_{\mathrm{drain},2} - q_{\mathrm{drain},3} L_{\mathrm{drain},3}) : (q_{\mathrm{drain},3} L_{\mathrm{drain},3}) \qquad (4.14)$$

In theory, the terms $(q_{\mathrm{drain},1} L_{\mathrm{drain},1} - q_{\mathrm{drain},2} L_{\mathrm{drain},2})$ and $(q_{\mathrm{drain},2} L_{\mathrm{drain},2} - q_{\mathrm{drain},3} L_{\mathrm{drain},3})$ can take negative values for specific combinations of $q_{\mathrm{drain},1} L_{\mathrm{drain},1}$, $q_{\mathrm{drain},2} L_{\mathrm{drain},2}$ and $q_{\mathrm{drain},3} L_{\mathrm{drain},3}$. When $(q_{\mathrm{drain},1} L_{\mathrm{drain},1} - q_{\mathrm{drain},2} L_{\mathrm{drain},2}) < 0$ it is assumed that D_1 will be zero and the nesting of superposed flows systems on top of the flow region assigned to drainage class 1 will not occur. Likewise, a separate nested flow region related to a drainage class will not show up when $(q_{\mathrm{drain},2} L_{\mathrm{drain},2} - q_{\mathrm{drain},3} L_{\mathrm{drain},3}) < 0$. These cases are depicted schematically in figure 4.8.
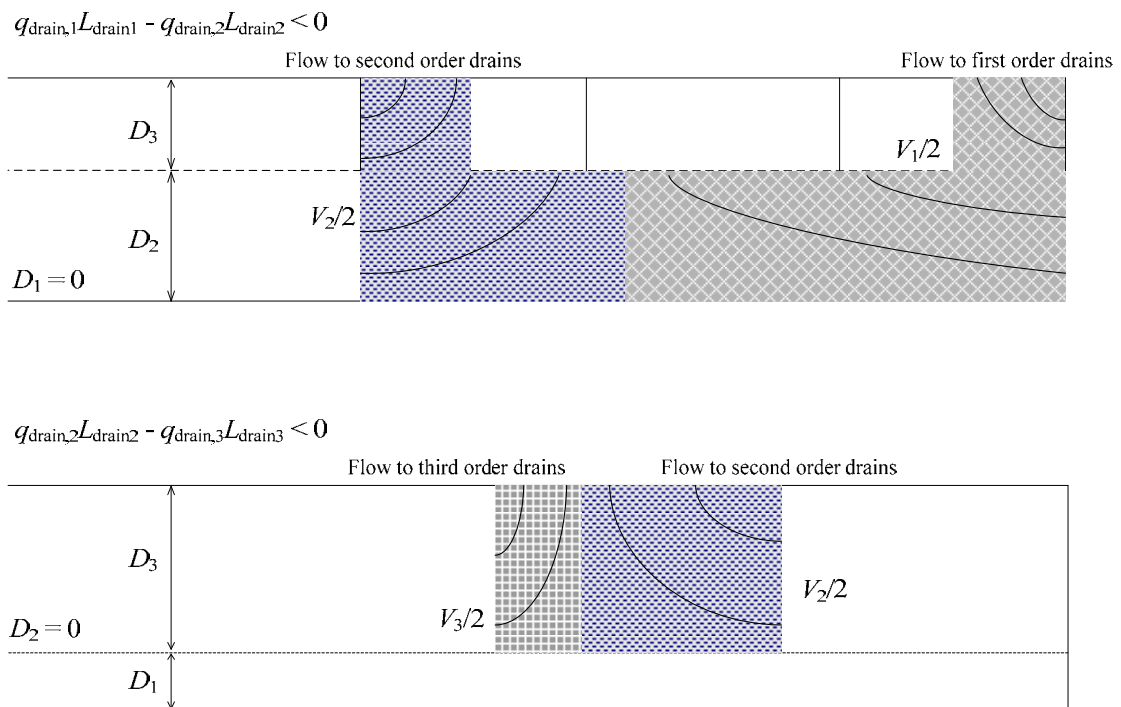
Figure 4.8 Schematization of regional groundwater flow to drains of three orders when either $q_{drain,1} L_{drain,1} - q_{drain,2} L_{drain,2} < 0$ *or* $q_{drain,2} L_{drain,2} - q_{drain,3} L_{drain,3}$

If the soil profile is stratified with respect to horizontal conductivities, the heterogeneity can be taken into account by substituting transmissivities kD for layer thicknesses in Eq. [4.33]:

$$KD_1 : KD_2 : KD_3 = \frac{q_{\mathrm{drain},1} L_{\mathrm{drain},1} - q_{\mathrm{drain},2} L_{\mathrm{drain},2}}{L_{\mathrm{drain},1}} : \frac{q_{\mathrm{drain},2} L_{\mathrm{drain},2} - q_{\mathrm{drain},3} L_{\mathrm{drain},3}}{L_{\mathrm{drain},2}} : q_{\mathrm{drain},3} \qquad (4.15)$$

Lateral drainage fluxes to a certain drainage system per nodal point are calculated by multiplying the flux and the transmissivity proportion of that nodal point in the total transmissivity of the discharge layer.

In deep aquifers, the thickness of a model discharge layer is limited by:

$$D \leq \frac{L_{\text{drain}}}{4} \sqrt{\frac{K_v}{K_h}} \qquad (4.16)$$

where K_v is the vertical conductivity and K_h is the horizontal conductivity. In stratified aquifers, the weighted arithmetic mean is used for the horizontal conductivity and the weighted harmonic mean is used for the vertical conductivity.

The top of any of the discharge layers is situated at the average groundwater level. This implies that solute transport to drains is calculated for the soil compartments between the simulated groundwater level and the bottom of the discharge layer. The groundwater level as the defined top of the zone that contributes to surface water loading may be inaccurate in case of concentration profiles with steep gradients. In reality the surface water load is determined by the present concentrations and water fluxes at the exfiltration zone in the drain. From Fig. 4.9 (left) it can be seen that the concentrations at the drain bottom and at the depth of the surface water level are lower than the ones at the groundwater level. In such case the concept will lead to an over estimation to the surface water load relative to the results of 2D models. The SWAP model provides an option to specify the top of the zone that contributes to surface water loading as a function of the average groundwater level and the drainage level (z_{top}, Fig. 4.9; right) according to:

$$z_{\text{top}} = f_{z\text{top}} \, \varphi_{\text{avg}} + (1 - f_{z\text{top}}) \, \varphi_{\text{drain}} \qquad (4.17)$$
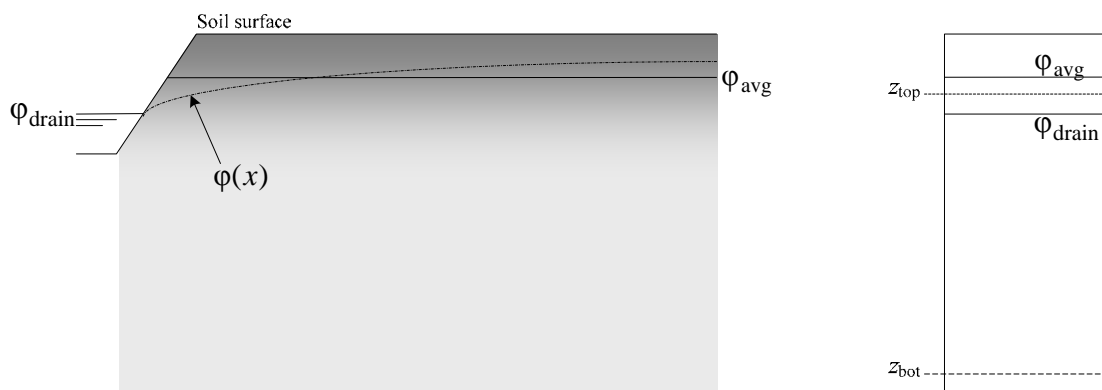
Figure 4.9 2D-schematization of the saturated flow domain with a hypothetical concentration profile indicated by gray shading (left) and the schematization of the top of the zone that contributes to surface water loading (right)

4.5 User instructions

4.5.1 Surface runoff

The maximum height of ponded water stored $h_{0,\text{threshold}}$ on the field surface is determined by the irregularities and the slope of the soil surface. Also the extend to which local field depressions are connected to each other and are connected to the surface water affects the $h_{0,\text{threshold}}$-value. Typical values range from 0.5 to 2 cm for well maintained agricultural fields in the Netherlands. Since it is impossible to measure the $h_{0,\text{threshold}}$-parameter directly, a value should be established by expert-judgement or model calibration.

As surface runoff is a rapid process, the resistance γ will typically take values of less than 1 d. When the dynamics of surface runoff are relevant, the values of γ and β might be derived from experimental data or from a hydraulic model of soil surface flow.

Box 4.1 Information on input of surface runoff in main file *.SWP

```
**********************************************************************************
* Part 2: Ponding, runoff and runon

* Ponding
  PONDMX  = 0.2  ! In case of ponding, minimum thickness for runoff, [0..1000 cm, R]

* Runoff
  RSRO     =  0.5 ! Drainage resistance for surface runoff [0.001..1.0 d, R]
  RSROEXP  =  1.0 ! Exponent in drainage equation of surface runoff [0.1..10.0 -, R]

* Runon
* Specify whether runon data are provided in extra input file
  SWRUNON = 0   ! 0 = No input of runon data
                ! 1 = Runon data are provided in extra input file

* If SWRUNON = 1, specify name of file with runon input data
* This file may be an output *.inc file (with only 1 header) of a previous Swap-simulation
  RUFIL = 'runon.inc' ! File name with extension [A80]
**********************************************************************************
```

4.5.2 Interflow

For describing the interflow process, a non-linear relation can be used. Such relation may useful for taking account for the horizontal flow in the saturated zone above drainage level may yield a non-linear relation contrary to relation based on the assumption made in the derivation of the horizontal resistance in the Ernst-equation. Another reason to introduce a non-linear relation for interflow may be the occurrence of hillslope. Sometimes it is possible to relate the parameters $A_{\text{interflow}}$ and $B_{\text{interflow}}$ to

a specific flow concept, but most of the model user has to rely on expert judgement of model calibration.

```
Box 4.2 Information on interflow in drainage file *.DRA

* Option for interflow in highest drainage level (shallow system with short residence time)
  SWINTFL = 0        ! Switch for interflow [0,1, I]

* If SWINTFL = 1, specify:
  COFINTFLB = 0.5    ! Coefficient for interflow relation  [0.01..10.0 d, R]
  EXPINTFLB = 1.0    ! Exponent for interflow relation  [0.1..1.0 -, R]
  ********************************************************************************
```

4.5.3 Drainage

The input requirements for the simulation of a field scale drainage relation according to Hooghoudt and Ernst is given in Box 4.3.

```
Box 4.3 Field scale drainage relation according to Hooghoudt and Ernst in drainage file
*.DRA
********************************************************************************
* Part 0: General

  DRAMET = 2 ! Switch, method of lateral drainage calculation:
*             METHOD 1 = Use table of drainage flux - groundwater level relation
*             METHOD 2 = Use drainage formula of Hooghoudt or Ernst
*             METHOD 3 = Use drainage/infiltration resistance, multi-level if needed

********************************************************************************
* METHOD 2 - Part 2: Drainage formula of Hooghoudt or Ernst (DRAMET = 2)

* Drain characteristics:
  LM2    = 11.       ! Drain spacing, [1..1000 m, R]
  SHAPE = 0.8        ! Shape factor to account for actual location between drain and water divide [0.0..1.0 -, R]
  WETPER =  30.0     ! Wet perimeter of the drain,  [0..1000 cm, R]
  ZBOTDR = -80.0     ! Level of drain bottom, [-1000..0 cm, R, neg. below soil surface]
  ENTRES =  20.0     ! Drain entry resistance, [0..1000 d, R]

* Soil profile characteristics:

  IPOS = 2   ! Switch for position of drain:
*             1 = On top of an impervious layer in a homogeneous profile
*             2 = Above an impervious layer in a homogeneous profile
*             3 = At the interface of a fine upper and a coarse lower soil layer
*             4 = In the lower, more coarse soil layer
*             5 = In the upper, more fine soil layer

* For all positions specify:
  BASEGW = -200.     ! Level of impervious layer, [-1d4..0 cm, R]
  KHTOP  =   25.     ! Horizontal hydraulic conductivity top layer, [0..1000 cm/d, R]

* In addition, in case IPOS = 3,4,5
  KHBOT  = 10.0      ! horizontal hydraulic conductivity bottom layer, [0..1000 cm/d, R]
  ZINTF  = -150.     ! Level of interface of fine and coarse soil layer, [-1d4..0 cm, R]

* In addition, in case IPOS = 4,5
  KVTOP  =  5.0      ! Vertical hydraulic conductivity top layer, [0..1000 cm/d, R]
  KVBOT  = 10.0      ! Vertical hydraulic conductivity bottom layer, [0..1000 cm/d, R]

* In addition, in case IPOS = 5
  GEOFAC = 4.8       ! Geometry factor of Ernst,  [0..100 -, R]
  ********************************************************************************
```

The input requirements for the simulation of a field scale drainage relation defined by a tabulated function is given in Box 4.4.

The input requirements for the simulation of multi-level drainage given in Box 4.5 for a basic system with fixed resistances and imposed levels. In Box 4.6 the requirements are given for an extended system with surface water dependent resistances and simulated drainage levels.

Up to five different drainage levels can be specified. For each level the user can specify whether drainage or infiltration or both are allowed. Both the drainage and infiltration resistance needs to be specified by the user. In case of sub-irrigation, the entrance resistance (then denoted as γ_{inf}) can be either higher or lower than that for drainage (γ_{drain}), depending on local conditions. A substantial raising of the surface water level can for instance result in infiltration through a more conductive 'bio-active' zone which will reduce the entrance resistance. In most situations with sub-irrigation the radial resistance will be higher than with drainage, because the wetted section of the subsoil is less than in the situation with drainage (the groundwater table becomes concave instead of convex). Especially if the conductivity is larger in the subsoil above the drainage base than in the deeper subsoil, γ_{inf} will be substantially higher than γ_{drain}. To deal with such cases, the model has the option for using sub-irrigation resistances that differ from the ones for drainage (e.g. $\gamma_{inf} \approx 3/2 \ \gamma_{drain}$ in Figure 4.5).

When calibrating SWAP against measured groundwater levels it should be realised that SWAP calculates a field-average groundwater level. Measured groundwater levels represent a point of the convex or concave shaped groundwater table, depending on the position of the piezometer in the field in relation to the drains. Piezometers in the middle of two parallel drains will display stronger fluctuations of the groundwater level than the field-average level. Calibrating SWAP against these strong fluctuating groundwater levels will result in a calibrated model that deviates

strongly from groundwater behavior at the field scale. To overcome this inaccuracy, it is advised to measure groundwater level movement in a row of piezometers perpendicular to the drain starting at a close (0.5 m) distance of the drain, including the drain level. From these measurements a shape-factor can be calculated that represents the relationship between the measured convex or concave groundwater table and the field average. This shape-factor can be used to convert measured levels into levels that are suitable for calibration of SWAP.

Box 4.5 Multi-level drainage with fixed resistances and imposed drainage levels in drainage file *.DRA

```
***********************************************************************************
* METHOD 3 - Part 3: Drainage and infiltration resistance (DRAMET = 3)

  NRLEVS = 2          ! Number of drainage levels, [1..5, I]

***********************************************************************************
* Part 3a: Drainage to level 1

  DRARES1 = 100    ! Drainage resistance, [10..1d5 d, R]
  INFRES1 = 100    ! Infiltration resistance, [0..1d5 d, R]
  SWALLO1 =   1    ! Switch, for allowance drainage/infiltration:
                   ! 1 = Drainage and infiltration are both allowed
                   ! 2 = Drainage is not allowed
                   ! 3 = Infiltration is not allowed
  ZBOTDR1 = -90.0  ! Level of drainage medium bottom, [-1000..0 cm, R]
  SWDTYP1 = 2      ! Type of drainage medium: 1 = drain tube, 2 = open channel

* If SWDIVD = 1 (drainage flux vertically distributed), specify the drain spacing:
  L1   = 20.       ! Drain spacing, [1..1000 m, R]

* In case of open channel (SWDTYP1 = 2), specify date DATOWL1 [dd-mmm-yyyy] and channel
* water level LEVEL1 [cm, negative if below soil surface], maximum MAOWL records:
       DATOWL1    LEVEL1
   12-jan-1981    -90.0
   14-dec-1981    -90.0
* End of table
***********************************************************************************

* Part 3b: Drainage to level 2

  DRARES2 = 100    ! Drainage resistance, [10..1E5 d, R]
  INFRES2 = 100    ! Infiltration resistance, [0..1E5 d, R]
  SWALLO2 =   1    ! Switch, for allowance drainage/infiltration:
                   ! 1 = Drainage and infiltration are both allowed
                   ! 2 = Drainage is not allowed
                   ! 3 = Infiltration is not allowed
  ZBOTDR2 = -90.0  ! Level of drainage medium bottom, [-1000..0 cm, R]
  SWDTYP2 = 2      ! Type of drainage medium: 1 = drain tube, 2 = open channel

* If SWDIVD = 1 (drainage flux vertically distributed), specify the drain spacing:
  L2 = 20.         ! Drain spacing, [1..1000 m, R]

* In case of open channel (SWDTYP2 = 2), specify date DATOWL2 [dd-mmm-yyyy] and channel
* water level LEVEL2 [cm, negative if below soil surface], maximum MAOWL records:
       DATOWL2    LEVEL2
   12-jan-1981    -90.0
   14-dec-1981    -90.0
* End of table
***********************************************************************************

If the Number of drainage levels (NRLEVS) is larger than 2, then
similar input is required for levels 3 - 5
```

Box 4.6 Multi-level drainage with surface water dependent resistances and simulated drainage levels in drainage file *.DRA

```
*** EXTENDED DRAINAGE SECTION ***


**********************************************************************************
* Part 0: Reference level

 ALTCU = 0.0 ! ALTitude of the Control Unit relative to reference level
*                 AltCu = 0.0 means reference level coincides with
*                 surface level [-300000..300000 cm, R]

**********************************************************************************
* Part 1a: drainage characteristics
*
 NRSRF  = 2     ! number of subsurface drainage levels [1..5, I]
*
*** Table with physical characteristics of each subsurface drainage level:
*
* LEVEL   ! drainage level number [1..NRSRF, I]
* SWDTYP  ! type of drainage medium [open=0, closed=1]
* L       ! spacing between channels/drains [1..1000 m, R]
* ZBOTDRE ! altitude of bottom of channel or drain [ALTCU-1000..ALTCU-0.01 cm,R]
* GWLINF  ! groundw. level for max. infiltr. [-1000..0 cm rel. to soil surf., R]
* RDRAIN  ! drainage resistance [1..100000 d, R]
* RINFI   ! infiltration resistance  [1..100000 d, R]
* Variables RENTRY, REXIT, WIDTHR and TALUDR must have realistic values when the
*          type of drainage medium is open (second column of this table:SWDTYP=0)
*          For closed pipe drains (SWDTYP=1) dummy values may be entered
* RENTRY  ! entry resistance  [1..100 d, R]
* REXIT   ! exit resistance   [1..100 d, R]
* WIDTHR  ! bottom width of channel [0..100 cm, R]
* TALUDR  ! side-slope (dh/dw) of channel [0.01..5, R]
*
 LEV SWDTYP     L    ZBOTDRE GWLINF RDRAIN RINFI RENTRY REXIT  WIDTHR TALUDR
  1   0      250.0  1093.0 -350.0 150.0  4000.0  0.8     0.8   100.0  0.66
  2   0      200.0  1150.0 -300.0 150.0  1500.0  0.8     0.8   100.0  0.66
* End_of_table
*
*
* Part 1b: Separate criteria for highest (shallow) drainage system
*
 SWNRSRF = 0     ! Switch to introduce rapid subsurface drainage [0..2, I]
*            0 = no rapid drainage
*            1 = rapid drainage in the highest drainage system (=NRSRF)
*                (implies adjustment of RDRAIN of highest drainage system)
*            2 = rapid drainage as interflow according to a power relation
*                (implies adjustment of RDRAIN of highest drainage system)
* When SWRNSRF = 1, then enter realistic values for rapid drainage
 RSURFDEEP    = 30.0  ! maximum resistance of rapid subsurface Drainage [0.001..1000.0 d, R]
 RSURFSHALLOW = 10.0  ! minimum resistance of Rapid subsurface Drainage [0.001..1000.0 d, R]
*
* When SWRNSRF = 2, then enter coefficients of power function
 COFINTFL = 0.1        ! coefficient of interflow relation [0.01..10.0 d-1, R]
 EXPINTFL = 0.5        ! exponent of interflow relation [0.1...1.0 -, R]
*
*
```

The input requirements to influence the distribution of drainage fluxes with depth are given in Box 4.7 and 4.8.

An implicit approach for travel times distribution (Section 4.4.1) requires specification of an anisotropy factor (COFANI) for each soil layer. This factor represents the division of horizontal over vertical saturated hydraulic conductivity and will generally increase with depth.

The exact location of the so-called discharge layers may be influenced by an adjustment of the upper boundary of the discharge layer (Box 4.8 and Section 4.4.2). This adjustment requires expert judgement and it is generally not recommended to apply/adjust it without thorough knowledge of the underlying processes.

```
Box 4.7 Implicit approach of travel times in drainage file *.DRA

**********************************************************************************
* Part 0: General

  SWDIVD = 1 ! Calculate vertical distribution of drainage flux in groundwater [Y=1, N=0]

* If SWDIVD = 1, specify anisotropy factor COFANI (horizontal/vertical saturated hydraulic
* conductivity) for each soil layer (maximum MAHO), [0..1000 -, R] :
  COFANI =    1.0    1.0
```

```
Box 4.8 Discharge layers in drainage file *.DRA

**********************************************************************************
* Switch to adjust upper boundary of model discharge layer [Y=1, N=0]
  SWDISLAY = 1
*
* If SWDISLAY = 1, specify for the drainage systems 1 - NRLEVS or NRSRF:
*  - swtopdislay(madr)  ! Switch, for each drainage level, to distribute drainage
*                         flux vertically with a given position of the top of the
*                         model discharge layers: [0,1 - , I]   0 = no; 1 = yes
*  - ztopdislay(Madr)   ! Array with depth of top of model discharge layer for
*                         each drain level, see also swtopdislay (L);
*                         ranges for extended drainageL  [1.0d3..-1.0d-2,cm-mv, R]
*                         ranges for extended drainageL  [(altcu-1.0d3) .. (altcu-1.0d-2),cm-ALTCU, R]
*
*  (level is a dummy array)
 level   swtopdislay   ztopdislay
   1          1          -200.0
   2          0           -0.01
   3          0           -0.01
   4          0           -0.01
   5          0           -0.01
* end of SWDISLAY-tabel
**********************************************************************************
```

5 Surface water management

5.1 Surface water balance

Surface water management options have been implemented in the SWAP model by taking account of the water balance of the surface water. The groundwater-surface water system is described at the scale of a horizontal subregion. The subregion has a single representative groundwater level and it is assumed that the soil profile occupies the whole surface area. This results in water balance terms of the soil profile that are computed per unit area (cm^3 cm^{-2}) and have the *same numerical value for the subregion as a whole.* The surface water system is simplified to a control unit for which the following surface water balance equation is formulated:

$$\frac{dV_{sur}}{dt} = q_{sup} - q_{dis} + q_{drain} + q_{crackfl} + q_{runoff} \tag{5.1}$$

where :

V_{sur}	regional surface water storage	(cm^3 cm^{-2})
q_{sup}	external supply to the control unit	(cm^3 cm^{-2} d^{-1})
q_{dis}	discharge from control unit	(cm^3 cm^{-2} d^{-1})
q_{drain}	regional drainage flow	(cm^3 cm^{-2} d^{-1})
$q_{crackfl}$	bypass flow through cracks of a clay soil to drains or ditches	(cm^3 cm^{-2} d^{-1})
q_{runoff}	surface runoff/runon	(cm^3 cm^{-2} d^{-1})

The regional surface water storage V_{sur} (cm^3 cm^{-2}) is the sum of the surface water storage in each order of the surface water system:

$$V_{sur} = \frac{1}{A_{reg}} \sum_{i=1}^{n} l_i A_{d,i} \tag{5.2}$$

in which A_{reg} is the total area of the sub-region (cm^2), l_i the total length of channels/drains of order i in the sub-region (cm), and $A_{d,i}$ is the wetted area of a channel vertical cross-section (cm^2). The wetted area $A_{d,i}$ is calculated from the surface water level ϕ_{sur}, the channel bed level, the bottom width, and the side-slope. Substitution of Eq. [4.22] in Eq. [5.2] yields the expression:

$$V_{sur} = \sum_{i=1}^{n} \frac{A_{d,i}}{L_i} \tag{5.3}$$

Channels of order i only contribute to the storage if $\phi_{sur} > z_{bed,i}$. The storage in tile drains is neglected. SWAP calculates the net discharge $q_{dis} - q_{sup}$ for a given timestep and for specified surface water levels φ_{sur}^j and φ_{sur}^{j+1} :

$$q_{dis} - q_{sup} = \frac{V_{sur}^{j}(\phi_{sur}^{j}) - V_{sur}^{j+1}(\phi_{sur}^{j+1})}{\Delta t^{j}} + q_{drain} + q_{crackfl} + q_{runoff} \qquad (5.4)$$

If the sum of the terms on the right hand side is positive, discharge has taken place and the supply is equal to zero. If the sum is negative, supply has taken place and the discharge is equal to zero.

The drainage flux is calculated by:

$$q_{drain} = \sum_{i=1}^{n} \frac{\varphi_{avg} - \varphi_{drain,i}}{\gamma_{drain,i}} \qquad (5.5)$$

where the drainage level $\varphi_{drain,i}$ is in this case equal to the channel bed level, $z_{bed,i}$.

When the groundwater level is situated above the highest bed level and with the surface water level is below the lowest one the total drainage flux. If the surface water level tends to rise to levels higher than the channel bed level $z_{bed,i}$, the latter is replaced by the surface water level.

Calculation of the discharge rate q_{dis} is the last step in solving Eq. (5.4):

1. If the supply rate q_{sup} takes a positive value, the discharge is set to zero. The calculation of the supply rate is based on the comparison the target level and that actual surface water level. After establishing a target level it is examined whether the surface water level can take the target value. If necessary, surface water supply is used to attain the target level. The water supply should meet to the following criteria:

    a. The supply rate should not exceed a user defined value of the maximum supply rate $q_{sup,max}$

    b. Water supply only occurs when the surface water level takes a value below the water supply level. This water supply level is defined as a tolerance value in relation to the target level.

2. For the fixed weir, the discharge follows from the iterative procedure to establish a target level from the stage – discharge relationship. This relationship can either be expressed in tabulated form or as a power function for "weir flow" (see Par 5.1.2.1).

3. For a soil moisture controlled weir, the discharge follows simply from the water balance equation as given by Eq. (5.4), with q_{sup} set to zero and the storage V_{sur}^{j+1} set equal to the storage for the target level. The discharge q_{dis} is then the only unknown left, and can be solved directly.

5.1.1 Multi-level drainage with imposed surface water levels

SWAP comprises an option for imposing a surface water level time series to be used as drainage level time series. When using this option it is assumed that the surface water level is equal for all drainage systems. Surface waters associated to the different drainage systems have open connections to each other and conduit resistances are neglected. This results to only one overall surface water level. The number of drainage systems to account for depends on the position of the groundwater level and the surface water level relative to the channel bed level.

5.1.2 Multi-level drainage with simulated surface water levels

Another option in the SWAP model is to simulate the surface water level on the basis of the control unit surface water balance. Then, the discharge is governed by a either a fixed weir or an automated weir. The user can specify different water management periods for which the settings of the weirs can be different. During each time step, SWAP determines in subsequent order:
1. the target level;
2. whether the target level is reached, and the amount of external supply that is needed (if any);
3. the discharge that takes place (if any) and the surface water level at the end of the time step.

Two options for describing the functioning of a weir are available: 1) the target level of a *fixed weir* coincides with the crest level, which has a constant value within a certain management period, or 2) the target level of *soil moisture controlled weir* is a function of a soil moisture state variable and is defined by a water management scheme.

5.1.2.1 Fixed weir

The *fixed weir*-option employs a power function based 'stage-discharge' relationship $q_{dis}(\phi_{sur})$ for which the parameters in the input are specified in SI-units[1] or a tabulated relationship. The power function based 'stage-discharge' relationship reads as:

$$q_{dis} = \frac{Q_{dis}}{A_{cu}} = \frac{\alpha_{weir} (\varphi_{sur} - z_{weir})^{\beta_{weir}}}{A_{cu}} \qquad (5.4)$$

in which Q_{dis} is the volumetric discharge (m^3 s^{-1}), A_{cu} is the area of the control unit (m^2), z_{weir} is the weir crest level (m), α_{weir} is the discharge coefficient (m$^{3-\beta}$ d^{-1}) and

---

[1] literature values are often given in these units. The conversion to internal units is handled by the SWAP model itself.

β_{weir} is the discharge exponent (-). For a broad-crested rectangular weir, α_{weir} is (approximately) given by $\alpha_{weir} = 1.7 \times "weir\ width"$

The stage-discharge relationship can optionally be specified by a table. Then, the relationship should be defined for each management period.

5.1.2.2 Soil moisture controlled weir management

This model option assumes the target level of a *weir* to be controlled by one or more soil moisture state variables. The so called water management scheme defines the setting of the water level $\phi_{sur,tar}$ aimed for in relation to a soil moisture state variable. The target level is defined as a combinational function of three state variables related to soil moisture:

1. the average groundwater level φ_{avg}. Lower target levels a higher groundwater levels may prevent waterlogging and can contribute to minimize crop yield reduction.
2. the soil water pressure head h (cm) at a certain depth. A soil water pressure value appears to be a better indicator for water logging in nature reserves than a groundwater level criterium..
3. the capacity of the unsaturated soil profile to store water V_{uns} (cm). This state variable is an indicator for the possibility of buffering extreme rainfall events. Maintaining a certain minimum amount of storage, reduces the risk of flooding and subsequent discharge peaks.

During the simulation, the SWAP model selects the target level for which all three criteria are met. A scheme maintained by a soil moisture controlled weir is illustrated in Table 5.1. The minimum target level is specified in the first column. The second, third and fourth column represent values for the corresponding groundwater level, soil water pressure head and soil water storage capacity. The first row contain zeros, indicating that irrespective the conditions, the minimum target level should never drop below that level.

Table 5.1 Example of a water management scheme, with $\phi_{sur,tar}$ as the target level, the groundwater level criterium $\phi_{avg,max}$, the pressure head criterium h_{max} and the soil water storage criterium $V_{uns,min}$.

$\phi_{sur,tar}$ (cm)	$\phi_{avg,max}$ (cm)	h_{max} (cm)	$V_{uns,min}$ (cm)
-180	0	0	0
-160	-80	-100	1.5
-140	-90	-150	2.0
-120	-100	-200	2.5
-100	-120	-250	3.0
-80	-130	-300	4.0

To avoid the target level reacting too fast on the prevailing groundwater level, a *maximum drop rate* parameter has been introduced specifying the maximum permitted change of the target level per time unit (cm d^{-1}). The limitation of the target level change can become effective in periods with surface water supply combined with a rising groundwater level.

In periods with heavy rainfall and high discharge, the maximum capacity of a soil moisture controlled weir can be reached and the crest level will drop to its minimum level. Then, the surface water level is not controlled by any of the criteria mentioned before any longer, but will be a function of the discharge characteristics of the surface water infrastructure. Therefore, the management scheme of a soil moisture controlled weir should always be combined with a table defining a stage discharge relationship. This tabulated relationship should be defined for every management period. The minimum level of management scheme should identical to the minimum level of the discharge relationship.

5.2   User instructions

5.2.1   Example case

The Wildenborch case is presented to explain the capabilities of the SWAP model to simulate surface water levels and to impose different options of water management. Input data were derived from the results of a monitoring program, which was carried out in several fields surrounding the "Wildenborch" estate in the eastern part of The Netherlands. Data series were collected on meteorology, soil, groundwater and surface water during several years. Here we focus on a field with a groundwater observation point (GWL in Fig. 5.1) and measurements in the adjacent surface water (SWL and weir in Fig. 5.1).

The SWAP model was applied assuming a seepage flux at the lower boundary described as a Cauchy condition due to regional flow and local flow to surface water systems at the lateral boundary. The surface water system was schematized in two systems. The first system has a weir with a movable crest and a depth of 1.0 meter below the soil surface. The second system has a depth of 0.6 meter below the soil surface. The drainage resistances of the two systems were calibrated with PEST (Doherty et al., 1995). The crest level was specified according to monitored data.

Figure 5.1 Location of monitoring site at the Wildenborch estate where groundwater levels (GWL) and surface water levels (SWL) were measured and controlled by a weir.

The flexible crest level resulted in a dynamic surface water level (Fig. 5.2), which follows the monitored levels of the weir crest. Periods of discharge mainly occur in the winter period. Surface water levels drop below the weir crest in dry summer periods, during which groundwater levels also decrease. Groundwater levels, using the calibrated drainage resistances, showed a good agreement between simulated and measures levels (Fig. 5.2).
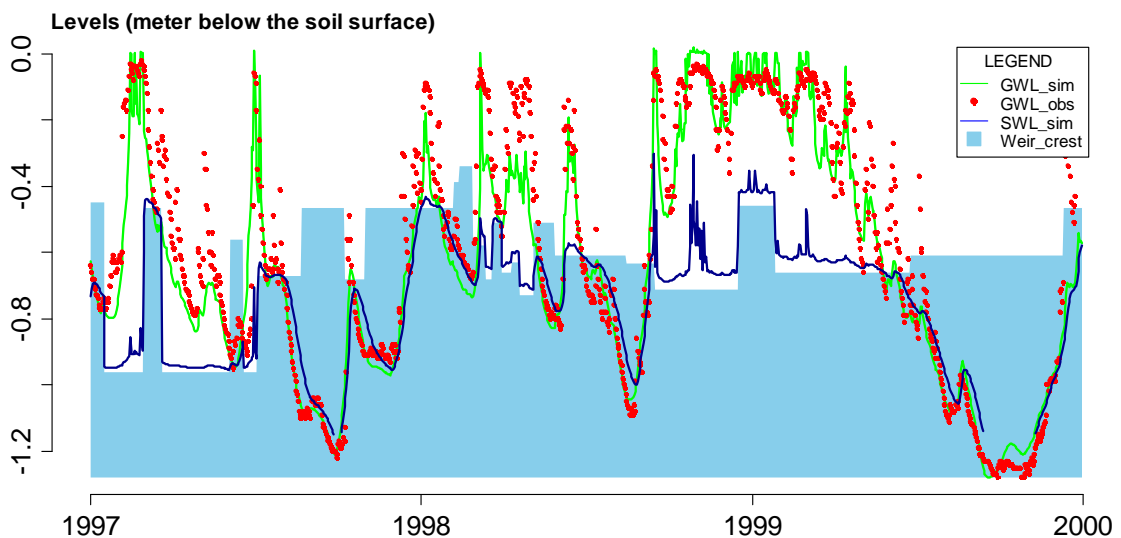
Figure 5.2 Calculated and measured groundwater levels (GWL simulated and GWL observed) and calculated surface water levels (SWL) and controlled by a weir with a variable crest level.

5.2.2 Input instructions

The user first has to select the option for extended drainage (Box 5.1).

```
Box 5.1 Extended drainage option in drainage file *.DRA

*** LATERAL DRAINAGE SECTION ***

**********************************************************************************
* Specify whether lateral drainage should be included

  SWDRA = 2  ! Switch, simulation of lateral drainage:
             ! 0 = No simulation of drainage
             ! 1 = Simulation with basic drainage routine
             ! 2 = Simulation with extended drainage routine (incl surf water man.)

* If SWDRA = 1 or SWDRA = 2 specify name of file with drainage input data:
  DRFIL = 'wg02' ! File name with drainage input data, no extension [A16]

*******************************************************************************
```

Parameters and input variables are specified in a separate file, indicated by the variable DRFIL.

The input data for the options described in this paragraph are given in 2 sections:
−   section 1: drainage characteristics (described in chapter 4)
−   section 2: surface water system

In section 1, the user should specify the altitude of the control unit (= soil surface), with respect to a certain reference level (ALTCU). In section 2, water management levels are given with respect to the same reference. The user may choose to define the soil as surface reference level by specifying zero for the altitude.

A flow chart of the input for the surface water module (section 2 in the input file) is given in figure 5.3. The user should make selections for the kind of surface water system (SWSRF) and the kind of control (SWSEC). The different parts of section 2 are described hereafter.
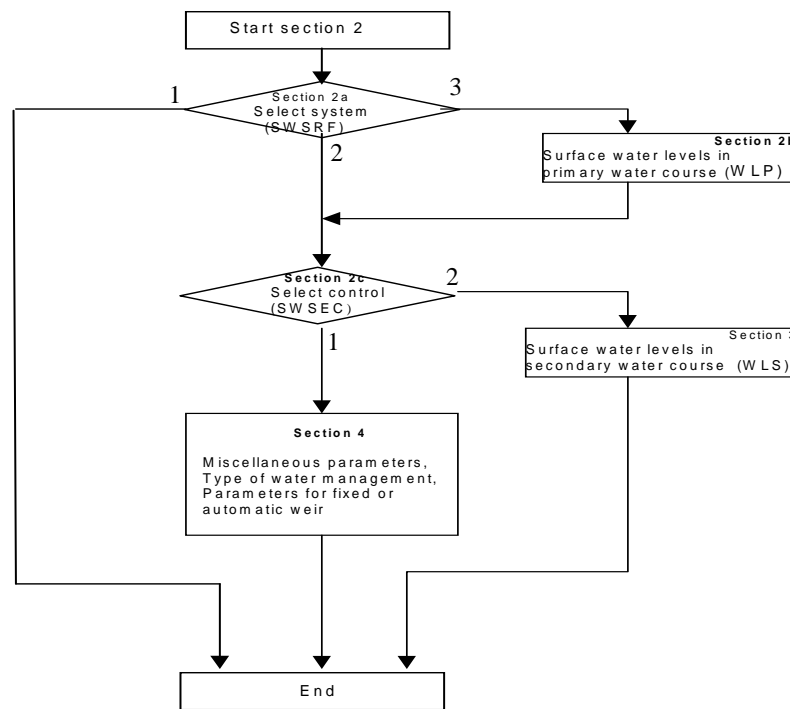
Figure 5.3 Flow chart for input data of surface water system

Section 2 starts with a switch (section 2a, variable SWSRF) for three options:

1. no surface water system is simulated;
2. surface water system is simulated with no separate primary water course;
3. surface water system is simulated with a primary water course (level 1) separate from the control unit

If the first option (SWSRF=1) has been chosen, the user may skip the rest of section 2.

For the second or third option (SWSRF=2 or 3) the user has also to specify how the surface water level in the control unit is determined (section 2c, variable SWSEC):

1. the surface water level is simulated;
2. the surface water level is obtained from input data.

If the third option (SWSRF=3) has been chosen, the user should also specify (section 2b) the time variation of the surface water level in the primary water course. The specification is done in terms of data pairs (date, water level). To obtain levels at intermediate dates, the model performs a linear interpolation.

```
**********************************************************************************
* Part 2a: Specification and control of surface water system
*
 SWSRF = 2 ! option for interaction with surface water system [1..3, I]
*            1 = no interaction with surface water system
*            2 = surf. water system is simulated with no separate primary system
*            3 = surf. water system is simulated with separate primary system
**********************************************************************************
*
* Part 2b: Surface water level of primary system
*
* Only if SWSRF = 3 then the following table must be entered
* Table with Water Levels in the Primary system [max. = 52]:
* no levels above soil surface for primary system
*
* Water level in primary water course WLP [ALTCU-1000..ALTCU-0.01 cm, R] as
* function of DATE1 [dd-mmm-yyyy]
        DATE1      WLP
 02-jan-1980     -100.
 14-jun-1980      -80.
 24-oct-1980     -120.
*End_of_table
**********************************************************************************
*
* Part 2c: Surface water level of secondary system
*
* If SWSRF =  2 or 3  then the variable SWSEC must be entered
*
 SWSEC = 2 ! option for surface water level of secondary system [1..2, I]
*            1 = surface water level is input
*            2 = surface water level is simulated
**********************************************************************************
```

If the option is chosen to obtain surface water levels from input data (SWSEC=1), the surface water level of the secondary watercourse has to be specified in the form of data pairs (section 3).

If the option is chosen to simulate surface water levels (SWSEC=2), the user has to specify how the surface water system in the control unit functions and how it is managed (section 4).

Section 4 starts with some miscellaneous parameters (section 4a):
−   the initial surface water level in the control unit;
−   the criterium for detecting oscillation of the surface water level;
−   the number of water management periods.

In the next section 4b the management period are defined as well as the type of watermanagent (1- fixed weir crest; 2- automatic weir), the water supply capacity and a tolerance value (WLDIP). The tolerance value WLDIP relates the water supply level to the target level preventing oscillations and too fast unrealistic responses of surface water management to the prevailing conditions. This tolerance can be seen as the allowed dip of the surface water level and can take a value of e.g. 10 cm. An appropriate setting of this parameter can save a substantial amount of water.

*Box 5.3 Input of surface water levels in drainage file *.DRA*

```
* Part 3: surface water level in secondary water course is input
*
* Table with Water Levels in the Secondary system [max. = 52]:
*
* Water level in secondary water course WLS [ALTCU-1000..ALTCU-0.01 cm, R] as
* function of DATE2 [dd-mmm-yyyy]
      DATE2       WLS
    24-Apr-1993,-77.0
    25-Apr-1993,-78.0
    26-Apr-1993,-79.0
    ................
    29-Dec-2000,-86.0
    30-Dec-2000,-86.0
    31-Dec-2000,-85.2
*End_of_table
********************************************************************************
```

*Box 5.4 Simulation of surface water levels in drainage file *.DRA*

```
********************************************************************************
* Part 4: surface water level is simulated
*
********************************************************************************
* Part 4a: Miscellaneous parameters
*
 WLACT  = -77.0 ! initial surface water level [ALTCU-1000..ALTCU cm,R]
 OSSWLM =   2.5 ! criterium for warning about oscillation [0..10 cm, R]
********************************************************************************
*
* Part 4b: management of surface water levels
*
 NMPER  = 34 ! number of management periods [1..10, I]
*
* For each management period specify:
* IMPER  index of management period [1..NMPER, I]
* IMPEND date that period ends [dd-mm-yyyy]
* SWMAN  type of water management [1..2, I]
*       1 = fixed weir crest (see part 4c and 4d)
*       2 = automatic weir (see part 4e)
* WSCAP  surface water supply capacity [0..100 cm/d, R]
* WLDIP  allowed dip of surf. water level, before starting supply [0..100 cm, R]
* INTWL  length of water-level adjustment period (SWMAN=2 only) [1..31 d, R]
IMPER_4b       IMPEND  SWMAN  WSCAP  WLDIP  INTWL
  1       21-Mar-1996    1     0.0    0.0     1
  2       15-Jan-1997    1     0.0    0.0     1
  ..       ..-...-....   ..    ...    ...     ..
 33       29-Aug-2000    1     0.0    0.0     1
 34       02-Oct-2000    1     0.0    0.0     1
*End_of_table
*
```

Dependent on the discharge relationship for the weir, the user has to specify:
−   either Section 4c (SWQHR=1, exponential relation)
−   or Section 4d (SWQHR=2, relation given as table)

If an exponential relations is chosen then, for each water management period with a fixed weir crest using weir characteristics, the user should specify (section 4c):
−   Size of the control unit (catchment) (ha);
−   A table with weir characteristics for each management period:
      o   Index for management period (-);
      o   Elevation (H) of the weir crest (cm);
      o   dischargecoefficient α_{input} ($m^{3-\beta}$ s^{-1});
      o   discharge exponent β (-)

Head-discharge relationships are given in SI-units, i.e. m for length and s for time and the discharge is computed as a volume rate (m^3 s^{-1}). To facilitate the input for the user we conformed to hydraulic literature. This implies that the user has to specify the weir characteristics that define a relationship of the following form:

$$Q = \alpha_{input} H^{\beta} \tag{5.7}$$

where Q is the discharge (m^3 s^{-1}), H is the head above the crest (m) and α_{input} is a weir coefficient ($m^{3-\beta}$ s^{-1}), β is a weir exponent (-).

The preparatory work that the user has to do is to compute the value of α_{input} from the various coefficients preceding the upstream head above the crest. For instance, for a broad-crested rectangular weir, α_{input} is (approximately) given by:

$$\alpha_{input} = 1.7 \ b \tag{5.8}$$

where 1,7 is the discharge coefficient of the weir (based on SI-units), b is the width of the weir (m).

To correct for units, the model carries out the following conversion:

$$\alpha_{weir} = \frac{8.65 * 100^{(1-\beta)}}{A_{cu}} \tag{5.9}$$

where A_{cu} is the size of the control unit (ha)

The model requires input of the size of the control unit (A_{cu}), which in simple cases will be identical to the size of the simulation unit.

If the discharge relation is described using a table (SWQHR=2) then, for each water management period with a fixed weir crest using weir characteristics, the user should specify a table in section 4d.

In section 4e of the input file the required parameters should be given to introduce an automatic weir (SWMAN=2) controlled by soil moisture characteristics (see also par. 5.1.2.2). For each management period with an automatic weir the user should specify in section 4e:

− the maximum allowed drop rate of the water level setting
− the depth (HDEPTH) in the soil profile for a comparison between simulated and required soil moisture criterium (HCRIT)

The three state variables (GWLCRIT, HCRIT, VCRIT) that define the target weir level are given in a separate table.

```
┌─────────────────────────────────────────────────────────────────────────────────────┐
│                                                                                       │
│  Box 5.5 Relation between groundwater and surface water levels in drainage file       │
│  *.DRA                                                                                 │
│                                                                                       │
│                                                                                       │
│  **********************************************************************************   │
│  * choice for type of discharge relationship                                          │
│  *                                                                                     │
│  SWQHR  = 1 ! option for type of discharge relationship [1..2, I]                      │
│  *            1 = exponential relationship (see part 4c)                               │
│  *            2 = table (see part 4d)                                                  │
│  *                                                                                     │
│  **********************************************************************************   │
│  *                                                                                     │
│  * Part 4c: exponential discharge relation (weir characteristics)                     │
│  *                                                                                     │
│  * If SWQHR=1 and for ALL periods specify:                                             │
│  *                                                                                     │
│   SOFCU = 100.0  ! Size of the control unit [0.1..100000.0 ha, R]                      │
│  *                                                                                     │
│  * IMPER  index of management period [1..NMPER, I]                                     │
│  * HBWEIR weir crest; levels above soil surface are allowed, but simulated            │
│  *        surface water levels should remain below 100 cm above soil surface;         │
│  *        the crest must be higher than the deepest channel bottom of the             │
│  *        secondary system (ZBOTDR(1 or 2), [ALTCU-ZBOTDR..ALTCU+100 cm,R].           │
│  *        If SWMAN = 2: HBWEIR represents the lowest possible weir position.           │
│  * ALPHAW alpha-coefficient of discharge formula [0.1..50.0, R]                        │
│  * BETAW  beta-coefficient of discharge formula [0.5..3.0, R]                          │
│  IMPER_4c  HBWEIR  ALPHAW  BETAW                                                        │
│    1       -96.0   1.7     1.5                                                          │
│    2       -45.0   1.7     1.5                                                          │
│   ..        ...     ...     ...                                                         │
│   33       -51.5   1.7     1.5                                                          │
│   34       -66.5   1.7     1.5                                                          │
│  *End_of_table                                                                         │
│  **********************************************************************************   │
│  *                                                                                     │
│  * Part 4d: table discharge relation                                                  │
│  *                                                                                     │
│  * If SWQHR=2 and for ALL periods specify:                                             │
│  *                                                                                     │
│  * IMPER  index of management period [1..NMPER, I]                                     │
│  * ITAB   index per management period [1..10, I]                                       │
│  * HTAB   surface water level [ALTCU-1000..ALTCU+100 cm, R]                            │
│  *        (first value for each period = ALTCU + 100 cm)                               │
│  * QTAB   discharge [0..500 cm/d, R]                                                   │
│  *        (should go down to a value of zero at a level that is higher than            │
│  *        the deepest channel bottom of secondary surface water system)               │
│  *                                                                                     │
│   IMPER_4d IMPTAB  HTAB   QTAB                                                          │
│      1       1     -75.0   2.0                                                          │
│  *End_of_table                                                                         │
│  **********************************************************************************   │
└─────────────────────────────────────────────────────────────────────────────────────┘
```

Box 5.6 Automatic and soil moisture controlled Weir management – in drainage file
*.DRA

```
* Part 4e: automatic weir control
*
* For the periods when SWMAN=2 specify next two tables:
*
*** Table #1
*
* IMPER  index of management period [1..NMPER, I]
* DROPR  maximum drop rate of surface water level [0..100 cm/d, positive, R]
*        if the value is set to zero, the parameter does not play any role at all
* HDEPTH depth in soil profile for comparing with HCRIT
*        [-100..0 cm below soil surface, R]
*
 IMPER_4E1 DROPR   HDEPTH
       1    0.0     -15.0
*End_of_table
*
*** Table #2
*
* IMPER   index of management period [1..NMPER, I]
* IPHASE  index per management period [1..10, I]
* WLSMAN  surface water level of phase IPHASE [ALTCU-500.0..ALTCU cm,R]
* GWLCRIT groundwater level of phase IPHASE,  max. value
*         [-500..0 cm  below soil surface, R]
* HCRIT   critical pressure head, max. value, (at HDEPTH, see above)
*         for allowing surface water level [-1000..0 cm, neg., R]
* VCRIT   critical unsaturated volume (min. value) for all
*         surface water level [0..20 cm, R]
*
*   Notes: 1) The zero's for the criteria on the first record are in fact
*             dummy's, because under all circumstances the scheme will set
*             the surface water level at least to wlsman(imper,1)
*          2) The lowest level of the scheme must still be above the
*             deepest channel bottom of the secondary surface water system
*
 IMPER_4E2 IMPPHASE WLSMAN GWLCRIT   HCRIT   VCRIT
        2     1   1114.0     0.0      0.0     0.0
        2     2   1124.0   -80.0      0.0     0.0
        2     3   1124.0   -90.0      0.0     0.0
        2     4   1154.0  -100.0      0.0     0.0
        3     1   1114.0     0.0      0.0     0.0
        3     2   1124.0   -80.0      0.0     0.0
        3     3   1124.0   -90.0      0.0     0.0
        3     4   1154.0  -100.0      0.0     0.0
*End_of_table
*******************************************************************************
```

6 Macropore flow

In structured soils such as clay and peat, preferential flow occurs through large pores or macropores in the (un)saturated soil matrix. Macropores are defined as pores with a diameter or width equal to or larger than 100 μm. Macroporosity can be caused by shrinking and cracking of soil, by plant roots, by soil fauna, or by tillage operations.

Due to the very rapid flow through macropores, water and solutes can reach large depths almost immediately after the start of a shower, bypassing the capacity of the soil matrix for storage, adsorption and transformation of potential pollutants. This process is known as 'bypass flow' or 'short-circuiting' (Hoogmoed and Bouma, 1980). Because of the great impact of macropores on water flow and solute transport through the vadose zone, a concept has been implemented in SWAP for simulating preferential flow at the field scale.

Cracked clay soils reveal a large spatial variability of water contents and solute concentrations at given depth (Beven and Germann, 1982; Bronswijk et al., 1995). Therefore, instead of trying to describe water flow and solute transport at each location, the field-average behaviour may be easier to catch in a model. In order to make the model suitable for process and scenario analysis, concepts should be used that are generally applicable, thus physically based. Furthermore, model calibration requires a limited number of parameters, and preferably parameters that can be measured directly in the field. The description of macropore flow in SWAP has been developed taking into account these requirements.

The macropore flow concept is described by Hendriks et al. (in prep). It is new in the present SWAP and therefore, and to promote a well-considered use of this option its description is rather extensive and detailed. The concept of macropore flow is described in Section 6.1. The numerical implementation in the SWAP model is discussed in Section 6.2. User instructions are given in Section 6.3.

6.1 Concept

In the SWAP model macropore water flow includes the following processes:
- uptake of water by macropores at the soil surface;
- vertical transport to deeper layers or the groundwater bypassing the soil matrix;
- lateral infiltration into and exfiltration out of the soil matrix;
- rapid drainage to drainage systems;
- water storage in the macropores.

The simulation of these processes is based on the description of the macropore geometry as proposed by Hendriks et al. (1999). The description of this geometry that SWAP uses, is discussed in Section 6.1.1. Water flowing into macropores is instantaneously added to the water storage at the bottom of the macropores. Lateral infiltration into the soil matrix of macropore water running rapidly downwards is neglected. Because such downward flow occurs in a low number of contracted films, contact areas with the matrix are small, and consequently this infiltration is negligible (Hoogmoed and Bouma, 1980; Booltink, 1993). Some of the macropore inflow is trapped in discontinuous macropores and is therefore forced to infiltrate into the unsaturated matrix at different depths. This process is called `internal catchment' (Bouma and Dekker, 1978; Van Stiphout et al., 1987). The water flow and balance are described in more detail in Section 6.1.2.

6.1.1 Macropore geometry

In SWAP the geometry of macropore structure is described by characterising the macropore volume according to three main properties:

1. <u>Continuity</u>: vertical continuity controls flow of water that is taken up at the soil surface to different depths in the profile and horizontal continuity controls exchange of water between macropores (Section 6.1.1.1);
2. <u>Persistency</u>: static macropore volume is permanent, while dynamic macropore volume (shrinkage cracks) depends on soil moisture status (Section 6.1.1.2);
3. <u>Horizontal distribution</u>: in the horizontal plane, macropore volume is distributed over cracks and holes. The shape of the horizontal cross-section of the macropore volume has a large impact on the water exchange between macropore volume and soil matrix, and on rapid drainage (Section 6.1.1.3).

The concept provides a functional rather than a meticulous description of these macropore geometry properties. With a limited number of input parameters it determines a functional macropore bottom depth distribution, and magnitude and horizontal shape of the macropore volume as a function of depth.

A basic assumption in the concept is that property 'persistency' is not correlated with both other properties. 'Persistency' refers to volume and not to pore structure: static macropore volume and dynamic macropore volume form together the total macropore volume. Characterisation according to the other two properties applies to the total volume. The properties 'continuity' and 'horizontal distribution' are correlated: the horizontal macropore volume distribution as a function of depth depends on the macropore bottom depth distribution.

6.1.1.1 Continuity

With respect to vertical and horizontal continuity the macropores are divided into two classes that are integrated in two domains:

1. Main Bypass (MB) flow domain: the network of continuous, horizontal interconnected macropores;
2. Internal Catchment (IC) domain: discontinuous non-interconnected macropores, ending at different depths.

The MB domain represents the main system of continuous structural and shrinkage cracks, as well as root and worm holes. These macropores penetrate relatively deep into the soil profile and are assumed to be horizontal interconnected, for example in a network of structural and shrinkage cracks. In the MB domain water is transported relatively fast and deep into the profile bypassing the soil matrix. This may lead to short-circuiting between soil surface and groundwater, and rapid drainage to drains.

The IC domain represents macropores − cracks and holes − that are not interconnected and not connected to the MB domain, and that end at different depths in the profile. In this domain macropore inflow is captured at the bottom of individual macropores, resulting in forced infiltration of macropore water into the (mainly) unsaturated soil matrix at different, relatively shallow depths.
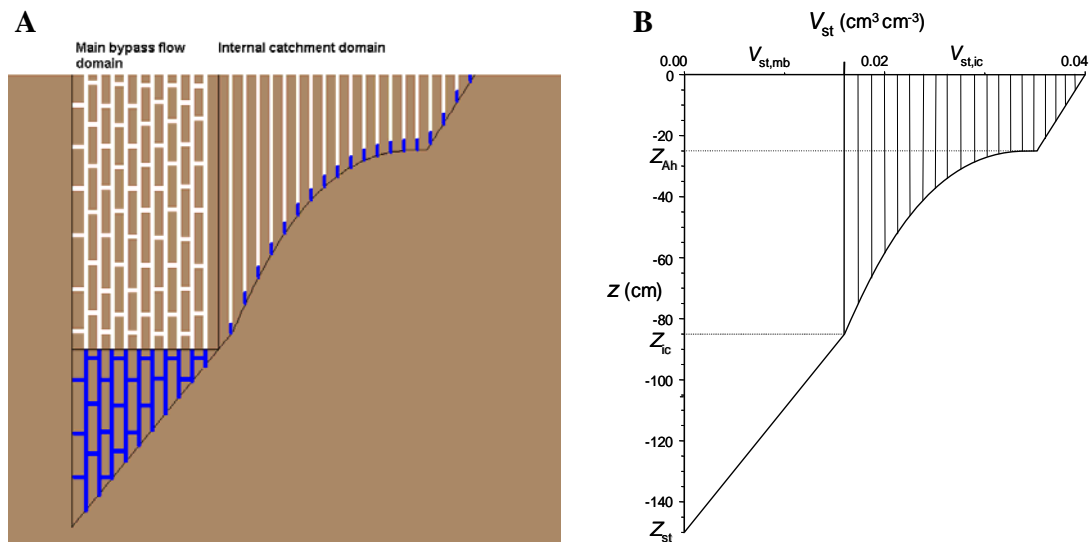
Figure 6.1 A: schematic representation of the two main domains: 1) Main bypass flow domain (MB): transporting water deep into the profile and possibly leading to rapid drainage, 2) Internal catchment domain (IC): infiltration of trapped water into the (mainly) unsaturated matrix at different depths; B: mathematical description of the two domains, as static macropore volume fraction V_{st} as a function of depth for the MB ($V_{st,mb}$) and IC ($V_{st,ic}$) domain, with the IC domain divided in several sub-domains.

Figure 6.1.A presents a conceptual visualisation of the two classes of macropores; Figure 6.1.B depicts a mathematical representation of the conceptual figure. It describes the static macropore volume fraction V_{st} (cm^3 cm^{-3}) of the two domains, $V_{st,mb}$ and $V_{st,ic}$, as a function of depth. From these two volume fractions the partition of the static macropore volume over the two domains at any depth can be calculated. This partition as a function of depth is a crucial property of macropore geometry in the concept. It determines the distribution of macropore volume and water flow over both domains. It is expressed in the volumetric proportion P_{dm} (-) of each domain dm:

$$P_{mb} = \frac{V_{st,mb}}{V_{st,mb} + V_{st,ic}} \quad \text{and} \quad P_{ic} = \frac{V_{st,ic}}{V_{st,mb} + V_{st,ic}} \qquad (6.1)$$

and

$$P_{mb} = 1 - P_{ic} \qquad (6.2)$$

where subscripts 'mb' and 'ic' refer to MB and IC domains, respectively.

In the concept, static macropore volume is not necessary always present. But even in the absence of this volume the volumetric proportions are required to partition the dynamic volume over the domains. Therefore, the calculation of the volumetric proportions as a function of depth is independent of the magnitude of the dynamic macropore volume. This calculation provides the 'blueprint' of the macropore domains. In order to visualize this 'blueprint' it is more illustrative to show only the static macropore volume as is done in Figure 6.1.B. Since the dynamic volume changes with time and depth, depending on shrinkage characteristic and soil moisture status that may differ at each depth, it would distort the image of the 'blueprint'.

The volumetric proportion of each domain as a function of depth is described by analytical equations with four basic input parameters: two depths (cm), Z_{AH} representing the bottom of the A-horizon and Z_{ic} representing the bottom of the IC domain, proportion $P_{ic,0}$ (-) of the IC domain at soil surface and power m (-), a shape factor. In order to describe the individual IC macropores, the IC domain is divided into sub-domains. Strictly speaking, this subdivision of the IC macropore volume is an aspect of the numerical implementation and therefore is discussed in Section 6.2.1.1.

The IC volumetric proportion at the soil surface $P_{ic,0}$ is an essential parameter of the concept. It determines the distribution over the two main domains of the precipitation water routed into the macropores at the soil surface, the major source of macropore water. It is assumed that the IC macropore volume consists of many individual small macropores that originates at the soil surface and functional end at different depths. In
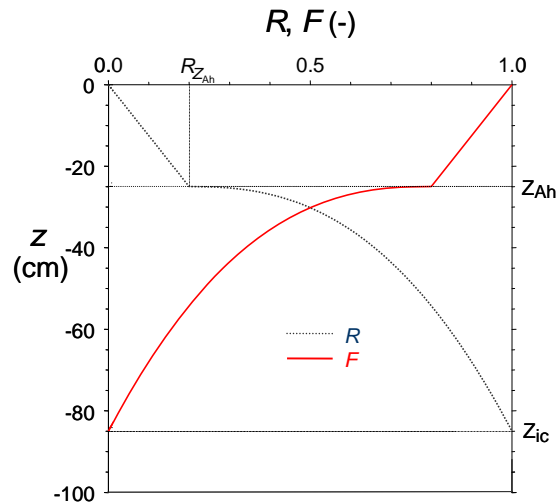
Figure 6.2 Cumulative frequency distribution R of the depth z at which the functional IC macropores end and the fraction F of IC macropores that is functional at depth z

this sense 'functional' implies that flow is blocked at the depth of ending of the macropores. Thus, the functional volume of IC macropores gradually declines to zero at depth Z_{ic}.

The cumulative frequency distribution of the depth z at which the functional IC macropores end in the concept is described with a power law function (Fig. 6.2):

$$R = R_{Z_{Ah}} \frac{z}{Z_{Ah}} \qquad \text{for} \ \ 0 \geq z > Z_{Ah} \qquad (6.3.a)$$

$$R = R_{Z_{Ah}} + \left(1 - R_{Z_{Ah}}\right)\left(\frac{Z_{Ah} - z}{Z_{Ah} - Z_{ic}}\right)^{m} \qquad \text{for} \ \ Z_{Ah} \geq z \geq Z_{ic} \qquad (6.3.b)$$

where the depths z, Z_{Ah} and Z_{ic} (cm) are defined negative downwards and the power m (-) is a shape-factor. Power $m < 1$ describes shallow IC systems, while $m > 1$ describes deep IC systems; $m = 1$ describes an intermediate system with a linear decline of functional IC macropores with depth. R_{ZAH} (-) is an optional parameter with which a linear increase of the *R*-curve over the thickness of the A-horizon can be described. Its default value is zero.

Curve *F* in Figure 6.2 depicts the complement of *R*, the cumulative frequency distribution of the depth at which IC macropores are not ended in the concept, i.e. the fraction of IC macropores that is functional at that depth *z*. Functional in the sense of downward transport and storage of water, and lateral infiltration of macropore water into the soil matrix:

$$F = 1 - R \qquad (6.4)$$

The volumetric proportion of IC macropore volume as a function of depth can be written in terms of the constant $P_{ic,0}$ and the function F:

$$P_{ic} = \frac{F}{\dfrac{1}{P_{ic,0}} + F - 1} \qquad \text{for } 0 \geq z > Z_{ic} \quad \text{and} \quad 0 < P_{ic,0} \leq 1 \qquad (6.5.a)$$

$$P_{ic} = 0 \qquad \text{for } z \leq Z_{ic} \qquad \text{and/or for } P_{ic,0} = 0 \qquad (6.5.b)$$

The volumetric proportion of MB macropore volume as a function of depth is calculated from function P_{ic} with Eq. [6.2]. This results in a proportion P_{mb} of 1 for depths below Z_{ic} where IC macropore volume is absent and all macropore volume is MB volume.

6.1.1.2 Persistency

With respect to persistency the macropore volume of each of the domains consists of:
1. Static macropore volume, expressed as volume fraction V_{st} (cm^3 cm^{-3}): macropores that are permanent present. The static volume as a function of depth is constant in time;
2. Dynamic macropore volume, expressed as volume fraction V_{dy} (cm^3 cm^{-3}) i.e. shrinkage cracks. The dynamic volume as a function of depth is not constant in time.

The dynamic shrinkage volume is added up to the static volume, if present, and in this way enlarges the total macropore volume (Fig. 6.3). The total macropore volume fraction V_{mp} (cm^3 cm^{-3}) is distributed over the two domains according to their volumetric proportion:

$$V_{mp} = V_{st} + V_{dy} \qquad (6.6.a)$$

$$V_{mb} = P_{mb}V_{mp} = P_{mb}\left(V_{st} + V_{dy}\right) = V_{st,mb} + P_{mb}V_{dy} \qquad (6.6.b)$$

$$V_{ic} = P_{ic}V_{mp} = P_{ic}\left(V_{st} + V_{dy}\right) = V_{st,ic} + P_{ic}V_{dy} \qquad (6.6.c)$$

This implies that below depth Z_{ic} all dynamic volume is part of the MB domain. And below depth Z_{st} dynamic volume only occurs.

Static macropore volume
The static macropore volume consists of structural shrinkage cracks, bio-pores (e.g., worm and root holes) and macropores that originate from tillage operations. Contrary to dynamic macropore volume, it is independent of the soil moisture status. The volu-
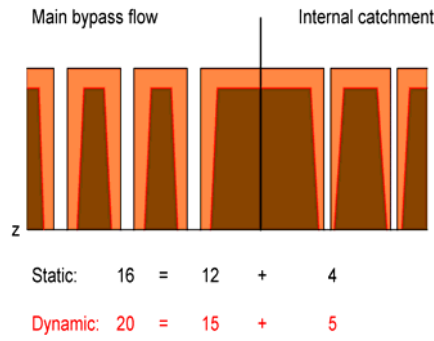
Figure 6.3 Partitioning of static and dynamic macropore volume over the two macropore domains according to the volumetric proportions of the domains (P_{ic} = 0.25): ratio between MB and IC domains is equal for static and dynamic macropore volume. White areas represent static and light areas dynamic macropore volume. Dark colour is the soil matrix. Numbers are imaginary macropore volumes meaning: Total = Main Bypass + Internal Catchment

me fraction of static macropores V_{st} (cm^3 cm^{-3}) as a function of depth z is described with the constant $P_{ic,0}$, the function F (Eq. [6.4]) and the two additional input parameters $V_{st,0}$ (-), describing the volume fraction of static macropores at the soil surface, and Z_{st} (cm), signifying the depth of static macropores.

In general (all V in cm^3 cm^{-3}):

$$V_{st} = V_{st,mb} + V_{st,ic} \quad \text{and thus} \quad V_{st,0} = V_{st,mb,0} + V_{st,ic,0} \tag{6.7.a}$$

where:

$$V_{st,ic,0} = P_{ic,0} V_{st,0} \quad \text{and} \quad V_{st,mb,0} = \left(1 - P_{ic,0}\right) V_{st,0} \tag{6.7.b}$$

The static macropore volume fraction of the MB domain as a function of depth is calculated as:

$$V_{st,mb} = V_{st,mb,0} \qquad \text{for } 0 \geq z > Z_{ic} \tag{6.8.a}$$

$$V_{st,mb} = V_{st,mb,0} \frac{z - Z_{st}}{Z_{ic} - Z_{st}} \qquad \text{for } Z_{ic} \geq z > Z_{st} \tag{6.8.b}$$

$$V_{st,mb} = 0 \qquad \text{for } z \leq Z_{st} \tag{6.8.c}$$

And the static macropore volume fraction of the IC domain as a function of depth:

$$V_{st,ic} = F\, V_{st,ic,0} \qquad \text{for } 0 \geq z > Z_{ic} \tag{6.9.a}$$

$$V_{st,ic} = 0 \qquad \text{for } z \leq Z_{ic} \tag{6.9.b}$$

Dynamic macropore volume

The dynamic macropore volume originates from the shrinking of the soil matrix due to soil moisture loss. In general, this process is restricted to soils that contain substantial amounts (> 10-15 mass-%) of clay minerals (except kaolonite) and/or organic matter. Mostly, the shrinkage volume occurs as shrinkage cracks. But shrinkage of the matrix may also enlarge cylinder-shaped macropores. In SWAP it is assumed that shrinkage enlarges the present permanent macropore volume and consequently the shrinkage volume is added up to the static volume (Eq. [6.3]).

Soil matrix shrinkage occurs in vertical and horizontal direction. Vertical shrinkage leads to soil surface subsidence, horizontal shrinkage to dynamic macropore volume. The dynamic volume is calculated from overall and vertical shrinkage as:

$$V_{dy} = V_{sh} - V_{su}$$ *(6.10)*

where V_{sh}, V_{dy} and V_{su} (all in cm^3 cm^{-3}) are the volume fraction of overall matrix shrinkage, the dynamic macropore volume fraction and the subsidence volume fraction, respectively.

In the present version of SWAP the vertical shrinkage does not affect the vertical coordinate system of SWAP. This approach avoids numerical problems that may result from solving Richards' equation for a dynamical vertical coordinate. We assume that at the field scale the effects of ignoring changes of the soil matrix in vertical direction are small as compared to effects of uncertainties in other processes and input parameters.

However, the approach of ignoring vertical changes in soil matrix does affect the calculation of the dynamic macropore volume. This volume is corrected for the vertical shrinkage according to:

$$V_{dy} = \frac{V_{sh} - V_{su}}{1 - V_{su}}$$ *(6.11)*

In this way the ratio between V_{dy} on one hand, and the matrix volume fraction and the static macropore volume fraction V_{st} on the other hand is consistent.

If static macropore volume is present, the horizontal area fraction of the matrix equals $1 - V_{st}$ cm^2 cm^{-2} and consequently the dynamic macropore volume fraction is calculated as:

$$V_{dy} = \left(1 - V_{st}\right) \frac{V_{sh} - V_{su}}{1 - V_{su}}$$ *(6.12)*

The vertical shrinkage component is determined from the overall matrix shrinkage as (Bronswijk, 1988):

$$V_{su} = 1 - \left(1 - V_{sh}\right)^{\frac{1}{r_s}} \qquad (6.13)$$

where exponent r_s (-) is the geometry factor (Rijniersce, 1983). In case of three-dimensional isotropic shrinkage, $r_s = 3$. When cracking dominates subsidence $r_s > 3$, when subsidence dominates cracking $1 < r_s < 3$. In case of subsidence only, $r_s = 1$. The geometry factor is an input parameter.

The matrix shrinkage volume fraction V_{sh} is a function of volumetric moisture content and shrinkage characteristic. A shrinkage characteristic describes the relationship between soil volume and soil moisture content. Many forms of shrinkage characteristics exist. A very convenient one is the characteristic that takes the constant volume fraction of the solid soil fraction V_{sol} as reference for all variable volume fractions and expresses the soil matrix volume fraction V_m in terms of pore volume fraction V_p relative to V_{sol} (Bronswijk, 1988) (all V in cm^3 cm^{-3}):

$$V_m = V_{sol} + V_p = (1 + e)V_{sol} \qquad (6.14)$$

where e (cm^3 cm^{-3}) is the void ratio:

$$e = \frac{V_p}{V_{sol}} \qquad (6.15)$$

The shrinkage volume fraction V_{sh} is equal to the fraction of volume loss of the matrix that in its turn equals the fraction loss of pore volume. The latter is expressed in terms of e and V_{sol}:

$$V_{sh} = -\Delta V_m = -\Delta V_p = -\Delta e V_{sol} = -\left(e - e_s\right)V_{sol} \qquad (6.16)$$

where e_s is the void ratio at saturation.

The shrinkage characteristic expresses the variable e as a function of the variable ϑ (cm^3 cm^{-3}), which represents the moisture ratio:

$$e = f\left(\vartheta\right) \qquad (6.17.a)$$

where the moisture ratio is defined as:

$$\vartheta = \frac{V_w}{V_{sol}} = \frac{\theta}{1 - \theta_s} \qquad (6.17.b)$$

with V_w (cm^3 cm^{-3}) the actual water volume fraction that equals θ, the volumetric moisture content of the matrix. Volume fraction of solids V_{sol} (cm^3 cm^{-3}) equals $1 - \theta_s$ ($\theta_s = \theta$ at saturation).

The exact form of the shrinkage characteristic depends on soil texture, in terms of content and nature of clay minerals, and organic matter. Shrinkage characteristics of clay and organic soils − peat and peaty soils − differ strongly.

Shrinkage characteristic of clay and clayey soils
Figure 6.4.A shows a typical shrinkage characteristic of a clay soil. Three stages can be distinguished (Stroosnijder, 1975; Bronswijk, 1988):
1. Normal shrinkage: volume decrease of clay aggregates is equal to moisture loss. The aggregates remain fully saturated;
2. Residual shrinkage: upon drying the volume of the aggregates still decreases, but moisture loss is greater than volume decrease. Air enters the pores of the aggregates;
3. Zero shrinkage: soil particles reach their most dense configuration. Upon further moisture extraction, the volume of the aggregates remains constant. Moisture loss equals air volume increase of the aggregates. Rigid soils, like sands, only show this stage.

A fourth shrinkage stage that precedes normal shrinkage may be recognized: structural shrinkage. When saturated soils dry, large water filled pores may be emptied. As a result, aggregates can get a somewhat denser packing. Overall, the volume changes in this stage are negligible, but water losses can be considerable. In SWAP, structural shrinkage is explicitly accounted for in the form of the static macropores, e.g. structural shrinkage cracks. The first three real shrinkage stages are computed as a function of moisture content with the equation of Kim (1992):

$$e = \alpha_K \exp(-\beta_K \vartheta) + \gamma_K \vartheta \quad \text{for } 0 < \vartheta < \vartheta_s \qquad \text{where} \quad \vartheta_s = \frac{\theta_s}{1 - \theta_s} \qquad (6.18)$$

with α_K (cm^3 cm^{-3}) equals e_0 the void ratio at $\vartheta = 0$, β_K, and γ_K are dimensionless fitting parameters and ϑ_s is void ratio at saturation. Using Eq. [6.18], e may become smaller than e_0, in which case the model sets e to e_0 (zero shrinkage).

Shrinkage characteristic of peat and peaty soils
According to Hendriks (2004), for peat soils three shrinkage stages can be distinguished as well (Fig. 6.4.B):
1. Near-normal shrinkage: volume reduction equals nearly moisture loss, little air enters the pores and the peat matrix remains close to saturation;
2. Subnormal shrinkage: upon drying moisture loss exceeds volume reduction, air enters the relatively large pores while the small pores in the organic fibres, that form the 'skeleton' around the larger pores, remain water-filled;
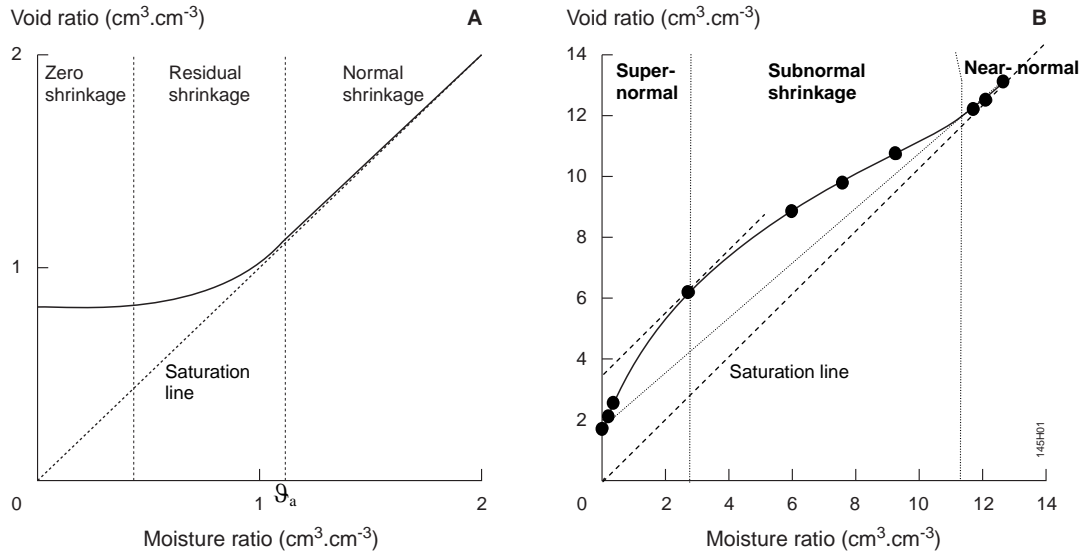
Figure 6.4 Typical shrinkage characteristic of A. clay (modified after Bronswijk, 1988) and B. peat (after Hendriks, 2004), expressed as void ratio e as a function of moisture ratio ϑ, showing the three shrinkage stages. Black dots in B. are measurements while solid line is fit with Eq.[6.19].

3. Supernormal shrinkage: volume reduction exceeds by far moisture loss, small pores are emptied and the skeleton collapses, so that air is driven out of the larger pores and the matrix reaches its final, smallest volume when the moisture content is zero.

Hendriks' (2004) equation for the shrinkage curve of peat and peaty soils reads:

$$e = e_t \left(1 + P_H \frac{\vartheta_t^{\alpha_H} \left(\exp(-\beta_H \vartheta_t) - \exp(-\beta_H) \right)}{\vartheta_{t,P}^{\alpha_H} \left(\exp(-\alpha_H) - \exp(-\beta_H) \right)} \right) \qquad \text{for } 0 < \vartheta < \vartheta_a \qquad (6.19.a)$$

$$e = e_t \qquad \qquad \text{for } \vartheta_a \le \vartheta < \vartheta_s \qquad (6.19.b)$$

with:

$$e_t = e_0 + \left(e_s - e_0 \right) \frac{\vartheta}{\vartheta_s} \; ; e_s = \vartheta_s = \frac{\theta_s}{1 - \theta_s} \qquad (6.19.c)$$

$$\vartheta_t = \frac{\vartheta}{\vartheta_a} \; ; \vartheta_{t,P} = \frac{\alpha_H}{\beta_H} \quad \text{for } 0 < \alpha_H < \beta_H \qquad (6.19.d)$$

where ϑ_a is the moisture ratio at the transition of the near-normal shrinkage stage to the subnormal shrinkage stage, when air entry increases substantially. α_H, β_H and P_H are dimensionless fitting parameters.

Overburden pressure

Shrinking and swelling behaviour in the field may deviate from that in the laboratory because of overburden pressure of overlaying soil layers in the field. This may result in delayed horizontal shrinkage in favour of vertical shrinkage. To account for this process, a threshold moisture content θ_{crack} is introduced. For moisture contents $\theta \geq \theta_{crack}$ all shrinkage is vertical and for $\theta < \theta_{crack}$ shrinkage is vertical and horizontal according to geometry factor r_s. This concept does not apply to swelling: shrinkage cracks are not closed before saturation. θ_{crack} is an input parameter.

6.1.1.3 Horizontal distribution

In the horizontal plane in the field, macropore volume is distributed over different forms of macropores: from holes with a diameter of 100 μm to several centimetres wide, several decimetres long cracks. This distribution determines the functional horizontal shape of the macropores, which forms the basis of the calculation of several important parameters:

1. two parameters that affect lateral water exchange between macropores and soil matrix:
   a. the vertical area of macropore walls per unit of volume, and
   b. the distance from macropore wall to centre of matrix polygons;
2. the lateral hydraulic conductivity of cracks in case of rapid drainage.

For simplicity and input parameter limitation, cracks and hole-shaped macropores are not explicitly distinguished. Instead, they are implicit in an effective functional horizontal macropore shape that is described by an effective matrix polygon diameter d_{pol} (cm) as a function of depth.

Assuming effective regular soil matrix polygons, the effective vertical area of macropore walls per unit of volume A^{*}_{wall} (cm^2 cm^{-3}) is equal to the quotient of the perimeter divided by the area of the polygons. For all even-sided regular polygons, from square to circle, this quotient equals (see 0 for derivation):

$$A^{*}_{wall} = \frac{4}{d_{pol}} \qquad (6.20)$$

The effective horizontal distance x_{pol} (cm) from macropore wall to matrix polygon centre is taken equal to:

$$x_{pol} = \frac{1}{2} d_{pol} \qquad (6.21)$$

The effect of horizontal macropore shape on rapid drainage is expressed through the effect on the lateral hydraulic conductivity of cracks which depends on the effective

crack width w_{cr} (cm) (see Section 6.1.2.3). This width is calculated from the effective polygon diameter and the volume fraction V_{mb} of macropores in the MB domain (see 0 for derivation):

$$w_{cr} = d_{pol}\left(1 - \sqrt{1 - V_{mb}}\right) \tag{6.22}$$

It is assumed that the effective diameter d_{pol} of the soil polygons is a function of depth with its minimum value at the soil surface where macropore density is maximal and consequently distances between macropores are relatively small, and its maximum value deeper in the profile where macropore density is minimal. d_{pol} as a function of depth is determined from a maximum $d_{p,max}$ and minimum $d_{p,min}$ polygon diameter, both input parameters, and the relative macropore density M (-) as a function of depth according to:

$$d_{pol} = d_{p,min} + \left(d_{p,max} - d_{p,min}\right)\left(1 - M\right) \tag{6.23.a}$$

where M depends on the static macropore volume if present:

$$M = \frac{V_{st}}{V_{st,0}} \qquad \text{for} \quad V_{st,0} > 0 \tag{6.23.b}$$

If no static macropore volume is present M depends on the volumetric proportion of the IC domain:

$$M = \frac{P_{ic}}{P_{ic,0}} \qquad \text{for} \quad V_{st,0} = 0 \quad \text{and} \quad P_{ic,0} > 0 \tag{6.23.c}$$

If no static macropore volume and no IC domain are present, M can be defined as a function of depth with Z_{dpmax} as the depth below which d_{pol} equals $d_{p,max}$:

$$M = \max\left(0, 1 - \frac{z}{Z_{dpmax}}\right) \quad \text{for} \quad V_{st,0} = 0 \quad \text{and} \quad P_{ic,0} = 0 \tag{6.23.d}$$

6.1.2 Water flow and balance

In SWAP macropore water flow and balance comprises (Fig. 6.5):
1. storage of water in the macropore domains S_{mp} (cm);
2. infiltration of water into macropores at soil surface, by precipitation, irrigation and snowmelt water falling directly into macropores I_{pr} and by overland flow (runoff) into the macropores I_{ru} (cm d^{-1});
3. lateral infiltration into the unsaturated soil matrix q_{lu} (cm d^{-1});
4. lateral infiltration into and exfiltration out of the saturated soil matrix q_{ls} (cm d^{-1});
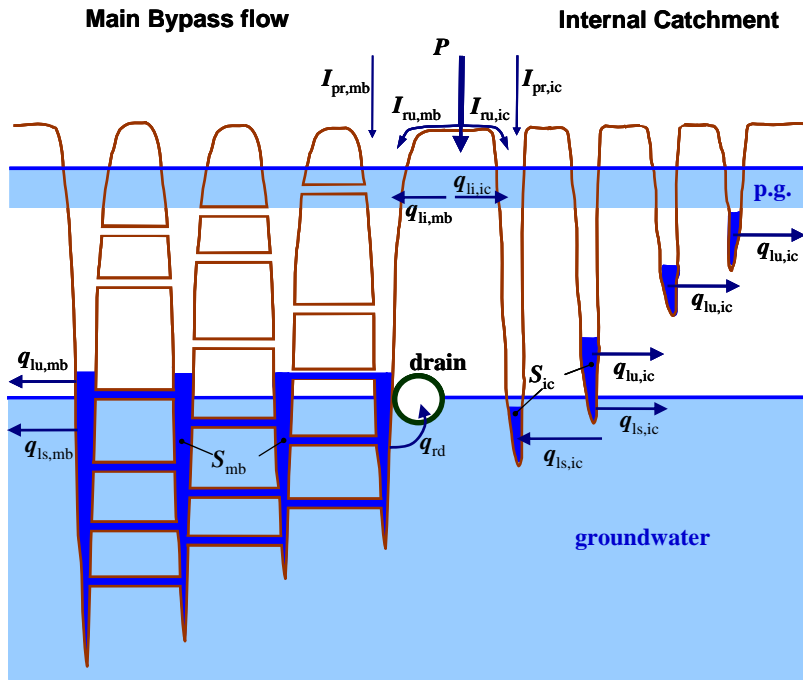
Figure 6.5 Schematic representation of the soil profile with soil matrix, drain, groundwater, perched groundwater (p.g.), macropores in MB and IC domains, and the various macropore water balance terms. Mark that the saturated lateral exchange flux q_{ls} can occur in two directions. See text for explanation of terms

5. lateral exfiltration out of the saturated soil matrix by interflow out of a zone with perched groundwater q_{li} (cm d^{-1});
6. rapid drainage to drainage systems q_{rd} (cm d^{-1}).

Water balance

The water balance of the MB domain for a given time interval d$t = t_0 \rightarrow t$ reads:

$$S_{mb}^t - S_{mb}^{t_0} = \int_{t_0}^{t} \left(I_{pr,mb} + I_{ru,mb} + q_{li,mb} - q_{lu,mb} - q_{ls,mb} - q_{rd} \right) dt \qquad (6.24.a)$$

where:

$$q_{li,mb} = \int_{z_{if,bot}}^{z_{if,top}} q_{li,mb}^* dz; \quad q_{lu,mb} = \int_{z_{uns,bot}}^{z=0} q_{lu,mb}^* dz; \quad q_{ls,mb} = \int_{z_{prof,bot}}^{z_{uns,bot}} q_{ls,mb}^* dz \qquad (6.24.b)$$

All balance terms are positive except q_{ls} which is positive in case of infiltration into the matrix and negative in case of exfiltration out of the matrix. The storage term is always less than or equal to the actual macropore volume. All flux densities q^* are defined per unit of depth (cm cm^{-1} d^{-1}). Depths $z_{if,top}$, $z_{if,bot}$, $z_{uns,bot}$ and $z_{prof,bot}$ (cm) refer to top and bottom of interflow zone, and bottom of unsaturated zone and soil profile, respectively.

The water balance calculation of the IC domain is equal to that of the MB domain with the exception of the rapid drainage term. Per definition, rapid drainage occurs exclusively in the MB domain.

Inflow at soil surface (I_{pr} and I_{ru})

The rate I_{pr} of precipitation, irrigation and snowmelt water routed directly into the macropores at the soil surface at a given precipitation/irrigation/snowmelt intensity P (cm d^{-1}) is calculated as:

$$I_{pr} = A_{mp}P \qquad (6.25)$$

where A_{mp} (cm^2 cm^{-2}) is the horizontal macropore area fraction at the soil surface which equals $V_{mp,0}$ (cm^3 cm^{-3}) the total macropore volume fraction at soil surface. For macropore domain dm (subscript dm = mb or ic) this direct infiltration reads:

$$I_{pr,dm} = A_{dm}P \quad \text{with} \quad A_{dm} = P_{dm,0}V_{mp,0} \qquad (6.26)$$

where $P_{dm,0}$ (-) is the volumetric proportion of domain dm at the soil surface. In case of a snowpack on top of the soil surface, it is assumed that the macropores are sealed off from the atmosphere and consequently $I_{pr} = 0$, except when snowmelt occurs.

Infiltration rate term I_{ru} occurs when the head boundary condition holds for the top boundary of the soil matrix (see Section 2.7.3.1). In that case the water balance of the ponding layer is calculated, which includes I_{ru}. Ponding occurs when the total of precipitation, irrigation, snow melt, runon and inundation intensity exceeds soil matrix infiltration capacity. Runoff into the macropores is described in the same form as used for regular runoff to surface water or adjacent fields (Section 4.1) to allow for similar incorporation into the numerical solution of the top boundary (Eq. [2.34] and [2.36]):

$$I_{ru} = \frac{h_0}{\gamma_{Iru}} \qquad (6.27)$$

where h_0 (cm) is the pressure head at the soil surface that equals the ponding height and γ_{Iru} (d) is the resistance for macropore inflow at the soil surface. The macropore inflow resistance is estimated from the maximum ponding height $h_{0,max}$ assuming no runoff, either into macropores or regular, and the vertical hydraulic conductivity of the macropores at soil surface $K_{ver,mp}$ (cm d^{-1}). The latter is derived as a function of effective macropore width at soil surface from a theoretical slit model presented by Bouma and Anderson (1973):

$$\gamma_{Iru} = \frac{h_{0,max}}{k_{ver,mp}} \quad \text{with} \quad K_{ver,mp} = 14.4 \cdot 10^8 \frac{w_{mp,0}^3}{d_{pol,0}} \qquad (6.28)$$

It can be seen that even the lower limit of macropore width (100 μm) yields large conductivities in the order of 100-1000 (cm d^{-1}) and consequently very low inflow resistances of 0.001-0.01 d. This implies that ponding water is routed preferentially into macropores. To account for the micro relief at the soil surface, mostly a threshold value for ponding height is used that must be exceeded before regular runoff starts. It is assumed that this does not apply to runoff into macropores, because it is very likely that micro depressions at the soil surface are connected to macropores. As a consequence, runoff into macropores is favoured over regular runoff and thus γ_{Iru} is not a very sensitive variable.

Distribution of I_{ru} over MB and IC domains is according to their proportions at the soil surface $P_{\mathrm{mb,0}}$ and $P_{\mathrm{ic,0}}$.

Lateral infiltration into the unsaturated matrix q_{lu}

Lateral infiltration of macropore water into the unsaturated soil matrix takes place strictly over the depth where stored macropore water is in contact with the unsaturated matrix. Two lateral infiltration mechanisms are relevant: absorption of macropore water when capillary forces dominate and Darcy flow due to a pressure head gradient from macropore wall to centre of the effective matrix polygon. Absorption is the dominant mechanism at low soil moisture contents. It will be negligible under wet conditions even when there is a large pressure head gradient. In the latter case Darcy flow will be dominant. Darcy flow is very small under dry conditions because of very low hydraulic conductivities. Therefore, for each situation the flow rates of both infiltration mechanisms are calculated and the unsaturated infiltration flux is set equal to the largest of these two rates.

Lateral absorption is described with Philip's sorptivity (Philip, 1957):

$$I^{*}_{\mathrm{ab},t} = A^{*}_{\mathrm{wall,mtx}} S_{\mathrm{P}} \sqrt{t - t_0} = \frac{4 S_{\mathrm{P}} \sqrt{t - t_0}}{d_{\mathrm{pol}} \sqrt{1 - V_{\mathrm{mp}}}} \tag{6.29}$$

where $I^{*}_{\mathrm{ab},t}$ is the lateral absorption per unit of depth (cm cm^{-1}) over time interval $t_0 \rightarrow t$ (d) and S_{P} is Philip's sorptivity (cm d$^{-0.5}$). The meaning of $A^{*}_{\mathrm{wall,mtx}}$ is explained in Appendix 2 (Eq.[A2.12]). S_{P} is a function of initial volumetric moisture content θ_0 (cm^3 cm^{-3}) at $t = t_0$, the time of first contact of macropore water with the matrix. It is empirically described as (adapted from Greco et al., 1996):

$$S_{\mathrm{P}} = S_{\mathrm{P,max}} \left(1 - \frac{\theta_0 - \theta_{\mathrm{r}}}{\theta_{\mathrm{s}} - \theta_{\mathrm{r}}} \right)^{\alpha_{\mathrm{S}}} = S_{\mathrm{P,max}} \left(\frac{\theta_{\mathrm{s}} - \theta_0}{\theta_{\mathrm{s}} - \theta_{\mathrm{r}}} \right)^{\alpha_{\mathrm{S}}} \tag{6.30}$$

where $S_{\mathrm{P,max}}$ is the maximum sorptivity when $\theta_0 = \theta_{\mathrm{r}}$ (residual moisture content) and α_{S} is a fitting parameter (-).

Average, constant absorption rate $q^*_{lu,ab}$ per unit of depth (cm cm^{-1} d^{-1}) for time interval $t_1 \rightarrow t_2$ is obtained from:

$$q^*_{lu,ab} = \frac{I^*_{ab,t_2} - I^*_{ab,t_1}}{t_2 - t_1}$$

(6.31)

Infiltration rate by Darcy flow per unit of depth $q^*_{lu,D}$ (cm cm^{-1} d^{-1}) reads:

$$q^*_{lu,D} = f_{shp} A^*_{wall} K_h \frac{\left(h_{mp} - h_{mt}\right)}{x_{pol}} = \frac{f_{shp} 8 K_h \left(h_{mp} - h_{mt}\right)}{d^2_{pol}}$$

(6.32)

where K_h (cm d^{-1}) is the hydraulic conductivity as a function of pressure head in the unsaturated matrix h_{mt} (cm) and term $(h_{mp} - h_{mt}) / x_{pol}$ is the lateral pressure head gradient between macropore and centre of the matrix polygon. Parameter f_{shp} (-) is a shape factor to account for the uncertainties in the theoretical description of lateral infiltration by Darcy flow originating from uncertainties in the exact shape of the soil matrix polygons. Depending on whether the polygons are more plate or cylinder shaped, the figure in Eq. [6.32] should be somewhere between 8 and 16. Thus, theoretically, the value of f_{shp} lies between 1 and 2. Pressure head h_{mp} as a function of depth is obtained from the macropore water level elevation φ_{mp} and depth z as:

$$h_{mp} = \varphi_{mp} - z$$

(6.33)

Finally, the lateral infiltration fluxdensity into the unsaturated matrix per unit of depth q^*_{lu} (cm cm^{-1} d^{-1}) is obtained by taking the largest flow rate:

$$q^*_{lu} = \max\left(q^*_{lu,ab}, q^*_{lu,D}\right)$$

(6.34)

Distribution of q^*_{lu} over MB and IC domains is according to their proportions P_{mb} and P_{ic} at the specific depth z.

Lateral infiltration into and exfiltration out of the saturated matrix q_{ls}

Lateral infiltration of macropore water into the saturated soil matrix and lateral exfiltration of soil matrix water into the macropores takes place strictly over the depth where stored macropore water is in contact with the saturated matrix. This only concerns static macropores below the groundwater table, since in the present concept in saturated condition the soil is assumed swollen to its maximum volume, without dynamic macropore volume.

The lateral in- and exfiltration rate per unit of depth $q^*_{ls,D}$ (cm cm^{-1} d^{-1}) in case of water filled macropores ($h_{mp} > 0$) is described by Darcy flow similar to Eq. [6.32]:

$$q^*_{ls,D} = f_{shp} A^*_{wall} K_{sat} \frac{\left(h_{mp} - h_{mt}\right)}{x_{pol}} = \frac{f_{shp} 8 K_{sat} \left(h_{mp} - h_{mt}\right)}{d^2_{pol}}$$

(6.35)

The same shape factor f_{shp} as in Eq. [6.32] is adopted since the same considerations about uncertainties in the exact shape of the soil matrix polygons apply. Infiltration occurs if $h_{mp} > h_{mt}$ and exfiltration if $h_{mp} < h_{mt}$.

Exfiltration rate out of the matrix into empty macropores ($h_{mp} = 0$) is described as a seepage face: $q^*_{ls,seep}$ (cm cm^{-1} d^{-1}). It is approached with a seepage resistance γ_{seep} (d) that is based on Ernst's drainage resistance equation Eq. [4.16] without term γ_{entr}:

$$q^*_{ls,seep} = -\frac{h_{mt}}{\gamma_{seep}} = -\frac{h_{mt}}{\gamma_{ver} + \gamma_{hor} + \gamma_{rad}} \qquad (6.36.a)$$

$$\gamma_{ver} = \frac{D_{seep}}{K_{sat}} \qquad \text{with } D_{seep} = \varphi_{gwl} - z_{seep} \qquad (6.36.b)$$

$$\gamma_{hor} = \frac{d^2_{pol}}{8 K_{sat} D_{seep}} \qquad (6.36.c)$$

$$\gamma_{rad} = \frac{d_{pol}}{\pi K_{sat}} \ln\left(\frac{D_{seep}}{u_{seep}}\right) \qquad (6.36.d)$$

where φ_{gwl} (cm) is the groundwater elevation, z_{seep} (cm) is bottom of seepage layer which equals depth of either bottom of macropores or macropore water level, D_{seep} (cm) is thickness of seepage zone and u_{seep} (cm) is thickness of seepage face which is set to 10% of D_{seep}. Eq. [6.36.b]-Eq. [6.36.d] are derived from Eq. [4.20]-Eq. [4.22].

Distribution of q^*_{li} over MB and IC domains is according to their proportions P_{mb} and P_{ic} at the specific depth z.

Lateral exfiltration out of the saturated matrix as interflow qli
Lateral exfiltration q^*_{li} (cm cm^{-1} d^{-1}) out of the saturated soil matrix into macropores by interflow (Section 4.2) out of a zone with perched groundwater occurs over the depth of perched groundwater. This process is a special case of exfiltration of soil water from the saturated zone into the macropores and is described in a similar way using Eq. [6.35] and Eq. [6.36], but with an opposite sign due to its definition in Eq. [6.24]. If $h_{mp} > h_{mt}$, infiltration into the saturated matrix in the perched groundwater zone occurs according to Eq. [6.35]. A perched groundwater zone is here defined as a saturated zone above groundwater level that is separated from the saturated zone below groundwater level by an unsaturated zone which contains at least a critical value $V_{undsat,crit}$ (default: 0.1 cm) of under-saturated volume $V_{undsat} (= \int[\theta_s - \theta]dz$ cm$)$.

Distribution of q^*_{li} over the MB and IC domains is according to their proportions P_{mb} and P_{ic} at the specific depth z.

Rapid drainage q_{rd}

Rapid drainage q_{rd}

Rapid drainage to drainage systems can occur via a network of lateral interconnected cracks or via otherwise (nearly) interconnected macropores. Also when macropores are separated by just thin walls of soil matrix they can enhance drainage considerably. Fed by macropore water, the small matrix barriers will become saturated even when the soil matrix as a whole remains unsaturated. They then form part of a saturated macropore-soil-matrix-system that conducts water better in vertical and horizontal direction than the bulk of the soil matrix (Nieber et al., 2006). Sidle et al. (2001) proposed the concept of a self-organising network of preferential flow pathways, where the connections in the network are controlled by moisture level.

In SWAP, the complex process of rapid drainage is described with a drainage resistance. This resistance may depend on the width of macropores and of shrinkage cracks in particular: wider cracks have higher hydraulic conductivities. It may also depend on macropore water level: the higher this level, the more macropore volume involved, the higher the hydraulic conductivity and the lower the resistance. Therefore, the functional input parameter 'drainage resistance' is considered as a reference drainage resistance: it is valid for a defined reference situation. The actual drainage resistance is derived from the reference resistance according to the deviations from the actual situation to the reference situation.

The reference situation is preferably an average situation at the field scale and should be based on a relevant reference level. In this SWAP version it is fixed. The reference level is chosen to be the drainage basis: drain depth or surface water level. The definition of the reference situation is: soil moisture is in hydrostatic equilibrium with groundwater level at depth of drainage basis and with the water level in the MB macropores at a depth of three-quarters of the drainage basis depth.

The actual drainage resistance γ_{act} (d) is calculated from the reference drainage resistance γ_{ref} (d) according to the ratio between actual and reference transmissivity *KD* of the MB macropores (cm^2 d^{-1}):

$$\gamma_{act} = \frac{\left[KD\right]_{act}}{\left[KD\right]_{ref}} \gamma_{ref} \qquad\qquad (6.37.a)$$

where:

$$\left[KD\right] = \int_{z_{botMB}}^{z_{levMB}} K_{lat} \, dz = \int_{z_{botMB}}^{z_{levMB}} C \frac{w_{cr}^{r_{rd}}}{d_{pol}} \, dz = C \int_{z_{botMB}}^{z_{levMB}} \frac{w_{cr}^{r_{rd}}}{d_{pol}} \, dz \qquad\qquad (6.37.b)$$

with K_{lat} (cm d^{-1}) the lateral hydraulic conductivity of the macropores, z_{botMB} and z_{levMB} (cm) the depths of the bottom of and the water level in the MB macropores. C

is a constant that follows from the slit model for conductivity (Eq. [6.28]). Its value is irrelevant because it is eliminated in Eq. [6.37.a]). The exponent r_{rd} (-) is a reaction coefficient that determines the effect of width w_{cr} (cm) on γ_{act}. It varies between 0 and 3. When $r_{rd} = 0$, γ_{act} becomes independent of w_{cr}.

Rapid drainage flux q_{rd} (cm d^{-1}) is calculated from MB domain water level elevation φ_{MB} (cm) above drainage level φ_{db} (cm) and γ_{act} (d^{-1}) at actual moisture content:

$$q_{rd} = \frac{\varphi_{MB} - \varphi_{db}}{\gamma_{act}} \tag{6.38}$$

6.2 Numerical implementation

SWAP applies the same vertical spatial (Δz) and temporal (Δt) discretisation for macropore flow as is used for matrix flow. Besides, SWAP uses a horizontal discretisation in the form of macropore domains for macropore flow. In this section the horizontal discretisation, its relationship with vertical and temporal discretisation, and the numerical implementation of water balance and flow equations are described.

6.2.1 Macropore geometry

6.2.1.1 Continuity

To obtain the required resolution in IC macropores, the IC domain is divided into n_{sd} sub-domains. This partition represents the horizontal discretisation of the macropore system. The IC volume at soil surface, minus the R_{ZAH}-volume, is equally distributed over the n_{sd} sub-domains. Thus, all n_{sd} sub-domains take up an equal amount of infiltrating water at the soil surface. The volumetric proportion $P_{sd,j}$ of sub-domain j as a function of z is calculated according to:

$$P_{sd,j} = \frac{1}{\frac{1}{P_{ic,0}} + F - 1} \frac{1 - R_{Z_{Ah}}}{n_{sd}} \qquad \text{for} \quad 0 \geq z > z_{sd,j+1} \tag{6.39.a}$$

$$P_{sd,j} = \frac{\left(F - \frac{j-1}{n_{sd}} \left(1 - R_{Z_{Ah}} \right) \right)}{\frac{1}{P_{ic,0}} + F - 1} \qquad \text{for} \quad z_{sd,j+1} \geq z > z_{sd,j} \tag{6.39.b}$$

$$P_{sd,j} = 0 \qquad \text{for} \quad z \leq z_{sd,j} \tag{6.39.c}$$

where $j = 1$ is the deepest and $j = n_{sd}$ the shallowest sub-domain (respectively left and right in Fig. 6.1.B), and $z_{sd,j}$ is the depth at which sub-domain j ends:

$$z_{sd,j} = Z_{Ah} - (Z_{Ah} - Z_{ic})\left(1 - \frac{j-1}{n_{sd}}\right)^{\frac{1}{m}} \qquad (6.40)$$

If option $R_{ZAH} > 0$ is chosen, an extra Ah-sub-domain $j = n_{sd} + 1$ is created with proportion:

$$P_{sd,n_{sd}+1} = \frac{R_{Z_{Ah}} + F - 1}{\dfrac{1}{P_{ic,0}} + F - 1} \qquad \text{for} \quad 0 \geq z > Z_{Ah} \qquad (6.41.a)$$

$$P_{sd,n_{sd}+1} = 0 \qquad \text{for} \quad z \leq Z_{Ah} \qquad (6.41.b)$$

Because the MB domain is always present, though sometimes with very low proportion, the total number of domains $n_{dm} = n_{sd} + 1$. In case of $R_{ZAH} > 0$, $n_{dm} = n_{sd} + 2$. All domains are numbered from $j = 1$ to n_{dm} with the MB domain being the first domain $j = 1$ and the deepest IC domain the second $j = 2$.

In the model, the vertical coordinate z is partitioned into discrete model compartments i with thickness $\Delta z_{,i}$ (cm) between $z_{b,i}$ and $z_{t,i}$ at the bottom and top of the compartment, respectively. For each compartment a discrete macropore volume per domain is required. Volumetric proportion $P_{j,i}$ for each combination of domain j and compartment i is obtained by integration of P_{MB} and $P_{sd,j}$ as a function of z over the compartment thickness and dividing by Δz_i:

$$P_{1,i} = \frac{\displaystyle\int_{z_{b,i}}^{z_{t,i}} P_{MB}\, dz}{\Delta z_i} \qquad \text{and} \quad P_{j,i} = \frac{\displaystyle\int_{z_{b,i}}^{z_{t,i}} P_{sd,j-1}\, dz}{\Delta z_i} \qquad \text{for} \quad 2 \leq j \leq n_{dm} \qquad (6.42)$$

Per domain the macropore volume is vertically interconnected over the soil compartments. Domains $j > 1$ to $j + n_{dl,j}$ inclusive, that end in the same model compartment, are functionally equal and therefore are lumped for all compartments $i = 1$ to ndb_j (compartment number that contains bottom of domain j):

$$P_{j,i} = P_{j,i} + \sum_{l=1}^{n_{dl,j}} P_{j+l,i} \quad \text{and} \quad P_{l,i} = P_{l+n_{dl,j},i} \quad \text{for all } l: \ j+1 \leq l \leq n_{dm} - n_{dl,j} \qquad (6.43)$$

For each lumped domain n_{dm} is reduced with 1. In this way, the resolution of the horizontal discretisation in terms of n_{dm} is determined by n_{sd}, the thickness of

compartments and the shape of curve F: the combination of large n_{sd}, small Δz's in the IC domain and a linear F-curve ($m = 1$) yields the largest n_{dm}.

6.2.1.2 Persistency

The volume of macropores $V_{mp,j,i}$ (cm^3 cm^{-2} unit of area) for domain j in compartment i is calculated for each time-step Δt as:

$$V_{mp,j,i} = P_{j,i} \left(V_{st,i} + V_{dy,i} \right) \tag{6.44}$$

Static $V_{st,i}$ and dynamic $V_{dy,i}$ macropore volume (cm^3 cm^{-2}) in each compartment i are obtained as explained below. Dynamic volume is changing in time, static volume is not. Consequently, if dynamic volume is present in compartment i, the total macropore volume in this compartment is changing in time as well.

The total volume $V_{dm,j}$ (cm^3 cm^{-2}) of macropore domain j equals:

$$V_{dm,j} = \sum_{i=1}^{ndb_j} V_{mp,j,i} \tag{6.45}$$

where ndb_j is the number of the compartment that contains the bottom of domain j.

Static macropore volume

The volumes of static macropores per compartment i for the MB and IC domain, $V_{st,mb,i}$ and $V_{st,ic,i}$ (cm^3 cm^{-2}), are obtained by integration over Δz_i:

$$V_{st,mb,i} = \int_{z_{b,i}}^{z_{t,i}} V_{st,mb} \, dz \quad \text{and} \quad V_{st,ic,i} = \int_{z_{b,i}}^{z_{t,i}} V_{st,ic} \, dz \tag{6.46}$$

The total volume of static macropores $V_{st,i}$ in compartment i equals:

$$V_{st,i} = V_{st,mb,i} + V_{st,ic,i} \tag{6.47}$$

Dynamic macropore volume

Dynamic macropore volume $V_{dy,i}$ (cm^3 cm^{-2}) in compartment i is computed for each time-step Δt by substituting Eq. [6.13] in Eq. [6.12] and multiplying with compartment thickness Δz_i:

$$V_{dy,i} = \left(1 - \frac{V_{st,i}}{\Delta z_i} \right) \frac{V_{sh,i} + \left(1 - V_{sh,i} \right)^{\frac{1}{r_{s,i}}} - 1}{\left(1 - V_{sh,i} \right)^{\frac{1}{r_{s,i}}}} \Delta z_i \tag{6.48}$$

The shrinkage volume fraction $V_{sh,i}$ (cm^3 cm^{-3}) is calculated from actual moisture content and shrinkage characteristic of compartment i at the beginning of Δt:

$$V_{\text{sh},i} = \left(e_{\text{s},i} - e_i \right) V_{\text{sol},i} \qquad\qquad (6.49.a)$$

where:

$$e_i = \text{f}\left(\vartheta_i \right)_i, \; \vartheta_i = \frac{\theta_i}{V_{\text{sol},i}}, \; e_{\text{s},i} = \vartheta_{\text{s},i} = \frac{\theta_{\text{s},i}}{V_{\text{sol},i}} \; \text{ and } \; V_{\text{sol},i} = 1\text{-}\theta_{\text{s},i} \qquad (6.49.b)$$

with θ_i is the actual and $\theta_{\text{s},i}$ the saturated volumetric moisture content (cm^3 cm^{-3}) of compartment i.

In order to correctly model infiltration into the soil matrix at soil surface, thin model compartments in the order of 1 cm thick are advised for the top of the soil profile (Van Dam and Feddes, 2000). Because of the dynamical conditions at soil surface and the small storage capacity of the thin compartments, moisture contents may change rapidly. As a result shrinkage volume at soil surface may appear and disappear faster than in reality. Because the quantity of shrinkage volume at the soil surface is crucial for determining the amount of precipitation water infiltrating into the macropores, shrinkage volume of the first compartments is calculated on the basis of moisture content of the compartment that contains a reference depth z_{crack}, where moisture conditions are less dynamical. z_{crack} is an input parameter.

6.2.1.3 Horizontal distribution

Effective diameter of soil polygons $d_{\text{pol},i}$ (cm) for compartment i is calculated with Eq. [6.23] by substituting $V_{\text{st},i}$, $1 - P_{1,i}$ and z_i for V_{st}, P_{ic} and z, respectively. z_i (cm) is the depth of node i which is in the middle of compartment i.

The effective vertical area of macropore walls per unit of horizontal area $A_{\text{wall},i}$ (cm^2 cm^{-2}) is obtained by multiplying the vertical area of macropore walls per unit of volume $A^{*}_{\text{wall},i}$ with compartment thickness Δz_i:

$$A_{\text{wall},i} = A^{*}_{\text{wall}}\Delta z_i = \frac{4}{d_{\text{pol},i}}\Delta z_i \qquad\qquad (6.50)$$

The effective horizontal distance $x_{\text{pol},i}$ (cm) is calculated with Eq. [6.21] by substituting $d_{\text{pol},i}$ for d_{pol}. The effective crack width $w_{\text{cr},i}$ (cm) in the MB domain for compartment i is calculated from Eq. [6.22] as:

$$w_{\text{cr},i} = d_{\text{pol},i}\left(1 - \sqrt{1 - \frac{V_{\text{mp},1,i}}{\Delta z_i}} \right) \qquad\qquad (6.50)$$

6.2.2 Water flow and balance

The water balance of macropore domain $j = 1$ (MB domain) for time-step Δt (d) reads in accordance with Eq. [6.24]:

$$S_j^t - S_j^{t-\Delta t} = \left(I_{\mathrm{pr},j} + I_{\mathrm{ru},j} + \sum_{i=nit}^{nib} q_{\mathrm{li},j,i}\Delta z_i - \sum_{i=1}^{nub} q_{\mathrm{lu},j,i}\Delta z_i - \sum_{i=nub+1}^{ndb_j} q_{\mathrm{ls},j,i}\Delta z_i - q_{\mathrm{rd}} \right)\Delta t \quad (6.52)$$

Water balance equations of all other domains $j > 1$ are equal to Eq. [6.52] but with exclusion of the rapid drainage term q_{rd} that only applies to domain 1, the MB domain. The compartment numbers nit, nib, nub and ndb_j refer to the top and bottom compartment with interflow from perched groundwater, the bottom (deepest) unsaturated compartment and the compartment with bottom of domain j, respectively. Storage S_j is always limited to $0 \leq S_j \leq V_{\mathrm{dm},j}$. In case of water deficit ($S_j < 0$) all outgoing fluxes are decreased with a part of the deficit according to their relative rate. In case of water excess ($S_j > V_{\mathrm{dm},j}$) all incoming fluxes are decreased with a part of the excess according to their relative rate. The excess of the inflow at soil surface is distributed over macropore domains that are not fully filled up, that is, if $S < V_{\mathrm{dm}}$ for a particular domain. The remaining excess is added to the ponding layer.

Inflow at soil surface (I_{pr} and I_{ru})

The inflow at the soil surface fluxes Ipr and Iru (cm d-1) are calculated according to Eq.'s [6.25] to [6.28] with the relevant properties of the first compartment. When these fluxes exceed storage capacity of total macropore volume, the inflow excess is added to the ponding layer before calculation of regular runoff takes place.

Distribution of I_{pr} and I_{ru} over all macropore domains j is according to the domains proportions at soil surface, that is, in model compartment 1:

$$I_{\mathrm{pr},j} = P_{j,1}I_{\mathrm{pr}} \quad \text{and} \quad I_{\mathrm{ru},j} = P_{j,1}I_{\mathrm{ru}} \qquad (6.53)$$

Lateral infiltration into the unsaturated matrix q_{lu}

Cumulative lateral absorption $I_{\mathrm{ab},j,i}$ (cm) for all compartments i of the unsaturated matrix that are in contact with water in macropore domain j is computed according to Eq. [6.29]:

$$I_{\mathrm{ab},j,i} = P_{j,i} A_{\mathrm{wall,mtx},i} S_{\mathrm{P},j,i} \sqrt{t_{\mathrm{cum},j,i}} = P_{j,i} \frac{4\Delta z_i S_{\mathrm{P},j,i} \sqrt{t_{\mathrm{cum},j,i}}}{d_{\mathrm{pol},i}\sqrt{1 - \left(V_{\mathrm{dy},i} + V_{\mathrm{st},i}\right)\Big/\Delta z_i}} \qquad (6.54)$$

where $t_{\mathrm{cum},j,i}$ (d) is the cumulative time since first contact of compartment i with water in macropore domain j. At each new contact event, $S_{\mathrm{P},j,i}$ and $t_{\mathrm{cum},j,i}$ are updated.

The sorptivity approach assumes that the moisture content is not influenced by another process then sorption. In the model, moisture content θ_i is also affected by vertical matrix flow and uptake by roots. To account for this inadequacy, for each time-step sorptivity $S_{P,j,i}$ is corrected according to the deviation $\Delta\theta_i$ between actual θ_i and theoretical $\theta_{thr,j,i}$ moisture content at the beginning of the time-step:

$$S_{P,j,i} = S_{P,\max,i} \left(\frac{\theta_{s,i} - \theta_{0,j,i} - \Delta\theta_{j,i}}{\theta_{s,i} - \theta_{r,i}} \right)^{\alpha_{s,i}} \qquad (6.55)$$

where $\Delta\theta_{j,i} = \theta_i - \theta_{thr,j,i}$. For further explanation, see Eq. [6.30]. $\theta_{thr,j,i}$ is computed with Eq. [6.54] on the basis of initial sorptivity $S_{P,j,i}$ that is obtained by Eq. [6.55] without term $\Delta\theta_{j,i}$.

The lateral absorption rate during time step Δt is linearised to obtain an average, constant rate $q_{lu,ab,j,i}$ (cm d^{-1}):

$$q_{lu,ab,j,i} = \frac{I_{ab,j,i}^{t} - I_{ab,j,i}^{t-\Delta t}}{\Delta t} \qquad (6.56)$$

Infiltration rate $q_{lu,D,j,i}$ (cm d^{-1}) by lateral Darcy flow from domain j into compartment i reads in accordance to Eq. [6.32]:

$$q_{lu,D,j,i} = P_{j,i} f_{shp} A_{wall,i} K_{h,i} \frac{\left(h_{mp,j,i} - h_{mt,i} \right)}{x_{pol,i}} = P_{j,i} \frac{f_{shp} 8 K_{h,i} \left(h_{mp,j,i} - h_{mt,i} \right)}{d_{pol,i}^{2}} \qquad (6.57)$$

where $h_{mp,j,i}$ is calculated with Eq. [6.33] by using $\varphi_{mp,j}$ (cm), the water level in domain j, and z_i.

The resulting lateral infiltration rate $q_{lu,j,i}$ (cm d^{-1}) from macropore domain j into unsaturated compartment i is derived from Eq. [6.34].

Lateral infiltration into and exfiltration out of the saturated matrix q_{ls}
Rate of lateral water exchange $q_{ls,j,i}$ (cm d^{-1}) between macropore domain j and saturated compartment i by Darcy flow is computed in accordance to Eq. (6.35):

$$q_{ls,D,j,i} = P_{j,i} f_{shp} A_{wall,i} K_{sat,i} \frac{\left(h_{mp,j,i} - h_{mt,i} \right)}{x_{pol,i}} = P_{j,i} \frac{f_{shp} 8 K_{sat,i} \left(h_{mp,j,i} - h_{mt,i} \right)}{d_{pol,i}^{2}} \qquad (6.58)$$

and in case of a seepage face ($h_{mp,j,I} = 0$) according to Eq. (6.36):

$$q_{ls,seep,j,i} = -\frac{h_{mt,i}}{\gamma_{ver,i} + \gamma_{hor,i} + \gamma_{rad,i}} \qquad (6.59.a)$$

$$\gamma_{\text{ver},i} = \frac{\Delta z_i}{K_{\text{sat},i}} \qquad (6.59.b)$$

$$\gamma_{\text{hor},i} = \frac{d_{\text{pol},i}^2}{8 K_{\text{sat},i} \Delta z_i} \qquad (6.59.c)$$

$$\gamma_{\text{rad},i} = \frac{d_{\text{pol},i}}{\pi K_{\text{sat},i}} \ln\left(\frac{\Delta z_i}{u_{\text{seep},i}}\right) \qquad (6.59.d)$$

where $u_{\text{seep},i}$ is set to 10% of Δz_i.

Lateral exfiltration out of the saturated matrix as interflow q_{li}

Lateral exfiltration rate qli,j,i (cm d−1) out of compartment i with perched groundwater into macropore domain j by interflow is calculated according to Eq. (6.58) and Eq. (6.59) with an opposite sign.

Rapid drainage q_{rd}

The actual drainage resistance γ_{act} (d^{-1}) for calculating rapid drainage flux q_{rd} (cm d^{-1}) according to Eq. [6.30] is obtained by:

$$\gamma_{\text{act}} = \frac{\displaystyle\sum_{i=nl_{\text{act}}}^{nb_{\text{act}}} \frac{w_{\text{cr},\text{act},i}^{r_{\text{rd}}}}{d_{\text{pol},i}} \Delta z_i}{\displaystyle\sum_{i=nl_{\text{ref}}}^{nb_{\text{ref}}} \frac{w_{\text{cr},\text{ref},i}^{r_{\text{rd}}}}{d_{\text{pol},i}} \Delta z_i} \gamma_{\text{ref}} \qquad (6.60)$$

where *nl* and *nb* are the numbers of the compartments with the water level and the bottom of the MB domain, respectively, for actual and reference situation.

For use in solute models, the rapid drainage flux q_{rd} is distributed over the compartments nl_{act} to nb_{act} according to their relative KD values:

$$q_{\text{rd},i} = \frac{\dfrac{w_{\text{cr},\text{act},i}^{r_{\text{rd}}}}{d_{\text{pol},i}} \Delta z_i}{\displaystyle\sum_{i=nl_{\text{act}}}^{nb_{\text{act}}} \frac{w_{\text{cr},\text{act},i}^{r_{\text{rd}}}}{d_{\text{pol},i}} \Delta z_i} q_{\text{rd}} \qquad (6.61)$$

Numerical solution

For the numerical solution of Richards' equation (Section 2.7.2) the partial derivative of the exchange between macropores and matrix to the pressure head must be added to the total partial derivative to the pressure head. For each compartment *i* the macropore contribution to this derivative is the sum of the derivatives of all $n_{\text{dm},i}$ macropore domains *j*:

$$\frac{\partial S_{m,i}^{l+1,p}}{\partial h_i^{l+1,p}} = \sum_{j=1}^{n_{dm,i}} \left(\frac{\partial S_{m,j,i}^{l+1,p}}{\partial h_i^{l+1,p}} \right) \tag{6.62}$$

where l refers to the time level and p to the iteration round. For the Darcy flow and seepage face fluxes $q_{lu,D}$, q_{ls} and q_{li} the derivative to the pressure head is calculated as:

$$\frac{\partial S_{m,j,i}^{l+1,p}}{\partial h_i^{l+1,p}} = \left(-\frac{q_{lu,D\_or\_ls,j,i}^{l+1,p}}{h_{mp,j,i}^l - h_{mt,i}^{l+1,p}} \right) \quad \text{and} \quad \frac{\partial S_{m,j,i}^{l+1,p}}{\partial h_i^{l+1,p}} = \left(-\frac{q_{li,j,i}^{l+1,p}}{h_{mp,j,i}^l - h_{mt,i}^{l+1,p}} \right) \tag{6.63}$$

For the absorption flux $q_{lu,ab}$ the derivative to the pressure head is obtained by:

$$\frac{\partial S_{m,j,i}^{l+1,p}}{\partial h_i^{l+1,p}} = \left(-\alpha_{S,i} \frac{q_{lu,ab,j,i}}{\left(\theta_{s,i} + \theta_{thr,j,i} - \theta_{0,j,i} - \theta_i \right)} \frac{\partial \theta_i}{\partial h_i} \right)^{l+1,p} \tag{6.64}$$

where $\dfrac{\partial \theta_i}{\partial h_i}$ is the differential water capacity (Section 2.2).

6.3 User instructions

6.3.1 General input parameters

The most important aspect of macropore flow is that precipitation water is routed into macropores at the soil surface. A relatively small part of precipitation enters the macropore volume directly. Inflow of precipitation excess via overland flow in case of precipitation intensity exceeding matrix infiltration rate is the dominant source of macropore inflow at soil surface. In order to describe these inflow processes accurately, realistic precipitation intensities and matrix infiltration rates should be simulated. The consequences of this for the SWAP parameterisation other than the macropore parameters, are discussed below.

Rainfall option
For realistic rainfall intensities, rainfall option SWRAIN 3 is preferred (Section 3.7.1). Less preferable are options 1 and 2. Option 0, daily rainfall sum, is not recommended. This option may seriously underestimate macropore inflow at soil surface because of far too small rainfall intensities.

Vertical discretisation
Realistic simulation of matrix infiltration at the soil surface requires thin compartments in the top of the profile in the order of 1 cm thick (Van Dam and Feddes, 2000). A typical vertical discretisation for a macroporous field soil could be: for the first 10-20 cm compartments of 1 cm thick, for the next 20-30 cm 2.5 cm

thick, until the depth of the bottom of the IC domain maximal 5 cm thick, until the depth of the bottom of the static macropores 5 to maximal 10 cm thick and below this depth compartments of 10-25 cm thick.

Soil hydraulic functions

The hydraulic functions of the soil matrix should be used. This implies that the saturated volumetric moisture content is without the static macropore volume. And that the saturated hydraulic conductivity concerns a soil physical conductivity of the matrix rather than a hydrological conductivity of the soil. The air-entry-value option should be switched off, thus he = 0 (see Sections 2.3 and 2.8.1).

Time step

It is recommended to take 10-5 or 10-6 (d) for the minimum time step and 10-1 (d) or less for the maximum time-step.

Output

Macropore simulation provides the option of output of a macropore water balance in the file *.BMA. For this option, switch SWBMA should have value 1 (see Box 1.4). Automatically generated are output files MacroGeom.csv and SoilShrinkChar.csv, which contain a tabular representation of the macropore geometry and the shrinkage characteristics as computed by the model on basis of the user's input.

6.3.2   Macropore input parameters

The typical macropore input parameters are discussed in this Section. They are listed in Boxes 6.1 (Section 6.3.2.1: Macropore geometry) and 6.2 (Section 6.3.2.2: Water flow). The presented values concern a field experiment on water, bromide tracer and pesticide transport in a tile-drained field on clay soil (Scorza Júnior et al., 2004). The field was located in the riverine area in the central part of the Netherlands. The soil concerned light to moderate clay (30-55 mass-% clay) and the crop was winter wheat. At 320 cm depth the clay soil was underlain by a coarse sand aquifer. The presented values are the first results of a calibration of SWAP against the dataset.

6.3.2.1 Macropore geometry

The input parameters of the macropore geometry are listed in Box 6.1. They are discussed below.
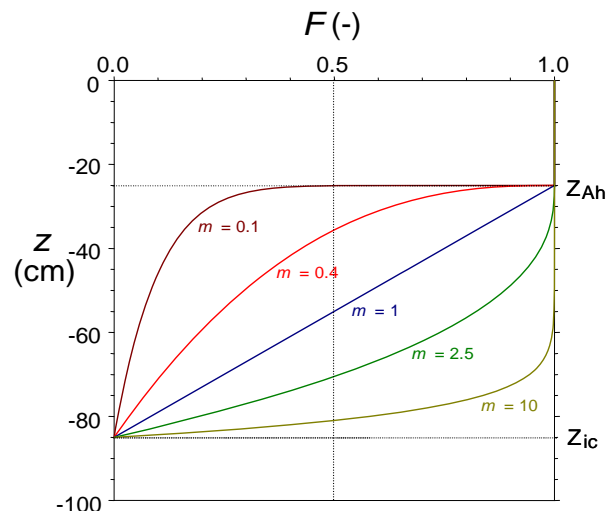
Figure 6.6 Fraction of functional IC macropores F as a function of depth is described by a power law function with power m. m = 1 describes a linear decline, while m < 1 represents shallow IC systems and m > 1 deep IC systems.

Illustration of the effect of parameters on macropore geometry

Curve F in Figure 6.6 illustrates the effect of shape-factor m in combination with other macropore geometry parameters on the fraction of IC macropores that is functional at depth z (in case that $R_{ZAH} = 0$). For $m = 0.1$, 0.4, 1.0, 2.5 and 10, respectively, depth z at which fraction F of functional IC macropores has declined to 0.5 equals -25.1, -35.6, -55, -70.5 and -81 cm, respectively. In general, $m < 1$ describes shallow IC systems, while $m > 1$ represents deep IC systems; $m = 1$ describes an intermediate system with linear decline of functional IC macropores with depth. Optionally, two more shape parameters can be used to describe IC macropores in more detail. The symmetry-point-parameter SPOINT allows for 'standing' ($m < 1$) and 'laying' ($m > 1$) S-shaped F-curves. In combination with switch SWPOWM turned on, these curves can be modified into double convex ($m < 1$) or double concave ($m > 1$) curves (see Appendix 3 for examples). This allows for a functional description of macropore volume for a wide range of macropore geometries.

Default value of R_{ZAH} is 0.0. In Figure 6.2 $R_{ZAH} = 0.2$, implying that at the bottom of the A-horizon ($z = -25$ cm) 20% of the IC macropores has ended. If $R_{ZAH} = 0$, no IC macropores end above the bottom of the A-horizon. This option may be used to describe effects of tillage of the A-horizon. Data of a dye tracer experiment from Booltink (1993) for an A-horizon in a clay soil in Flevoland, the Netherlands, point out that this option may be relevant.

Box 6.1 Macropore flow input: geometry. Case: Andelst (Scorza Júnior et al., 2004)

```
********************************************************************************
* Part 10: Preferential flow due to macro pores
  SwMacro = 1   ! Switch for macro pores, [0..1, I]

* If SwMacro = 1, specify parameters for macropore flow:
  Z_AH = -26.0    ! Depth bottom A-horizon [-1000..0 cm, R]
  Z_IC = -90.0    ! Depth bottom Internal Catchment (IC) domain [-1000..0 cm, R]
  Z_ST = -180.0   ! Depth bottom Static macropores [-1000..0 cm, R]
  VlMpStSs = 0.04 ! Volume of Static Macropores at Soil Surface [0..0.5 cm3/cm3, R]
  PpIcSs = 0.6    ! Proportion of IC domain at Soil Surface [0..0.99 -, R]
  NumSbDm = 4     ! Number of Sub-domains in IC domain [0..MaDm-2 -, I]
  PowM = 0.8      ! Power M for frequency distrib. curve IC domain (OPTIONAL, default 1.0) [0..100 -, R]
  RZah = 0.0      ! Fraction macropores ended at bottom A-horizon [OPTIONAL, default 0.0] [0..1 -, R]
  SPoint = 1.     ! Symmetry Point for freq. distr. curve [OPTIONAL, default 1.0] [0..1 -, R]
  SwPowM = 0      ! Switch for double convex/concave freq. distr. curve (OPTIONAL, Y=1, N=0; default: 0)
                                                                            [0..1 -, I]
  DiPoMi = 10.0   ! Minimal diameter soil polygons (shallow) [0.1..1000 cm, R]
  DiPoMa = 50.0   ! Maximal diameter soil polygons (deep)    [0.1..1000 cm, R]
  ZDiPoMa = -180.0! Depth below which diameter polygons is max. (OPTIONAL, default 0.) [-1000..0 cm, R]

* Start of Tabel with shrinkage characteristics
* ISOILLAY3 = indicator (number) of soil layer, as defined in part 4 [1..MAHO, I]
* SWSoilShr = Switch for kind of soil for shrinkage curve: 0 = rigid, 1 = clay, 2 = peat [0..2 -, I]
* SWShrInp  = Switch for determining shrinkage curve [1..2 -, I]:  1 = parameters of curve are given;
*                                                                  2 = typical points of curve given;
*                                                                  3 = (only peat) intersection points
*                                                                      of 3-straight-line-model given
* ThetCrMP  =  Threshold moisture content below which horizontal shrinkage [0..1 cm3/cm3, R]
* GeomFac   =  Geometry factor (3.0 = isotropic shrinkage), [0..100, R]
*
* ShrParA to ShrParE = parameters for describing shrinkage curves,
*                   depending on combination of SWSoilShr and SwShrInp [-1000..1000, R]:
*              SWSoilShr = 0              : 0 variables required (all dummies)
*              SWSoilShr = 1,  SwShrInp 1 = : 3 variables required (ShrParA to ShrParC) (rest dummies)
*              SWSoilShr = 1,  SwShrInp 2 = : 2 variables required (ShrParA to ShrParB) (rest dummies)
*              SWSoilShr = 2,  SwShrInp 1 = : 5 variables required (ShrParA to ShrParE)
*              SWSoilShr = 2,  SwShrInp 2 = : 5 variables required (ShrParA to ShrParE)
*              SWSoilShr = 2,  SwShrInp 3 = : 4 variables required (ShrParA to ShrParD) (rest dummy)

  ISOILLAY3  SWSoilShr  SwShrInp  ThetCrMP  GeomFac  ShrParA ShrParB ShrParC ShrParD ShrParE
      1          1          2       0.5001     3.0     0.343  0.6558    0.0     0.0     0.0
      2          1          2       0.3994     3.0     0.343  0.5392    0.0     0.0     0.0
      3          1          2       0.3895     3.0     0.415  0.6281    0.0     0.0     0.0
      4          1          2       0.3843     3.0     0.400  0.6233    0.0     0.0     0.0
      5          1          2       0.3894     3.0     0.412  0.5340    0.0     0.0     0.0
      6          1          2       0.4052     3.0     0.406  0.6583    0.0     0.0     0.0
      7          1          2       0.4052     3.0     0.446  0.5536    0.0     0.0     0.0
*End of Tabel with shrinkage characteristics

 ZnCrAr = -5.0  ! Depth at which crack area of soil surface is calculated [-100..0 cm, R]
```

Figure 6.7 illustrates a macropore geometry with six domains: MB-domain, four IC sub-domains and Ah-sub-domain. In this example V_{st} at soil surface = 0.04 cm^3 cm^{-3}, $P_{ic,0} = 0.6$, $m = 0.4$, $n_{dm} = 6$, $n_{sd} = 4$, $R_{ZAH} = 0.2$, $Z_{AH} = -25$ cm and $Z_{ic} = -85$ cm. $V_{st,ic}$ at soil surface equals 0.6 x 0.04 = 0.024 cm^3 cm^{-3}. This volume is equally divided over the $n_{sd} + 1$ sub-domains, including the Ah-sub-domain, because at soil surface $P_{sd,j}$ is equal for all five sub-domains and amounts to 0.6 / 5 = 0.12. Depth $z_{sd,j}$ of bottom of domains 2 to 6, equals -85, -54.2, -35.6, -26.9 and -25 cm, respectively.

Figure 6.8 presents an example of lumped sub-domains.
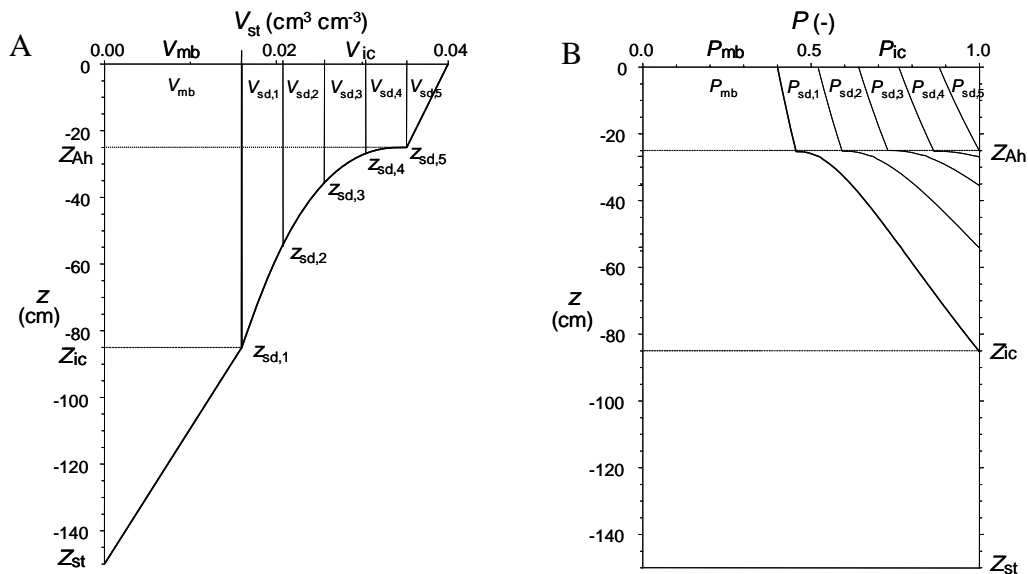
Figure 6.7 Example of macropore geometry with the IC domain partitioned in four sub-domains and an Ah-sub-domain. Static macropore volume V_{st} (left) and volumetric proportion P (right) for MB, IC and IC-sub-domains. $V_{st,0} = 0.04\ cm^3\ cm^{-3}$, $P_{ic,0} = 0.6$, $m = 0.4$, $n_{dm} = 6$, $n_{sd} = 4$, $R_{ZAH} = 0.2$, $Z_{AH} = -25\ cm$ and $Z_{ic} = -85\ cm$. $z_{sd,j}$ is bottom of sub-domain j.
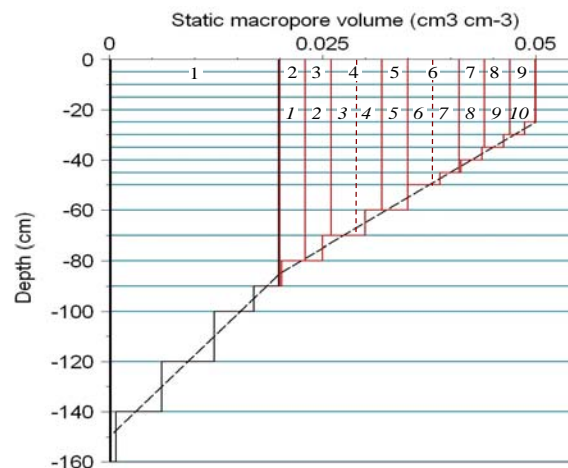
Figure 6.8 Example of a combination of horizontal and vertical discretisation: number of IC sub-domains $n_{sd} = 10$ (italic figures) while resulting total number of domains $n_{dm} = 9$ (regular figures). Former sub-domains 2 and 3 are lumped to obtain present domain 3, and former sub-domains 4 and 5 are lumped to obtain present domain 4.
$V_{st,0} = 0.1\ cm3\ cm-3$, $P_{ic,0} = 0.6$, $m = 1$, $R_{ZAH} = 0$, $Z_{AH} = -20\ cm$, $Z_{ic} = -80\ cm$, $Z_{st} = -120\ cm$.

Obtaining parameter values for macropore continuity and distribution

Most macropore input parameters are functional parameters with a physical relevancy. Information on their values can be derived from field and lab research. This especially counts for the depths Z_{Ah}, Z_{ic} and Z_{st}. Depth of A-horizon Z_{Ah} may be

known from soil mapping or field investigation. Z_{st} could be taken at or some decimetres above the mean annual lowest groundwater table. Processes leading to the presence of static macropores like ripening of clay and peat soils, and biological activities like soil penetration by plant roots, worms, insects and small mammals, will very likely be limited to this depth. Z_{ic} might be found at the depth of a clear shift in macropore density by investigation of a vertical soil profile in a pit or by taking relatively large soil samples (e.g. 20 cm diameter and 10-20 cm height).

Information about macropore volume to obtain a value for static macropore volume fraction at soil surface $V_{st,0}$ (VlMpStSs in Box 6.1) and the distribution of macropore volume with depth, can be obtained by comparing pore volume of large samples with fitted values for θ_{sat} of the original, unmodified Mualem-Van Genuchten functions. The latter expresses the pore volume of the soil matrix, while the first may comprise macropore volume as well.

Parameters which are relevant for the distribution of macropore volume with depth, PpIcSs, NumSbDm, PowM, DiPoMi, DiPoMa, and optional RZah, SPoint, SwPowM, ZDiPoMa, may be derived from inverse modelling of field experiments on tracer transport, with dye, conservative solutes or isotope tracers.

To illustrate the concept of the effective polygon diameter in case of combinations of cracks and hole-shaped macropores in the field, we consider the following equation:

$$d_{pol} = \frac{1}{\dfrac{1}{d_{pf}} + \pi \dfrac{\left(N_{h,1}d_{hf,1} + N_{h,2}d_{hf,2} + ...\right)}{4A_h}} \tag{6.65}$$

where d_{pol} (cm) is the effective polygon diameter, d_{pf} (cm) is the actual average polygon diameter in the field, $d_{hf,1}$ and $d_{hf,2}$ (cm) are the diameters of two classes of hole-shaped macropores in the field and $N_{h,1}$ and $N_{h,2}$ are their numbers per area A_{hf} (cm^2). If we assume that d_{pf} =15 cm, that there are two classes of hole-shaped parameters with an average diameter of 0.4 and 1.0 cm and with numbers per dm^2 of 3 and 1, then the effective polygon diameter will be 11.9 cm.

Shrinkage characteristics
The SWAP user needs to specify either the parameters of Kim's or Hendriks' relationship (see Section 6.1.1.2), or the values of typical points of the shrinkage characteristic curve. The different options and required parameters are listed in Table 6.1. The option to specify the original parameters of both relationships is especially relevant for the development of pedotransfer functions for shrinkage characteristics. Alterra is working on pedotransfer functions for shrinkage characteristics of clay and peat soils. The options to use typical points of the shrinkage characteristic curves are

Table 6.1 Overview of required shrinkage parameters for clay and peat soils (Fig. 6.4.A and 6.9)

Soil	Input option	Shrinkage parameters				
		ShrParA	ShrParB	ShrParC	ShrParD	ShrParE
Clay	1	$\alpha_K(e_0)$	β_K	γ_K	–	–
	2	$\alpha_K(e_0)$	ϑ_a	–	–	–
Peat	1	e_0	ϑ_a	α_H	β_H	P_H
	2	e_0	ϑ_a	ϑ_r	ϑ_P	P_H
	3	e_0	ϑ_a	ϑ_i	e_i	–

useful when limited information about the exact curves is available. When just a (rough) sketch of a curve is available it may be possible to recognize these typical points.

For clay soils, the typical points are the void ratio e_0 (α_K) at $\vartheta = 0$ and the moisture ratio ϑ_a at transition of residual to normal shrinkage (Fig. 6.4). With these two input data, SWAP generates the parameters of Kim's relationship. For peat soils, there are two options to use typical points of the shrinkage curve. The first, option 2 in Table 6.1, requires typical points with which the parameters of Hendriks' curve can be generated. The second, option 3 in Table 6.1, enables to describe the shrinkage with three straight line-pieces.
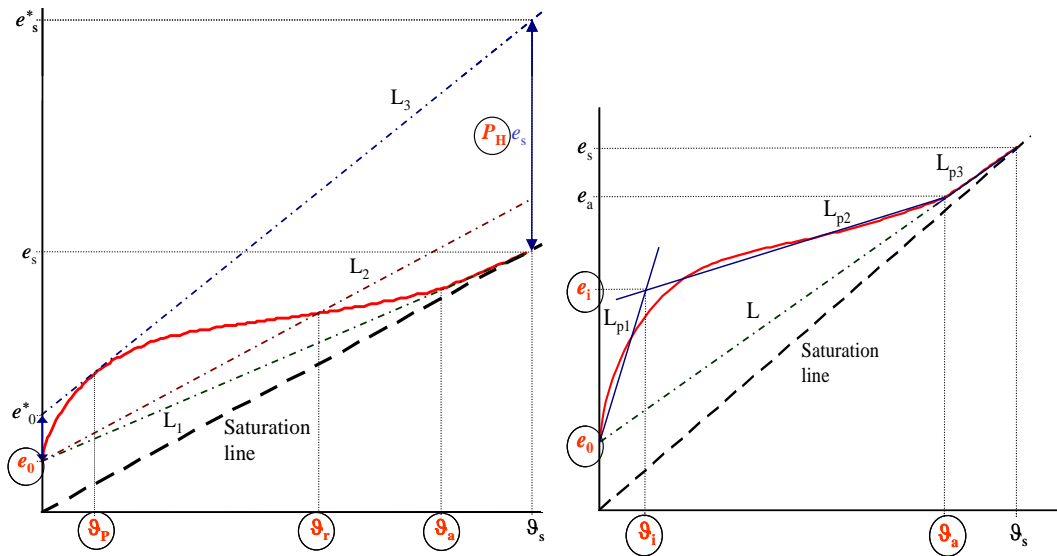
Figure 6.9 Construction of support-lines and line-pieces in the graph of the peat-shrinkage curve to find values of input parameters for Option 2 of Table 6.1: 'typical points' (left) and for Option 3 of Table 6.1: '3 straight line-pieces' (right). Symbols in circles represent input parameters.

Option 2 requires the construction of three support-lines, L_1, L_2 and L_3, in the graph of the shrinkage curve (Fig. 6.9). L_1 connects the points $(0,e_0)$ and (ϑ_s,e_s). L_2 is parallel to the saturation line and starts at point $(0,e_0)$. L_3 connects the points $(0,e^*_0)$ and (ϑ_s,e^*_s) and is tangent to the shrinkage curve. In order to construct this line, parameter P_H should be found so that $e^*_0 = (1 + P_H) e_0$ and $e^*_s = (1 + P_H) e_s$. This can easily be done by trial-and-error in a spreadsheet or on paper. When $P < 0$, L_2 must start at point $(0,\frac{1}{2}e_0)$ instead of point $(0,e_0)$ (e.g. samples A-15 and V-10 in Appendix 11). For values of $|P| < 0.1$, option 3 is recommended (e.g. sample A-25 in Appendix 11). Input parameters are (Table 6.1): e_0, P_H, ϑ_a (moisture ratio at transition of 'near-normal' to 'subnormal' shrinkage on L_1, Fig. 6.4.B), ϑ_r (moisture ratio at intersection point of L_2 and curve) and ϑ_P (moisture ratio at tangency point of L_3 to curve). Values must be given with an accuracy of at least 1% of saturated moisture ratio (ϑ_s).

Option 3 requires the construction of three line-pieces L_{p1}, L_{p2} and L_{p3} and one support-line L in the graph of the shrinkage curve (Fig. 6.9). L_{p1} connects the points $(0,e_0)$ and (ϑ_i,e_i), L_{p2} the points (ϑ_i,e_i) and (ϑ_a,e_a), and L_{p3} the points (ϑ_a,e_a) and (ϑ_s,e_s). L connects the points $(0,e_0)$ and (ϑ_s,e_s). Point (ϑ_a,e_a) is situated on this line and represents the point of transition of 'near-normal' to 'subnormal' shrinkage. Point (ϑ_i,e_i) should be chosen in such a way that the three line-pieces describe the shrinkage curve as accurate as possible. For use in the model, L_{p2} and L_{p3} are much more important than L_{p1}. So emphasis should be put on these two line-pieces. Input parameters are (Table 6.1): e_0, ϑ_a, e_i and ϑ_i.

```
********************************************************************************
* Start of Tabel with sorptivity characteristics
* ISOILLAY4  = Indicator (number) of soil layer, as defined in part 4 [1..MAHO, I]
* SWSorp     = Switch for kind of sorptivity function [1..2 -, I]:
*              1 = calculated from hydraulic functions according to Parlange
*              2 = empirical function from measurements
* SorpFacParl = Factor for modifying Parlange function (OPTIONAL, default 1.0) [0..100 -, R]
* SorpMax    = Maximal sorptivity at theta residual [0..100 cm/d**0.5, R]
* SorpAlfa   = Fitting parameter for empirical sorptivity curve [-10..10 -, R]

  ISOILLAY4  SwSorp   SorpFacParl  SorpMax  SorpAlfa
      1        1         0.33        0.0      0.0
      2        1         0.33        0.0      0.0
      3        1         0.50        0.0      0.0
      4        1         0.50        0.0      0.0
      5        1         0.50        0.0      0.0
      6        1         0.50        0.0      0.0
      7        1         0.50        0.0      0.0
*End of Tabel with sorptivity characteristics
*
 ShapeFacMp    = 1.0     ! Shape factor for lateral Darcy flow (theoret. 1-2) [0..100 -, R]
 CritUndSatVol = 0.1     ! Critical value for under-saturation volume [0..10 -, R]
*
 SwDrRap     = 1         ! Switch for simulating rapid drainage,[Y=1, N=0]
 RapDraResRef = 1 * 15.  ! Reference rapid drainage resistance [0..1.E+10 /d, R]
                         ! an array with a single element must be indicated using a multiplier
                         ! asterix  (see TTUTIL-manual, par. 5.2  Defining arrays)
 RapDraReaExp = 1.0      ! Exponent for reaction rapid drainage to dynamic crack width
                         !                                             [0..100 -, R]
 ZDrLv       = -79.75    ! Depth of drain level: only required when SwBotB = 3 [-1000..0 cm, R]
```

If there is no information available to decide otherwise, ThetCrMP could be taken at 90-100% θ_{sat}, GeomFac as 3.0 and ZnCrAr around -5.0 cm.

Measured shrinkage characteristics of seven clay profiles in the Netherlands, as described by Bronswijk and Evers-Vermeer (1990), are listed in 0. Yule and Ritchie (1980a, 1980b) described shrinkage characteristics of eight Texas Vertisols, using small and large cores. Garnier et al. (1997) propose a simple evaporation experiment to determine simultaneously the moisture retention curve, hydraulic conductivity function and shrinkage characteristic. Measured shrinkage characteristics of four peat soil profiles in the Netherlands, as described by Hendriks (2004), are listed in 0.

6.3.2.2 Water flow

The input parameters of the water flow concept are listed in Box 6.2. They are discussed below.

The sorptivity parameters can be obtained by fitting Eq. [6.30] against measured values to derive a relationship between sorptivity and initial moisture content. The advantage of measured sorptivities is that they may reflect the influence of water-repellent coatings on the surface of clay aggregates which often hamper infiltration into these aggregates (Thoma et al., 1992; Dekker and Ritsema, 1996). If measured

sorptivities are not available, sorptivity as a function of moisture content is derived from the soil hydraulic characteristics (Parlange, 1975). To account for water-repellent coatings a correction factor SorpFacParl can be entered. Greco et al. (1996) found values for this factor of 0.33 for the topsoil and 0.5 for the sub-soil of a Dutch clay soil similar to the Andelst soil. They describe a simple way of measuring sorptivity as a function of moisture content.

ShapeFacMp can be used to decrease or increase exchange fluxes between macropores and soil matrix. Theoretically, its value lies between 1 and 2 (see Section 6.1.2); default value is 1.0. RapDraResRef depends on the system of macropores and their connection to drains or ditches. In case of a network of structural cracks, RapDraResRef will be smaller than in case of mainly hole shaped macropores. The opposite applies to RapDraReaExp.

7   Crop growth

7.1   Introduction

SWAP contains three crop growth routines: a simple module, a detailed module for all kind of crops (WOFOST, WOrld FOod STudies), and a detailed module for grass (re)growth.

The simple module prescribes crop development, independent of external stress factors. Its main function is to provide proper upper boundary conditions for soil water movement. The simple model is useful when crop growth doesn't need to be simulated or when crop growth input data are insufficient. Section 7.2 provides a description of the simple module.

In the footsteps of De Wit and co-workers (De Wit et al., 1978; Goudriaan, 1977; Penning de Vries and Van Laar, 1982), in the 1980s a wide range of scientists in Wageningen became involved in the development and application of crop growth models. The generic crop model SUCROS for the potential production situation was developed (Spitters et al., 1989). SUCROS formed the basis of a range of Wageningen crop models, as reviewed by Bouman et al. (1996) and Van Ittersum et al. (2003). One of the developed models is the WOFOST model, which simulates in detail photosynthesis and crop development, taking into account growth reductions due to water and/or salt stress. WOFOST has been implemented in SWAP and is described in Section 7.3.

The detailed module for grass is a modified version of WOFOST. The only species occuring in the sward is supposed to be perennial ryegrass (Lolium perenne L.). The sward is regular mowed and remains vegetative. No grazing takes place and the grassland is permanent. The settings for regrowth after grass cutting have a large effect on the LAI development, and the application of this module requires expert judgement. For more information of this module we refer to the SWAP source code, subroutine GRASS.

7.2   Simple crop module

The simple crop growth model represents a green canopy that intercepts precipitation, transpires water vapour and shades the ground. The user specifies as a function of development stage either leaf area index or soil cover fraction, along with crop height and rooting depth. The development stage can be controlled either by the temperature sum or can be linear in time.

The simple model does not calculate the crop potential or actual yield. However, the user may define yield response factors (Doorenbos and Kassam, 1979; Smith, 1992) for various growing stages as a function of development stage. For each growing stage k the actual yield $Y_{a,k}$ (kg ha^{-1}) relative to the potential yield $Y_{p,k}$ (kg ha^{-1}) during this growing stage is calculated by:

$$1 - \frac{Y_{a,k}}{Y_{p,k}} = K_{y,k}\left(1 - \frac{T_{a,k}}{T_{p,k}}\right) \qquad (7.1)$$

where $K_{y,k}$ (-) is the yield response factor of growing stage k, and $T_{p,k}$ (cm) and $T_{a,k}$ (cm) are the potential and actual transpiration, respectively, during growing stage k.

The relative yield of the whole growing season is calculated as the product of the relative yields of each growing stage:

$$\frac{Y_a}{Y_p} = \prod_{k=1}^{n}\left(\frac{Y_{a,k}}{Y_{p,k}}\right) \qquad (7.2)$$

where Y_a is the cumulative actual yield (kg ha^{-1}) of the whole growing season, Y_p is the cumulative potential yield (kg ha^{-1}) of the whole growing season, index k is the growing stage and n is the number of defined growing stages.

7.3 Detailed crop module

Three groups of growth factors (Fig. 7.1) may be distinguished to obtain a hierarchy of production levels in crop production (Van Ittersum et al., 2003). Growth defining factors determine the potential production that can be achieved in a given physical environment and for a plant species. Radiation intensity, carbon dioxide concentration, temperature and crop characteristics are the major growth defining factors. Their management, at least in open, non-controlled environments, is only possible through tactical decisions such as sowing date, sowing density and breeding. To achieve the potential production the crop must be optimally supplied with water and nutrients and completely protected against weeds, pests, diseases and other factors that may reduce growth.
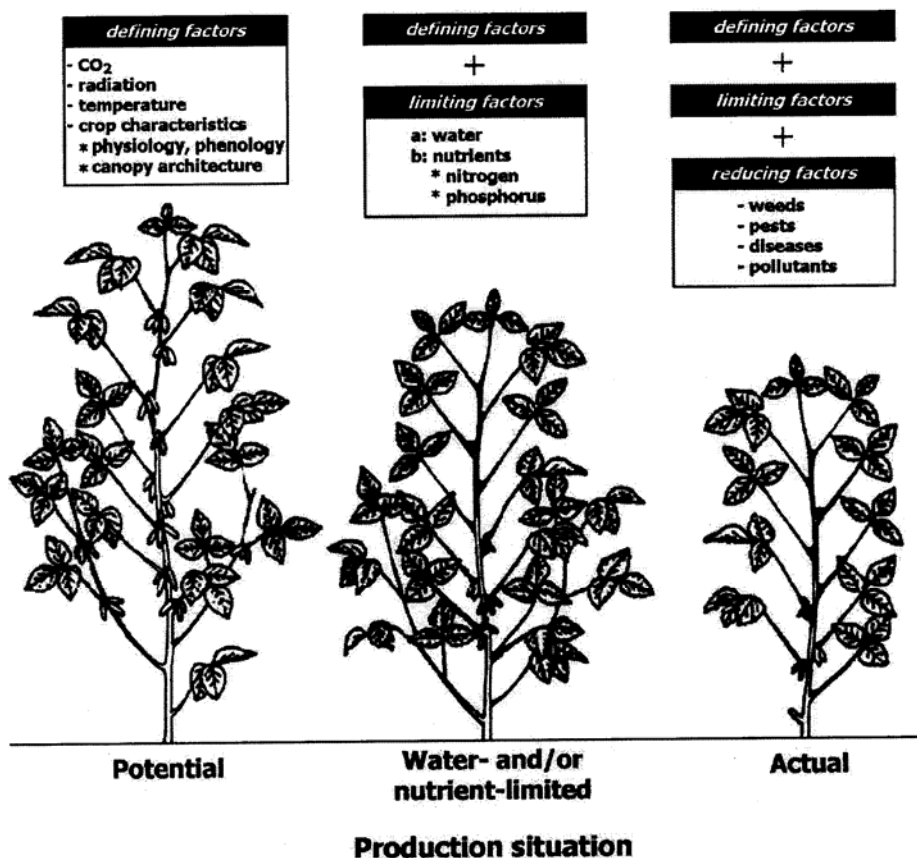
Figure 7.1 A hierarchy of growth factors, production situations and associated production levels (Van Ittersum et al., 2003).

Growth-limiting factors comprise water and nutrients and determine water- or nutrient-limited production levels in a given physical environment. Here, management can be used to control availability of water and nutrients, and may increase production towards potential levels. Growth reducing factors reduce or hamper growth and comprise biotic factors such as weeds, pests and diseases, and abiotoc factors such as pollutants and Al-toxicity. Crop protection aims at effective management of these growth factors. In the actual production situation, the productivity achieved is usually the results of a combination of growth-limiting and – reducing factors (Van Ittersum et al., 2003).

The model WOFOST (Van Keulen and Wolf, 1986; Spitters et al., 1989; Supit et al., 1994; Hijmans et al., 1994; Boogaard et al., 1998) has been developed to simulate potential production and limited production due to water and/or salinity stress. Figure 7.2 shows the processes and relations incorporated in WOFOST. The radiation energy absorbed by the canopy is a function of incoming radiation and crop leaf area. Using the absorbed radiation and taking into account photosynthetic leaf characteristics the potential gross photosynthesis is calculated. The latter is reduced due to water and/or salinity stress, as quantified by the relative transpiration, and yields the actual gross photosynthesis.
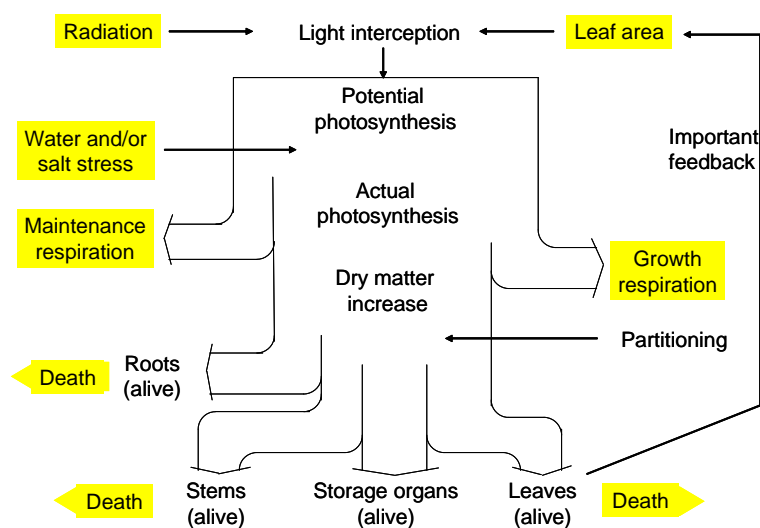
Figure 7.2 Overview of crop growth processes incorporated in WOFOST.

Part of the carbohydrates (CH_2O) produced are used to provide energy for the maintenance of the living biomass (maintenance respiration). The remaining carbohydrates are converted into structural matter. In this conversion, some of the weight is lost as growth respiration. The dry matter produced is partitioned among roots, leaves, stems and storage organs, using partitioning factors that are a function of the phenological development stage of the crop (Spitters et al., 1989). The fraction partitioned to the leaves, determines leaf area development and hence the dynamics of light interception. The dry weights of the plant organs are obtained by integrating their growth rates over time. During the development of the crop, part of living biomass dies due to senescence.

Light interception and CO_2 assimilation are the main growth driving processes. Some simulated crop growth processes are influenced by temperature, like for example the maximum rate of photosynthesis and the maintenance respiration. Other processes, like the partitioning of assimilates or decay of crop tissue, are a function of the phenological development stage.

7.3.1 Phenological development stage

As many physiological and morphological processes change with the phenological stage of the plant, quantification of phenological development is essential in any crop growth simulation model. For many annual crops, the phenological development can conveniently be expressed in development stage D_s (-), having the value 0 at seedling emergence, 1 at flowering and 2 at maturity (Van Heemst, 1986a; 1986b). The most important phenological change is the one from vegetative $(0 < D_s < 1)$ to reproductive stage $(1 < D_s < 2)$, which changes drastically the dry matter allocation to organs.

WOFOST starts crop growth simulation at emergence, of which the date should be specified by the user. A crop passes through successive phenological development stages, of which the length depends on the development rate. Development rates before floral initiation or anthesis $(D_s = 1)$ are controlled by day length and temperature. After anthesis only temperature will affect development
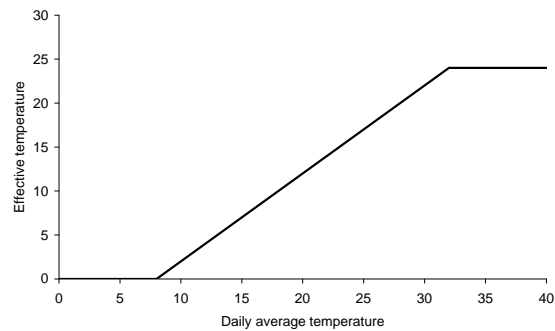
Figure 7.3 Example of effective temperature for temperature sum as function of daily average temperature.

rate. Higher temperatures accelerate the development rate, leading to shorter growing periods. It has often been demonstrated, that over a wide range of temperatures, the development rate increases more or less linearly with temperature (Van Dobben, 1962; Van Keulen and Seligman, 1987). Therefore WOFOST uses the temperature sum to account for the effect of temperature on the development stage. An effective temperature T_{eff} (°C) is calculated as function of daily average temperature T_{air} (°C). For species originating from temperate regions $T_{eff} = 0$ at $T_{air} = 0\text{-}3$ °C, while for species of subtropical and tropical origins $T_{eff} = 0$ at $T_{air} = 9\text{-}14$ °C (Angus et al., 1981). In a table the WOFOST user should specify the relation between T_{eff} and T_{air}. An example is given in Fig. 7.3. Within a species, cultivars may vary substantially in their temperature requirements. Therefore, the temperature sum is characteristic for each cultivar, and is input to WOFOST. Accordingly, the development stage, D_s (-), is calculated as:

$$D_s^{j+1} = D_s^j + \frac{T_{eff}}{T_{sum,i}} \tag{7.3}$$

where superscript j is the day number and $T_{sum,i}$ is the temperature sum required to complete either the vegetative or the reproductive stage.

For some species or cultivars, during the vegetative stage, the effect of day length should be taken into account. Approaches that describe such effects quantitatively are given, amongst others, by Weir et al. (1984), Hadley et al. (1984) and Reinink et al. (1986). In the model, a reduction factor for the development rate as function of day length f_{lday} (-) is computed:

$$f_{\text{lday}} = \frac{L_{\text{day}} - L_{\text{cday}}}{L_{\text{oday}} - L_{\text{cday}}} \qquad \text{with} \qquad 0 < f_{\text{lday}} < 1 \tag{7.4}$$

with L_{day} the actual day length (d), L_{cday} the shortest day length for any development (d), and L_{oday} the minimum day length for optimum development (d). Note that in modern cultivars, photosensitivity is much less pronounced than in traditional cultivars, and that for the purpose of modelling the day length influence can be ignored by choosing an appropriate temperature sum, which leads to an equivalent crop life cycle.

The simulation of crop growth stops when the development stage reaches the stage at which the crop will be harvested. The development stage at harvest time should be provided by the user.

7.3.2 Radiation fluxes above the canopy

Measured or estimated daily global radiation (wavelength band 300-3000 nm) is input for the model. Incoming radiation is partly direct, with the angle of incidence equal to the angle of the sun, and partly diffuse, with incidence under various angles. The sine of solar elevation as a function of the day hour, can be calculated with:

$$\sin \beta_{\text{sun}} = \sin L_{\text{g}} \sin \sigma_{\text{sun}} + \cos L_{\text{g}} \cos \sigma_{\text{sun}} \cos \left(\frac{2\pi (t_{\text{h}} + 12)}{24} \right) \tag{7.5}$$

with β_{sun} the solar elevation (degrees), σ_{sun} is solar declination (degrees), L_{g} is geographic latitude (degrees) and t_{h} is hour of the day.

Only about 50 percent of the global radiation is photosynthetically active (PAR, Photosynthetically Active Radiation, wavelength band 400-700 nm). The daily incoming PAR (J m^{-2} d^{-1}) is calculated by multiplying half of the daily global radiation with the ratio of the actual effective solar elevation and the integral of the effective solar height, taking into account reduced atmospheric transmission at low solar elevations:

$$PAR = 0.5 \, R_{\text{s}} \, \frac{\sin \beta_{\text{sun}} \left(1 + 0.4 \sin \beta_{\text{sun}} \right)}{\int \sin \beta_{\text{mod, sun}}} \tag{7.6}$$

where R_s is daily global radiation (J m^{-2} d^{-1}) and $\int$sin $\beta_{mod,sun}$ the integral of sin β_{sun} over the day (-) which is corrected for reduced atmospheric transmission at low solar elevations.

A diffuse radiation flux results from scattering of sun rays by clouds, gases and dust in the atmosphere. To quantify the degree of scattering, the measured daily total radiation is compared with the amount that would have reached the Earth's surface in the absence of an atmosphere, S_{sun}, which can be calculated as:

$$S_{sun} = 1.18 \, 10^8 \left(1 + 0.033 \left(\frac{2j\pi}{365} \right) \right) \tag{7.7}$$

where S_{sun} is the solar constant (J m^{-2} d^{-1}) and j the day number in the year (DOY). The ratio of potential and measured daily total radiation is called atmospheric transmission A_t (-). The proportion of diffuse radiation, I_{fdif} (-), is derived from the atmospheric transmission by an empirical relationship (Spitter et al., 1989). Taking also into account that only 50 percent of the solar radiation is photosynthetically active, the diffuse photosynthetically active radiation PAR_{dif} (J m^{-2} d^{-1}) can thus be calculated by:

$$PAR_{dif} = 0.5 \, I_{fdiff} \, A_t \, S_{sun} \sin \beta_{sun} \tag{7.8}$$

The direct radiation flux, PAR_{dir} (J m^{-2} d^{-1}), is obtained by subtracting the diffuse part from the photosynthetically active radiation flux:

$$PAR_{dir} = PAR - PAR_{dif} \tag{7.9}$$

7.3.3 Radiation profiles within the canopy

The incoming PAR is partly reflected by the canopy. The reflection coefficient is defined as the fraction of the downward radiation flux that is reflected by the entire canopy. According to Goudriaan (1977), the reflection coefficient ρ_{rad} (-) of a green leaf canopy with a random spherical leaf angle distribution equals:

$$\rho_{rad} = \left(\frac{1 - \sqrt{1 - \sigma_{leaf}}}{1 + \sqrt{1 - \sigma_{leaf}}} \right) \left(\frac{2}{1 + 1.6 \sin \beta_{sun}} \right) \tag{7.10}$$

with σ_{leaf} the scattering coefficient of single leaves for visible radiation (-), which is taken to be 0.2. The first right-hand-side term of Eq. (7.10) denotes the reflection of a canopy of horizontal leaves and the second term is the approximate correction factor for a spherical leaf angle distribution. The fraction $(1-\rho_{rad})$ of the incoming visible radiation is available for absorption by the canopy.

Light intensity, adjusted for crop reflection, decreases approximately exponentially with leaf area index when going deeper into the canopy:

$$PAR_{\mathrm{L}} = \left(1 - \rho_{\mathrm{rad}}\right) PAR\, e^{-\kappa L} \qquad\qquad (7.11)$$

where L is the cumulative leaf area index, ΣLAI (m^2 leaf m^{-2} ground), counted from the top of the canopy downwards, PAR_{L} is the net light intensity (J m^{-2} d^{-1}) at depth L, and κ is the radiation extinction coefficient (-).

The profiles of the net diffuse flux and the net flux caused by direct irradiance can be characterized analogously (Goudriaan, 1982). Diffuse and direct fluxes each attenuate at a different rate, and both extinction coefficients are input in SWAP. For a random spherical leaf angle distribution the extinction coefficient of the direct flux component, κ_{dir} (-), might be approximated by (Goudriaan, 1977, 1982):

$$\kappa_{\mathrm{dir}} = \frac{0.5}{\sin \beta_{\mathrm{sun}}} \qquad\qquad (7.12)$$

and the extinction coefficient of the diffuse flux component, κ_{dif} (-), might be calculated as:

$$\kappa_{\mathrm{dif}} = \kappa_{\mathrm{dir}} \sqrt{1 - \sigma_{\mathrm{leaf}}} \qquad\qquad (7.13)$$

In Eq. (7.12), the factor 0.5 represents the average projection on the ground surface of leaves showing a spherical angle distribution. Averaging $0.5/\sin\beta$ during a day with an overcast sky, gives a value of $\kappa_{\mathrm{dir}} = 0.8$ (-). The value of κ_{dif} can be measured directly under completely overcast sky conditions, when only diffuse radation reaches the canopy. The average value is about 0.72 (-) (Goudriaan, 1977).

In many situations, the leaf angle distribution is not spherical. Therefore, in WOFOST the actual leaf angle distribution is accounted for by using a so called cluster factor which is the measured extinction coefficient for diffuse radiation, relative to the theoretical one for a spherical leaf area distribution.

On its way through the canopy, part of the direct flux is intercepted and scattered by the leaves. Hence, the direct flux segregates into a diffuse, scattered component and another component which remains direct. Attenuation of the remaining direct component proceeds like in a hypothetical canopy of black, non scattering leaves. The diffuse component is obtained as the difference between the total direct flux and its direct component.

The rate of light absorption at depth L in the canopy, $PAR_{\mathrm{L,a}}$ (J m^{-2} leaf d^{-1}), is obtained by taking the derivative of Eq. (7.11) with respect to L:

$$PAR_{L,\mathrm{a}} = \kappa\left(1 - \rho_{\mathrm{rad}}\right) PAR\, e^{-\kappa L} \qquad\qquad (7.14)$$

Similar expressions can be derived for the separate light components: the diffuse flux, the total direct radiation flux and the direct component of the direct radiation flux. The absorbed diffuse component of the direct flux is obtained by subtracting the direct component from the total direct flux.

7.3.4 Instantaneous assimilation rates per leaf layer

The CO_2 assimilation rate of a canopy layer is obtained by substituting the absorbed amount of light energy into the assimilation-light response of single leaves (Peat, 1970):

$$A_L = A_{max}\left(1 - e^{\frac{-\varepsilon_{PAR}\, PAR_{L,a}}{A_{max}}}\right) \hspace{2cm} (7.15)$$

where A_L is the gross assimilation rate (kg CO_2 m^{-2} leaf d^{-1}), A_{max} the gross assimilation rate at light saturation (kg CO_2 m^{-2} leaf d^{-1}), and ε_{PAR} the initial slope or light use efficiency (kg CO_2 J^{-1} absorbed).

Two leaf classes are distinguished: shaded leaves and sunlit leaves. The shaded leaf area absorbs the diffuse flux and the diffuse component of the direct flux. The sunlit leaf area receives diffuse and direct radiation. At every horizon within the canopy, the intensity of the unobstructed direct beam equals its intensity above the crop. llumination intensity of sunlit leaves varies strongly with leaf angle. In the model, the assimilation rate of the sunlit leaf area is therefore integrated over the leaf angle distribution.

The assimilation rate per unit leaf area in a canopy, is the sum of the assimilation rates of sunlit and shaded leaves, taking into account their proportion in each layer. The proportion of sunlit leaf area at depth L in the canopy equals the proportion of the direct component of the direct flux reaching that depth. This proportion is calculated analogous to Eq. (7.14), using the extinction coefficient of the direct radiation component.

Figure 7.4 shows the CO_2 assimilation rate at different sunlight intensities as measured for different crops. Striking are the higher assimilation rates of so-called C_4 crops in comparison to C_3 crops. The reason is that C_4 plants are more effective in fixation of CO_2 within the leaf. The internal CO_2 concentration amounts 120 ppm at C_4 plants and 210 ppm at C_3 plants. Currently the CO_2 concentration in the atmosphere is about 370 ppm. This means that at C_4 plants the gradient for diffusion of CO_2 throught the stomata is 250/160 = 1.56 times as large as at C_3 plants.
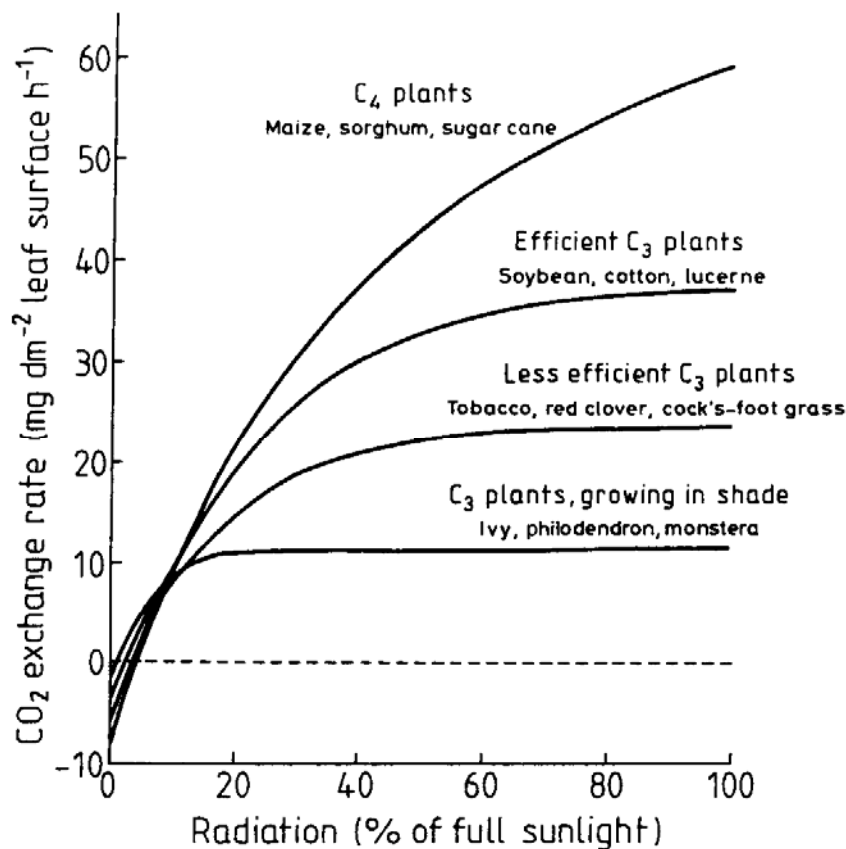
Figure 7.4 CO$_2$ exchange rate as function of radiation amount for C$_3$ and C$_4$ plants.

Therefore, at a certain light intensity, the CO$_2$ uptake rate and the photosynthesis are much higher in case of C$_4$ plants.

7.3.5 Daily gross assimilation rate of the canopy

The instantaneous rates per leaf layer need to be integrated over the canopy leaf area index and over the day. This is efficiently achieved using the Gaussian integration method (Press et al., 1989). This method specifies the discrete points at which function values have to be calculated, and the weighting factors with which the function values have to be multiplied in order to minimize deviation from analytical integration. A three-point algorithm evaluates the function at 0.1127a, 0.5a and 0.8873a of the interval (0,a), with weighting coefficients 1.0, 1.6 and 1.0, respectively. The Gaussian integration method is remarkably accurate in case of trigonometric (radiation) and exponential (light absorption) functions. WOFOST computes at three selected moments of the day incoming *PAR* just above the canopy. Using this radiation, assimilation is computed at three selected depths in the canopy (Spitters et al., 1989). Gaussian integration of these values results in the daily rate of potential gross CO$_2$ assimilation, A_{pgross} (kg CO$_2$ ha^{-1} d^{-1}).

Until now the assimilation has been treated as a function of the intercepted light and of photosynthetic crop characteristics such as initial light use efficiency and maximum leaf CO_2 assimilation at light saturation. Other factors that may reduce the daily assimilation rate are typical crop characteristics, unfavourable temperatures and water stress.

Typical crop characteristics depend on the phenological crop stage. Therefore the WOFOST user should specify a maximum CO_2 assimilation rate, A_{max} (kg CO_2 ha^{-1} d^{-1}), as function of development stage.

A reduction factor f_{tday} (-), which is a function of the average daytime temperature T_{day} (°C), accounts for sub-optimum temperatures. T_{day} is calculated by:

$$T_{day} = 0.75\,T_{max} + 0.25\,T_{min} \qquad (7.16)$$

where T_{max} and T_{min} (°C) are the daily maximum and minimum temperature, respectively. The shape of the reduction function is entered as a table in WOFOST.

The crop characteristics and temperature effect reduce A_{pgross} to A_{pgross}^1 (kg CO_2 ha^{-1} d^{-1}):

$$A_{pgross}^1 = \max\left(A_{pgross}, f_{tday}, A_{max}\right) \qquad (7.17)$$

In addition, low nighttime temperatures affect assimilation. At night, assimilates produced during daytime, are transformed into structural biomass. This process is hampered by low temperature. If these low temperatures prevail for several days, the assimilates accumulate in the plant and the assimilation rate diminishes and ultimately halts. In the model, this temperature effect is accounted for by a reduction factor f_{7min}, which is a function of the minimum temperature during the previous seven days.

Other important factors that may reduce assimilation are water and salinity stress. WOFOST uses the ratio of actual transpiration and potential transpiration, T_a/T_p, as reduction coefficient.

Reduction due to low minimum temperatures, water stress, and salinity stress, and taking into account that for each kg CO_2 30/44 kg biomass (CH_2O) is formed, results in the following daily gross assimilation rate A_{gross} (kg ha^{-1} d^{-1}):

$$A_{gross} = \frac{30}{44} f_{7min} \frac{T_a}{T_p} A_{pgross}^1 \qquad (7.18)$$

7.3.6 Maintenance respiration

Some of the carbohydrates formed are respired to provide energy for maintaining the existing bio structures. This maintenance respiration consumes roughly 15 - 30% of the carbohydrates produced by a crop in a growing season (Penning de Vries et al., 1979). This underlines the importance of accurate quantification of this process in the model.

WOFOST estimates the maintenance costs using the approach proposed by Penning de Vries and Van Laar (1982), assuming that the reference maintenance requirements R_{mref} (kg ha^{-1} d^{-1}) are proportional to the dry weights of the plant organs to be maintained:

$$R_{mref} = c_{m,leaf}W_{leaf} + c_{m,stem}W_{stem} + c_{m,stor}W_{stor} + c_{m,root}W_{root} \qquad (7.19)$$

where $c_{m,i}$ denotes the maintenance coefficient of organ i (kg kg^{-1} d^{-1}) and W_i the organ dry weight (kg ha^{-1}). The maintenance coefficients should be specified by the user.

The maintenance respiration rate still has to be corrected for senescence and temperature. The reduction factor for senescence f_{senes} (-) is crop-specific and is defined as a function of development stage. Higher temperatures accelerate the turnover rates in plant tissue and hence the costs of maintenance. An increase in temperature of 10°C typically increases maintenance respiration by a factor of about 2 (Kase and Catsky, 1984; Penning de Vries and Van Laar, 1982). However, to be more flexible, the user may specify the increase factor of the respiration rate per 10°C temperature increase, Q_{10} (-):

$$R_m = f_{senes}R_{mref}Q_{10}^{\frac{T_{avg}-25}{10}} \qquad (7.20)$$

where R_m is the actual maintenance respiration rate (kg ha^{-1} d^{-1}).

It may be assumed that the vegetation will not be 'self-consuming' in terms of carbohydrates. Therefore the maintenance respiration rate cannot exceed the gross assimilation rate. The net assimilation rate A_{net} (kg ha^{-1} d^{-1}) is the amount of carbohydrates available for conversion into structural material:

$$A_{net} = A_{gross} - R_m \qquad \text{with} \qquad A_{net} \geq 0 \qquad (7.21)$$

7.3.7 Dry matter partitioning and growth respiration

The primary assimilates in excess of the maintenance costs, are available for conversion into structural plant material. In this conversion process CO_2 and H_2O are released. The magnitude of growth respiration is determined by the composition of
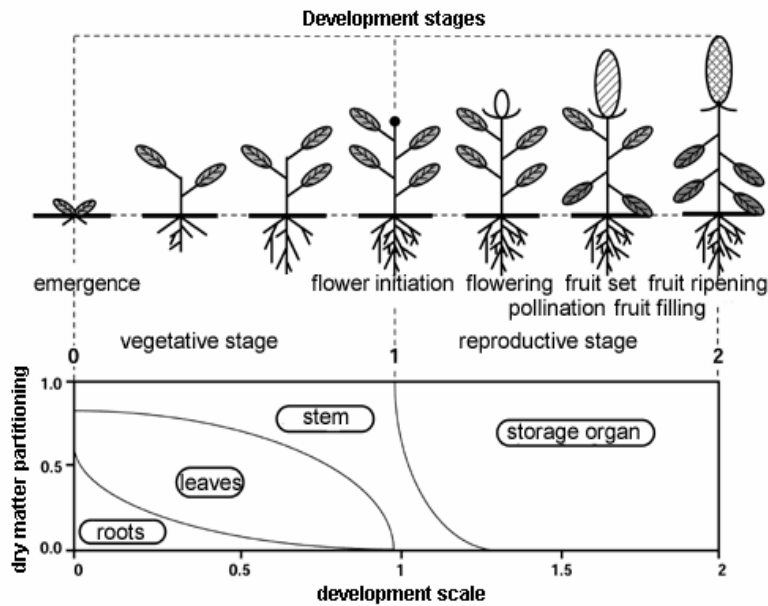
Figure 7.5 Typical partitioning of assimilated dry matter among leaves, stem, roots and storage organs as function of development stage.

the end product formed (Penning de Vries et al., 1974). Thus the weight efficiency of conversion of primary photosynthates into structural plant material varies with the composition of that material. Fats and lignin are produced at high costs; structural carbohydrates and organic acids are relatively cheap. Proteins and nucleic acids form an intermediate group.

At higher temperatures the conversion processes are accelerated, but the pathways are identical (Spitters et al. 1989). Hence, the assimilate requirements do not vary with temperature.

In the vegetative stage, the increase in total dry weight of the crop is partitioned over the plant organs: roots, leaves, stems and storage organs. Storage organs, however, may not only be formed from current photosyntheses but also from carbohydrates and proteins that have been stored temporarily in vegetative parts and that are redistributed during the reproductive stage. In the model, the latter process is not incorporated. The total growth of the crop is partitioned among the plant organs according to partitioning factors that are introduced as forcing functions; their values only change with the development stage of the crop.

In WOFOST, average (crop specific) conversion factors $C_{e,i}$ (kg kg^{-1}) should be specified for leaf, storage organ, stem and root biomass. WOFOST calculates a weighted average, C_e (kg kg-1), of these organ specific conversion factors by multiplying the organ specific values with the partitioning factors:

$$C_e = \frac{1}{\left(\dfrac{\xi_{leaf}}{C_{e,leaf}} + \dfrac{\xi_{stor}}{C_{e,stor}} + \dfrac{\xi_{stem}}{C_{e,stem}}\right)\left(1 - \xi_{root}\right) + \dfrac{\xi_{root}}{C_{e,root}}} \tag{7.22}$$

where ξ_i is the partitioning factor for organ i.

The gross dry matter growth rate w_{gross} (kg ha^{-1} d^{-1}) is related to the net assimilation rate A_{net} by:

$$w_{gross} = C_e A_{net} \tag{7.23}$$

Gross dry matter growth is first partitioned between shoots (leafs, stems and storage organs together) and roots:

$$w_{gross,root} = \xi_{root} w_{gross} \qquad \text{and} \qquad w_{gross,sh} = \left(1 - \xi_{root}\right) w_{gross} \tag{7.24}$$

where ξ_{root} is the partitioning factor for roots (-) and $w_{gross,root}$ and $w_{gross,sh}$ are the gross growing rates (kg ha^{-1} d^{-1}) of the roots and the shoots, respectively. The gross growth rate of leaves, stems and storage organs is simply the product of the gross dry matter growth rate of the shoots and the fraction allocated to these organs. The partitioning factors are a function of development stage and are crop specific. Figure 7.5 gives a typical example of the partitioning.

7.3.8 Senescence

The death rate of storage organs is assumed to be zero. The death rate of stem and roots is crop specific and is defined as the daily amount of the living biomass that no longer participates in the plant processes. The death rate of stems and roots is considered to be a function of development stage as specified by the user.

The death rate of leaves is more complicated. Leaf senescence occurs due to water stress, shading (high LAI), and also due to exceedance of the life span.

The potential death rate of leaves due to water stress $\zeta_{leaf,water}$ (kg ha^{-1} d^{-1}) is calculated as:

$$\zeta_{leaf,water} = W_{leaf}\left(1 - \frac{T_a}{T_p}\right)\zeta_{leaf,p} \tag{7.25}$$

where W_{leaf} is the leaf dry matter weight (kg ha^{-1}), T_a and T_p are the actual and potential transpiration rates (cm d^{-1}), respectively, and $\zeta_{leaf,p}$ is the maximum relative death rate of leaves due to water stress (kg kg^{-1} d^{-1}). The latter is crop specific and should be provided by the user.

A potential death rate due to self-shading, $\zeta_{leaf,shade}$ (kg ha^{-1} d^{-1}), is defined which increases linearly from zero at a critical leaf area index LAI_c (-), to its maximum value at $2LAI_c$:

$$\zeta_{leaf,shade} = 0.03\, W_{leaf} \left(\frac{LAI - LAI_c}{LAI_c} \right) \qquad \text{with} \qquad 0 < \left(\frac{LAI - LAI_c}{LAI_c} \right) < 1 \qquad (7.26)$$

with $LAI_c = 3.2/\kappa_{df}$ (see, section 7.4). Typical values for $\zeta_{leaf,p}$ and LAI_c are 0.03 d^{-1} and 4 m^{2}m^{-2}, respectively (Spitters et al., 1989).

WOFOST uses the highest value of $\zeta_{leaf,water}$ and $\zeta_{leaf,shade}$ for the combined effect of water stress and mutual shading.

Leaves that have escaped from premature death due to water stress or mutual shading, inevitably die due to exceedance of the life span for leaves. Life span is defined as the maximum time a leaf can live at a constant temperature of 35°C. A physiologic ageing factor, f_{age} (-), is calculated each day:

$$f_{age} = \frac{T - T_{b,age}}{35 - T_{b,age}} \qquad \text{with} \qquad f_{age} \geq 0 \qquad (7.27)$$

with $T_{b,age}$ the lower threshold temperature for physiologic ageing (°C), which is crop specific and should be provided by the user.

The integral of the physiologic ageing factor over time yields the physiologic age, P_{age} (d):

$$P_{age}^{j+1} = P_{age}^{j} + f_{age}\Delta t \qquad (7.28)$$

In order to correct for leaf senescence, the specific leaf area of each day, S_{la}^{j} (ha kg^{-1}), the growth of the dry matter weight of leaves per day, w_{leaf}, and the physiological age, P_{age}, are stored in 3 corresponding arrays. The first element of the arrays represents the most recent day and the last element of the arrays represents the oldest day.

The weight of the leaves that have died during a day due to water stress or mutual shading is subtracted from the weight of the oldest leaf class. When senescence is larger than the amount available in the oldest leaf class, the remaining senescence is subtracted from the next oldest leaf class. Emptying of the leaf classes continues,

until the amount of senescence is dissipated completely or the remaining amount of leaves becomes zero.

Leaves may maximally attain the age defined by the crop specific life span. WOFOST checks the leaf classes ages. The first class younger than the defined life span becomes the oldest class.

7.3.9 Net growth

The initial amount of total dry crop weight should be provided by the user. This amount is multiplied by the partitioning factors, ξ_i, to yield the dry weight values at emergence.

The net growth rates of the plant organs, $w_{net,i}$ (kg ha^{-1} d$^{-1)}$) result from the gross growth rates (Section 7.8) and the senescence rates, ζ_i (kg kg^{-1} d^{-1}):

$$w_{net,i} = w_{gross,i} - \zeta_i W_i \qquad (7.29)$$

By integrating $w_{net,i}$ over time, the dry matter weight of organ i, W_i (kg ha^{-1}), is calculated.

An exception has to be made for the growth of leaves. In the initial stage, the rate of leaf appearance and final leaf size are constrained by temperature through its effect on cell division and extension, rather than by the supply of assimilates. For a relative wide range of temperatures the growth rate responds more or less linearly to temperature (Hunt et al., 1985; Causton and Venus, 1981; Van Dobben, 1962). The growth rate of the leaf area index, w_{LAI} (ha ha^{-1} d^{-1}), in this so-called exponential stage, is described by:

$$w_{LAI} = LAI \; w_{LAI, max} T_{eff} \qquad (7.30)$$

where $w_{LAI,max}$ is the maximum relative increase of leaf area index (°C^{-1} d^{-1}).

WOFOST assumes that the exponential growth rate of leaf area index will continue until it equals the assimilation limited growth rate of the leaf area index. During this second, source limited growth stage, w_{LAI} is described by:

$$w_{LAI} = w_{net,leaf} S_{la} \qquad (7.31)$$

where S_{la} is the specific leaf area (ha kg^{-1}).

The green parts of stems and storage organs, may absorb a substantial amount of radiation. Therefore the so-called green area index GAI_i (ha ha^{-1}) should be added to the leaf area index. The green area index of the stems and storage organs, are calculated from the dry matter weights of the organs:

$$GAI_i = S_{ga,i} W_i \qquad\qquad (7.32)$$

with $S_{ga,i}$ the specific green area (ha kg^{-1}) of either stems or storage organ. $S_{ga,i}$ are crop specific and should be provided by the user.

7.3.10 Root growth

Root extension is computed in a straightforward way. The user needs to specify the initial rooting depth, the maximum rooting depth as determined by the crop and by the soil, and the maximum daily increase in rooting depth, $d_{root,max}$ (cm). Daily increase in rooting depth is equal to the maximum daily increase, unless maximum rooting depth is reached or no assimilates are available for root growth:

$$D_{root}^{j+1} = D_{root}^{j} + d_{root,\,max} \qquad \text{if} \qquad D_{root}^{j+1} \leq D_{root,\,max} \qquad \text{and} \qquad w_{net,\,root} \geq 0 \qquad (7.33)$$

where D_{root}^{j} is the rooting depth (cm) at day j.

7.4   User instructions

7.4.1   Simple crop module

An example of the input file is given in Box 7.1. Most data are specified as function of crop development stage, which ranges from 0 to 2. In part 1, the development stage can be defined either linear in time (specify only duration of crop growth) or based on the temperature sums in the vegetative and reproductive stage.

In part 2, light extinction coefficients are used to quantify the decrease of solar radiation within a canopy (Chapter 3). Default values of $\kappa_{dir} = 0.8$ and $\kappa_{dif} = 0.72$ will suffice in most cases.

In part 3, either leaf area or soil cover during crop development should be specified, in order to distribute evapotranspiration fluxes over evaporation and transpiration, as discussed in Chapter 3.

In part 4 a choice should be made between input of crop factors or crop heights. Crop factors should be used when ET_{ref} values are used as input, or when the Penman-Monteith method is used to calculate ET_{ref}. Crop heights should be specified if the potential evapotranspiration fluxes are derived directly for the actual crop (see Table 3.2). In that case also the reflection coefficient and stomatal resistance of the crop should be defined.

Rooting depth during crop development (part 5) in combination with a dimensionless root length density distribution (part 10) will be used by SWAP to determine the distribution of rootwater extraction rates.

In part 6, yield response factors as function of development stage should be specified. In case of a linear relation between Y_a/Y_p and T_a/T_p during the whole growing period, or when no information is available of the yield response factors as function of development stage D_s for the particular crop, specify $K_{y,k} = 1$ for $0 < D_s < 2$ and specify one growing stage k. Please, note that increasing the number of growing stages reduces the relative yield as calculated by Eq. (7.1).

Part 7 describes the reduction function of root water uptake for either too wet or too dry conditions (Fig. 3.4). Critical pressure head values of this sink term function for a number of crops are given by Taylor and Ashcroft (1972), see 0. In part 7 also the minimum canopy resistance for the Penman-Monteith method should be specified.

Part 8 specifies the parameters which describe the reduction of root water uptake as function of salinity concentrations (Fig. 3.5). Critical salinity concentrations have been experimentally determined for many crops (Maas, 1990). 0 lists salt tolerance data for a number of crops.

Interception input data are specified in Part 9. For agricultural crops, just one interception coefficient for the Von Hoyningen-Hune and Braden concept is required. The default value of $a = 0.25$ mm will suffice for most agricultural crops. In case of trees and forests (Gash concept) SWAP requires average rainfall and evaporation fluxes as function of crop development. These values are independent of other specified weather data.

---

*Box 7.1 Crop input data for simple model in file *.crp.*

```
**********************************************************************************************
*** PLANT GROWTH SECTION ***


**********************************************************************************************
* Part 1: Crop development

  IDEV = 1 ! length of crop cycle: 1 = fixed, 2 = variable

* If fixed growth length (IDEV = 1), specify:
  LCC  =   168 ! Length of the crop cycle [1..366 days, I]

* If variable growth length (IDEV = 2), specify:
  TSUMEA = 1050.0    ! Temperature sum from emergence to anthesis [0..10000 C, R]
  TSUMAM = 1000.0    ! Temperature sum from anthesis to maturity  [0..10000 C, R]
  TBASE  = 0.0       ! Start value of temperature sum [-10..30 C, R]
**********************************************************************************************

**********************************************************************************************
* Part 2: Light extinction

  KDIF  =     0.60 ! Extinction coefficient for diffuse visible light [0..2 -, R]
  KDIR  =     0.75 ! Extinction coefficient for direct visible light  [0..2 -, R]
**********************************************************************************************

**********************************************************************************************
* Part 3: Leaf area index or soil cover fraction

  SWGC = 1 ! choice between LAI [=1] or soil cover fraction [=2]

* If SWGC = 1, list leaf area index [0..12 ha/ha, R],    as function of dev. stage [0..2 -,R]:
* If SWGC = 2, list soil cover fraction [0..1 m2/m2, R], as function of dev. stage [0..2 -,R]:

*        DVS   LAI or SCF  ( maximum 36 records)
  GCTB =
```

```
                  0.00    0.05
                  0.30    0.14
                  0.50    0.61
                  0.70    4.10
                  1.00    5.00
                  1.40    5.80
                  2.00    5.20
* End of table
***********************************************************************************************


***********************************************************************************************
* Part 4: crop factor or crop height

  SWCF = 2 ! choice between crop factor [=1] or crop height [=2]
* Choose crop factor if ETref is used, either from meteo input file (SWETR = 1) or with PM
* Choose crop height if PM should be used with actual crop height, albedo and resistance

* If SWCF = 1, list crop factor CF [0.5..1.5, R],   as function of dev. stage DVS [0..2 -,R]:
* If SWCF = 2, list crop height CH [0..1000 cm, R], as function of dev. stage DVS [0..2 -,R]:
* (maximum 36 records)

     DVS       CH      CF
     0.0       1.0     0.8
     0.3      15.0     0.8
     0.5      40.0     0.9
     0.7     140.0     1.0
     1.0     170.0     1.1
     1.4     180.0     1.2
     2.0     175.0     1.2
* End of table

* If SWCF = 2, in addition to crop height list crop specific values for:
  ALBEDO =    0.23 ! crop reflection coefficient [0..1.0 -, R]
  RSC    =   70.0 ! Minimum canopy resistance [0..10^6 s/m, R]
***********************************************************************************************


***********************************************************************************************
* Part 5: rooting depth

* List rooting depth [0..1000 cm, R], as a function of development stage [0..2 -,R]:

*         DVS    RD    (maximum 36 records)
  RDTB =
          0.00     5.00
          0.30    20.00
          0.50    50.00
          0.70    80.00
          1.00    90.00
          2.00   100.00
* End of table
***********************************************************************************************


***********************************************************************************************
* Part 6: yield response

* List yield response factor [0..5 -,R], as function of development stage [0..2 -,R]:

*         DVS    KY    (maximum 36 records)
  KYTB =
          0.00   1.00
          2.00   1.00
* End of table
***********************************************************************************************


***********************************************************************************************
* Part 7: soil water extraction by plant roots

  HLIM1  =      -15.0 ! No water extraction at higher pressure heads, [-100..100 cm, R]
  HLIM2U =     -30.0 ! h below which optimum water extr. starts for top layer, [-1000..100 cm, R]
  HLIM2L =     -30.0 ! h below which optimum water extr. starts for sub layer, [-1000..100 cm, R]
  HLIM3H =    -325.0 ! h below which water uptake red. starts at high Tpot, [-10000..100 cm, R]
  HLIM3L =    -600.0 ! h below which water uptake red. starts at low Tpot, [-10000..100 cm, R]
  HLIM4  =   -8000.0 ! No water extraction at lower pressure heads, [-16000..100 cm, R]
  ADCRH  =       0.5 ! Level of high atmospheric demand, [0..5 cm/d, R]
  ADCRL  =       0.1 ! Level of low atmospheric demand,  [0..5 cm/d, R]
***********************************************************************************************


***********************************************************************************************
* Part 8: salt stress

  ECMAX  =        2.0 ! ECsat level at which salt stress starts, [0..20 dS/m, R]
```

```
   ECSLOP =        0.0 ! Decline of rootwater uptake above ECMAX [0..40 %/dS/m, R]
********************************************************************************************



********************************************************************************************
* Part 9: interception

  SWINTER =  1  ! Switch for rainfall interception method:
               ! 0 = No interception calculated
               ! 1 = Agricultural crops (Von Hoyningen-Hune and Braden)
               ! 2 = Closed forest canopies (Gash)

* In case of interception method for agricultural crops (SWINTER = 1) specify:
  COFAB  =       0.25 ! Interception coefficient Von Hoyningen-Hune and Braden, [0..1 mm, R]

* In case of interception method for closed forest canopies (SWINTER = 2) specify as function
* of time of the year T [0..366 d, R], maximum 36 records:
* PFREE = free throughfall coefficient, [0.d0..1.d0 -, R]
* PSTEM = stem flow coefficient, [0.d0..1.d0 -, R]
* SCANOPY = storage capacity of canopy, [0.d0..10.d0 cm, R]
* AVPREC = average rainfall intensity, [0.d0..100.d0 cm, R]
* AVEVAP = average evaporation intensity during rainfall from a wet canopy, [0.d0..10.d0 cm, R]

      T       PFREE     PSTEM    SCANOPY    AVPREC    AVEVAP
    0.0       0.9       0.05       0.4       6.0       1.5
  365.0       0.9       0.05       0.4       6.0       1.5
* End of table
********************************************************************************************


********************************************************************************************
* Part 10: Root density distribution and root growth

* List relative root density [0..1 -, R], as function of rel. rooting depth [0..1 -, R]:

*    Rdepth Rdensity  (maximum 11 records)
  RDCTB =
      0.00      1.00
      1.00      0.00
* End of table
*************************************************************************************
```

7.4.2 Detailed crop module

Input of the detailed crop module has been divided in 13 parts:

1. Crop factor of crop height
2. Crop development
3. Initial values
4. Green surface area
5. Assimilation
6. Conversion of assimilates into biomass
7. Maintenance respiration
8. Partitioning
9. Death rates
10. Crop water use
11. Salt stress
12. Interception
13. Root growth and root density profile

An example of the input file is given in Box 7.2. In general the theorie description in Section 7.3 in combination with the descriptions in the input file will be sufficient to guide the model user. However a few additional remarks should be made here.

In part 4 a choice should be made between input of crop factors or crop heights. Crop factors should be used when ET_{ref} values are used as input, or when the Penman-Monteith method is used to calculate ET_{ref}. Crop heights should be specified if the potential evapotranspiration fluxes are derived directly for the actual crop (see Table 3.2). In that case also the reflection coefficient and stomatal resistance of the crop should be defined.

In part 8 the user should specify the partitioning factors as function of crop development stage. As explained in Section 7.3.7, WOFOST first divides the gross dry matter among roots and shoots (leafs, stems and storage organs together), using the partitioning factor for roots. Next WOFOST divides the gross dry matter directed to the shoots among leafs, stems and storage organs, using the partitioning factors for these plant organs. At any development stage the sum $\xi_{leaf}+\xi_{stem}+\xi_{stor}$ must equal one.

The theoretical background of Parts 10-12 (Crop water use, Salt stress and Interception) applies to both the simple and detailed crop model and has been explained in Chapter 3.

Boons-Prins et al. (1993) documented specific parameters for the crops winter wheat, grain maize, spring barley, rice, sugar beet, potato, field bean, soy bean, winter oilseed rape and sunflower. WOFOST input files for these crops will be provided with the SWAP program.

```
*************************************************************************************************
*** PLANT GROWTH SECTION ***


*************************************************************************************************
* Part 1: Crop factor or crop height

  SWCF = 1 ! choice between crop factor [=1] or crop height [=2]
* Choose crop factor if ETref is used, either from meteo input file (SWETR = 1) or with PM
* Choose crop height if PM should be used with actual crop height, albedo and resistance

* If SWCF = 1, list crop factor CF [0.5..1.5, R],   as function of dev. stage DVS [0..2 -,R]:
* If SWCF = 2, list crop height CH [0..1000 cm, R], as function of dev. stage DVS [0..2 -,R]:
* (maximum 36 records)

    DVS       CH      CF
    0.0      1.0     1.0
    1.0     40.0     1.1
    2.0     50.0     1.1
* End of Table

* If SWCF = 2, list crop specifi values for:
```

Box 7.2 Crop input data for detailed model in file *.crp.

```
   ALBEDO =   0.23 ! crop reflection coefficient [0..1.0 -, R]
   RSC    =   70.0 ! Minimum canopy resistance [0..10^6 s/m, R]
**********************************************************************************************



**********************************************************************************************
* Part 2 : Crop development

   IDSL   = 0 ! Switch for crop development:
              ! 0 = Crop development before anthesis depends on temperature only
              ! 1 = Crop development before anthesis depends on daylength only
              ! 2 = Crop development before anthesis depends on both

* If IDSL = 1 or 2, specify:
   DLO    = 14.0    ! Optimum day length for crop development [0..24 h, R]
   DLC    = 8.0     ! Minimum day length, [0..24 h, R]

* If IDSL = 0 or 2 specify:
   TSUMEA =   152.00 ! Temperature sum from emergence to anthesis, [0..10000 C, R]
   TSUMAM =  1209.00 ! Temperature sum from anthesis to maturity  [0..10000 C, R]

* List increase in temperature sum [0..60 C, R] as function of daily average temp. [0..100 C, R]

*          TAV  DTSM    (maximum 15 records)
   DTSMTB =
              0.00   0.00
              2.00   0.00
             13.00  11.00
             29.00  11.00
* End of Table

   DVSEND =     2.00 ! development stage at harvest [-]
**********************************************************************************************


**********************************************************************************************
* Part 3: Initial values

   TDWI   =    33.0 ! Initial total crop dry weight [0..10000 kg/ha, R]
   LAIEM  = 0.0589 ! Leaf area index at emergence [0..10 m2/m2, R]
   RGRLAI = 0.01200 ! Maximum relative increase in LAI [0..1 m2/m2/d, R]
**********************************************************************************************


**********************************************************************************************
* Part 4: Green surface area

   SPA    = 0.0000 ! Specific pod area  [0..1 ha/kg, R]
   SSA    = 0.0000 ! Specific stem area [0..1 ha/kg, R]
   SPAN   = 35.00 ! Life span under leaves under optimum conditions, [0..366 d, R]
   TBASE  =  2.00 ! Lower threshold temperature for ageing of leaves ,[-10..30 C, R]

* List specific leaf area [0..1 ha/kg, R] as function of devel. stage [0..2, R]

*          DVS  SLA    (maximum 15 records)
   SLATB =
             0.00 0.0030
             1.10 0.0030
             2.00 0.0015
* End of Table
**********************************************************************************************


**********************************************************************************************
* Part 5: Assimilation

   KDIF   =    1.00 ! Extinction coefficient for diffuse visible light, [0..2 -, R]
   KDIR   =    0.75 ! Extinction coefficient for direct visible light, [0..2 -, R]
   EFF    =    0.45 ! Light use efficiency for real leaf [0..10 kg/ha/hr/(Jm2s), R]

* List max CO2 assimilation rate [0..100 kg/ha/hr, R] as function of development stage [0..2 -, R]

*          DVS    AMAX    (maximum 15 records)
   AMAXTB =
             0.00 30.000
             1.57 30.000
             2.00  0.000
* End of table

* List reduction factor of AMAX [-, R] as function of average day temp. [-10..50 C, R]
*          TAVD   TMPF   (maximum 15 records)
```

```
  TMPFTB =
             0.00   0.010
             3.00   0.010
            10.00   0.750
            15.00   1.000
            20.00   1.000
            26.00   0.750
            33.00   0.010
* End of table

* List reduction factor of AMAX [-, R] as function of minimum day temp. [-10..50 C, R]

*           TMNR    TMNF   (maximum 15 records)
  TMNFTB =
             0.00   0.000
             3.00   1.000
* End of table
*************************************************************************************************

*************************************************************************************************
* Part 6: Conversion of assimilates into biomass

  CVL    = 0.7200 ! Efficiency of conversion into leaves,         [0..1 kg/kg, R]
  CVO    = 0.8500 ! Efficiency of conversion into storage organs, [0..1 kg/kg, R]
  CVR    = 0.7200 ! Efficiency of conversion into roots,          [0..1 kg/kg, R]
  CVS    = 0.6900 ! Efficiency of conversion into stems,          [0..1 kg/kg, R]
*************************************************************************************************

*************************************************************************************************
* Part 7: Maintenance respiration

  Q10    = 2.0000 ! Rel. increase in respiration rate with temperature, [0..5 /10 C, R]
  RML    = 0.0300 ! Rel. maintenance respiration rate of leaves,  [0..1 kgCH2O/kg/d, R]
  RMO    = 0.0045 ! Rel. maintenance respiration rate of st. org.,[0..1 kgCH2O/kg/d, R]
  RMR    = 0.0100 ! Rel. maintenance respiration rate of roots,   [0..1 kgCH2O/kg/d, R]
  RMS    = 0.0150 ! Rel. maintenance respiration rate of stems,   [0..1 kgCH2O/kg/d, R]

* List reduction factor of senescence [-, R] as function of dev. stage [0..2 -, R]

*          DVS    RFSE   (maximum 15 records)
  RFSETB =
             0.00   1.00
             2.00   1.00
* End of table
*************************************************************************************************

*************************************************************************************************
* Part 8: Partitioning

* List fraction of total dry matter increase partitioned to the roots [kg/kg, R]
* as function of development stage [0..2 -, R]

*          DVS    FR    (maximum 15 records)
  FRTB =
             0.00   0.20
             1.00   0.20
             1.36   0.00
             2.00   0.00
* End of table

* List fraction of total above ground dry matter incr. part. to the leaves [kg/kg, R]
* as function of development stage [0..2 -, R]

*          DVS     FL   (maximum 15 records)
  FLTB =
             0.00   0.75
             1.00   0.75
             1.27   0.00
             2.00   0.00
* End of table

* List fraction of total above ground dry matter incr. part. to the stems [kg/kg, R]
* as function of development stage [0..2 -, R]
*          DVS    FS    (maximum 15 records)
  FSTB =
             0.00   0.25
             1.27   0.25
             1.36   0.00
             2.00   0.00
* End of table
```

```
* List fraction of total above ground dry matter incr. part. to the st. organs [kg/kg, R]
* as function of development stage [0..2 -, R]
*         DVS    FO    (maximum 15 records)
  FOTB =
         0.00   0.00
         1.00   0.00
         1.27   0.75
         1.36   1.00
         2.00   1.00
* End of table
*****************************************************************************************
* Part 9: Death rates

  PERDL =   0.030 ! Maximum rel. death rate of leaves due to water stress [0..3 /d, R]

* List relative death rates of roots [kg/kg/d] as function of dev. stage [0..2 -, R]

*         DVS    RDRR    (maximum 15 records)
  RDRRTB =
         0.0000 0.0000
         1.5000 0.0000
         1.5001 0.0200
         2.0000 0.0200
* End of table

* List relative death rates of stems [kg/kg/d] as function of dev. stage [0..2 -, R]

*         DVS    RDRS    (maximum 15 records)
  RDRSTB =
         0.0000 0.0000
         1.5000 0.0000
         1.5001 0.0200
         2.0000 0.0200
* End of table
*****************************************************************************************

*****************************************************************************************
* Part 10: Crop water use

  HLIM1  =     -10.0 ! No water extraction at higher pressure heads, [-100..100 cm, R]
  HLIM2U =     -25.0 ! h below which optimum water extr. starts for top layer, [-1000..100 cm, R]
  HLIM2L =     -25.0 ! h below which optimum water extr. starts for sub layer, [-1000..100 cm, R]
  HLIM3H =    -300.0 ! h below which water uptake red. starts at high Tpot, [-10000..100 cm, R]
  HLIM3L =    -500.0 ! h below which water uptake red. starts at low Tpot, [-10000..100 cm, R]
  HLIM4  =  -10000.0 ! No water extraction at lower pressure heads, [-16000..100 cm, R]
  ADCRH  =       0.5 ! Level of high atmospheric demand, [0..5 cm/d, R]
  ADCRL  =       0.1 ! Level of low atmospheric demand,  [0..5 cm/d, R]
*****************************************************************************************

*****************************************************************************************
* Part 11: Salt stress

  ECMAX  =       1.7 ! ECsat level at which salt stress starts, [0..20 dS/m, R]
  ECSLOP =      12.0 ! Decline of rootwater uptake above ECMAX [0..40 %/dS/m, R]
*****************************************************************************************

*****************************************************************************************
* Part 12: Interception

  COFAB  =      0.25 ! Interception coefficient Von Hoyningen-Hune and Braden, [0..1 cm, R]
*****************************************************************************************

*****************************************************************************************
* Part 13: Root growth and root density profile

  RDI    =  10.00 ! Initial rooting depth, [0..1000 cm, R]
  RRI    =   1.20 ! Maximum daily increase in rooting depth, [0..100 cm/d, R]
  RDC    =  50.00 ! Maximum rooting depth crop/cultivar, [0..1000 cm, R]

* List relative root density [0..1 -, R], as function of rel. rooting depth [0..1 -, R]:
*       Rdepth Rdensity   (maximum 11 records)
  RDCTB =
         0.00     1.00
         1.00     1.00
* End of table
*****************************************************************************************
```

8 Solute transport

8.1 Introduction

Many solutes enter the natural system at the soil surface. The solute residence time in the unsaturated zone is important for soil- and groundwater pollution management. For instance organic compounds are mainly decomposed in the unsaturated zone, where the biological activity is concentrated. Most plants are able to extract water and nutrients from the soil only in the unsaturated zone. In irrigated areas, the long term salinity in the root zone will depend on the amount of percolation from the unsaturated zone. Whereas in the unsaturated zone the transport of solutes is predominantly vertical, once being in the groundwater solutes may diverge in any direction, threatening surface waters, nature reserves and drinking wells. Using an analytical model, Beltman et al. (1995) show the importance of the transport processes in the unsaturated zone as compared to the transport processes in the saturated zone. It is clear that a thorough understanding is needed of the processes that govern the transport, adsorption, root uptake and decomposition of the solutes in the unsaturated zone, in order to analyse and manage soil and water related environmental problems.

SWAP is designed to simulate basic transport processes at field scale level. Although for management purposes most farmers try to have more or less the same soil and drainage condition per field, still the existing soil spatial heterogeneity within a field may cause a large variation of solute fluxes (Biggar and Nielsen, 1976; Van de Pol et al., 1977; Van der Zee and Van Riemsdijk, 1987). Most of this variation is caused by spatial variation of the soil hydraulic functions, preferential flow due to macropores in structured soils or unstable wetting fronts in unstructured soils. In many cases it will not be possible to determine the variation (including the correlations) of all the physical parameters (Hopmans and Stricker, 1989). SWAP confines to the physical processes in order to be flexible in parameter input and allow the simulation of all kind of design and management scenarios. The spatial variability can be taken into account by inverse modelling or Monte Carlo simulation. Inverse modelling has been applied by Groen (1997). He measured for a period of time the solute concentrations in the soil profile and drainage water and determined 'field effective' transport parameters by inverse modelling. In case of Monte Carlo simulations the model is run a large number of times, while the input parameters and boundary conditions are varied according to the variation at comparable fields (Boesten and Van der Linden, 1991).

SWAP focuses on the transport of salts, pesticides and other solutes that can be described with relatively simple physical relations: convection, diffusion, dispersion, root uptake, Freundlich adsorption and first order decomposition. Transport related processes that are not considered in SWAP are:

- volatilization and gas transport
- transport of non-mixing or immiscible fluids (e.g. oil and water)
- chemical equilibria of various solutes (e.g. between Na^+, Ca^{2+} and Mg^{2+})
- chemical and biological chain reactions (e.g. mineralization, nitrification)

In case of advanced pesticide transport, including volatilization and kinetic adsorption, SWAP can be used in combination with the model PESTLA (Van den Berg and Boesten, 1998) and PEARL (Leistra et al., 2000; Tiktak et al., 2000). For nutrient transport (nitrogen and phosphorus), SWAP can be used in combination with the model ANIMO (Rijtema et al., 1997; Kroes and Roelsma, 1998).

In this chapter, we first describe the solute transport processes that are considered in SWAP. Next, we discuss the boundary conditions applied. Also, we consider how SWAP deals with solute transport in water repellent soils and in cracked clay soils. Finally we describe the input data for solute transport.

8.2 Basic equations

8.2.1 Transport processes

The three main solute transport mechanisms in soil water are diffusion, convection and dispersion. *Diffusion* is solute transport caused by the solute gradient. Thermal motion of the solute molecules within the soil solution causes a net transport of molecules from high to low concentrations. The solute flux J_{dif} (g cm^{-2} d^{-1}) is generally described by Fick's first law:

$$J_{dif} = -\theta D_{dif} \frac{\partial c}{\partial z} \qquad (8.1)$$

with D_{dif} the diffusion coefficient (cm^2 d^{-1}) and c the solute concentration in soil water (g cm^{-3}). D_{dif} is very sensitive to the actual water content, as it strongly affects the solute transport path and the effective cross-sectional transport area. In SWAP we employ the relation proposed by Millington and Quirk (1961):

$$D_{dif} = D_w \frac{\theta^{7/3}}{\phi_{por}^2} \qquad (8.2)$$

with D_w the solute diffusion coefficient in free water (cm^2 d^{-1}) and ϕ_{por} the soil porosity (cm^3 cm^{-3}).
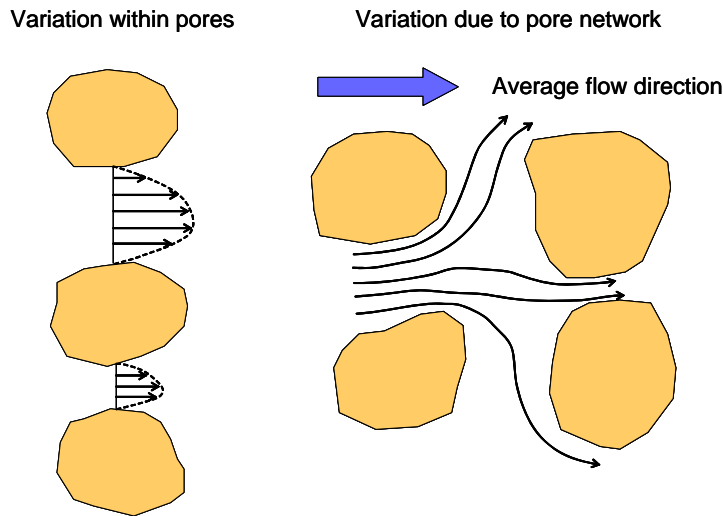
Figure 8.1 Flow velocity variation within pores and within the pore network.

The bulk transport of solutes occurs when solutes are carried along with the moving soil water. The mean flux of this transport is called the *convective* flux, J_{con} (g cm^{-2} d^{-1}), and can be calculated from the average soil water flux:

$$J_{con} = qc \qquad (8.3)$$

When describing water flow, we usually consider the Darcy flux q (cm d^{-1}), which is averaged over a certain cross section. In case of solute transport, we have to account for the water velocity variation between pores of different size and geometry and also the water velocity variation inside a pore itself (Fig. 8.1). The variety of water velocities cause some solutes to advance faster than the average solute front, and other solutes to advance slower. The overall effect will be that steep solute fronts tends to smoothen or to disperse. Solutes seem to flow from high to low concentrations. If the time required for solutes to mix in the transverse direction is small, compared to the time required for solutes to move in the flow direction by mean convection, the *dispersion* flux J_{dis} (g cm^{-2} d^{-1}) is proportional to the solute gradient (Bear, 1972):

$$J_{dis} = -\theta D_{dis} \frac{\partial c}{\partial z} \qquad (8.4)$$

with D_{dis} the dispersion coefficient (cm^2 d^{-1}). Under laminar flow conditions D_{dis} itself is proportional to the pore water velocity $v = q/\theta$ (Bolt, 1979):

$$D_{dis} = L_{dis} |v| \qquad (8.5)$$

with L_{dis} the dispersion length (cm). Unless water is flowing very slowly through repacked soil, the dispersion flux is usually much larger than the diffusion flux.

The total solute flux J (g cm^{-2} d^{-1}) is therefore described by:

$$J = J_{con} + J_{dif} + J_{dis} = qc - \theta\left(D_{dif} + D_{dis}\right)\frac{\partial c}{\partial z} \qquad (8.6)$$

8.2.2   Continuity and transport equation

By considering conservation of mass in an elementary volume, we may derive the continuity equation for solute transport:

$$\frac{\partial X}{\partial t} = -\frac{\partial J}{\partial z} - S_s \qquad (8.7)$$

with X being the total solute concentration in the soil system (g cm^{-3}) and S_s the solute sink term (g cm^{-3} d^{-1}) accounting for decomposition and uptake by roots.

The solutes may be dissolved in the soil water or may be adsorbed to organic matter or to clay minerals:

$$X = \theta c + \rho_b Q \qquad (8.8)$$

with ρ_b being the dry soil bulk density (g cm^{-3}) and Q the amount adsorbed (g g^{-1}). The adsorption isotherm describes the amount of solutes adsorbed in equilibrium with the dissolved concentration. At this stage we will assume instantaneous equilibrium between c and Q and use the non-linear Freundlich equation, which is a flexible function for many organic and inorganic solutes. Freundlich adsorption can be written as:

$$Q = K_f c_{ref}\left(\frac{c}{c_{ref}}\right)^{N_f} \qquad (8.9)$$

with K_f the Freundlich coefficient (cm^3 g^{-1}), N_f is the Freundlich exponent (-) and c_{ref} is a reference value of the solute concentration (g cm^{-3}) which is used to make N_f dimensionless.

The solute sink term S_s can be written as:

$$S_s = \mu\left(\theta c + \rho_b Q\right) + K_r S c \qquad (8.10)$$

where μ is the first order rate coefficient of transformation (d^{-1}), K_r is the root uptake preference factor (-) and S the root water extraction rate (d^{-1}). At the right hand side of Eq. (8.10), the first term accounts for linear decomposition and the second term for root uptake proportional to water uptake. K_r accounts for positive or negative selection of solute ions relative to the amount of soil water that is extracted.

The coefficient μ is affected by soil temperature, water content and depth. Analogous to Boesten and Van der Linden (1991), SWAP calculates μ from:

$$\mu = f_T \, f_\theta \, f_z \, \mu_{ref} \qquad (8.11)$$

in which f_T is a soil temperature factor (-), f_θ and f_z are reduction factors (-) accounting for the effect of soil water content and soil depth, and μ_{ref} (d⁻¹) is μ at reference conditions (e.g. soil from the plough layer at 20 °C and at soil water pressure head $h = -100$ cm).

The factor f_T is described according to Boesten (1986) as:

$$f_T = e^{\gamma_T (T - 20)} \qquad (8.12)$$

where γ_T is a parameter (°C⁻¹), and T is the soil temperature in °C.

Wolfe et al. (1990) describe the importance of the water content in transformation processes. Realizing that it is a large simplification, in SWAP we adopt the relation as proposed by Walker (1974) :

$$f_\theta = \left(\frac{\theta}{\theta_{ref}} \right)^B \qquad \text{with} \quad f_\theta \leq 1.0 \qquad (8.13)$$

where θ_{ref} is θ at $h = -100$ cm and B is a constant (-).

The transformation reduction factor for soil depth, f_z, should be derived from in situ measurements. The user may specify f_z as function of soil depth in the input file.

Combination of Eq. (8.6), (8.7), (8.8), and (8.10), yields the transport equation applied in SWAP which is valid for dynamic, one-dimensional, convective-dispersive mass transport, including non-linear adsorption, linear decay and proportional root uptake in unsaturated/saturated soil (Van Genuchten and Cleary, 1979; Nielsen et al., 1986; Boesten and Van der Linden, 1991):

$$\frac{\partial(\theta c + \rho_b Q)}{\partial t} = -\frac{\partial(qc)}{\partial z} + \frac{\partial \left[\theta \left(D_{dif} + D_{dis} \right) \frac{\partial c}{\partial z} \right]}{\partial z} - \mu(\theta c + \rho_b Q) - K_r S c \qquad (8.14)$$

An explicit, central finite difference scheme is used to solve Eq. (8.14):

$$\frac{\theta_i^{j+1} c_i^{j+1} + \rho_b Q_i^{j+1} - \theta_i^j c_i^j - \rho_b Q_i^j}{\Delta t^j} =$$

$$\frac{q_{i-\frac{1}{2}}^j c_{i-\frac{1}{2}}^j - q_{i+\frac{1}{2}}^j c_{i+\frac{1}{2}}^j}{\Delta z_i} + \frac{1}{\Delta z_i}\left[\frac{\theta_{i-\frac{1}{2}}^j D_{i-\frac{1}{2}}^j \left(c_{i-1}^j - c_i^j\right)}{\frac{1}{2}\left(\Delta z_{i-1} + \Delta z_i\right)} - \frac{\theta_{i+\frac{1}{2}}^j D_{i+\frac{1}{2}}^j \left(c_i^j - c_{i+1}^j\right)}{\frac{1}{2}\left(\Delta z_i + \Delta z_{i+1}\right)} \right] -$$

$$\mu_i^j \left(\theta_i^j c_i^j + \rho_b Q_i^j\right) - K_r S_i^j c_i^j$$

(8.15)

where D (= $D_{dif} + D_{dis}$) is the overall dispersion coefficient (cm^2 d^{-1}); the superscript j denotes the time level, subscript i the node number and subscripts i-1/2 and i+1/2 refer to linearly interpolated values at the upper and lower compartment boundary, respectively. Compared to an implicit, iterative scheme, above explicit scheme has the advantage that incorporation of non-linear adsorption, mobile/immobile concepts, and other non-linear processes is relatively easy. In order to ensure stability of the explicit scheme, the time step Δt^j should meet the criterium (Van Genuchten and Wierenga, 1974):

$$\Delta t^j \leq \frac{\Delta z_i^2 \, \theta_i^j}{2 D_i^j}$$

(8.16)

This stability criterium applies to non-sorbing substances and is therefore also safe for sorbing substances.

8.3   Boundary conditions

As *initial condition*, the user needs to specify the solute concentrations, c_i (g cm^{-3}), in the soil water and the average solute concentration, c_{gr} (g cm^{-3}), in the groundwater.

For the *top boundary condition*, the solute concentrations in irrigation and rain water, c_{irr} and c_{prec} (g cm^{-3}), need to be specified. During evaporation no solutes leave the soil profile at the surface. During infiltration, the solute concentration of water that enters the soil profile at the top, c_{pond} (g cm^{-3}), is affected by the ponding layer and its concentration at the former time step, the solute amounts coming in by rain and irrigation, and the solute amounts transported laterally to cracks:

$$c_{pond}^j = \frac{\left(P_{net}^j c_{prec} + I_{net}^j c_{irr}\right)\Delta t^j + h_{pond}^{j-1} c_{pond}^{j-1}}{h_{pond}^j - \left(q_{top} + q_{lat}\right)\Delta t^j}$$

(8.17)

where P_{net} is the net precipitation rate (cm d^{-1}, I_{net} is the net irrigation rate (cm d^{-1}), h_{pond} is the height of water ponding on the soil surface, q_{top} is the water flux at the soil surface (cm d^{-1}, positive upward) and q_{lat} is the water flux flowing to cracks (cm d^{-1}, see Section 8.4). The solute flux J_{top} (g cm^{-2}) entering the soil at the surface, equals:

$$J_{top} = q_{top} c_{pond} \left(1.0 - A_c\right)$$

(8.18)

where A_c is the relative crack area (cm^2 cm^{-2}).

For the *drainage boundary condition*, during drainage ($q_{drain} > 0$) the solute flux J_{drain} (g cm^{-2}) that leaves the one-dimensional soil profile is accumulated for each compartment below groundwater level:

$$J_{drain} = \sum_{i=n_{gwl}}^{n} q_{drain,i}\, c_i \tag{8.19}$$

where n_{gwl} is the compartment with the groundwater level and $q_{drain,i}$ is the lateral drainage flux (cm d^{-1}) of compartment i. During infiltration ($q_{drain} < 0$), J$_{drain}$ follows from:

$$J_{drain} = \sum_{i=n_{gwl}}^{n} q_{drain,i}\, c_{gr} \tag{8.20}$$

where c_{gr} is the average solute concentration in the groundwater (g cm^{-3}).

For the *bottom boundary condition*, SWAP uses the flux through the bottom of the soil profile q_{bot} (cm d^{-1}). In case of upward flow ($q_{bot} > 0$), the solute flux J_{bot} (g cm^{-2}, positive is upwards) equals:

$$J_{bot} = q_{bot} c_{gr} \tag{8.21}$$

If q_{bot} is directed downwards ($q_{bot} < 0$), the solute flux J_{bot} (g cm^{-2}) equals:

$$J_{bot} = q_{bot} c_n \tag{8.22}$$

8.4 Crack solute transport

In order to calculate solute transport in combination with macropore flow, SWAP may generate soil water fluxes which are input to the pesticide model PEARL or the nutrient model ANIMO.

8.5 Residence time in the saturated zone

In the case of heterogeneous groundwater flow or multi-level drainage, the residence time approach described in Chapter 4 is used. This section describes an alternative concept assuming a homogeneous aquifer and field drainage at one level.

Ernst (1973) and Van Ommen (1985) showed that the breakthrough curve of a field with fully penetrating drainage canals, is identical to the breakthrough curve of a reservoir with complete mixing. This is also valid if adsorption can be described by a linear isotherm and transformation occurs proportional to the existing concentration (Van Ommen, 1985).

Linear adsorption might be described by:

$$Q = k_{ads} c_{gr} \qquad (8.23)$$

where k_{ads} is the linear adsorption coefficient in the saturated zone (cm^3 g^{-1}). Numerical analysis by Duffy and Lee (1992) showed that dispersion in the saturated zone has only a minor effect for $L_{drain}/d_{aquif} \geq 10$, where L_{drain} is the distance between the drainage canals (cm) and d_{aquif} the thickness of the aquifer (cm). Generally L_{drain}/d_{aquif} will be around 10 or larger, therefore SWAP ignores dispersion.

In order to derive the breakthrough curve, the similarity is used between breakthrough curves of drained fields and mixed reservoirs. Starting point is the solute transport equation of the unsaturated zone, Eq. (8.14). Replacement of non-linear adsorption by linear adsorption, and removal of dispersion and root water uptake, results in the mass balance equation of the saturated zone:

$$\frac{\partial \left(\theta_s c_{gr} + \rho_b k_{ads} c_{gr} \right)}{\partial t} = \frac{q_{drain}}{d_{aquif}} \left(c_{in} - c_{gr} \right) - \mu_{gr} \left(\theta_s c_{gr} + \rho_b k_{ads} c_{gr} \right) \qquad (8.24)$$

where θ_s is the saturated water content (cm^3 cm^{-3}), q_{drain} is the drainage flux (cm d^{-1}), c_{in} is the solute concentration of water percolating from the unsaturated zone (g cm^{-3}) and μ_{gr} is the first order rate coefficient for transformation in the saturated zone (d^{-1}). Eq. (8.24) applies to a drainage situation ($q_{drain} > 0$). In case of infiltration ($q_{drain} < 0$), SWAP assumes the infiltrating water from the drainage system to be solute free, and Eq. (8.24) transforms into:

$$\frac{\partial \left(\theta_s c_{gr} + \rho_b k_{ads} c_{gr} \right)}{\partial t} = \frac{q_{drain}}{d_{aquif}} c_{gr} - \mu_{gr} \left(\theta_s c_{gr} + \rho_b k_{ads} c_{gr} \right) \qquad (8.25)$$

Eq. (8.24) and (8.25) are discretized as an explicit, forward difference scheme. The boundary conditions that apply to the saturated zone, are included in Eq. (8.24) and (8.25).

8.6   User instructions

Box 8.1 lists the input data for solute transport, which are divided over 7 parts:
1. Main switch
2. Top and initial boundary condition
3. Miscellaneous parameters as function of soil depth
4. Diffusion coefficient and solute uptake by roots
5. Adsorption
6. Decomposition
7. Solute residence in the saturated zone

In general the theorie description in Sections 8.2 – 8.6 in combination with the descriptions in the input file will be sufficient to guide the model user. A few additional remarks are appropriate at this place.

In case conservative solute are simulated, like salts are non-reactive tracers, we need only to consider the transport processes convection, diffusion, dispersion and passive uptake by plant roots.

At most field conditions we may neglect the effect of diffusion with respect to dispersion and therefore may specify $D_{dif} = 0$. The parameter dispersion length, L_{dis} (cm), depends on the scale over which the water flux and solute convection are averaged. Typical values of L_{dis} are 0.5 - 2.0 cm in packed laboratory columns and 5-20 cm in the field (Jury et al., 1991).

In case of high salinity levels, SWAP will reduce the root water uptake according to the reduction function of Maas and Hoffman (1977), see Fig. 3.5. In order to calculate this reduction, SWAP calculates the electrical conductivity of the saturation extract, EC_{sat} (dS m^{-1}) from the soil water solute concentration c (mg cm^{-3}) with:

$$EC_{sat} = 1.492 c_i \frac{\theta_i}{\theta_{sat}}$$

(8.26)

where θ_i is the actual water content (cm^3 cm^{-3}) and θ_{sat} is the saturated water content (cm^3 cm^{-3}).

SWAP supports two methods to account for the residence time of solutes in the saturated zone. The first one by proper distribution of the lateral drainage flux over the saturated compartments (Chapter 4). In that case we may set SWBR = 0 and specify the solute concentration in the groundwater as boundary condition for upward

flow (Box 8.1, Part 7). The second method has been described in this chapter and views the saturated zone as one mixed reservoir (Section 8.5). In that case we should set SWBR = 0 and provide the effective transport properties of the saturated zone (Box 8.1, Part 7).

```
*************************************************************************************
Box 8.1 Information on solute transport in main file *.SWP

*************************************************************************************
* Part 1: Specify whether simulation includes solute transport

  SWSOLU = 1 ! Switch for simulation of solute transport, [Y=1, N=0]
*************************************************************************************


*************************************************************************************
* Part 2: Top boundary and initial condition

  CPRE = 0.0     ! Solute concentration in precipitation, [0.0..100.0 mg/cm3, R]

* If SWINCO = 1 or 2, list initial solute concentration CML [0.0..1000.0 mg/cm3, R]
* as function of soil depth ZC [-10000..0 cm, R], max. MACP records:
      ZC        CML
   -10.0       0.0
   -95.0       0.0
* End of table
*************************************************************************************


*************************************************************************************
* Part 3: Miscellaneous parameters as function of soil depth

* Specify for each soil layer (maximum MAHO)
* ISOILLAY6 = number of soil layer, as defined in soil water section (part 4) [1..MAHO, I]
* LDIS      = dispersion length, [0.0..100.0 cm, R]
* KF        = Freundlich adsorption coefficient, [0.0..100.0 cm3/mg, R]
* BDENS     = dry soil bulk density, [500.0..3000.0 mg/cm3, R]
* DECPOT    = potential decomposition rate, [0.0..10.0 /d, R]

 ISOILLAY6    LDIS         KF     BDENS   DECPOT
    1         5.00   0.0001389   1315.00     0.0
    2         5.00   0.0001378   1318.00     0.0
* --- end of Table
*************************************************************************************


*************************************************************************************
* Part 4: Diffusion constant and solute uptake by roots

  DDIF = 0.0     ! Molecular diffusion coefficient, [0..10 cm2/day, R]
  TSCF = 0.0     ! Relative uptake of solutes by roots, [0..10 -, R]
*************************************************************************************


*************************************************************************************
* Part 5: Adsorption

  SWSP = 0       ! Switch, consider solute adsorption, [Y=1, N=0]

* In case of adsorption (SWSP = 1), specify:
  FREXP = 0.9   ! Freundlich exponent, [0..10 -, R]
  CREF  = 1.0   ! Reference solute concentration for adsorption, [0..1000 mg/cm3, R]
*************************************************************************************
```

```
********************************************************************************
* Part 6: Decomposition

  SWDC = 0        ! Switch, consideration of solute decomposition, [Y=1, N=0]

* In case of solute decomposition (SWDC = 1), specify:
  GAMPAR = 0.0  ! Factor reduction decomposition due to temperature, [0..0.5 /ºC, R]
  RTHETA = 0.3  ! Minimum water content for potential decomposition, [0..0.4 cm3/cm3, R]
  BEXP   = 0.7  ! Exponent in reduction decomposition due to dryness, [0..2 -, R]

* List the reduction of pot. decomposition for each soil type, [0..1 -, R]:

  ISOILLAY7  FDEPTH              ! (maximum MAHO records)
      1       1.00
      2       0.65
* End of table
********************************************************************************


********************************************************************************
* Part 7: Solute residence in the saturated zone

  SWBR = 0        ! Switch, consider mixed reservoir of saturated zone [Y=1, N=0]

* Without mixed reservoir (SWBR = 0), specify:
  CDRAIN = 0.1  ! solute concentration in groundwater, [0..100 mg/cm3, R]

* In case of mixed reservoir (SWBR = 1), specify:
  DAQUIF = 110.0 ! Thickness saturated part of aquifer, [0..10000 cm, R]
  POROS  = 0.4  ! Porosity of aquifer, [0..0.6 -, R]
  KFSAT  = 0.2  ! Linear adsorption coefficient in aquifer, [0..100 cm3/mg, R]
  DECSAT = 1.0  ! Decomposition rate in aquifer, [0..10 /d, R]
  CDRAINI = 0.2 ! Initial solute concentration in groundwater, [0..100 mg/cm3, R]
********************************************************************************
```

9 Soil temperature

Soil temperature affects many physical, chemical and biological processes in the top soil, for instance the surface energy balance, soil hydraulic properties, decomposition rate of solutes and growth rate of roots. Currently SWAP uses the soil temperatures only to adjust the solute decomposition rate, but other temperature relations may readily be included. SWAP calculates the soil temperatures either analytically or numerically. In the following sections the heat flow equations and the applied analytical and numerical solutions are discussed.

9.1 Temperature conductance equation

If we consider heat transport only by convection, the one-dimensional soil heat flux, q_{heat} (J cm^{-2} d^{-1}), can be described as:

$$q_{heat} = -\lambda_{heat} \frac{\partial T}{\partial z} \qquad (9.1)$$

where λ_{heat} is the thermal conductivity (J cm^{-1} ^{o}C^{-1} d^{-1}) and T is the soil temperature ($^{\circ}$C).

Conservation of energy results in:

$$C_{heat} \frac{\partial T}{\partial t} = \frac{-\partial q_{heat}}{\partial z} \qquad (9.2)$$

where C_{heat} is the soil heat capacity (J cm^{-3} ^{o}C^{-1}).

Combination of Eq. (9.1) and (9.2) yields the differential equation for soil heat flow:

$$C_{heat} \frac{\partial T}{\partial t} = \frac{\partial \left(\lambda_{heat} \frac{\partial T}{\partial z} \right)}{\partial z} \qquad (9.3)$$

In general in the liquid phase, radiation and convection will also transport heat. As the contribution of radiation and convection to soil heat transport in general is small compared to conductance, SWAP only considers conductance. In the vapour phase, diffusion may contribute to soil heat transport. The rate of heat transfer by water vapour diffusion is small and proportional to the temperature gradient (De Vries, 1975). Therefore, such diffusion can be taken into account by slightly increasing the soil thermal diffusivity. This approach is followed in SWAP as well. Apparent thermal properties rather than real thermal properties are assumed to account for both conductive and non-conductive heat flow.

9.2　Numerical solution

The parameters λ_{heat} and C_{heat} strongly depend on the soil moisture content. Therefore in general Eq. 9.3 can only be solved with a numerical solution. SWAP employs a fully implicit finite difference numerical scheme to solve Eq. 9.3:

$$C_i^{j+1}\left(T_i^{j+1} - T_i^{j}\right) = \frac{\Delta t^{j}}{\Delta z_i}\left[\lambda_{i-\frac{1}{2}}^{j+\frac{1}{2}}\frac{T_{i-1}^{j+1} - T_i^{j+1}}{\Delta z_{\text{u}}} - \lambda_{i+\frac{1}{2}}^{j+\frac{1}{2}}\frac{T_i^{j+1} - T_{i+1}^{j+1}}{\Delta z_{\ell}}\right] \tag{9.4}$$

where superscript j denotes the time level, subscript i is the node number, $\Delta z_{\text{u}} = z_{i+1} - z_i$ and $\Delta z_{\text{l}} = z_i - z_{i+1}$. As the coefficients C_{heat} and λ_{heat} are not affected by the soil temperature itself, Eq. (9.4) is a linear equation.

Both volumetric heat capacity and thermal conductivity depend on the soil composition. The volumetric heat capacity is calculated as weighted mean of the heat capacities of the individual components (De Vries, 1963):

$$C_{\text{heat}} = f_{\text{sand}}C_{\text{sand}} + f_{\text{clay}}C_{\text{clay}} + f_{\text{organic}}C_{\text{organic}} + \theta C_{\text{water}} + f_{\text{air}}C_{\text{air}} \tag{9.5}$$

where f and C on the right hand side of Eq. (9.5) are the volume fraction (cm^3 cm^{-3}) and volumetric heat capacity (J cm^{-3} °C^{-1}) of each component, respectively, and the components are indicated in the subscripts. Table 9.1 gives values of C for the different soil components.

Table 9.1 Volumetric heat capacity and thermal conductivity of the soil components.

Component	Volumetric heat capacity (J cm^{-3} °C^{-1})	Thermal conductivity (J cm^{-1} °C^{-1} d^{-1})
Sand	2.128	7603
Clay	2.385	2523
Organic	2.496	216
Water	4.180	492
Air (20°C)	1.212	22

In order to calculate C_{heat} (and λ_{heat}) from (9.10), the percentage (by volume) of sand and clay, denoted VP_{sand} and VP_{clay}, respectively, must be specified by the SWAP user. VP_{sand} and VP_{clay} should be provided as percentages of the total *solid* soil matter and may differ for each soil layer. The total volume fraction of solid matter is given by:

$$\theta_{\text{solid}} = 1 - \theta_{\text{sat}} \tag{9.6}$$

where θ_{sat} is the saturated volumetric water content. The volume fraction of air is equal to the saturated minus the actual water content:

$$f_{\text{air}} = \theta_{\text{sat}} - \theta \tag{9.7}$$

$f_{\text{sand}}, f_{\text{clay}}$ and f_{organic} are then calculated by:

$$f_{\text{sand}} = \frac{VP_{\text{sand}}}{100} \theta_{\text{solid}} \qquad (9.8)$$

$$f_{\text{clay}} = \frac{VP_{\text{clay}}}{100} \theta_{\text{solid}} \qquad (9.9)$$

$$f_{\text{organic}} = \theta_{\text{solid}} - f_{\text{sand}} - f_{\text{clay}} \qquad (9.10)$$

where it has been assumed that solid matter that is not sand or clay, is organic.

Table 9.1 also lists the thermal conductivities, which are greatest for sand and clay, an order smaller for organic material and water, and again an order smaller for air. Hence the space-average thermal conductivity of a soil depends upon its mineral composition and organic matter content, as well as the volume fractions of water and air. Since the thermal conductivity of air is much smaller than that of water or solid matter, a high air content (or low water content) corresponds to a low thermal conductivity.

The components that affect λ_{heat} are the same as those affecting C_{heat}. However, the variation in λ_{heat} is much greater than that of C_{heat}. In the range of soil wetness normally experienced in the field, C_{heat} may undergo a threefold or fourfold change, whereas the corresponding change in λ_{heat} may be hundredfold or more. Unlike heat capacity, thermal conductivity is also sensitive to the sizes, shapes, and spatial arrangements of the soil particles (Hillel, 1980).

The thermal conductivity is found by considering the soil as a continuous liquid or gaseous phase in which soil and respectively gas or liquid 'particles' are dispersed. In the case of a 'wet' soil ($\theta > \theta_{\text{wet}}$) liquid water is assumed to be the continuous phase and the thermal conductivity is given by:

$$\lambda_{\text{heat}} = \frac{x_{\text{sand-water}} f_{\text{sand}} \lambda_{\text{sand}} + x_{\text{clay-water}} f_{\text{clay}} \lambda_{\text{clay}} + x_{\text{organic-water}} f_{\text{organic}} \lambda_{\text{organic}} + x_{\text{water-water}} \theta \lambda_{\text{water}} + x_{\text{air-water}} f_{\text{air}} \lambda_{\text{air}}}{x_{\text{sand-water}} f_{\text{sand}} + x_{\text{clay-water}} f_{\text{clay}} + x_{\text{organic-water}} f_{\text{organic}} + x_{\text{water-water}} \theta + x_{\text{air-water}} f_{\text{air}}} \qquad (9.11)$$

The k –values on the right hand side of Eq. (9.11) refer to the thermal conductivities (J cm^{-1} $^{\circ}$C^{-1} d^{-1}) of each individual component, as listed in Table 9.1. The weighting factors x_{mn} for component m particles suspended in the continuous phase n phase depend on the ratio of the specific thermal conductivities of component m and n and on the shape of m particles in the direction of the temperature gradient. When we assume the particles to be spheroids whose axes are randomly oriented in the soil (Ten Berge, 1986), the weighting factors can be calculated by:

$$x_{\text{mn}} = \frac{2}{3 + 3g_{\text{m}}\left(k_{\text{m}}/k_{\text{n}} - 1\right)} + \frac{1}{3\left(1 + \left(k_{\text{m}}/k_{\text{n}} - 1\right)\left(1 - 2g_{\text{m}}\right)\right)} \qquad (9.12)$$

The shape factors and weights calculated using Eq. (9.12) are given in Table 9.2.

For 'dry' soil ($\theta < \theta_{dry}$) air is considered as the continuous phase and the conductivity is given by:

$$\lambda_{heat} = 1.25 \frac{x_{sand\text{-}air} f_{sand} \lambda_{sand} + x_{clay\text{-}air} f_{clay} \lambda_{clay} + x_{organic\text{-}air} f_{organic} \lambda_{organic} + x_{water\text{-}air} \theta \lambda_{water} + x_{air\text{-}air} f_{air} \lambda_{air}}{x_{sand\text{-}air} f_{sand} + x_{clay\text{-}air} f_{clay} + x_{organic\text{-}air} f_{organic} + x_{water\text{-}air} \theta + x_{air\text{-}air} f_{air}} \qquad (9.13)$$

which is similar to Eq. (9.11) with an empirical correction factor.

In the case that neither water nor air can be considered as the continuous phase ($\theta_{dry} < \theta < \theta_{wet}$) λ_{heat} is found by interpolation between values at the wet and dry limits:

$$\lambda_{heat}\left(\theta\right) = \lambda_{heat}\left(\theta_{dry}\right) + \frac{\lambda_{heat}\left(\theta_{wet}\right) - \lambda_{heat}\left(\theta_{dry}\right)}{\theta_{wet} - \theta_{dry}}\left(\theta - \theta_{dry}\right) \qquad (9.14)$$

The values of θ_{dry} and θ_{wet} are taken as 0.02 and 0.05 respectively. We refer to De Vries (1975) and Ten Berge (1986) for more detail on the calculation of λ_{heat} and further references.

Table 9.2 Shape and weight factors for different components in water and air phases, as used for thermal conductivity calculations (Ashby et al., 1996).

	Component				
	Sand	Clay	Organic	Water	Air
Shape factor	g_{sand}	g_{clay}	$g_{organic}$	g_{water}	g_{air}
	0.14	0.00	0.50	0.14	0.05
Weight factor for water as continuous phase	$x_{sand\text{-}water}$	$x_{clay\text{-}water}$	$x_{organic\text{-}water}$	$x_{water\text{-}water}$	$x_{air\text{-}water}$
	0.2474	0.7244	1.2476	1.0000	3.0592
Weight factor for air as continuous phase	$x_{sand\text{-}air}$	$x_{clay\text{-}air}$	$x_{organic\text{-}air}$	$x_{water\text{-}air}$	$x_{air\text{-}air}$
	0.0145	0.6628	0.4500	0.1826	1.0000

At the soil surface either the daily average air temperature T_{avg} or measured soil surface temperatures can be used as boundary condition. In case of a snow layer and the use of T_{avg}, SWAP will adjust T_{avg} as described in Chapter 10. At the bottom of the soil profile either soil temperatures can be specified or $q_{heat} = 0.0$ can be selected. The latter option is valid for large soil columns.

Application of Eq. (9.4) to each node and including the boundary conditions at the top and bottom of the soil profile, results in a tri-diagonal system of equations, as shown in 0. SWAP efficiently solves the equations with *LU*-decomposition for tridiagonal systems (Press et al., 1989).

9.3 Analytical solution (sinus wave)

If the values of λ_{heat} and C_{heat} are considered to be constant with depth and time, the soil thermal diffusivity D_{heat} (cm^2 d^{-1}) can be defined as:

$$D_{heat} = \frac{\lambda_{heat}}{C_{heat}} \tag{9.15}$$

and Eq. (9.3) simplifies to:

$$\frac{\partial T}{\partial t} = D_{heat} \frac{\partial^2 T}{\partial z^2} \tag{9.16}$$

This partial differential equation can be solved for simple boundary conditions, assuming D_{heat} constant or very simple functions for D_{heat} (Van Wijk, 1966; Feddes, 1971; Wesseling, 1987). A commonly used top boundary condition is a sinusoidally varying soil surface temperature:

$$T(0,t) = T_{mean} + T_{ampl} \sin\left(\tfrac{1}{2}\pi + \omega(t - t_{max})\right) \tag{9.17}$$

where T_{mean} is the mean yearly temperature (°C), T_{ampl} is the wave amplitude (°C), $\omega = 2\pi / \tau$ is the angular frequency, where τ is the period of the wave (d), t is time (d) starting January 1st and t_{max} equals t when the temperature reaches its maximum. In case of a semi-infinite soil profile with constant D_{heat} and using Eq. (9.17), the solution to Eq. (9.16) is:

$$T(z,t) = T_{mean} + T_{ampl} e^{\frac{z}{d_{temp}}} \sin\left(\tfrac{1}{2}\pi + \omega(t - t_{max}) + \frac{z}{d_{temp}}\right) \tag{9.18}$$

where d_{temp} is the damping depth (cm), which equals:

$$d_{temp} = \sqrt{\frac{2D_{heat}}{\omega}} \tag{9.19}$$

Equation (9.18) can be used for daily or yearly fluctuations. Measured values of D_{heat} for various dry and wet soils are given in Table 9.3. Figure 9.1 gives an example of calculated soil temperatures for a dry and wet sand soil. The sinusoidal temperature fluctuations at each depth are reduced in amplitude and delayed in time with respect to the top boundary condition. Although the heat capacity of wet sand is higher than of dry sand, the temperature wave in the wet sand is less attenuated due to the higher thermal conductivity.

Table 9.3 Thermal diffusivity Dheat (cm2/d) for various dry and wet soils (Jury et al., 1991).

| Sand		Loam		Clay		Peat	
Dry	Wet	Dry	Wet	Dry	Wet	Dry	Wet
147	380	156	518	156	320	112	104
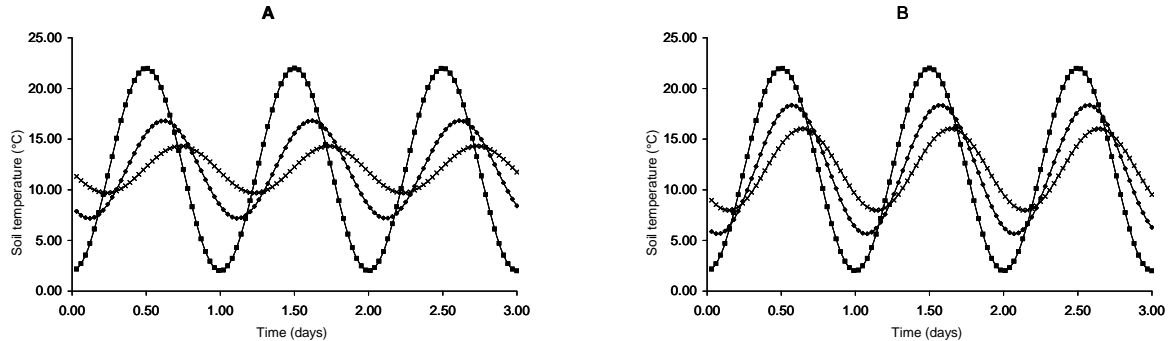
Figure 9.1 Calculated soil temperatures at depths z = 0, z = -5 en z = -10 cm for a dry (A) and a wet (B) sand soil. The following input date were used: T_{mean} = 12 °C, T_{ampli} = 10 °C, τ = 1 d, t_{max} = 0.5 d en D_{heat} = 147 (droog) en 380 (nat) $cm^2 d^{-1}$.

9.4   User instructions

Box 9.1 lists the input data for heat transport. When the analytical method is used, the parameters describing the soil surface temperature wave and the demping depth should be specified. The demping depth might be derived from Eq. (9.19) and the thermal diffusivity values in Table 9.3. When the numerical method is used, information should be given of the soil texture, initial soil temperatures and type of bottom boundary condition.

Box 9.1 Information on heat transport in main file *.SWP.

```
********************************************************************************
* Part 1: Specify whether simulation includes heat flow

  SWHEA  = 1 ! Switch for simulation of heat transport, [Y=1, N=0]
********************************************************************************

********************************************************************************
* Part 2: Heat flow calculation method

  SWCALT = 2     ! Switch for method: 1 = analytical method, 2 = numerical method
********************************************************************************

********************************************************************************
* Part 3: Analytical method

* If SWCALT = 1 specify the following heat parameters:
  TAMPLI = 10.0 ! Amplitude of annual temperature wave at soil surface, [0..50 C, R]
  TMEAN  = 15.0 ! Mean annual temperature at soil surface, [5..30 C, R]
  TIMREF = 90.0 ! Time in the year with top of sine temperature wave [1..366 d, R]
  DDAMP  = 50.0 ! Damping depth of temperature wave in soil, [0..500 cm, R]
********************************************************************************

********************************************************************************
* Part 4: Numerical method

* If SWCALT = 2 specify the following heat parameters:

* Specify for each soil type the soil texture (g/g mineral parts)
* and the organic matter content (g/g dry soil):

  ISOILLAY5  PSAND    PSILT    PCLAY    ORGMAT            ! (maximum MAHO records)
    1         0.80     0.15     0.05     0.100
    2         0.80     0.15     0.05     0.100
* End of table

* If SWINCO = 1 or 2, list initial temperature TSOIL [-20..40 C, R] as function of
* soil depth ZH [-1.0d5..0 cm, R]:

     ZH    TSOIL    ! (maximum MACP records)
   -10.0    15.0
   -40.0    12.0
   -70.0    10.0
   -95.0     9.0
* End of table

* Define top boundary condition:
  SwTopbHea = 1     ! 1 = use air temperature of meteo input file as top boundary
                    ! 2 = use measured top soil temperature as top boundary

* If SwTopbHea = 2, specify name of input file with soil surface temperatures
  TSOILFILE = 'Haarweg' ! File name without extension .TSS, [A16]

* Define bottom boundary condition:
  SwBotbHea = 1     ! 1 = no heat flux; 2 = prescribe bottom temperature

* If SwBotbHea = 2, specify a tabel with dates and temperatures at bottom boundary

  DATET          TBOT    ! (maximum MABBC records)
  01-jan-1980    -15.0
  30-jun-1980    -20.0
  23-dec-1980    -10.0
* End of table
```

10   Snow and frost

The SWAP model contains separate switches for simulating snow and frost conditions. When these two switches are turned off, in the simulations precipitation and soil water remain unfrozen at temperatures below zero ^{o}C. Snow is described in Section 10.1 and frost in Section 10.2.

10.1   Snow

When the snow option is switched on, SWAP simulates snowfall, accumulation of snow in a snowpack and the water balance of the snowpack. The present approach is quite simple and consists of the more basic processes, including a description of the insulating effect of snow on soil temperature. Simulation of snowfall and water balance of the snowpack is performed on a daily basis. Snowfall and snowpack are described in the next two Sections.

10.1.1 Snowfall

Snowfall occurs when air temperature drops below a threshold value. In that case precipitation falls partly or completely as snow. The division of total precipitation P (cm d^{-1}) into snow P_s (cm d^{-1}) and rain P_r (cm d^{-1}) depends on the daily average air temperature. For air temperatures T_{av} (^{o}C) below the threshold temperature T_{snow} (^{o}C) all precipitation is snow, while for air temperatures above the threshold temperature T_{rain} (^{o}C) all precipitation is rain. Between both threshold temperatures the snow fraction f_{snow} (-) and rain fraction f_{rain} (-) of the precipitation are obtained by linear interpolation:

$$f_{snow} = 1 \qquad\qquad \text{for } T_{av} \le T_{snow} \qquad\qquad (10.1.a)$$

$$f_{snow} = \frac{T_{rain} - T_{av}}{T_{rain} - T_{snow}} \qquad \text{for } T_{snow} < T_{av} < T_{rain} \qquad (10.1.b)$$

$$f_{snow} = 0 \qquad\qquad \text{for } T_{av} \ge T_{rain} \qquad\qquad (10.1.c)$$

$$f_{rain} = 1 - f_{snow} \qquad\qquad\qquad\qquad\qquad (10.1.d)$$

$$P_s = f_{snow} P \quad \text{and} \quad P_r = f_{rain} P \qquad\qquad\qquad (10.1.e)$$

10.1.2 Snowpack

Snow that falls on the soil surface is accumulated in a snowpack, on condition that the temperature of the soil surface is below 0.5 °C. The water balance of the snowpack includes storage, the incoming fluxes snow and rain and the outgoing fluxes melt and sublimation (Figure 10.1) and reads:

$$S_{snow}^{t} - S_{snow}^{t-1} = \left(P_r + P_s - q_{melt} - q_{melt,r} - E_s \right) \Delta t \tag{10.2}$$
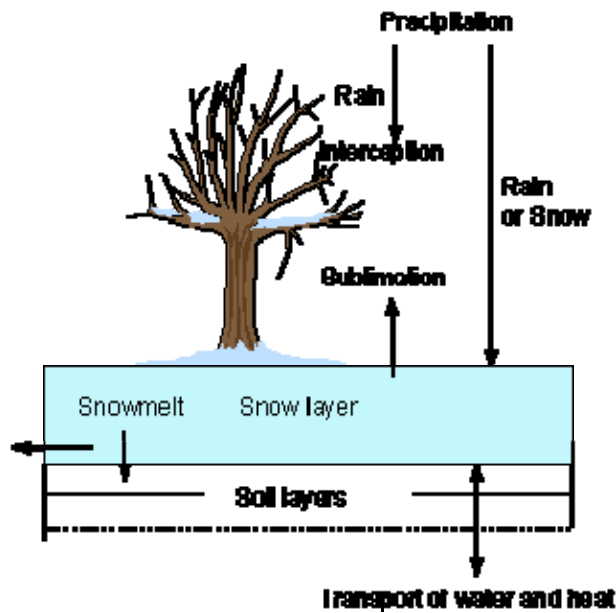

Figure 10.1 Water fluxes to and from the snow layer

in which S_{snow} is storage of snow at day t or the previous day t-1 in cm water equivalent (cm w.e.), P_s and P_r are the two precipitation terms (cm w.e. d^{-1}), q_{melt} and $q_{melt,r}$ are two snow melt terms (cm w.e. d^{-1}), E_s is sublimation of snow (cm w.e. d^{-1}) and Δt is the time-step of one day.

Two forms of snowmelt are included in the model:
1. air temperature rise above a threshold value, the 'degree-day model' (Kustas & Rango, 1994):

$$q_{melt} = a\,(T_{av} - T_b) \qquad \text{for } T_{av} > T_b \tag{10.3.a}$$

$$q_{melt} = 0 \qquad\qquad \text{for } T_{av} \leq T_b \tag{10.3.b}$$

where a is the 'degree-day factor' (cm $^{\circ}$C^{-1} d^{-1}), T_{av} is the daily average air temperature ($^{\circ}$C) and T_b is the base temperature ($^{\circ}$C) which is set to 0 $^{\circ}$C according to Kustas & Rango (1994). The value of a can be specified by the user, and ranges under most circumstances between 0.35 and 0.60 cm $^{\circ}$C^{-1} d^{-1}.

2. heat release from rainfall P_r on the snowpack: additional melt will occur due to heat released by splashing raindrops. This snowmelt rate $q_{melt,r}$ is calculated with (Fernández, 1998; Singh et al., 1997):

$$q_{\text{melt,r}} = \frac{P_{\text{r}} C_{\text{m}} (T_{\text{av}} - T_{\text{snow}})}{L_{\text{f}}} \quad \text{for } T_{\text{av}} > T_{\text{snow}} \tag{10.4.a}$$

$$q_{\text{melt,r}} = 0 \quad \text{for } T_{\text{av}} \leq T_{\text{snow}} \tag{10.4.b}$$

where C_m is the heat capacity of water (4180 J kg^{-1} $^{\circ}$C^{-1}), L_f is the latent heat of fusion (333580 J kg^{-1}) and T_{snow} is the temperature of the snowpack, which is set to 0 $^{\circ}$C.

The melt fluxes leave the snow pack as infiltration into the soil and/or runoff when infiltration capacity of the soil is exceeded.

Snow can evaporate directly into the air, a process called sublimation. The sublimation rate E_s is taken equal to the potential evaporation rate E_p (see Chapter 3). When a snow pack exists, the evapotranspiration from the soil and vegetation is set to zero.

A snowpack on top of the soil surface has great effect on soil temperature. Because of the low thermal conductivity of snow (0.1-0.4 times thermal conductivity of water), a snowpack can form a perfect insulating layer that will considerably damp the effects on soil temperature of strong changes in air temperature. The insulating effect of a snowpack on soil temperature is accounted for by calculating the temperature at the soil surface, the driving force for soil temperature calculations (see Chap. 9), taking into account the thermal conductivity and thickness of the snowpack. Therefore, the surface temperature T_{ss} ($^{\circ}$C) is calculated as a weighted average derived from the distances from the top of the snow cover and the first soil temperature node to the surface and the respective temperatures of air and soil, and thermal conductivities of snow and soil (Granberg et al., 1999):

$$T_{\text{ss}} = \frac{T_1 + a T_{\text{av}}}{1 + a} \tag{10.5a}$$

where:

$$a = \frac{\lambda_{snow}\left(\dfrac{\Delta z_1}{2}\right)}{\lambda_1 \Delta z_{snow}} \qquad (10.5b)$$

with λ_1 (J cm^{-1} $^{\circ}$C^{-1} d^{-1}) and Δz_1 (cm) are thermal conductivity and thickness of the first soil compartment. Thermal conductivity of the snowpack λ_{snow} (J cm^{-1} $^{\circ}$C^{-1} d^{-1}) depends on density ρ_{snow} (kg cm^{-3}) of the snowpack (Granberg et al., 1999):

$$\lambda_{snow} = k_{snow}\rho_{snow}^2 \qquad (10.6)$$

where k_{snow} is a thermal conductivity parameter for snow (24.71·10^8 J cm^5 kg^{-2} $^{\circ}$C^{-1} d^{-1}). For ρ_{snow} the average value of 170·10^{-6} kg cm^{-3} is taken (Granberg et al., 1999), so that λ_{snow} equals 71.4 J cm^{-1} $^{\circ}$C^{-1} d^{-1} (15% of λ_{water}).

Thickness of the snowpack Δz_{snow} (cm) is calculated from storage and density of snow, and density of water (1000·10^{-6} kg cm^{-3}):

$$\Delta z_{snow} = \frac{\rho_{water}}{\rho_{snow}} S_{snow} = \frac{1000}{170} S_{snow} \qquad (10.7)$$

10.2 Frost

If the option for frost is switched on, SWAP simulates freezing of soil water when soil temperature drops below a threshold value T_{frz} ($^{\circ}$C). Soil ice has a markedly impact on water flow and storage in the soil. To express this impact in simulations where soil ice occurs, some transport parameters are adjusted. This is achieved by using a factor $f_T(z)$, which introduces a correction when soil temperatures are below T_{frz} at depth z. This correction factor is assumed to be linear related to the fraction of soil ice $f_{ice}(z)$ (-) at depth z:

$$f_T(z) = 1 - f_{ice}(z) \qquad (10.8)$$

where $f_{ice}(z)$ is the fraction of the actual freezable volumetric soil water content (actual water content minus residual water content) at depth (z).

According to measured data from Kujala (1991), $f_{ice}(z)$ can reasonably well be described by a linear function of soil temperature $T(z)$ ($^{\circ}$C) between two threshold temperatures:

$$f_{ice}(z) = 0 \qquad \text{for } T(z) \geq T_{frz} \qquad (10.9.a)$$

$$f_{ice}(z) = \frac{T_{frz} - T(z)}{T_{frz} - T_{mlt}} \qquad \text{for } T_{mlt} < T(z) < T_{frz} \qquad (10.9.b)$$

$$f_{\text{ice}}(z) = 1 \qquad \text{for} \ \ T(z) \le T_{\text{mlt}} \qquad\qquad (10.9.c)$$

where T_{frz} is the temperature below which soil water starts freezing, and T_{mlt} is the temperature above which soil ice starts melting and below which all soil water except θ_{res} is frozen. A value of $T_{\text{frz}} < 0$ $^{\circ}$C expresses freezing point depression. T_{frz} and T_{mlt} are model input with default values of 0 and -1 $^{\circ}$C.

The following parameters are adjusted in case of soil ice:

1. hydraulic conductivity K:

$$K^{*}(z) = f_{T}(z)(K(z) - K_{\text{min}}) + K_{\text{min}} \qquad\qquad (10.10)$$

where $K^{*}(z)$ is the adjusted hydraulic conductivity at depth z (cm d^{-1}) and K_{min} is a very small hydraulic conductivity (cm d^{-1}). For K_{min} a default value is taken of 10^{-10} cm d^{-1};

2. actual crop uptake is reduced as:

$$S_{\text{a}}(z) = \alpha_{\text{rf}} \, S_{\text{a}}(z) \qquad \text{with} \ \ \alpha_{\text{rf}} = 0 \qquad \text{for} \qquad T(z) < 0 \ ^{0}\text{C} \qquad (10.11)$$

where α_{rf} is a multiplication factor for soil temperatures (-);

3. drainage fluxes of all drainage levels:

$$q_{drain,i}(z) = f_{T}(z) \, q_{drain,i}(z) \qquad\qquad (10.12)$$

where $q_{drain,i}(z)$ is the drainage flux at depth z from drainage level i (cm d^{-1});

4. bottom flux:

$$q_{bot} = f_{T}(z) \, q_{bot} \qquad\qquad (10.13)$$

where q_{bot} is the flux across the bottom of the modelled soil profile and z the bottom depth;

5. boundary fluxes (drainage and bottom) when the available air volume is very low:

    When drainage does not occur and the available air volume is very low (<0.01 cm cm^{-3}), the bottom flux is reduced to zero.
    When drainage occurs and the available air volume is very low (<0.01 cm cm^{-3}), the drainage fluxes of frozen soil compartments above the drainage level are reduced to zero.

The (available) air volume in the soil V_{air} (cm) for a soil profile that becomes saturated equals:

$$V_{air} = \sum_{i=n}^{m} \left\{ \left(\theta_{s,i} - \theta_i \right) \Delta z_i \right\}$$

(10.14)

where $\theta_{s,i}$ is the saturated water content (cm cm^{-3}), θ_i is the actual water content (cm^3 cm^{-3}), i is a node number, n is the node number of the bottom compartment, m is the node number of the highest soil compartment with a temperature below T_{mlt} starting to count from the bottom compartment, and Δz_l is the nodal distance $(z_i - z_{i+1})$

When a soil compartment is frozen ($T(z) < T_{mlt}$) the pore volume of the total soil profile becomes smaller, because only the compartments below this layer are used in the calculation.

An example is a soil in spring that is melting (figure 10.2). The lower compartments were never frozen and the melting starts at the soil surface. It is possible that the first 4 compartments have melted and only the compartments 5 - 8 are frozen. Now the air volume is only calculated for compartments n (bottom) to m=5 (frozen). The following is then valid:

−   When drainage does not occur and the available air volume is very low (<0.01 cm cm^{-3}), the bottom flux is reduced to zero

−   When drainage does occur and the available air volume is very low (<0.01 cm cm^{-3}), the drainage fluxes of all drainage systems, that have a drainage level above the lowest frozen soil compartment, are reduced to zero.
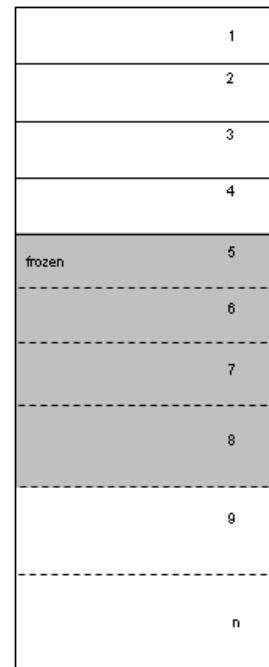

Figure 10.2 Partly frozen soil profile

10.3 User instructions

Both the options for snow and frost can only be used in combination with the option for simulation of soil temperature.

For the snow option, the two threshold temperatures T_{rain} and T_{snow}, the initial storage of snow at the beginning of the simulations S_{snow} and the 'degree-day factor' a are required as model input (Box 10.1).
The frost option requires input for the two threshold temperatures T_{frz} and T_{mlt} (Box 10.1).

Box 10.1 Input for snow and frost modules in file *.SWP

```
********************************************************************************
* Part 11: Snow and frost
*
  SWSNOW = 1   ! Switch, calculate snow accumulation and melt. [Y=1, N=0]
*
* If SWSNOW = 1, then specify initial snow water equivalent and snowmelt factor
  SNOWINCO = 22.0  ! Initial snow storage in w.e. (water equivalent) [0.0...1000.0 cm, R]
  TePrRain =  2.0  ! Temperature above which all precipitation is rain [ 0.0...5.0 oC, R]
  TePrSnow = -2.0  ! Temperature below which all precipitation is snow [-5.0...0.0 oC, R]
  SNOWCOEF =  0.3  ! Degree-day factor for snowmelt, [0.0...10.0 cm/oC/d, R]
*
  SWFROST = 1      ! Switch, in case of frost: stop soil water flow, [Y=1, N=0]
* If SWFROST = 1, then specify soil temperature to start end end flux-reduction
  tfroststa =  0.0 ! Tfrz, soil temperature below which soil water starts freezing [-10.0,5.0,oC, R]
  tfrostend = -1.0 ! Tmlt, soil temperature above which soil ice starts melting and
                                     below which all soil water is frozen [-10.0,5.0, oC, R]

********************************************************************************
```

11 Irrigation

The SWAP water balance simulations may be used to develop optimal irrigation schedules by evaluating alternative application strategies.

Irrigation strategies may be applied with a fixed or a scheduled regime. The fixed regime is defined by the time and depth of irrigation application. The scheduled regime is defined by different criteria for time and depth of an irrigation application. A combination of a fixed and a scheduled regime is also possible. This regime allows the evaluation of water productivity in relation to several degrees of water stress.

11.1 Fixed irrigation regime

At user-defined dates a fixed application depth may be applied as an observed gross irrigation dose (I_g). Interception of irrigation water may occur, dependent on the type of application (surface irrigation or sprinkling):

$$I_n = I_g - E_i \qquad\qquad (11.1)$$

where I_n is the net amount of irrigation water (cm/d), I_g is the gross given amount of fixed irrigation water (cm/d), E_i is the amount of intercepted irrigation water (cm/d). The interception irrigation water (E_i) is assumed to evaporate within the same day as the day of irrigation.

11.2 Scheduled irrigation regime

A specific combination of timing and depth criteria is valid from a user-defined date in the growing season until the end of crop growth. Both timing and depth criteria may be defined as a function of crop development stage. Scheduled irrigation only occurs when a crop is present.

11.2.1 Timing criteria

For the timing of the irrigation schedule one out of five different criteria must be selected:
- *Allowable daily stress*
- *Allowable depletion of readily available water in the root zone*
- *Allowable depletion of totally available water in the root zone*
- *Allowable depletion amount of water in the root zone*
- *Critical pressure head or moisture content at sensor depth*

At the start of each day the selected criterion is evaluated based on state variables at the start of the day. The outcome of this evaluation may generate an irrigation event on that same day.

In addition the user may prescribe a minimum interval between irrigated applications.

11.2.1.1 Allowable daily stress

The level of soil water shortage by drought and salinity stress may be diagnosed from a threshold defined by the ratio of reduced transpiration T_r to potential transpiration T_p. Irrigation is applied whenever reduced transpiration becomes lower than a limit defined by this threshold:

$$T_r \leq f_1 \, T_p \tag{11.2}$$

where T_r is the transpiration reduced by drought and salinity stress (cm d^{-1}), T_p is the potential transpiration (cm d^{-1}), f_1 (-) is a user defined factor for allowable daily stress.

11.2.1.2 Allowable depletion of readily available water

In order to optimize irrigation scheduling where irrigation is always secured before conditions of soil moisture stress occur, the maximum amount of depletion of readily available water in the root zone can be specified. Irrigation is then applied whenever the water depletion exceeds fraction f_2 of the readily available water amount:

$$\left(U_{\text{field}} - U_{\text{a}}\right) \geq f_2 \left(U_{\text{field}} - U_{\text{h3}}\right) \tag{11.3}$$

where U_a (cm) is the actual water storage in the root zone, U_{field} (cm) is the root zone water storage at $h =$ given value for field capacity, and U_{h3} (cm) is the root zone water storage at $h = h_3$, the pressure head from where root water extraction starts being reduced due to drought stress, f_2 (-) is a user-defined depletion fraction.

U_a is calculated by integrating numerically the water content in the rooting layer. For deficit irrigation purposes, stress can be allowed by specifying $f_2 > 1$.

11.2.1.3 Allowable depletion of totally available water

Depletion of water in the root zone can also be evaluated relative to the total amount of water available in the root zone as given by the difference between the field capacity and the wilting point. Irrigation is then applied whenever the depletion of water in the root zone exceeds fraction f_3 (-) of the available water:

$$\left(U_{\text{field}} - U_{\text{a}}\right) \geq f_3 \left(U_{\text{field}} - U_{\text{h4}}\right) \tag{11.4}$$

where U_{h4} (cm) is the root zone water storage at $h = h_4$, the pressure head at which root water extraction is reduced to zero, f_3 (-) is a user-defined factor depletion fraction.

11.2.1.4 Allowable depletion of field capacity water

In case of high-frequency irrigation systems (drip) it may be useful to specify the maximum amount of water that may be extracted below field capacity, ΔU_{max} (cm). Irrigation is then applied if:

$$U_a \leq U_{field} - \Delta U_{max}$$

(11.5)

11.2.1.5 Critical pressure head or moisture content

The user may specify a soil moisture threshold value θ_{min} (cm^3 cm^{-3}) or pressure head threshold value h_{min} (cm) and a corresponding depth for which the threshold values are valid.

This option may be used to simulate irrigation with automated systems relying on soil moisture measurements. Irrigation is then applied whenever a threshold is exceeded:

$$\theta_{sensor} \leq \theta_{min} \qquad \text{or} \qquad h_{sensor} \leq h_{min}$$

(11.6)

where θ_{sensor} and h_{sensor} are the threshold values for soil moisture and pressure head, respectively.

11.2.1.6 Fixed interval

By default an irrigation interval has a minimum of one day and the length of the interval is variable and determined by the moment when one of the previously mentioned timing criteria becomes valid.

The user may optionally choose a fixed interval of one week between possible irrigation events. Irrigation events occur weekly during crop growth when the required amount of water to bring the rootzone to field capacity exceeds a given threshold value. This threshold value is input to the model.

11.2.1.7 Minimum interval

The length of the interval between irrigation events may also be variable and be determined by the moment when one of the timing criteria becomes valid.

The user may select this option in addition to one of the previous five criteria (par. 11.2.1.1 - 11.2.1.5) to have a minimum time interval between irrigation applications.

11.2.2 Depth criteria

Scheduled irrigation results in gross irrigation depths. Interception of irrigation water may occurin case of sprinkling irrigation:

$$I_n = I_g - E_i$$

(11.7)

Two option are available for the amount of irrigation:

- *An application depth which is brings the root zone back to field capacity*
- *A fixed application depth*

In addition to one of these 2 options the actual depth of the application may be limited by a minimum and a maximum level.

The 2 criteria and the option for limited depth will be explained hereafter.

11.2.2.1 Back to Field Capacity (+/- specified amount)

The soil water content in the root zone is brought back to field capacity. An additional irrigation amount can be defined to leach salts, while the user may define a smaller irrigation amount when rainfall is expected. This option may be useful in case of sprinkler and micro irrigation systems, which allow variation of irrigation application depth.

11.2.2.2 Fixed irrigation depth

A specified amount of water is applied. This option applies to most gravity systems, which allow little variation in irrigation application depth.

11.2.2.3 Limited depth

With this option enabled the scheduled irrigation depth occurs only when the calculated irrigation depth lies between a minimum and maximum limit:

$$I_{g,\min} \leq I_g \leq I_{g.\max}$$

(11.8)

where $I_{g,min}$ and $I_{g,max}$ are the threshold values for minimum and maximum irrigation depth (mm), respectively.

11.3 User instructions

Fixed irrigation depths must be entered in the *.SWP file (Box 11.1).

Scheduled irrigation enters the model by means of timing and depth criteria in the .CRP-file, see respectively Boxes 11.2 and 11.3

Box 11.1 Fixed irrigation in the input file *.SWP, CROP-Section part 2

```
**********************************************************************************
* Part 2: Fixed irrigation applications

  SWIRFIX = 1    ! Switch for fixed irrigation applications
                 ! SWIRFIX = 0: no irrigation applications are prescribed
                 ! SWIRFIX = 1: irrigation applications are prescribed

* If SWIRFIX = 1:

  SWIRGFIL  = 0  ! Switch for file with fixed irrigation applications:
                 ! SWIRGFIL = 0: data are specified in the .swp file
                 ! SWIRGFIL = 1: data are specified in a separate file

* If SWIRGFIL  = 0 specify information for each fixed irrigation event (max. MAIRG):
* IRDATE   = date of irrigation, [dd-mmm-yyyy]
* IRDEPTH  = amount of water, [0.0..100.0 mm, R]
* IRCONC   = concentration of irrigation water, [0.0..1000.0 mg/cm3, R]
* IRTYPE   = type of irrigation: sprinkling = 0, surface = 1

      IRDATE    IRDEPTH     IRCONC    IRTYPE
 05-jan-1980       5.0     1000.0         1
* --- end of table

* If SWIRGFIL  = 1 specify name of file with data of fixed irrigation applications:
  IRGFIL = 'testirri'     ! File name without extension .IRG [A16]
**********************************************************************************
```

Box 11.2 Scheduled irrigation in the input file *.CRP, IRRIGATION SCHEDULING part 1

```
*** IRRIGATION SCHEDULING SECTION ***

**********************************************************************************
* Part 1: General

  SCHEDULE = 0  ! Switch for application irrigation scheduling [Y=1, N=0]

* If SCHEDULE = 0, no more information is required in this input file!
* If SCHEDULE = 1, continue ....

  STARTIRR = 30 3 ! Specify day and month after which irrigation scheduling is allowed [dd mm]
  ENDIRR  = 31 12 ! Specify day and month after which irrigation scheduling is NOT allowed [dd mm]
  CIRRS = 0.0     ! solute concentration of scheduled irrig. water, [0..100 mg/cm3, R]
  ISUAS = 1       ! Switch for type of irrigation method:
                  ! 0 = sprinkling irrigation
                  ! 1 = surface irrigation

* Specify pressure head at field capacity
* required for timing options  TCS = 2, 3, or 4 and depth option DCS = 1, else dummy
  phFieldCapacity = -100.0   ! soil hydraulic pressure head [-1000.0 .. 0.0,cm, R]

**********************************************************************************
```

```
**********************************************************************************
* Part 2: Irrigation time criteria

*** Choose one of the following 5 timing options:
  TCS = 1  ! Switch, timing criterion  [1..5, I]]
!            1 = Daily Stress
!            2 = Depletion of Readily Available Water
!            3 = Depletion of Totally Available Water
!            4 = Depletion Water Amount
!            5 = Pressure head or moisture content
!            6 = Fixed weekly irrigation, rootzone to field capacity

*** Daily stress criterion (TCS = 1)
* If TCS = 1, specify mimimum of ratio actual/potential transpiration Trel [0..1, R],
* as function of development stage DVS_tc1 [0..2, R], maximum 7 records:
  DVS_tc1  Trel
      0.0  0.95
      2.0  0.95
* End of table


*** Depletion of Readily Available Water (TCS = 2)
* If TCS = 2, specify minimal fraction of readily available water RAW [0..1, R],
* as function of development stage DVS_tc2 [0..2, R], maximum 7 records:
  DVS_tc2   RAW
      0.0  0.95
      2.0  0.95
* End of table


*** Depletion of Totally Available Water (TCS = 3)
* If TCS = 3, specify minimal fraction of totally available water TAW [0..1, R],
* as function of development stage DVS_tc3 [0..2, R], maximum 7 records:
  DVS_tc3   TAW
      0.0  0.50
      2.0  0.50
* End of table


*** Depletion Water Amount (TCS = 4)
* If TCS = 4, specify maximum amount of water depleted below field cap. DWA [0..500 mm, R],
* as function of development stage DVS_tc4 [0..2, R], maximum 7 records:
  DVS_tc4   DWA
      0.0  40.0
      2.0  40.0
* End of table


*** Pressure head or Moisture content (TCS = 5)
* If TCS = 5, specify:
  PHORMC = 0   ! Switch, use pressure head (PHORMC=0) or water content (PHORMC=1)
  DCRIT = -30.0! Depth of the sensor [-100..0 cm, R]
* Also specify critical pressure head [-1.d6..-100 cm, R] or moisture content
* [0..1.0 cm3/cm3, R], as function of development stage DVS_tc5 [0..2, R]:
  DVS_tc5  Value_tc5
      0.0    -1000.0
      2.0    -1000.0
* End of table


*** fixed irrigation time (weekly during crop growth) (TCS = 6)
* If TCS = 6, specify:
* Threshold for weekly irrigation only when deficit is higher then threshold
  irgthreshold = 1.0         ! Threshold value [0.0..20.0 mm, R]


*** Select (optional) minimum time interval:
  tcsfix = 0   ! Switch, minimum timing criterion  [0 or 1, I]]
* If tcsfix = 1, specify:
  irgdayfix = 7     !  minimum length of interval between irrigations [1..365 d, I]
```

```
***********************************************************************************
* Part 3: Irrigation depth criteria

*** Choose one of the following 2 options for irrigation depth:
  DCS = 1  ! Switch, depth criterion  [1..2, I]]
!           1 = Back to Field Capacity
!           2 = Fixed Irrigation Depth


*** Back to Field Capacity (DCS = 1)
* If DCS = 1, specify amount of under (-) or over (+) irrigation dI [-100..100 mm, R],
* as function of development stage DVS_dc1 [0..2, R], maximum 7 records:
  DVS_dc1   dI
     0.0  10.0
     2.0  10.0
* End of table


*** Fixed Irrigation Depth (DCS = 2)
* If DCS = 2, specify fixed irrigation depth FID [0..400 mm, R],
* as function of development stage DVS_dc2 [0..2, R], maximum 7 records:
  DVS_dc2   FID
     0.0  60.0
     2.0  60.0
* End of table


*** Select (optional) limitations of irrigation depth:
  dcslim = 0  ! Switch, limited irrigation depth  [0=No, 1=Yes]   [0..1, I]
* If dcslim = 1, specify:
  irgdepmin = 0.0    !   minimum irrigation depth [0.0d0 .. 100.0d0, mm, I]
  irgdepmax = 0.0    !   maximum irrigation depth [irgdepmin .. 1.0d7, mm, I]
```

References

Abenney-Mickson, S., A. Yomota, and T. Miura, 1997. *Water balance of field plots planted with soybean and pumpkin.* Trans. ASAE, 40: 899-909.

Allen, R.G., M.E. Wright and R.D. Burman, 1989. *Operational estimates of evapotranspiration.* Agron. J., 81, 650-662.

Allen, R.G., 1991. *REF-ET Reference evapotranspiration calculator, version 2.1.* Utah State University, Logan, 39 pp.

Allen, R.G., L.S. Pereira, D. Raes, and M. Smith, 1998. *Crop evapotranspiration. Guidelines for computing crop water requirements.* Irrigation and Drainage Paper 56, FAO, Rome, Italy, 300 p.

Angus, J.F., R.B. Cunningham, M.W. Moncur and D.H. Mackenzie, 1981. *Phasic development in field crops. I. Thermal response in seedling phase.* Field Crops Research 3, 365-378.

Ashby, M., A.J. Dolman, P. Kabat, E.J. Moors and M.J. Ogink-Hendriks, 1996. *SWAPS version 1.0. Technical reference manual.* Technical document 42, Winand Staring Centre, Wageningen.

Bear, J., 1972. *Dynamics of fluids in porous media.* Elsevier, Amsterdam.

Belmans, C., J.G. Wesseling and R.A. Feddes, 1983. *Simulation of the water balance of a cropped soil: SWATRE.* J. Hydrol., 63, 271-286.

Beltman, W.H.J., J.J.T.I. Boesten and S.E.A.T.M. van der Zee, 1995. *Analytical modelling of pesticide transport from the soil surface to a drinking water well.* J. Hydrol., 169, 209-228.

Beven, K. and P. Germann, 1982. *Macropores and water flow in soils.* Water Resour. Res., 18: 1311-1325.

Biggar, J.W. and D.R. Nielsen, 1976. *The spatial varability of the leaching characteristics of a field soil.* Water Resour. Res., 12, 78-84.

Black, T.A., W.R. Gardner and G.W. Thurtell, 1969. *The prediction of evaporation, drainage, and soil water storage for a bare soil.* Soil Sci. Soc. Am. J., 33, 655-660.

Boesten, J.J.T.I., 1986. *Behaviour of herbicides in soil : Simulation and experimental assessment.* Ph.D. thesis Winand Staring Centre, Wageningen.

Boesten, J.J.T.I. and L. Stroosnijder, 1986. *Simple model for daily evaporation from fallow tilled soil under spring conditions in a temperate climate.* Neth. J. Agric. Sci., 34, 75-90.

Boesten, J.J.T.I. and A.M.A. van der Linden, 1991. *Modeling the influence of sorption and transformation on pesticide leaching and persistence.* J. Environ. Qual., 20, 425-435.

Bolt, G.H., 1979. *Movement of solutes in soils: principles of adsorption/exchange chromatography.* In: G.H. Bolt (Ed.), Soil Chemistry B, Physico-Chemical Models. Elsevier, Amsterdam. p. 285-348.

Boogaard, H.L., C.A. van Diepen, R.P. Rötter, J.C.M.A. Cabrera, and H.H. van Laar, 1998. *WOFOST 7.1. User guide for the WOFOST 7.1 crop growth simulation model and WOFOST Control Center 5.1.* Techn. Doc. 52, Alterra, WUR, Wageningen, The Netherlands, pp. 144.

Booltink, H.W.G., 1993. *Morphometric methods for simulation of water flow*. PhD-thesis, Wageningen University, 169 p.

Booltink, H.W.G. and J. Bouma, 1993. *Sensitivity analysis on processes affecting bypass flow.* Hydrol. Process., 7: 33-43.

Boons-Prins, E.R., G.H.J. de Koning, C.A. van Diepen and F.W.T. Penning de Vries, 1993. *Crop specific simulation parameters for yield forecasting across the European Community.* Simulation Rep. 32, CABO-DLO and SC-DLO, Wageningen, The Netherlands.

Bos, M.G., J. Vos and R.A. Feddes, 1996. *CRIWAR 2.0. A simulation model on crop irrigation water requirements.* ILRI publ. 46, Wageningen, The Netherlands.

Bouma, J. and J.L. Anderson, 1973. *Relationships between soil structure characteristics and hydraulic conductivity.* p. 77-105. In: R.R. Bruce (ed.). Field soil moisture regime. SSSA Special Publ. no. 5. Am. Soc. of Agron. Madison, Wis.

Bouma, J. and L.W. Dekker, 1978. *A case study on infiltration into a dry clay soil. I. Morphological observations.* Geoderma, 20: 27-40.

Bouma, J., C. Belmans, L.W. Dekker and W.J.M. Jeurissen, 1983. *Assessing the suitability of soils with macropores for subsurface liquid waste disposal.* J. Environ. Qual. 12, 305-311.

Bouma, J., 1990. *Using morphometric expressions for macropores to improve soil physical analyses of fields soils.* Geoderma 46, 3-11.

Bouman, B.A.M., H. van Keulen, H.H. van Laar and R. Rabbinge, 1996. *The 'School of de Wit' crop growth simulation models: a pedigree and historical overview.* Agric. Systems 56, 171-198.

Bouten, W., 1992. *Monitoring and modelling forest hydrological processes in support of acidification research.* Diss. Univ. A'dam. 218 pp.

Braden, H., 1985. *Ein Energiehaushalts- und Verdunstungsmodell for Wasser und Stoffhaushaltsuntersuchungen landwirtschaftlich genutzer Einzugsgebiete.* Mittelungen Deutsche Bodenkundliche Geselschaft, 42, 294-299.

Bresler, E., and G. Dagan, 1983. *Unsaturated flow in spatially variable fields. 2. Application of water flow models to various fields.* Water Resour. Res., 19: 421-428.

Bronswijk, J.J.B. 1988. *Modeling of water balance, cracking and subsidence of clay soils.* J. Hydrol., 97: 199-212.

Bronswijk, J.J.B. and J.J. Evers-Vermeer, 1990. *Shrinkage of Dutch clay soil aggregates.* Neth. J. of Agric. Sci., 38, 175-194.

Bronswijk, J.J.B., W. Hamminga and K. Oostindie, 1995. *Field-scale solute transport in a heavy clay soil.* Water Resour. Res., 31, 517-526.

Brooks, R.H. and A.T. Corey, 1964. *Hydraulic properties of porous media.* Colorado State Univ., Hydrology paper no. 3, p. 27.

Bruin, R.A., 1998. Micrometeorology. Lecture notes 06252207, Wageningen University, 156 p.

Brunt, D., 1952. *Physical and dynamical meteorology.* Second edition, University Press, Cambridge, 428 pp.

Burman, R.D., M.E. Jensen and R.G. Allen, 1987. *Thermodynamic factors in evapotranspiration.* In 'Proc. Irrig. and Drain. Spec. Conf.', L.G. James and M.J. English (Eds.), ASCE, Portland, Ore., July, p. 28-30.

Carrera, J. and S.P. Neuman, 1986. *Estimation of aquifer parameters under transient and steady state conditions. 2. Uniqueness, stability, and solution algorithms.* Water Resour. Res. 22, 211-27.

Carsel, R.F. and R.S. Parrish, 1988. *Developing joint probability distributions of soil water characteristics.* Water Resour. Res., 24, 755-769.

Causton, D.R. and J.C. Venus, 1981. *The biometry of plant growth.* Edward Arnold, London. 307 pp.

Celia, M.A., E.T. Bouloutas and R.L. Zarba, 1990. *A general mass-conservative numerical solution for the unsaturated flow equation.* Water Resour. Res., 26, 1483-1496.

Clausnitzer, V., J.W. Hopmans and D.R. Nielsen, 1992. *Simultaneous scaling of soil water retention and hydraulic conductivity curves.* Water Resour. Res., 28, 19-31.

Clothier, B.E., M.B. Kirkham and J.E. McLean, 1992. *In situ measurement of the effective transport volume for solute moving through soil.* Soil Sci. Soc. Am. J., 56, 733-736.

Dane, J.H., and G.C. Topp, 2002. *Methods of soil analysis. Part 4. Physical methods.* SSSA Book series, number 5, Madison, Wisconsin, 1692 p.

Dekker, L.W. and P.D. Jungerius, 1990. *Water repellency in the dunes with special reference to the Netherlands.* In 'Dunes of the European Coasts', Catena Suppl., 18, 173-183.

Dekker, L.W. and C.J. Ritsema, 1994. *How water moves in a water repellent sandy soil. 1. Potential and actual water repellency.* Water Resour. Res., 30, 2507-2517.

Dekker, L.W. and C.J. Ritsema, 1996. *Preferential flow paths in a water repellent clay soil with grass cover.* Water. Resour. Res. 32: 1239-1249.

Dekker, L.W., 1998. *Moisture variability resulting from water repellency in Dutch soils.* PhD-thesis Wageningen University, 240 p.

De Rooij, G.H., 1996. *Preferential flow in water-repellent sandy soils. Model development and lysimeter experiments.* Ph.D. thesis, Wageningen Agricultural University, The Netherlands, 229 p.

Desbarats, A.J., 1995. *An interblock conductivity scheme for finite difference models of steady unsaturated flow in heterogeneous media.* Water Resour. Res., 31, 2883-2889.

De Smedt, F. and P.J. Wierenga, 1979. *A generalized solution for solute flow in soils with mobile and immobile water.* Water Resour. Res., 1137-1141.

De Vries, D.A., 1975. *Heat transfer in soils.* In 'Heat and mass transfer in the biosphere. I. Transfer processes in plant environment', De Vries, D.A. and N.H. Afgan (eds.), Scripts Book Company, Washington D.C., p. 5-28.

De Wit, C.T. et al., 1978. *Simulation of assimilation and transpiration of crops.* Simulation Monographs, Pudoc, Wageningen, The Netherlands. 100 pp.

Dirksen, C., 1979. *Flux-controlled sorptivity measurements to determine soil hydraulic property functions.* Soil Sci. Soc. Am. J., 43, 827-834.

Dirksen, C., 1987. *Water and salt transport in daily irrigated root zone.* Neth. J. Agric. Sci., 35: 395-406.

Dirksen, C., 1991. *Unsaturated hydraulic conductivity.* In 'Soil analysis, physical methods', K.A. Smith and C.E. Mullins (eds), Marcel Dekker, New York, p. 209-269.

Dirksen, C., J.B. Kool, P. Koorevaar and M.Th. van Genuchten, 1993. *Hyswasor: simulation model of hysteretic water and solute transport in the root zone.* In: D. Russo and G. Dagan (Eds.), Water flow and solute transport in soils. Springer-Verlag, Adv. Series in Agric. Sci., 20, 99-122.

Dirksen, C. and S. Matula, 1994. *Automatic atomized water spray system for soil hydraulic conductivity measurements.* Soil Sci. Soc. Am. J., 58, 319-325.

Doorenbos, J. and W.O. Pruitt, 1977. *Guidelines for predicting crop water requirements.* Irrigation and Drainage Paper 24, FAO, Rome, Italy.

Doorenbos, J. and A.H. Kassam, 1979. *Yield response to water.* FAO Irrigation and Drainage Paper 33, FAO, Rome, Italy.

Elrick, D.E. and W.D. Reynolds, 1992. *Infiltration from constant-head well permeameters and infiltrometers.* In 'Advances in measurement of soil physical properties: bringing theory into practice', G.C. Topp, W.D. Reynolds and R.E. Green (eds.), SSSA special publication no. 30, p. 1-24.

Ernst, L.F., 1956. *Calculation of the steady flow of groundwater in vertical cross-sections.* Netherlands Journal of Agricultural Science 4, 126-131.

Ernst, L.F. 1962. *Groundwater flow in the saturated zone and its calculation when parallel open conduits are present.* Thesis (Dutch with English summary), University of Utrecht, 189 pp.

Ernst, L.F., 1973. *The determination of residence times in case of groundwater flow.* Nota 755 I.C.W., now Winand Staring Centre, Wageningen (in Dutch).

Ernst, L.F. 1978. *Drainage of undulating sandy soils with high groundwater tables. I en II.* Journal of Hydrology 39, 1-50.

Ernst, L.F. and R.A. Feddes, 1979. *Invloed van grondwateronttrekking voor beregening en drinkwater op de grondwaterstand.* Report 1116, ICW (currently Winand Staring Centre), Wageningen, The Netherlands.

Feddes, R.A., 1971. *Water, heat and crop growth.* Ph.D. thesis, Wageningen Agricultural University, The Netherlands.

Feddes, R.A., P.J. Kowalik and H. Zaradny, 1978. *Simulation of field water use and crop yield.* Simulation Monographs. Pudoc. Wageningen. 189 pp.

Feddes, R.A., 1987. *Crop factors in relation to Makking reference crop evapotranspiration.* In 'Evaporation and weather', TNO Committee on Hydrological Research, Proceedings and information no 39, p. 33-46.

Feddes, R.A., P. Kabat, P.J.T. van Bakel, J.J.B. Bronswijk and J. Halbertsma, 1988. *Modelling soil water dynamics in the unsaturated zone - state of the art.* J. Hydrol., 100, 69-111.

Feddes, R.A., G.H. de Rooij, J.C. van Dam, P. Kabat, P. Droogers, and J.N.M. Stricker, 1993a. *Estimation of regional effective soil hydraulic parameters by inverse modelling.* In 'Water flow and solute transport in soils: modelling and application', D. Russo and G. Dagan (Eds.), Springer Verlag, Berlin, p. 211-231.

Feddes, R.A., M. Menenti, P. Kabat, and W.G.M. Bastiaanssen, 1993b. *Is large scale inverse modelling of unsaturated flow with areal average evaporation and surface soil moisture as estimated from remote sensing feasible?* J. Hydrol., 143: 125-152.

Feddes, R.A. and K.J. Lenselink, 1994. *Evapotranspiration.* In 'Drainage priciples and applications', H.P. Ritzema (ed.), ILRI publication 16, second ed., Wageningen, p. 145-174.

Fernández, A., 1998. *An Energy Balance Model of Seasonal Snow Evolution.* Physical Chemistry of the Earth 23, 5-6: 661-666.

Flury, M. and H. Flühler, 1995. *Tracer characteristics of Brilliant Blue FCF.* Soil Sci. Soc. Am. J., 59, 22-27.

Garnier, P., Rieu, M., Boivin, P., Vauclin, M., and Baveye, P. 1997. *Determining the hydraulic properties of a swelling soil from a transient evaporation experiment.* Soil Sci. Soc. Am. J., 61: 1555-1563.

Gash, J.H.C., 1979. *An analytical model of rainfall interception by forests.* Q. J. R. Meteor. Soc. 105, 43-55.

Gash, J.H.C., C.R. Lloyd and G. Lachaud, 1995. Estimating sparse forest rainfall interception with an analytical model. *Journal of Hydrology 170 (1995) 79-86.*

Gelhar, L.W. and J.L. Wilson, 1974. *Groundwater quality modeling.* Ground Water, 12, 399-408.

Gerke, H.H. and M.Th van Genuchten, 1993. *A dual-porosity model for preferential movement of water and solutes in structured porous media.* Water Resour. Res., 29, 305-319.

Goudriaan, J., 1977. *Crop meteorology: a simulation study.* Simulation monographs, Pudoc, Wageningen.

Goudriaan, J., 1982. *Some techniques in dynamic simulation.* In 'Simulation of plant growth and crop production', F.W.T. Penning de Vries and H.H. van Laar (Eds.), Simulation Monographs, Pudoc, Wageningen, p. 66-84.

Granberg, G., H. Grip, M. Ottoson Lofvenius, I. Sundh, B.H. Svensson and M. Nilsson, 1999. *A simple model for simulation of water content, soil frost, and soil temperatures in boreal mixed mires.* Water Resources Research 35: 3771-3782.

Greco, R., R.F.A. Hendriks and W. Hamminga, 1997. *Clay soil aggregate sorptivity measurements under different water contents.* Proceedings of the National Hydraulics Conference, Turin, Italy, November 1996.

Groen, K.P., 1997. *Pesticide leaching in polders. Field and model studies on cracked clays and loamy sand.* PhD thesis, Wageningen Agricultural University, Wageningen, The Netherlands, 296 pp.

Groenendijk, P., L.V. Renaud, and J. Roelsma, 2005. *Prediction of Nitrogen and Phosphorus leaching to groundwater and surface waters; Process descriptions of the ANIMO 4.0 model.* Alterra–Report 983. Wageningen.

Groenendijk, P. and J.G. Kroes (in prep). *Performance of the numerical implementation of the Richards' equation and associated boundary conditions in the SWAP model.*

Hadley, P., E.H. Roberts, R.J. Summerfield and F.R. Minchin, 1984. *Effects of temperature and photoperiod on flowering in soya bean: a quantitative model.* Annals of Botany, 53, 669-681.

Hargreaves, G.L., and Z.A. Samani, 1985. *Reference crop evapotranspiration from temperature.* Applied Engineer. In Agric., 1, 2, 96-99.

Harrison, L.P., 1963. *Fundamental concepts and definitions relating to humidity.* In 'Humidity and moisture', A. Wexler (Ed.), Vol. 3, Reinhold Publishing Company, New York.

Haverkamp, R., M. Vauclin, J. Touma, P.J. Wierenga and G. Vachaud, 1977. *A comparison of numerical simulation models for one-dimensional infiltration.* Soil Sci. Soc. Am. J., 41, 285-294.

Haverkamp, R., and M. Vauclin, 1979. *A note on estimating finite difference interblock hydraulic conductivity values for transient unsaturated flow problems.* Water Resour. Res., 15, 181-187.

Hendriks, R.F.A., K. Oostindie, and P. Hamminga, 1999. *Simulation of bromide tracer and nitrogen transport in a cracked clay soil with the FLOCR/ANIMO model combination.* J. Hydrol., 215: 94-115.

Hendriks, R.F.A. (2004). *An analytical equation for describing the shrinkage characteristics of peat soils.* In J. Päivänen (Ed.) Wise use of Peatlands. Proceedings of the 12th International Peat Congress. Tampere, Finland.

Hendriks, R.F.A., J.J.T.I. Boesten, J.C. van Dam, and P. Groenendijk. in prep. *Modelling macropore flow in swelling/shrinking clay and peat soils on the basis of macropore geometry.*

Hijmans, R.J., I.M. Guiking-Lens and C.A. van Diepen, 1994. *User's guide for the WOFOST 6.0 crop growth simulation model.* Technical Document 12, Winand Staring Centre, Wageningen, The Netherlands, 144 p.

Hillel, D., 1980. *Fundamentals of soil physics.* Academic Press, San Diego, CA, 412 p.

Hooghoudt, S.B., 1940. *Algemene beschouwing van het probleem van de detailontwatering en de infiltratie door middel van parallel lopende drains, greppels, sloten en kanalen.* Versl. Landbouwk. Onderz., 46, B, 193 p.

Hoogmoed, W.B., and Bouma, J. 1980. *A simulation model for predicting infiltration into a cracked clay soil.* Soil Sci. Soc. Am. J., 44: 458-461.

Homaee, M., 1999. *Root water uptake under non-uniform transient salinity and water stress.* PhD- thesis, Wageningen University, 173 p.

Hopmans, J.W., and J.N.M. Stricker, 1989. *Stochastic analysis of soil water regime in a watershed.* J. Hydrol., 105, 57-84.

Hopmans, J.W., K.C. Roy, and W.W. Wallender, 1991. *Irrigation water management and soil-water hysteresis - a computer modeling study with stochastic soil hydraulic properties.* Transactions of the ASAE, 34: 449-459.

Hopmans, J.W., J.C. van Dam, S.O. Eching and J.N.M. Stricker, 1994. *Parameter estimation of soil hydraulic functions using inverse modeling of transient outflow experiments.* Trends in Hydrology, 1, 217-242.

Hornung, U., and W. Messing, 1983. *Truncation errors in the numerical solution of horizontal diffusion in saturated/unsaturated media.* Adv. Water Resour., 6, 165-168.

Huang, K., B.P Mohanty and M.Th. van Genuchten, 1996. *A new convergence criterion for the modified Picard iteration method to solve the variably saturated flow equation.* J. Hydrol., 178, 69-91.

Hunt, E.R., J.A. Weber and D.M. Gates, 1985. *Effects of nitrate application on Amaranthuspowellii Wats. I. Changes in photosynthesis, growth rates, and leaf area.* Plant Physiology 79, 609-613.

Ippisch, O., H.-J. Vogel and P. Bastian, 2006. *Validity limits for the van Genuchten-Mualem model and implications for parameter estimation and numerical simulation.* Adv. Water Resour., 29, 1780-1789.

Jacucci, G., P. Kabat, L. Pereira, P. Verrier, P. Steduto, C. Uhrik, G. Bertanzon, J.Huygen, B. van den Broek, J. Teixeira, R. Fernando, G. Giannerini, F. Carboni, M. Todorovic, G. Toller, G. Tziallas, E. Fragaki, J. Vera Munoz, D. Carreira, P. Yovchev, D. Calza, E. Valle and M. Douroukis, 1994. *The Hydra Project: a*

Decision Support System for Irrigation Water Management. Proceedings of the International Conference on Land and Water Resources Management in the Mediterranean Region. 4-8 September 1994, Valenzano (Bari), Italy.

Jarvis, N.J., 1989. *CRACK - A model of water and solute movement in cracking clay soils. Technical description and user notes.* Report 159, Dept. Soil Sci., Swedish Univ. Agric. Sci., Uppsala, Sweden, 37 pp.

Jaynes, D.B., 1984. *Comparison of soil water hysteresis models.* J. Hydrol., 75, 287-299.

Jensen, M.E., R.D. Burman and R.G. Allen, 1990. *Evapotranspiration and irrigation water requirements.* ASCE manuals and reports on enigineering practice 70, ASCE, New York. 332 pp.

Jury, W.A., 1982. *Simulation of solute transport using a transfer function mode.* Water Resour. Res., 18, 363-368.

Jury, W.A., D. Russo and G. Sposito, 1987. *The spatial variability of water and solute transport properties in unsaturated soil, II Scaling of water transport.* Hilgardia, 55, 33-56.

Jury, W.A., W.R. Gardner and W.H. Gardner, 1991. *Soil Physics.* Fifth edition. Wiley, New York. 330 pp.

Kabat, P., B.J. Broek, van den and R.A. Feddes, 1992. *SWACROP: A water management and crop production simulation model.* ICID Bulletin 92, vol. 41 No. 2, 61-84.

Kaluarachchi, J.J., and J.C. Parker, 1987. *Effects of hysteresis with air entrapment on water flow in the unsaturated zone.* Water Resour. Res., 23: 1967-1976.

Kase, M. and J. Catský, 1984. *Maintenance and growth components of dark respiration rate in leaves of C_3 and C_4 plants as affected by leaf temperature.* Biologia Plantarum 26, 461-470.

Kim, D.J., 1992. *Characterization of swelling and shrinkage behaviour, hydraulic properties and modelling of water movement in a physically ripening marine clay soil.* PhD thesis, Catholic University Leuven.

Kim, R., 1995. *The water budget of heterogeneous areas.* Doctoral thesis. Wageningen Agricultural University, Wageningen, The Netherlands, 182 pp.

Kool, J.B., J.C. Parker and M.Th. van Genuchten, 1985. *Determining soil hydraulic properties from One-step outflow experiments by parameter estimation: I. Theory and numerical studies.* Soil Sci. Soc. Am. J.,49, 1348-1354.

Kool, J.B., and J.C. Parker, 1987. *Development and evaluation of closed form expressions for hysteretic soil hydraulic properties.* Water Resour. Res., 23, 105-114.

Kool, J.B., J.C. Parker and M.Th. van Genuchten, 1987. *Parameter estimation for unsaturated flow and transport models - a review.* J. Hydrol., 91, 255-293.

Kool, J.B., and M.Th. van Genuchten, 1991. *HYDRUS, One-dimensional variably saturated flow and transport model including hysteresis and root water uptake.* Research Report 124, U.S. Salinity Laboratory, USDA, ARS, Riverside, CA.

Koorevaar, P., G. Menelik and C. Dirksen, 1983. *Elements of soil physics.* Developments in Soil Science 13, Elsevier, Amsterdam, p. 223.

Klute, A., 1986. *Water retention: laboratory methods.* In 'Methods of soil analysis; Part 1; Physical and Mineralogical methods', A. Klute (Ed.), Agronomy series n. 9, ASA and SSSA, Madison, Wisconsin, p. 635-662.

Klute, A., and C. Dirksen, 1986. *Hydraulic conductivity and diffusivity: laboratory methods.* In 'Methods of soil analysis; Part 1; Physical and Mineralogical methods', A. Klute (Ed.), Agronomy series n. 9, ASA and SSSA, Madison, Wisconsin, p. 687-734.

Kraalingen, D. W. G, and C. Rappoldt, 2000. *Reference manual of the FORTRAN utility library TTUTIL v. 4.* Report 5. Plant Research International, Wageningen.

Krammes, J.S., and L.F. DeBano, 1965. *Soil wettability: a neglected factor in watershed management.* Water Resour. Res., 1, 283-288.

Kraijenhoff van de Leur, D.A., 1958. *A study of non-steady groundnwater flow with special references to a reservoir coefficient.* Ingenieur, 70: B87-B94.

Kroes, J.G., and J. Roelsma, 1997. *User's Guide ANIMO 3.5; input instructions and technical programme description.* Technical Document 46, DLO Winand Staring Centre, Wageningen.

Kroes, J.G., P.J.T. van Bakel, J. Huygen, T. Kroon en R. Pastoors, 2001. *Actualisatie van de hydrologie voor STONE 2.0.* Rapport 298, Alterra, Wageningen, 68 p.

Kropff, M.J., H.H. van Laar and H.F.M. ten Berge (Eds.), 1993. *ORYZA1 A basic model for irrigated lowland rice production.* IRRI, Los Banos, The Philippines.

Kujala, K., 1991. *Factors affecting frost susceptibility and heaving pressure in soils.* Acta Univ. Oul. C 58. Department of Civil Engineering, University of Oulu, Finland, 104 pag.

Kustas, W., A. Rango, 1994. *A simple energy algorithm for the snowmelt runoff model.* Water Resources Research 30: 1515-1527.

Leij, F.J., W.J. Alves, M. Th. van Genuchten and J.R. Williams, 1996. *The UNSODA Unsaturated Soil Hydraulic Database. User's manual Version 1.0*, Soil Salinity Laboratory, Riverside, California.

Leistra, M., A.M.A. van der Linden, J.J.T.I.Boesten, A. Tiktak and F. van den Berg. 2001. *PEARL model for pesticide behaviour and emissions in soil-plant systems. Description of processes.* Alterra report 13, RIVM report 711401009, Alterra, Wageningen, 107 pp.

Lin, H.C., Richards, D.R., Yeh, G.T., Cheng, J.R., Cheng, H.P., Jones, N.L., 1997. *FEMWATER: A Three-Dimensional Finite Element Computer Model for Simulating Density-Dependent Flow and Transport in Variably Saturated Media.* Technical Report CHL-97-12. Waterways Experiment Station, U.S. Army Corps of Engineers, Vicksburg, MS 39180-6199

Maas, E.V., and G.J. Hoffman, 1977. *Crop salt tolerance-current assessment.* J. Irrig. and Drainage Div., ASCE 103, 115-134.

Maas, E.V., 1990. *Crop salt tolerance.* In 'Agricultural salinity assessment and management', K.K. Tanji (Ed.), ASCE Manuals and Reports on Engineering practice, No 71, New York.

Makkink, G.F., 1957. *Testing the Penman formule by means of lysimeters.* J. Int. Water Eng., 11:277-288.

Massop, H.Th.L., and P.A.J.W. de Wit, 1994. *Hydrologisch onderzoek naar de gewasweerstanden van het tertiair ontwateringsstelsel in Oost-Gelderland.* Report 373, Winand Staring Centre, Wageningen, The Netherlands, 132 p.

Miller, E.E., and R.D. Miller, 1956. *Physical theory for capillary flow phenomena.* J. Appl. Phys., 27, 324-332.

Millington, R.J., and J.P. Quirk., 1961. *Permeability of porous solids.* Trans. Faraday Soc., 57, 1200-1207.

Milly, P.C.D., 1985. *A mass conservative procedure for time-stepping in models of unsaturated flow.* Adv. Water Resour., 8, 32-36.

Monteith, J.L., 1965. *Evaporation and the Environment.* In: G.E. Fogg (ed.), The state and movement of water in living organisms. Cambridge University Press, p. 205-234.

Monteith, J.L., 1981. *Evaporation and surface temperature.* Quarterly J. Royal Soc., 107, 1-27.

Mualem, Y., 1976. *A new model for predicting the hydraulic conductivity of unsaturated porous media.* Water Resour. Res., 12, 513-522.

Murray, F.W., 1967. *On the computation of saturation vapor pressure.* J. Appl. Meteor., 6, 203-204.

Nieber, John, L., Tammo S. Steenhuis, Todd Walter & Mark Bakker, 2006. *Enhancement of seepage and lateral preferential flow by biopores on hillslopes*, in Biologia.

Nielsen, D.R., M.Th. van Genuchten and J.W. Biggar, 1986. *Water flow and solute transport in the unsaturated zone.* Water Resour. Res., 22, supplement, 89S-108S.

Nimmo, J.R., J. Rubin and D.P. Hammermeister, 1987. *Unsaturated flow in a centrifugal field: Measurement of hydraulic conductivity and testing of Darcy's law.* Water Resour. Res., 32, 124-134.

Parlange, J.Y., 1975. *On solving the flow equation in unsaturated soils by optimization: horizontal infiltration.* Soil Sci. Soc. Am. Proc. 39, 415-418.

Peat, W.E., 1970. *Relationships between photosynthesis and light intensity in the tomato.* Annal Bot., 34, 319-328.

Peck, A.J., R.J. Luxmoore and J.L. Stolzy, 1977. *Effects of spatial variability of soil hydraulic properties in water budget modeling.* Water Resour. Res., 13, 348-354.

Penning de Vries, F.W.T., A.H.M. Brunsting and H.H. van Laar, 1974. *Products requirements and efficiency of biosynthesis: a quantitative approach.* Journal of Theoretical Biology 45, 339-377.

Penning de Vries, F.W.T., J.M. Witlage and D. Kremer, 1979. *Rates of respiration and of increase in structural dry matter in young wheat, ryegrass and maize plants in relation to temperature, to water stress and to their sugar content.* Annals of Botany (London) 44, 595-609.

Penning de Vries, F.W.T. and H.H. van Laar, 1982. *Simulation of growth processes and the model BACROS.* In Penning de Vries, F.W.T. and H.H. van Laar (Eds.) Simulation of plant growth and crop production. Simulation Monographs, Pudoc, Wageningen, The Netherlands. p. 114-135.

Penning de Vries, F.W.T., D.M. Jansen, H.F.M. ten Berge and A. Bakema, 1989. *Simulation of ecophysiological processes of growth in several annual crops.* Pudoc, Wageningen, the Netherlands, 271 pp.

Penman, H.L., 1948. *Natural evaporation from open water, bare soil, and grass.* Proc. Royal Society, London 193, 120-146.

Philip, J.R., 1957. *The theory of infiltration: 4. Sorptivity and algebraic infiltration equations.* Soil Science 84, 264-275.

Press, W.H., B.P. Flannery, S.A. Teukolsky and W.T. Vetterling, 1989. *Numerical Recipes. The art of scientific computing.* Cambridge University Press. 702 pp.

Priestley, C.H.B., and R.J. Taylor, 1972. *On the assessment of surface heat flux and evaporation using large scale parameters.* Mon. Weath. Rev., 100, 81-92.

Raats, P.A.C., 1973. *Unstable wetting fronts in uniform and nonuniform soils.* Soil Sci. Soc. Am. J., 37, 681-685.

Raes, D., H. Lemmens, P. van Aelst, M. van der Bulcke and M. Smith, 1988. *IRSIS (Irrigation Scheduling Information System), reference manual.* Laboratory of Land Management, K.U. Leuven, Belgium.

Reinink, K., I. Jorritsma and A. Darwinkel, 1986. *Adaption of the AFRC wheat phenology model for Dutch conditions.* Neth. J. Agric. Science, 34, 1-13.

Rijniersce, K., 1983. *A simulation model for physical ripening in the IJsselmeerpolders.* Rijksdienst voor IJsselmeerpolders. Lelystad, The Netherlands, 216 pp.

Rijtema, P.E., P. Groenendijk and J.G. Kroes, 1997. *ANIMO, a dynamic simulation model for transport and transformation of nutrients and organic materials in soils.* Report 30, DLO Winand Staring Centre, Wageningen, in press.

Ritchie, J.T., 1972. *A model for predicting evaporation from a row crop with incomplete cover.* Water Resour. Res., 8, 1204-1213.

Ritsema, C.J., L.W. Dekker, J.M.H. Hendrickx and W. Hamminga, 1993. *Preferential flow mechanism in a water repellent sandy soil.* Water Resour. Res., 29, 2183-2193.

Ritsema, C.J., and L.W. Dekker, 1994. *How water moves in a water repellent sandy soil. 2. Dynamics of fingered flow.* Water Resour. Res., 30, 2519-2531.

Ritsema, C.J., 1998. *Flow and transport in water repellent sandy soils.* PhD-thesis Wageningen University, 213 p.

Ritzema, H.P., 1994. *Subsurface flow to drains.* In 'Drainage principles and applications', H.P. Ritzema (Ed. in Chief), ILRI publication 16, second edition, Wageningen, p. 263-304.

Ross, P.J., 1990. *Efficient numerical methods for infiltration using Richards' equation.* Water Resour. Res., 26, 279-290.

Russo, D., E. Bresler, U. Shani and J. Parker, 1991. *Analysis of infiltration events in relation to determining soil hydraulic properties by inverse problem methodology.* Water Resour. Res., 27, 1361-1373.

Saxena, R.K., N.J. Jarvis and L. Bergström, 1994. *Interpreting non-steady state tracer breakthrough experiments in sand and clay soils using a dual-porosity model.* J. Hydrol., 162, 279-298.

Schaap, Marcel G. and Martinus Th. Van Genuchten, 2006. *A Modified Mualem–van Genuchten Formulation for Improved Description of the Hydraulic Conductivity Near Saturation.* In: Vadose Zone Journal 5:27–34.

Scorza Júnior, R.P., J.H. Smelt, J.T.I. Boesten, R.F.A. Hendriks and S.E.A.T.M. van der Zee (2004). *Preferential flow of bromide, bentazon and imidacloprid in a Dutch clay soil.* J. Environ. Qual. 33:1473-1486.

Scott, P.S., G.J. Farquhar and N. Kouwen, 1983. *Hysteretic effects on net infiltration.* In 'Advances in infiltration', American Society of Agricultural Engineers, St. Joseph, Mich, p. 163-170.

Shalhevet, J., 1994. *Using water of marginal quality for crop production: major issues.* Agric. Water Man., 25, 233-269.

Sidle, R.C., S. Noguchi, Y. Tsuboyama and K. Laursen, 2001. *A conceptual model of preferential flow systems in forested hillslopes: evidence of self-organization.* Hydrol. Process., 15: 1675-1692.

Singh, P., G. Spitzbart, H. Hübl, H. W. Weinmeister, 1997. *Hydrological response of snowpack under rain-on-snow events: a field study.* Journal of Hydrology 202: 1-20.

Šimůnek, J., T. Vogel and M.Th. van Genuchten, 1992. *The SWMS-2D code for simulating water flow and solute transport in two-dimensional variably saturated media.* Version 1.1. Res. Rep. 126, U.S. Salinity Lab., Agric. Res. Ser., U.S. Dept. of Agric., Riverside, Calif.

Šimůnek, J., K. Huang, M. Šejna, and M. Th. van Genuchten. 1998. *The HYDRUS-1D Software Package for Simulating the One-Dimensional Movement of Water, Heat and Multiple Solutes in Variably-Saturated Media, Version 1.0.* IGWMC-TPS-70, Int. Ground Water Modeling Center, Colorado School of Mines, Golden, CO., 186 p.

Šimůnek, J., R. Kodesova, M.M. Gribb and M.T. van Genuchten, 1999. *Estimating hysteresis in the soil water retention function from cone permeameter experiments.* Water Resour. Res., 35: 1329-1345.

Šimůnek, J., M. Šejna and M. Th. van Genuchten, 2007. *The HYDRUS Software Package for Simulating the Two- and Three-Dimensional Movement of Water, Heat, and Multiple Solutes in Variably-Saturated Media.* User Manual Version 1.0. PC-Progress, Prague, Czech Republic

Skaggs, T.H., M.Th van Genuchten, P.J. Shouse, and J.A. Poss, 2006. *Macroscopic approaches to root water uptake as a function of water and salinity stress.* Agric. Water Man., 86, 140-149.

Smith, M., 1992. *CROPWAT, a computer program for irrigation planning and management.* FAO Irrigation and Drainage Paper 46. Rome, Italy.

Spitters, C.J.T., H. van Keulen and D.W.G. van Kraalingen, 1989. *A simple and universal crop growth simulator: SUCROS87.* In: R. Rabbinge, S.A. Ward and H.H. van Laar (Eds.) Simulation and systems management in crop protection. Simulation Monographs, Pudoc, Wageningen, The Netherlands. p. 147-181.

Stolte, J., J.I. Freijer, W. Bouten, C. Dirksen, J.M. Halbertsma, J.C. van Dam, J.A. van den Berg, G.J. Veerman and J.H.M. Wösten, 1994. *Comparison of six methods to determine unsaturated soil hydraulic conductivity.* Soil Sci. Soc. Am. J., 58, 1596-1603.

Stroosnijder, L. 1975. *Infiltration and redistribution of water in the soil.* PhD-thesis, Wageningen University, 213 p. (in Dutch)

Supit, I., A.A. Hooyer and C.A. van Diepen (Eds.), 1994. *System description of the WOFOST 6.0 crop simulation model implemented in CGMS. Vol. 1: Theory and algorithms.* EUR publication 15956, Agricultural series, Luxembourg, 146 p.

Taylor, S.A., and G.M. Ashcroft, 1972. *Physical Edaphology.* Freeman and Co., San Francisco, California, p. 434-435.

Ten Berge, H.F.M., 1986. *Heat and water transfer at the bare soil surface: aspects affecting thermal images.* PhD thesis, Wageningen Agricultural University, Wageningen, The Netherlands.

Tetens, O., 1930. *Uber einige meteorologische Begriffe.* Z. Geophys, 6, 297-309.

Thoma , S.G., D.P. Gallegos and D.M. Smith, 1992. *Impact of fracture coatings on fracture/matrix flow interactions in unsaturated porous media.* Water Resources Res., 28, 1357-1367.

Thoms, R.B., R.L. Johnson, and R.W. Healy, 2006. *User's guide to the variability saturated flow (VSF) process for MODFLOW.* USGS Techniques and Methods 6-A18. Reston, Virginia: U.S. Geological Survey.

Tiktak, A., F. van den Berg, J.J.T.I. Boesten, M. Leistra, A.M.A. van der Linden, and D. van Kraalingen, 2000. *Pesticide Emission at Regional and Local scales: Pearl version 1.1 User Manual.* RIVM report 711401008, report 29, Alterra Green World Research, Wageningen.

Van Bakel, P.J.T., 1986. *Planning, design and operation of surface water management systems; a case study.* PhD thesis, Wageningen Agricultural University.

Van Dam, J.C., J.M.H. Hendrickx, H.C. van Ommen, M.H. Bannink, M.Th. van Genuchten and L.W. Dekker, 1990. *Water and solute movement in a coarse-textured water-repellent field soil.* J. Hydrol., 120, 359-379.

Van Dam, J.C., J.N.M. Stricker and P. Droogers, 1994. *Inverse method to determine soil hydraulic functions from multi-step outflow experiments.* Soil Sci. Soc. Am. J., 58, 647-652.

Van Dam, J.C., J.H.M. Wösten and A. Nemes, 1996. *Unsaturated soil water movement in hysteretic and water repellent soils.* J. Hydrol., 184, 153-173.

Van Dam, J.C., J. Huygen, J.G. Wesseling, R.A. Feddes, P. Kabat, P.E.V. van Walsum, P. Groenendijk and C.A. van Diepen, 1997. *Theory of SWAP version 2.0. Simulation of water flow, solute transport and plant growth in the Soil-Water-Atmosphere-Plant environment.* Wageningen University and Alterra. Technical Document 45.

Van Dam, J.C, 2000. *Field scale water flow and solute transport. SWAP model concepts, parameter estimation and case studies.* PhD thesis, Wageningen Universiteit, 167 p.

Van Dam, J.C., and R.A. Feddes, 2000. *Simulation of infiltration, evaporation and shallow groundwater levels with the Richards' equation.* J. of Hydrol., 233, 72-85.

Van Dam, J.C., P. Groenendijk, R.F.A. Hendriks and J.G. Kroes, 2008. Advances of modeling water flow in variably saturated soils with SWAP. Vadose Zone Journal, in press.

Van de Pol, R.M., P.J. Wierenga and D.R. Nielsen, 1977. *Solute movement in a field soil.* Soil Sci. Soc. Am. J., 41, 10-13.

Van den Berg, F., and J.J.T.I. Boesten, 1998. *PEsticide Leaching and Accumulation model (PESTLA) version 3.4; description and user's guide.* Technical Document 43, Alterra Green World Research, Wageningen, 150 p.

Van den Broek, B.J., J.C. van Dam, J.A. Elbers, R.A. Feddes, J. Huygen, P. Kabat and J.G. Wesseling, 1994. *SWAP 1993, input instructions manual.* Report 45, Dep. Water Resources, Wageningen Agricultural University.

Van der Molen, W.H., and J. Wesseling, 1991. *A solution in closed form and a series solution to replace the tables for the thickness of the equivalent layer in Hooghoudt's drain spacing formula.* Agricultural Water Management 19, p. 1-16.

Van der Zee, S.E.A.T.M., and W.H. van Riemsdijk, 1987. *Transport of reactive solute in spatially variable soil systems.* Water Resour. Res., 23, 2059-2069.

Van Dobben, W.H., 1962. *Influence of temperature and light conditions on dry matter distribution, development rate and yield in arable crops.* Netherlands Journal of Agricultural Science 10, 377-389.

Van Genuchten, M.Th., and P.J. Wieringa, 1974. *Simulation of one-dimensional solute transfer in porous media.* New Mexico State University Agric. Exp. Stn. Bull. 628, New Mexico.

Van Genuchten, M.Th., and R.W. Cleary, 1979. *Movement of solutes in soil : computer simulated and laboratory results.* In: G.H. Bolt (Ed.), Soil Chemistry B, Physico-Chemical Models. Elsevier, Amsterdam, pp. 349-386.

Van Genuchten, M.Th., 1980. *A closed form equation for predicting the hydraulic conductivity of unsaturated soils.* Soil Sci. Soc. Am. J., 44, 892-898.

Van Genuchten, M.Th., 1982. *A comparison of numerical solutions of the one-dimensional unsaturated-saturated flow and transport equations.* Adv. Water Resour., 5, 47-55.

Van Genuchten, M.Th., 1987. *A numerical model for water and solute movement in and below the root zone.* Res. Report, US Salinity Laboratory, Riverside, CA.

Van Genuchten, M.Th., and R.J. Wagenet, 1989. *Two-site/two-region models for pesticide transport and degradation: Theoretical development and analytical solutions.* Soil Sci. Soc. Am. J., 53, 1303-1310.

Van Genuchten, M.Th., F.J. Leij and S.R. Yates, 1991. *The RETC code for quantifying the hydraulic functions for unsaturated soils.* U.S. Salinity Laboratory, Riverside, California.

Van Genuchten, M.Th., and F.J. Leij, 1992. *On estimating the hydraulic properties of unsaturated soils.* In 'Indirect methods for estimating hydraulic properties of unsaturated soils', M.Th. van Genuchten and F.J. Leij (eds.), Proc. Int. Workshop, Riverside, California, p. 1-14.

Van Grinsven, J.J.M., C. Dirksen and W. Bouten, 1985. *Evaluation of hot air method for measuring soil water diffusivity.* Soil Sci. Soc. Am. J., 49, 1093-1099.

Van Heemst, H.D.J., 1986a. *The distribution of dry matter during growth of a potato crop.* Potato Research 29, 55-66.

Van Heemst, H.D.J., 1986b. *Crop phenology and dry matter distribution.* In: H. van Keulen and J. Wolf (Eds.). Modelling of agricultural production: soil, weather and crops. p. 13-60.

Van Ittersum, M.K., P.A. Leffelaar, H. van Keulen, M.J. Kropff, L. Bastiaans and J. Goudriaan, 2003. *On approaches and applications of the Wageningen crop models.* Europ. J. Agronomy 18, 201-234.

Van Keulen, H., 1975. *Simulation of water use and herbage growth in arid regions.* Simulation Monographs. Pudoc, Wageningen, the Netherlands. 184 pp.

Van Keulen, H., N.G. Seligman and R.W.Benjamin, 1981. *Simulation of water use and herbage growth in arid regions - A re-evaluation and further development of the model 'Arid Crop'.* Agricultural systems 6, 159-193.

Van Keulen, H., and J. Wolf, 1986. *Modelling of agricultural production: weather, soil and crops.* Simulation Monographs. Pudoc, Wageningen, The Netherlands, pp. 479.

Van Keulen, H., and N.G. Seligman, 1987. *Simulation of water use, nitrogen nutrition and growth of a spring wheat crop.* Simulation Monographs. Pudoc, Wageningen, The Netherlands. 310 pp.

Van Laar, H.H., J. Goudriaan and H. van Keulen (Eds.), 1992. *Simulation of crop growth for potential and water-limited production situations (as applied to*

spring wheat). Simulation reports CABO-TT 27. CABO-DLO, WAU-TPE, Wageningen. 72 pp.

Van Ommen, H.C., M.Th. van Genuchten, W.H. van der Molen, R. Dijksma and J. Hulshof, 1989. *Experimental assessment of preferential flow paths in a field soil.* J. Hydrol., 105, 253-262.

Van Stiphout, T.P.J., H.A.J. van Lanen, O.H. Boersma, and J. Bouma, 1987. *The effect of bypass flow and internal catchment of rain on the water regime in a clay loam grassland soil.* J. Hydrol. 95, 1-11.

Van Wijk, W.R. (Ed.), 1966. *Physics of plant environment.* North Holland Publ. Comp., Amsterdam, The Netherlands, 2nd edition. 382 pp.

Vogel T., M.Th. van Genuchten, M. Cislerova, 2001. *Effect of the shape of the soil hydraulic functions near saturation on variably-saturated flow predictions.* In: Advances in WaterResources 24 (2001) 133-144.

Von Hoyningen-Hüne, J., 1983. *Die Interception des Niederschlags in landwirtschaftlichen Beständen.* Schriftenreihe des DVWK 57, 1-53.

Voss, C. I., and A.M. Provost, 2002. *SUTRA, A model for saturated-unsaturated variable-density ground-water flow with solute or energy transport.* U.S. Geological Survey Water-Resources Investigations Report 02-4231, 250 p.

Walker, A., 1974. *A simulation model for prediction of herbicide persistence.* J. Environ. Qual., 3, 396-401.

Warrick, A.W., 1991. *Numerical approximations of darcian flow through unsaturated soil.* Water Resour. Res., 27, 1215-1222.

Weir, A.H., P.L. Bragg, J.R. Porter and J.H. Rayner, 1984. *A winter wheat crop simulation model without water and nutrient limitations.* Journal of Agricultural Science 102, 371-382.

Wendroth, O., W. Ehlers, J.W. Hopmans, H. Kage, J. Halbertsma and J.H.M. Wösten, 1993. *Reevaluation of the evaporation method for determining hydraulic functions in unsaturated soils.* Soil Sci. Soc. Am. J., 57, 1436-1443.

Wesseling, JG; Wesseling, J, 1984. *Influence of seepage on the depth of water tables in drainage.* J. Hydrol., 73, 289-297

Wesseling, J.G., 1987. *Invloed van bodemsoort en vochtgehalte op de bodemtemperatuur. Een theoretische beschouwing.* Cultuurtechnisch tijdschrift, 27(2), 117-128.

Wesseling, J.G., J.A. Elbers, P. Kabat and B.J. van den Broek, 1991. *SWATRE; instructions for input.* Internal note, Winand Staring Centre, Wageningen.

Wesseling, J.G., J.G. Kroes, and K. Metselaar, 1998. *Global sensitivity analysis of the Soil-Water-Atmosphere-Plant (SWAP) model.* Report 160, Alterra, Wageningen, 67 p.

Wolfe, N.L., U. Mingelgrin, G.C. Miller, 1990. *Abiotic transformations in water, sediments and soil.* In: H.H. Cheng (Ed.), Pesticides in the soil environment: processes, impacts and modeling. SSSA Book Series no. 2, Madison, Wisconsin, USA.

Wösten, J.H.M., G.J. Veerman and J. Stolte, 1994. *Water retention and hydraulic conductivity functions of top- and subsoils in The Netherlands: The Staring series.* Technical Document 18, Winand Staring Centre, Wageningen, The Netherlands, 66 p. (in Dutch).

Wösten, J.H.M., A. Lilly, A. Nemes and C. Le Bas, 1998. *Using existing soil data to derive hydraulic properties for simulation models in environmental studies and in land use planning.* Report 156, Winand Staring Centre, The Netherlands.

Wösten, J.H.M., G.J. Veerman, W.J.M. de Groot, and J. Stolte, 2001. *Water retention and hydraulic conductivity functions of top- and subsoils in The Netherlands: The Staring series.* Alterra report 153, Wageningen, The Netherlands, 86 p. (in Dutch).

Yates, S.R., M.Th. van Genuchten, A.W. Warrick and F.J. Leij, 1992. *Analysis of measured, predicted and estimated hydraulic conductivity using the RETC computer program.* Soil Sci. Soc. Am. J., 56, 347-354.

Youngs, E.G., and R.I. Price, 1981. *Scaling of infiltration behaviour in dissimilar porous materials.* Water Resour. Res., 17, 1065-1070.

Yule, D.F., and J.T. Ritchie, 1980a. *Soil shrinkage relationships of Texas Vertisols: I. Small cores.* Soil Sci. Soc. Am. J., 44: 1285-1291.

Yule, D.F., and J.T. Ritchie, 1980b. *Soil shrinkage relationships of Texas Vertisols: II. Large cores.* Soil Sci. Soc. Am. J., 44: 1291-1295.

Zaidel, J., and D. Russo, 1992. *Estimation of finite difference interblock conductivities for simulation of infiltration into initially dry soils.* Water Resour. Res., 28, 2285-2295.

Appendix 1 Application Penman Monteith method

After Allen et al. (1998)

The original form of the Penman-Monteith equation can be written as (Monteith, 1965, 1981):

$$ET_p = \frac{\dfrac{\Delta_v}{\lambda_w}(R_n - G) + \dfrac{p_1 \rho_{air} C_{air}}{\lambda_w}\dfrac{e_{sat} - e_a}{r_{air}}}{\Delta_v + \gamma_{air}\left(1 + \dfrac{r_{crop}}{r_{air}}\right)}$$

where ET_p is the potential transpiration rate of the canopy (mm d^{-1}), Δ_v is the slope of the vapour pressure curve (kPa °C^{-1}), λ_w is the latent heat of vaporization (J kg^{-1}), R_n is the net radiation flux at the canopy surface (J m^{-2} d^{-1}), G is the soil heat flux (J m^{-2} d^{-1}), p_1 accounts for unit conversion (=86400 s d^{-1}), ρ_{air} is the air density (kg m^{-3}), C_{air} is the heat capacity of moist air (J kg^{-1} °C^{-1}), e_{sat} is the saturation vapour pressure (kPa), e_a is the actual vapour pressure (kPa), γ_{air} is the psychrometric constant (kPa °C^{-1}), r_{crop} is the crop resistance (s m^{-1}) and r_{air} is the aerodynamic resistance (s m^{-1}).

To facilitate analysis of the combination equation, an aerodynamic and radiation term are defined:

$$ET_p = ET_{rad} + ET_{aero}$$

where ET_p is potential transpiration rate of crop canopy (cm d^{-1}), ET_{rad} is the radiation term (cm d^{-1}) and ET_{aero} is the aerodynamic term (cm d^{-1}).

The radiation term equals:

$$ET_{rad} = \frac{\Delta_v(R_n - G)}{\lambda_w(\Delta_v + \gamma_{air}^*)}$$

where the modified psychrometric constant (kPa °C^{-1}) is:

$$\gamma_{air}^* = \gamma_{air}\left(1 + \frac{r_{crop}}{r_{air}}\right)$$

The aerodynamic term equals:

$$ET_{aero} = \frac{p_1 \rho_{air} C_{air}(e_{sat} - e_a)}{\lambda_w(\Delta_v + \gamma_{air}^*)r_{air}}$$

Many meteorological stations provide mean daily values of air temperature T_{air} (°C), global solar radiation R_s (J m^{-2} d^{-1}), wind speed u_0 (m s^{-1}) and air humidity e_{act} (kPa). These basic meteorological data are used to apply the Penman Monteith equation.

Radiation term

The net radiation R_n (J m^{-2} d^{-1}) is the difference between incoming and outgoing radiation of both short and long wavelengths. It is the balance between the energy adsorbed, reflected and emitted by the earth's surface:

$$R_n = (1 - \alpha_r) R_s - R_{nl}$$

where α_r is the reflection coefficient or albedo (-) and R_{nl} is the net longwave radiation (J m^{-2} d^{-1}). The albedo is highly variable for different surfaces and for the angle of incidence or slope of the ground surface. It may be as large as 0.95 for freshly fallen snow and as small as 0.05 for a wet bare soil. A green vegetation cover has an albedo of about 0.20-0.25 (De Bruin, 1998). SWAP will assume in case of a crop $\alpha_r = 0.23$, in case of bare soil $\alpha_r = 0.15$.

The earth emits longwave radiation, which increases with temperature and which is adsorbed by the atmosphere or lost into space. The longwave radiation received by the atmosphere increases its temperature and, as a consequence, the atmosphere radiates energy of its own. Part of this radiation finds its way back to the earth's surface. As the outgoing longwave radiation is almost always greater than the incoming longwave radiation, the net longwave radiation R_{nl} represents an energy loss. Allen et al. (1998) recommend the following formula for the net longwave radiation:

$$R_{nl} = \sigma_{sb} \left[\frac{T_{max}^4 + T_{min}^4}{2} \right] \left(0.34 - 0.14 \sqrt{e_{act}} \right) \left(0.1 + 0.9 N_{rel} \right)$$

where σ_{sb} is the Stefan-Boltzmann constant (4.903 10^{-3} J K^{-4} m^{-2} d^{-1}), T_{min} and T_{max} are the minimum and maximum absolute temperatures during the day (K), respectively, e_{act} is the actual vapour pressure (kPa), and N_{rel} is the relative sunshine duration. The latter can be derived from the measured global solar radiation R_n and the extraterrestrial radiation R_a (J m^{-2} d^{-1}), which is received at the top of the Earth's atmosphere on a horizontal surface:

$$N_{rel} = \left(\frac{R_s}{R_a} - a \right) \frac{1}{b}$$

where a and b are empirical coefficients which depend on the local climate. For international use Allen et al. (1998) recommend $a = 0.25$ and $b = 0.50$.

The extraterrestrial radiation R_a depends on the latitude and the day of the year. R_a is calculated with:

$$R_a = \frac{G_{sc}}{\pi} d_r \left[\omega_s \sin(\varphi) \sin(\delta) + \cos(\varphi) \cos(\delta) \sin(\omega_s) \right]$$

where G_{sc} is the amount of solar radiation striking a surface perpendicular to the sun's rays at the top of the Earth's atmosphere, called the solar constant (J m^{-2} d^{-1}), d_r is the inverse relative distance Earth-Sun (-), ω_s is the sunset hour angle (rad), φ is the latitude (rad) and δ is the solar declination (rad). The inverse relative distance Earth-Sun and the solar declination are given by:

$$d_r = 1 + 0.033 \cos\left(\frac{2\pi}{365} J\right)$$

$$\delta = 0.409 \sin\left(\frac{2\pi}{365} J - 1.39\right)$$

where J is the number of the day in the year (1-365 or 366, starting January 1). The sunset hour angle expresses the day length and is given by:

$$\omega_s = \arccos\left[-\tan(\varphi)\tan(\delta)\right]$$

Aerodynamic term

Latent heat of vaporization, λ_w (J g^{-1}), depends on the air temperature T_{air} (°C) (Harrison, 1963):

$$\lambda_w = 2501 - 2.361 T_{air}$$

Saturation vapour pressure, e_{sat} (kPa), also can be calculated from air temperature (Tetens, 1930):

$$e_{sat} = 0.611 \exp\left(\frac{17.27\, T_{air}}{T_{air} + 237.3}\right)$$

The slope of the vapour pressure curve, Δ_v (kPa °C^{-1}), is calculated as (Murray, 1967):

$$\Delta_v = \frac{4098\, e_{sat}}{(T_{air} + 237.3)^2}$$

The psychrometric constant, γ_{air} (kPa °C^{-1}), follows from (Brunt, 1952):

$$\gamma_{air} = 1.63 \frac{p_{air}}{\lambda_w}$$

with p_{air} the atmospheric pressure (kPa) at elevation z_0 (m), which is calculated from (Burman et al., 1987):

$$p_{air} = 101.3 \left(\frac{T_{air,K} - 0.0065 z_0}{T_{air,K}}\right)^{5.256}$$

Employing the ideal gas law, the atmospheric density, ρ_a (g cm^{-3}), can be shown to depend on p and the virtual temperature T_{vir} (K):

$$\rho_{air} = 3.486\, 10^{-3} \frac{p_{air}}{T_{vir}}$$

where the virtual temperature is derived from:

$$T_{vir} = \frac{T_{air,K}}{1 - 0.378\dfrac{e_{act}}{p_{air}}}$$

The heat capacity of moist air, C_{air} (J g^{-1} °C^{-1}), follows from:

$$C_{air} = 0.622 \frac{\gamma_{air} \lambda_w}{p_{air}}$$

Aerodynamic resistance

The aerodynamic resistance r_{air} depends on the wind speed profile and the roughness of the canopy and is calculated as (Allen et al., 1998):

$$r_{air} = \frac{\ln\left(\dfrac{z_m - d}{z_{om}}\right) \cdot \ln\left(\dfrac{z_h - d}{z_{oh}}\right)}{\kappa_{vk}^2 \cdot u}$$

where z_m is height of wind speed measurements (m), z_h is height of temperature and humidity measurements (m), d is zero plane displacement of wind profile (m), z_{om} is roughness parameter for momentum (m) and z_{oh} is roughness parameter for heat and vapour (m), κ_{vk} is von Karman constant = 0.41 (-), u is wind speed measurement at height z_m (m s^{-1}).

The parameters d, z_{om} and z_{oh} are defined as:

$$d = \tfrac{2}{3} h_{crop}$$

$$z_{om} = 0.123 \; h_{crop}$$

$$z_{oh} = 0.1 \, z_{om}$$

with h_{crop} the crop height (cm)

A default height of 2 m is assumed for wind speed measurements (z_m) and height of temperature and humidity measurements (z_h).

Meteorological stations generally provide 24 hour averages of wind speed measurements, according to international standards, at an altitude of 10 meter.

To calculate r_{air}, the average daytime wind (7.00 - 19.00 h) should be used. For ordinary conditions we assume (Smith, 1991) for the average daytime windspeed ($u_{0,day}$):

$$u_{0,day} = 1.33 \, u_0$$

where u_0 is the measured average wind speed over 24 hours (m s^{-1}).

When crop height (h_{crop}) reaches below or above measurement height ($z_{m,meas}$), the wind speed is corrected with the following assumptions:

- a uniform wind pattern at an altitude of 100 meter;
- wind speed measurements are carried out above grassland;
- a logarithmic wind profile is assumed;

- below 2 meter wind speed is assumed to be unchanged with respect to a value at an altitude of 2 meter; applying a logarithmic wind profile at low altitudes is not carried out due to the high variation below 2 meter.

These assumptions result in the following equation for wind speed correction:

$$
u = \frac{\ln\left(\dfrac{z_{act} - d_{act}}{z_{om,act}}\right)}{\ln\left(\dfrac{z_{100} - d_{act}}{z_{om,act}}\right)} \; \frac{\ln\left(\dfrac{z_{100} - d_{grass}}{z_{om,grass}}\right)}{\ln\left(\dfrac{z_{m,meas} - d_{grass}}{z_{om,grass}}\right)} \; u_{0,day}
$$

where: u wind speed at crop height (m s^{-1}), z_{act} is the actual crop height with a minimum value of 2 m, d_{act} and d_{grass} are zero plane displacement of actual crop and grass (m), $z_{om,act}$ and $z_{om,grass}$ are roughness parameter for momentum actual crop and grass (m).

Appendix 2 Derivation of some macropore geometry equations

Basis of the determination of the effective vertical macropore wall area and the effective crack width is the assumption that the natural variety of soil matrix polygons can be described in terms of one effective regular soil matrix polygon. Crucial condition for this polygon is that many of it should fit together without any gaps to 'tile the plane'. From the regular polygons, only equilateral triangles, squares and regular hexagons have this quality. Empirical experience points out that squares and hexagons in particular are the most likely candidates for these polygons. Which of the two should be chosen, is irrelevant. They are both regular polygons with an even number of sides. All of these even-sided regular polygons, from square to circle, have two relevant, special qualities: the quotient of their perimeter divided by their area is independent of the number of sides and their area is a function of the squared diameter.

Effective vertical macropore wall area

All even-sided regular polygons with n sides are built up of n equal isosceles triangles with base of length x (cm) and height $\frac{1}{2} d_{pol}$ (cm) (Fig. A2.1). The perimeter of the polygon equals n times x and the area equals n times the area of the triangle. The latter equals $\frac{1}{4} d_{pol} x$ (cm^2), so that:

$$\frac{perimeter_{pol}}{area_{pol}} = \frac{nx}{n\frac{1}{4}d_{pol}x} = \frac{4}{d_{pol}} \qquad (A2.1)$$
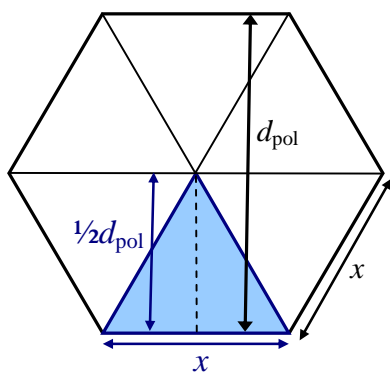
Figure A2.1 Hexagon: 6-sided regular polygon, consists of 6 isosceles triangles with area $\frac{1}{2}d_{pol} \cdot \frac{1}{2}x = \frac{1}{4} d_{pol}x$. Area of polygon $= 6 \cdot \frac{1}{4} d_{pol}x$ and perimeter $= 6 x$. Vertical wall area per unit of volume $A^*_{wall} = 6 x / (6 \cdot \frac{1}{4} d_{pol}x) = 4 / d_{pol}$.

The vertical area of the wall of the polygon of Figure A2.1 per unit of depth is equal to the perymeter of the polygon. In order to express this area per unit of horizontal area it is divided by the area of the polygon. Thus, the effective vertical area of the wall of the matrix polygons A^*_{wall} per unit of depth and horizontal area, which implies

per unit of volume, equals the quotient of the polygons' perimeter divided by their area, which equals $4 / d_{\text{pol}}$ (cm^{-1}).
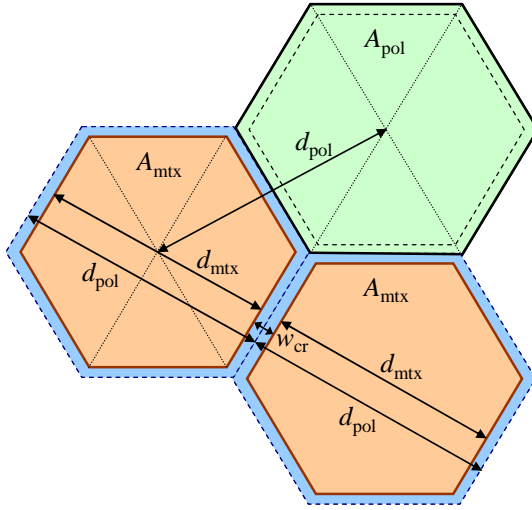
*Figure A2.2 Area A and diameter d of basis polygon (pol) and matrix polygon (mtx). Crack width w_{cr} is equal to the difference between d_{pol} and d_{mtx}.*

Effective crack width

For even-sided regular polygons it can be derived that their sides x (Fig. A2.1) can be expressed as $(C_n / n) d_{\text{pol}}$, where C_n (-) is a constant that depends on n. For squares, hexagons and circles, C_n equals, 4, 2√3 and π, respectively. With C_n a general equation for the area A_{pol} (cm^2) of an even-sided regular polygon as function of d^2_{pol} can be derived:

$$A_{\text{pol}} = n\frac{1}{4}d_{\text{pol}}x = n\frac{1}{4}d_{\text{pol}}\frac{C_n}{n}d_{\text{pol}} = \frac{1}{4}C_n d^2_{\text{pol}} \qquad (A2.2)$$

For this equation, we define d_{pol} as the distance between the centres of two adjacent basis polygons (Fig. A2.2). The value of this diameter is fixed. The value of the actual soil matrix polygon diameter d_{mtx} depends on the crack width, which is not fixed in case of a shrinking matrix. Thus, the crack width w_{cr} can be calculated as (Fig. A2.2):

$$w_{cr} = d_{\text{pol}} - d_{\text{mtx}} \qquad (A2.3)$$

The horizontal area of the cracks A_{cr} (cm^2) as fraction of A_{pol} depends on the macropore volume fraction V_{mp} (cm^3 cm^{-3}) as:

$$A_{\text{cr}} = V_{\text{mp}}A_{\text{pol}} \qquad (A2.4)$$

The horizontal area of the matrix polygon A_{mtx} (cm^2) is a function of d^2_{mtx} according to Eq. [A2.2]:

$$A_{\text{mtx}} = \frac{1}{4}C_n d^2_{\text{mtx}} \qquad (A2.5)$$

A_{mtx} is also equal to the difference between basis polygon area A_{pol} and crack area A_{cr}:

$$A_{\mathrm{mtx}} = A_{\mathrm{pol}} - A_{\mathrm{cr}} = A_{\mathrm{pol}} - V_{\mathrm{mp}} A_{\mathrm{pol}} = \left(1 - V_{\mathrm{mp}}\right) A_{\mathrm{pol}} = \left(1 - V_{\mathrm{mp}}\right) \frac{1}{4} C_n d_{\mathrm{pol}}^2 \qquad (A2.6)$$

Combining the right hands terms of Eq. [A2.5] and Eq. [A2.6] yields:

$$\frac{1}{4} C_n d_{\mathrm{mtx}}^2 = \left(1 - V_{\mathrm{mp}}\right) \frac{1}{4} C_n d_{\mathrm{pol}}^2 \qquad (A2.7)$$

and:

$$d_{\mathrm{mtx}}^2 = \left(1 - V_{\mathrm{mp}}\right) d_{\mathrm{pol}}^2 \qquad (A2.8)$$

so that:

$$d_{\mathrm{mtx}} = d_{\mathrm{pol}} \sqrt{1 - V_{\mathrm{mp}}} \qquad (A2.9)$$

And finally, the crack width is expressed as:

$$w_{\mathrm{cr}} = d_{\mathrm{pol}} - d_{\mathrm{mtx}} = d_{\mathrm{pol}} \left(1 - \sqrt{1 - V_{\mathrm{mp}}}\right) \qquad (A2.10)$$

Figure A2.3 shows the crack width w_{cr} as function of the macropore volume fraction V_{mp} for different polygon diameters d_{pol}.
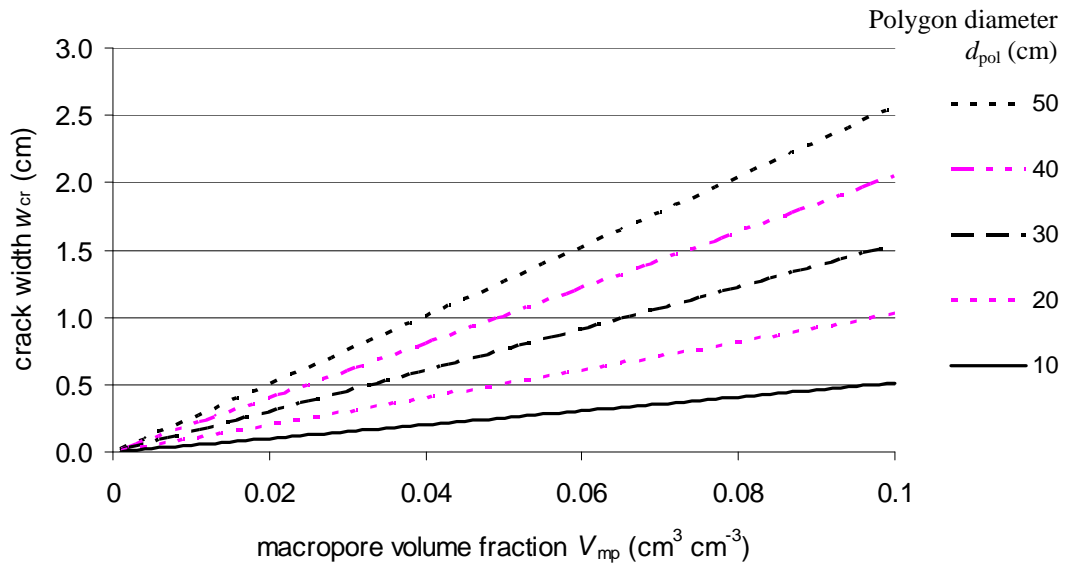
Figure A2.3   Crack width w_{cr} as function of the macropore volume fraction V_{mp} for different polygon diameters d_{pol}

***Effect of crack width w_{cr} on calculation of area of vertical wall A^*_{wall} and distance x_{pol}***

Strictly speaking, the vertical macropore wall area A^*_{wall} and the horizontal distance x_{pol} should be calculated on the basis of d_{mtx} instead of d_{pol}. However, x_{pol} is always used in combination with A^*_{wall} as: A^*_{wall} / x_{pol} (Eq. [6.32], Eq. [6.35] and Eq. [6.36]). This quotient is similar for using d_{mtx} and d_{pol}:

$$\frac{A^*_{wall,mtx}}{x_{pol,mtx}} = \frac{\dfrac{4}{d_{mtx}} \dfrac{A_{mtx}}{A_{pol}}}{\dfrac{1}{2} d_{mtx}} = \frac{\dfrac{4}{d_{mtx}} \dfrac{d^2_{mtx}}{d^2_{pol}}}{\dfrac{1}{2} d_{mtx}} = \frac{4}{\dfrac{1}{2} d^2_{pol}} = \frac{A^*_{wall}}{x_{pol}} \qquad (A2.11)$$

Only in Eq. [6.29], the calculation of the absorption, A^*_{wall} is used without dividing by x_{pol}. In that case, $A^*_{wall,mtx}$ is used for A^*_{wall}. Therefore, A^*_{wall} is corrected with Eq. [A2.9] according to:

$$A^*_{wall,mtx} = \frac{d_{mtx}}{d_{pol}} A^*_{wall} = \frac{d_{pol}\sqrt{1-V_{mp}}}{d_{pol}} A^*_{wall} = \sqrt{1-V_{mp}}\, A^*_{wall} \qquad (A2.12)$$

Appendix 3 Examples of description of macropore geometry
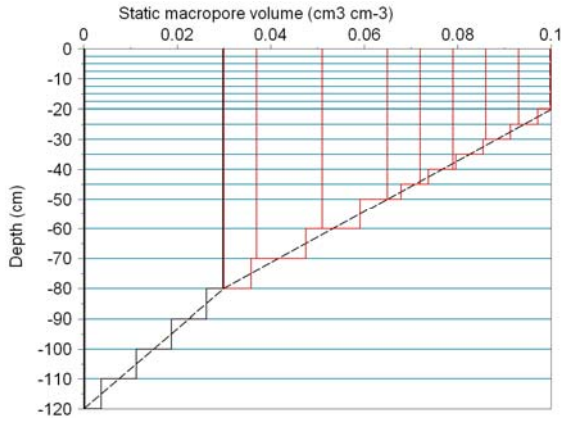
VLMPSTSS	=	$V_{st,0}$
PPICSS	=	$P_{ic,0}$
NUMSBDM	=	n_{sd}
POWM	=	m
RZAH	=	R_{ZAh}
SPOINT	=	S_p
SWPOWM	=	Sw_{powm}

$Z_{ah} = -20$ cm; $Z_{ic} = -80$ cm; $Z_{st} = -120$ cm;
$V_{st,0} = 0.1$ cm^3 cm^{-3}; $P_{ic,0} = 0.7$; $m = 1.0$; $n_{sd} = 10$
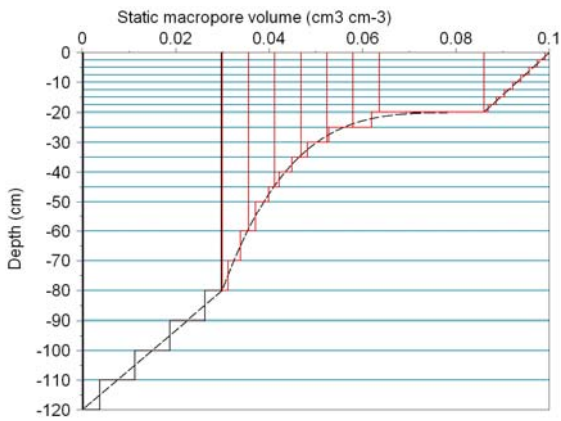
$m = 0.25$; $R_{ZAh} = 0.2$

$m = 4.0$

$m = 4.0$; $S_p = 0.5$

$m = 0.25$; $S_p = 0.5$

$m = 0.25$; $S_p = 0.25$

$m = 0.25$; $S_p = 0.75$

$S_p = 0.5$; $Sw_{powm} = 1$

$m = 4.0$; $S_p = 0.5$; $Sw_{powm} = 1$

$m = 4.0$; $S_p = 0.25$; $Sw_{powm} = 1$

$m = 4.0$; $S_p = 0.75$; $Sw_{powm} = 1$
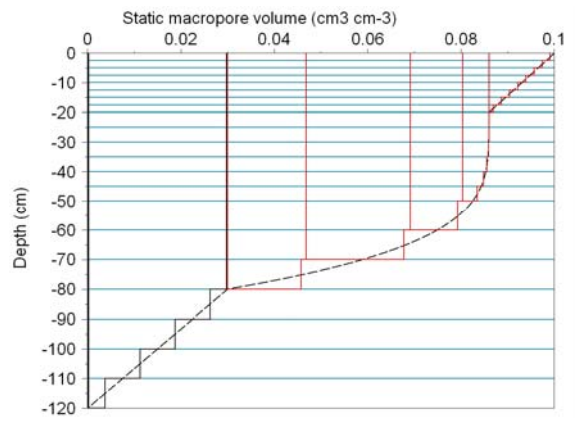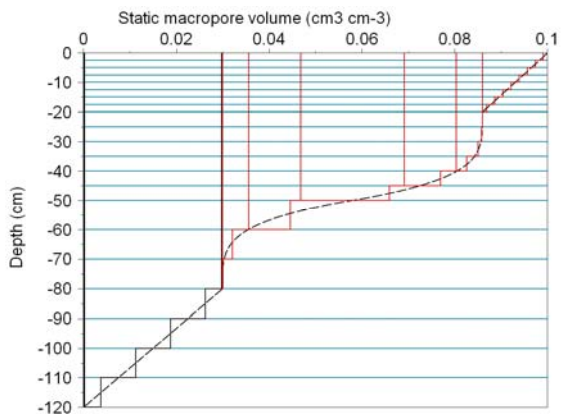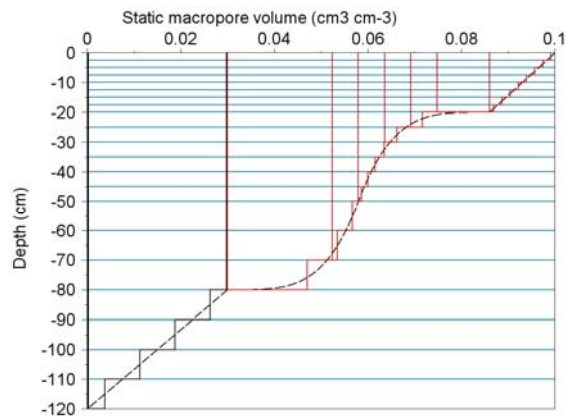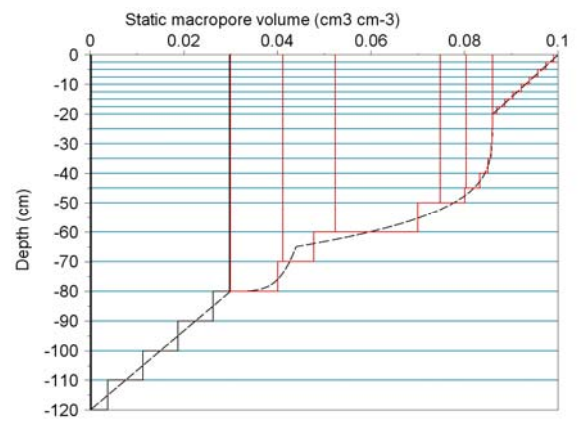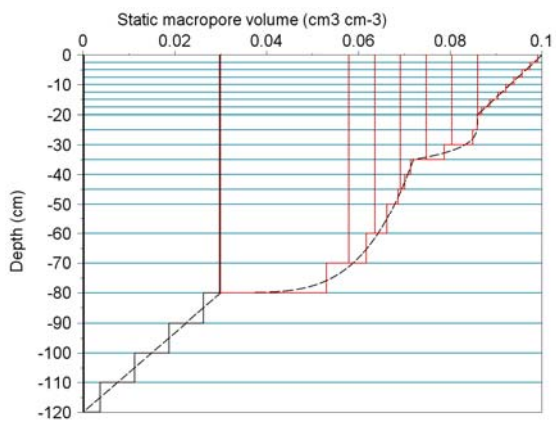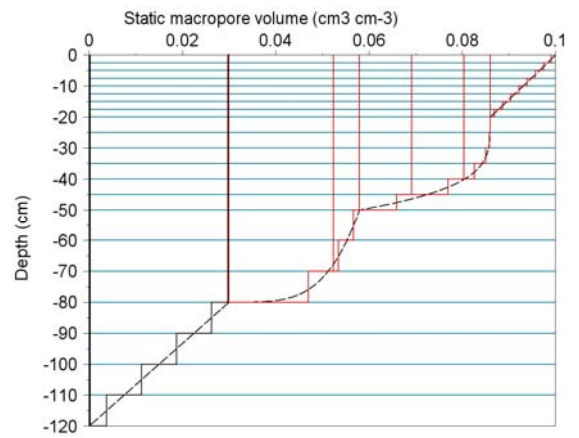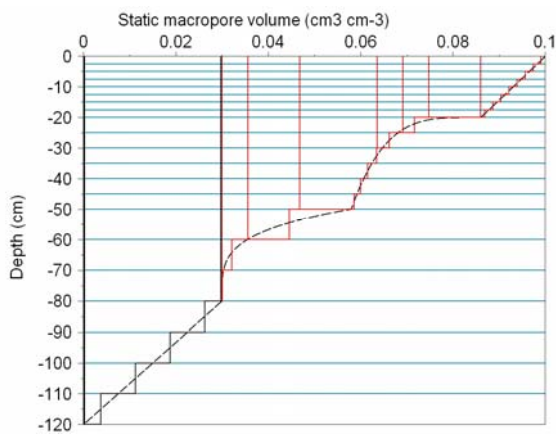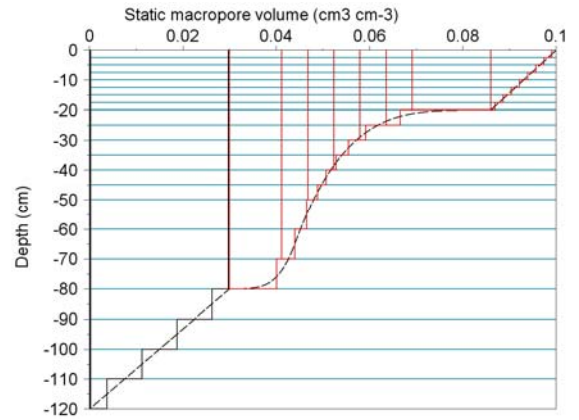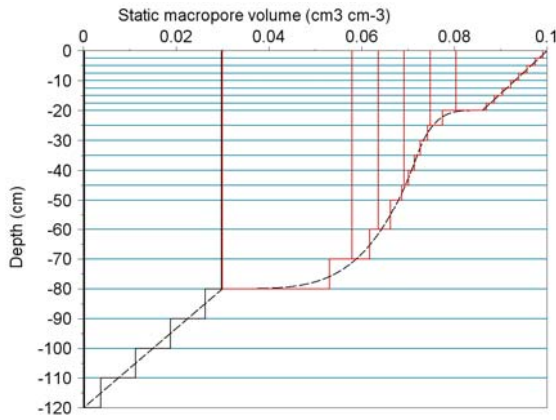
Appendix 4 Partial derivatives of F_i to pressure heads

The coefficients of the Jacobian are given by:

$$\frac{\partial F_i}{\partial h_{i-1}^{j+1,p}} = -\frac{K_{i-\frac{1}{2}}^{j+\kappa,\kappa p}}{\frac{1}{2}(\Delta z_{i-1} + \Delta z_i)} - \kappa \frac{\partial K_{i-\frac{1}{2}}^{j+\kappa,\kappa p}}{\partial h_{i-1}^{j+1,p}} \left(\frac{h_{i-1}^{j+1,p} - h_i^{j+1,p}}{\frac{1}{2}(\Delta z_{i-1} + \Delta z_i)} + 1 \right)$$

$$\frac{\partial F_i}{\partial h_i^{j+1,p}} = \frac{\Delta z_i}{\Delta t^j} C_i^{j+1,p} + \Delta z_i \frac{\partial S_{m,i}^{j+1,p}}{\partial h_i^{j+1,p}} + \frac{K_{i-\frac{1}{2}}^{j+\kappa,\kappa p}}{\frac{1}{2}(\Delta z_{i-1} + \Delta z_i)} + \frac{K_{i+\frac{1}{2}}^{j+\kappa,\kappa p}}{\frac{1}{2}(\Delta z_i + \Delta z_{i+1})}$$

$$- \kappa \frac{\partial K_{i-\frac{1}{2}}^{j+\kappa,\kappa p}}{\partial h_i^{j+1,p}} \left(\frac{h_{i-1}^{j+1,p} - h_i^{j+1,p}}{\frac{1}{2}(\Delta z_{i-1} + \Delta z_i)} + 1 \right) + \kappa \frac{\partial K_{i+\frac{1}{2}}^{j+\kappa,\kappa p}}{\partial h_i^{j+1,p}} \left(\frac{h_i^{j+1,p} - h_{i+1}^{j+1,p}}{\frac{1}{2}(\Delta z_i + \Delta z_{i+1})} + 1 \right)$$

$$\frac{\partial F_i}{\partial h_{i+1}^{j+1,p}} = -\frac{K_{i+\frac{1}{2}}^{j+\kappa,\kappa p}}{\frac{1}{2}(\Delta z_i + \Delta z_{i+1})} + \kappa \frac{\partial K_{i+\frac{1}{2}}^{j+\kappa,\kappa p}}{\partial h_{i+1}^{j+1,p}} \left(\frac{h_i^{j+1,p} - h_{i+1}^{j+1,p}}{\frac{1}{2}(\Delta z_i + \Delta z_{i+1})} + 1 \right)$$

Where $C_i^{j+1,p}$ is the differential moisture capacity (cm-1). $\dfrac{\partial K_{i-\frac{1}{2}}^{j+\kappa,\kappa p}}{\partial h_i^{j+1,p}}$ and $\dfrac{\partial K_{i+\frac{1}{2}}^{j+\kappa,\kappa p}}{\partial h_i^{j+1,p}}$ are

the partial derivatives of the internodal conductivity to the pressure head, further elaborated in 0. The calculation of the partial derivatives for the top and bottom compartment requires special attention.

The Jacobian coefficient for the first compartment reads as:
Flux controlled top boundary condition

$$\frac{\partial F_1}{\partial h_1^{j+1}} = \frac{\Delta z_1}{\Delta t^j} C_1^{j+1} + \Delta z_1 \frac{\partial S_{m,1}^{j+1}}{\partial h_1^{j+1}} + \frac{K_{1\frac{1}{2}}^{j+\kappa}}{\frac{1}{2}(\Delta z_i + \Delta z_{i+1})} + \kappa \frac{\partial K_{1\frac{1}{2}}^{j+\kappa}}{\partial h_1^{j+1}} \left(\frac{h_1^{j+1} - h_2^{j+1}}{\frac{1}{2}(\Delta z_1 + \Delta z_2)} + 1 \right)$$

Head controlled top boundary condition

$$\frac{\partial F_1}{\partial h_1^{j+1}} = \frac{\Delta z_1}{\Delta t^j} C_1^{j+1} + \Delta z_1 \frac{\partial S_{m,1}^{j+1}}{\partial h_1^{j+1}} + \frac{K_{\frac{1}{2}}^{j+1}}{\frac{1}{2}\Delta z_i} + \frac{K_{1\frac{1}{2}}^{j+\kappa}}{\frac{1}{2}(\Delta z_i + \Delta z_{i+1})}$$

$$- \frac{\partial K_{\frac{1}{2}}^{j+1}}{\partial h_1^{j+1}} \left(\frac{h_0^{j+1} - h_1^{j+1}}{\frac{1}{2}\Delta z_1} + 1 \right) + \kappa \frac{\partial K_{1\frac{1}{2}}^{j+\kappa}}{\partial h_1^{j+1}} \left(\frac{h_1^{j+1} - h_2^{j+1}}{\frac{1}{2}(\Delta z_1 + \Delta z_2)} + 1 \right)$$

The internodal conductivity $K_{\frac{1}{2}}^{j+1}$ is irrespective the value of κ always treated implicitly.

The Jacobian coefficient for the last compartment reads as:
Flux controlled bottom boundary

$$\frac{\partial F_1}{\partial h_n^{j+1}} = \frac{\Delta z_n}{\Delta t^j} C_n^{j+1} + \Delta z_n \frac{\partial S_{m,n}^{j+1}}{\partial h_n^{j+1}} + \frac{K_{n-\frac{1}{2}}^{j+\kappa}}{\frac{1}{2}(\Delta z_{n-1} + \Delta z_n)} - \kappa \frac{\partial K_{n-\frac{1}{2}}^{j+\kappa}}{\partial h_n^{j+1}} \left(\frac{h_{n-1}^{j+1} - h_n^{j+1}}{\frac{1}{2}(\Delta z_{n-1} + \Delta z_n)} + 1 \right)$$

Head controlled bottom boundary

$$\frac{\partial F_n}{\partial h_n^{j+1,p}} = \frac{\Delta z_n}{\Delta t^j} C_n^{j+1} + \Delta z_n \frac{\partial S_{m,n}^{j+1}}{\partial h_n^{j+1}} + \frac{K_{n-\frac{1}{2}}^{j+\kappa}}{\frac{1}{2}(\Delta z_{n-1} + \Delta z_n)} + \frac{K_{n+\frac{1}{2}}^{j+\kappa}}{\frac{1}{2}\Delta z_n}$$

$$- \kappa \frac{\partial K_{n-\frac{1}{2}}^{j+\kappa}}{\partial h_n^{j+1}} \left(\frac{h_{n-1}^{j+1} - h_n^{j+1}}{\frac{1}{2}(\Delta z_{n-1} + \Delta z_n)} + 1 \right) + \kappa \frac{\partial K_{n+\frac{1}{2}}^{j+\kappa}}{\partial h_n^{j+1}} \left(\frac{h_n^{j+1} - h_{bot}}{\frac{1}{2}\Delta z_n} + 1 \right)$$

Predefined groundwater levels

$$\frac{\partial F_i}{\partial h_{n^*}^{j+1}} = \frac{\Delta z_i}{\Delta t^j} C_{n^*}^{j+1} + \Delta z_{n^*} \frac{\partial S_{m,n^*}^{j+1}}{\partial h_{n^*}^{j+1}} + \frac{K_{n^*-\frac{1}{2}}^{j+\kappa}}{\frac{1}{2}(\Delta z_{n^*-1} + \Delta z_{n^*})} - \kappa \frac{\partial K_{n^*-\frac{1}{2}}^{j+\kappa}}{\partial h_{n^*}^{j+1}} \left(\frac{h_{n^*-1}^{j+1} - h_{n^*}^{j+1}}{\frac{1}{2}(\Delta z_{n^*-1} + \Delta z_{n^*})} + 1 \right)$$

$$+ \left(\frac{z_{n^*} - z_{n^*+1}}{z_{n^*} - gwl} \right) \frac{K_{n^*+\frac{1}{2}}^{j+\kappa}}{\frac{1}{2}(\Delta z_{n^*} + \Delta z_{n^*+1})} + \kappa \frac{\partial K_{n^*+\frac{1}{2}}^{j+\kappa}}{\partial h_{n^*}^{j+1}} \left(\left(\frac{z_{n^*} - z_{n^*+1}}{z_{n^*} - gwl} \right) \frac{h_{n^*}^{j+1}}{\frac{1}{2}(\Delta z_{n^*} + \Delta z_{n^*+1})} + 1 \right)$$

Cauchy relation for the bottom boundary

$$\frac{\partial F_n}{\partial h_n^{j+1,p}} = \frac{\Delta z_n}{\Delta t^j} C_n^{j+1} + \Delta z_n \frac{\partial S_{m,n}^{j+1}}{\partial h_n^{j+1}} + \frac{K_{n-\frac{1}{2}}^{j+\kappa}}{\frac{1}{2}(\Delta z_{n-1} + \Delta z_n)} + \frac{K_{n+\frac{1}{2}}^{j+\kappa}}{\frac{1}{2}\Delta z_n + cK_{n+\frac{1}{2}}^{j+\kappa}}$$

$$- \kappa \frac{\partial K_{n-\frac{1}{2}}^{j+\kappa}}{\partial h_n^{j+1}} \left(\frac{h_{n-1}^{j+1} - h_n^{j+1}}{\frac{1}{2}(\Delta z_{n-1} + \Delta z_n)} + 1 \right) + \kappa \frac{\partial K_{n+\frac{1}{2}}^{j+\kappa}}{\partial h_n^{j+1}} \frac{1}{2}\Delta z_n \left(\frac{h_n^{j+1} - (\varphi - z_n)}{\left(\frac{1}{2}\Delta z_n + cK_{n+\frac{1}{2}}^{j+\kappa} \right)^2} \right)$$

Seepage face

$$h_n^{j+1} + \frac{1}{2}\Delta z_n < 0 \quad \rightarrow$$

$$\frac{\partial F_1}{\partial h_1^{j+1}} = \frac{\Delta z_1}{\Delta t^j} C_1^{j+1} + \Delta z_1 \frac{\partial S_{m,1}^{j+1}}{\partial h_1^{j+1}} + \frac{K_{1\frac{1}{2}}^{j+\kappa}}{\frac{1}{2}(\Delta z_i + \Delta z_{i+1})} + \kappa \frac{\partial K_{1\frac{1}{2}}^{j+\kappa}}{\partial h_1^{j+1}} \left(\frac{h_1^{j+1} - h_2^{j+1}}{\frac{1}{2}(\Delta z_1 + \Delta z_2)} + 1 \right)$$

$$h_n^{j+1} + \frac{1}{2}\Delta z_n \not< 0 \quad \rightarrow \qquad \frac{\partial F_n}{\partial h_n^{j+1,p}} = \frac{\Delta z_n}{\Delta t^j} C_n^{j+1} + \Delta z_n \frac{\partial S_{m,n}^{j+1}}{\partial h_n^{j+1}} + \frac{K_{n-\frac{1}{2}}^{j+\kappa}}{\frac{1}{2}(\Delta z_{n-1} + \Delta z_n)} + \frac{K_{n+\frac{1}{2}}^{j+\kappa}}{\frac{1}{2}\Delta z_n}$$

$$- \kappa \frac{\partial K_{n-\frac{1}{2}}^{j+\kappa}}{\partial h_n^{j+1}} \left(\frac{h_{n-1}^{j+1} - h_n^{j+1}}{\frac{1}{2}(\Delta z_{n-1} + \Delta z_n)} + 1 \right) + \kappa \frac{\partial K_{n+\frac{1}{2}}^{j+\kappa}}{\partial h_n^{j+1}} \left(\frac{h_n^{j+1}}{\frac{1}{2}\Delta z_n} + 1 \right)$$

Free drainage

$$\frac{\partial F_n}{\partial h_n^{j+1,p}} = \frac{\Delta z_n}{\Delta t^j} C_n^{j+1} + \Delta z_n \frac{\partial S_{m,n}^{j+1}}{\partial h_n^{j+1}} + \frac{K_{n-\frac{1}{2}}^{j+\kappa}}{\frac{1}{2}(\Delta z_{n-1} + \Delta z_n)} + \frac{K_{n+\frac{1}{2}}^{j+1}}{\frac{1}{2}\Delta z_n}$$

$$- \kappa \frac{\partial K_{n-\frac{1}{2}}^{j+\kappa}}{\partial h_n^{j+1}} \left(\frac{h_{n-1}^{j+1} - h_n^{j+1}}{\frac{1}{2}(\Delta z_{n-1} + \Delta z_n)} + 1 \right) + \kappa \frac{\partial K_{n+\frac{1}{2}}^{j+1}}{\partial h_n^{j+1}}$$

The internodal conductivity $K_{n+\frac{1}{2}}^{j+1}$ is in the case of free drainage irrespective the value of κ always treated implicitly

Appendix 5 Implicit linearization of hydraulic conductivities

An implicit linearization of hydraulic conductivities in the numerical elaboration of Eq. () requires expressions for the derivative of the conductivity to the pressure head:

Arithmetic mean:

$$\frac{\partial K_{i-\frac{1}{2}}^{j+\kappa,\kappa\,p}}{\partial h_{i-1}^{j+1,p}} = \frac{1}{2}\frac{\partial K_{i-1}^{j+1,p}}{\partial h_{i-1}^{j+1,p}}$$

$$\frac{\partial K_{i-\frac{1}{2}}^{j+\kappa,\kappa\,p}}{\partial h_{i}^{j+1,p}} = \frac{1}{2}\frac{\partial K_{i}^{j+1,p}}{\partial h_{i}^{j+1,p}}$$

Weighted arithmetic mean:

$$\frac{\partial K_{i-\frac{1}{2}}^{j+\kappa,\kappa\,p}}{\partial h_{i-1}^{j+1,p}} = \frac{\Delta z_{i-1}}{\Delta z_{i-1}+\Delta z_i}\frac{\partial K_{i-1}^{j+1,p}}{\partial h_{i-1}^{j+1,p}}$$

$$\frac{\partial K_{i-\frac{1}{2}}^{j+\kappa,\kappa\,p}}{\partial h_{i}^{j+1,p}} = \frac{\Delta z_{i}}{\Delta z_{i-1}+\Delta z_i}\frac{\partial K_{i}^{j+1,p}}{\partial h_{i}^{j+1,p}}$$

Geometric mean:

$$\frac{\partial K_{i-\frac{1}{2}}^{j+\kappa,\kappa\,p}}{\partial h_{i-1}^{j+1,p}} = \frac{1}{2}\left(\frac{K_i^{j+1,p}}{K_{i-1}^{j+1,p}}\right)^{\frac{1}{2}}\frac{\partial K_{i-1}^{j+1,p}}{\partial h_{i-1}^{j+1,p}}$$

$$\frac{\partial K_{i-\frac{1}{2}}^{j+\kappa\,p}}{\partial h_{i}^{j+1,p}} = \frac{1}{2}\left(\frac{K_{i-1}^{j+1,p}}{K_{i}^{j+1,p}}\right)^{\frac{1}{2}}\frac{\partial K_{i}^{j+1,p}}{\partial h_{i}^{j+1,p}}$$

Weighted geometric mean:

$$\frac{\partial K_{i-\frac{1}{2}}^{j+\kappa,\kappa\,p}}{\partial h_{i-1}^{j+1,p}} = \frac{\Delta z_{i-1}}{\Delta z_{i-1}+\Delta z_i}\left(\frac{K_i^{j+1,p}}{K_{i-1}^{j+1,p}}\right)^{\frac{\Delta z_i}{\Delta z_{i-1}+\Delta z_i}}\frac{\partial K_{i-1}^{j+1,p}}{\partial h_{i-1}^{j+1,p}}$$

$$\frac{\partial K_{i-\frac{1}{2}}^{j+\kappa\,p}}{\partial h_{i}^{j+1,p}} = \frac{\Delta z_{i}}{\Delta z_{i-1}+\Delta z_i}\left(\frac{K_{i-1}^{j+1,p}}{K_{i}^{j+1,p}}\right)^{\frac{\Delta z_{i-1}}{\Delta z_{i-1}+\Delta z_i}}\frac{\partial K_{i}^{j+1,p}}{\partial h_{i}^{j+1,p}}$$

A relation for the conductivity derivative to the pressure head $\partial K/\partial h$ is given by:

$$\frac{\partial K}{\partial h} = \frac{\partial K}{\partial S_e}\frac{\partial S_e}{\partial h}$$

Where:

$$\frac{\partial K}{\partial S_e} = K_{sat} S_e^{\lambda-1} \left[1 - \left(1 - S_e^{\frac{1}{m}} \right)^m \right] \left[\lambda + \left(1 - S_e^{\frac{1}{m}} \right)^{m-1} \left((2+\lambda) S_e^{\frac{1}{m}} - \lambda \right) \right]$$

$$\frac{\partial S_e}{\partial h} = \frac{C}{\theta_{sat} - \theta_{res}}$$

The coefficients of the Jacobian are given by:

$$\frac{\partial F_i}{\partial h_{i-1}^{j+1,p}} = -\frac{K_{i-\frac{1}{2}}^{j+\kappa,\kappa p}}{\frac{1}{2}(\Delta z_{i-1} + \Delta z_i)} - \kappa \frac{\partial K_{i-\frac{1}{2}}^{j+\kappa,\kappa p}}{\partial h_{i-1}^{j+1,p}} \left(\frac{h_{i-1}^{j+1,p} - h_i^{j+1,p}}{\frac{1}{2}(\Delta z_{i-1} + \Delta z_i)} + 1 \right)$$

$$\frac{\partial F_i}{\partial h_i^{j+1,p}} = \frac{\Delta z_i}{\Delta t^j} C_i^{j+1,p} + \Delta z_i \frac{\partial S_{m,i}^{j+1,p}}{\partial h_i^{j+1,p}} + \frac{K_{i-\frac{1}{2}}^{j+\kappa,\kappa p}}{\frac{1}{2}(\Delta z_{i-1} + \Delta z_i)} + \frac{K_{i+\frac{1}{2}}^{j+\kappa,\kappa p}}{\frac{1}{2}(\Delta z_i + \Delta z_{i+1})}$$

$$- \kappa \frac{\partial K_{i-\frac{1}{2}}^{j+\kappa,\kappa p}}{\partial h_i^{j+1,p}} \left(\frac{h_{i-1}^{j+1,p} - h_i^{j+1,p}}{\frac{1}{2}(\Delta z_{i-1} + \Delta z_i)} + 1 \right) + \kappa \frac{\partial K_{i+\frac{1}{2}}^{j+\kappa,\kappa p}}{\partial h_i^{j+1,p}} \left(\frac{h_i^{j+1,p} - h_{i+1}^{j+1,p}}{\frac{1}{2}(\Delta z_i + \Delta z_{i+1})} + 1 \right)$$

$$\frac{\partial F_i}{\partial h_{i+1}^{j+1,p}} = -\frac{K_{i+\frac{1}{2}}^{j+\kappa,\kappa p}}{\frac{1}{2}(\Delta z_i + \Delta z_{i+1})} + \kappa \frac{\partial K_{i+\frac{1}{2}}^{j+\kappa,\kappa p}}{\partial h_{i+1}^{j+1,p}} \left(\frac{h_i^{j+1,p} - h_{i+1}^{j+1,p}}{\frac{1}{2}(\Delta z_i + \Delta z_{i+1})} + 1 \right)$$

Appendix 6 Numerical solution heat flow equation

The discretized form of the heat flow equation as described in Chapter 9, is:

$$C_i^{j+\frac{1}{2}}\left(T_i^{j+1} - T_i^j\right) = \frac{\Delta t^j}{\Delta z_i}\left[\lambda_{i-\frac{1}{2}}^{j+\frac{1}{2}}\frac{T_{i-1}^{j+1} - T_i^{j+1}}{\Delta z_u} - \lambda_{i+\frac{1}{2}}^{j+\frac{1}{2}}\frac{T_i^{j+1} - T_{i+1}^{j+1}}{\Delta z_\ell}\right]$$ *(A6.1)*

where for notational convencience the subscript heat of thermal conductivity λ and soil heat capacity C is omitted. Equation [A6.1] can be rewritten as:

$$-\frac{\Delta t^j}{\Delta z_i \Delta z_u}\lambda_{i-\frac{1}{2}}^{j+\frac{1}{2}}T_{i-1}^{j+1} + \left[C_i^{j+\frac{1}{2}} + \frac{\Delta t^j}{\Delta z_i \Delta z_u}\lambda_{i-\frac{1}{2}}^{j+\frac{1}{2}} + \frac{\Delta t^j}{\Delta z_i \Delta z_\ell}\lambda_{i+\frac{1}{2}}^{j+\frac{1}{2}}\right]T_i^{j+1} - \frac{\Delta t^j}{\Delta z_i \Delta z_\ell}\lambda_{i+\frac{1}{2}}^{j+\frac{1}{2}}T_{i+1}^{j+1} = C_i^{j+\frac{1}{2}}T_i^j$$ *(A6.2)*

Application of Eq. A6.2 to each node results in a tri-diagonal matrix:

$$\begin{bmatrix} \beta_1 & \gamma_1 & & & & \\ \alpha_2 & \beta_2 & \gamma_2 & & & \\ & \alpha_3 & \beta_3 & \gamma_3 & & \\ & & & & & \\ & & & \alpha_{n-1} & \beta_{n-1} & \gamma_{n-1} \\ & & & & \alpha_n & \beta_n \end{bmatrix}\begin{bmatrix} T_1^{j+1} \\ T_2^{j+1} \\ T_3^{j+1} \\ \\ T_{n-1}^{j+1} \\ T_n^{j+1} \end{bmatrix} = \begin{bmatrix} f_1 \\ f_2 \\ f_3 \\ \\ f_{n-1} \\ f_n \end{bmatrix}$$ *(A6.3)*

where n is the number of nodal points. Next the coefficients α_i, β_i, γ_i, and f_i are explained for the intermediate nodes and for the top and bottom node.

Intermediate nodes

From Eq. [A6.2] and Eq. [A6.3] we may derive the coefficients:

$$\alpha_i = -\frac{\Delta t^j}{\Delta z_i \Delta z_u} \lambda_{i-\frac{1}{2}}^{j+\frac{1}{2}} \tag{A6.4}$$

$$\beta_i = C_i^{j+\frac{1}{2}} + \frac{\Delta t^j}{\Delta z_i \Delta z_u} \lambda_{i-\frac{1}{2}}^{j+\frac{1}{2}} + \frac{\Delta t^j}{\Delta z_i \Delta z_\ell} \lambda_{i+\frac{1}{2}}^{j+\frac{1}{2}} \tag{A6.5}$$

$$\gamma_i = -\frac{\Delta t^j}{\Delta z_i \Delta z_\ell} \lambda_{i+\frac{1}{2}}^{j+\frac{1}{2}} \tag{A6.6}$$

$$f_i = C_i^{j+\frac{1}{2}} T_i^j \tag{A6.7}$$

Top node

The temperature at soil surface is set equal to the daily average air temperature, T_{avg}. Therefore, in case of the top node, Eq. [A6.1] transforms to:

$$C_1^{j+\frac{1}{2}}\left(T_1^{j+1} - T_1^j\right) = \frac{\Delta t^j}{\Delta z_1}\left[\lambda_{\frac{1}{2}}^{j+\frac{1}{2}}\frac{T_{avg} - T_1^{j+1}}{\Delta z_u} - \lambda_{1\frac{1}{2}}^{j+\frac{1}{2}}\frac{T_1^{j+1} - T_2^{j+1}}{\Delta z_\ell}\right] \tag{A6.8}$$

which can be written as:

$$\left[C_1^{j+\frac{1}{2}} + \frac{\Delta t^j}{\Delta z_1 \Delta z_u}\lambda_{\frac{1}{2}}^{j+\frac{1}{2}} + \frac{\Delta t^j}{\Delta z_1 \Delta z_\ell}\lambda_{1\frac{1}{2}}^{j+\frac{1}{2}}\right]T_1^{j+1} - \frac{\Delta t^j}{\Delta z_1 \Delta z_\ell}\lambda_{1\frac{1}{2}}^{j+\frac{1}{2}}T_2^{j+1} = C_1^{j+\frac{1}{2}}T_1^j + \frac{\Delta t^j}{\Delta z_1 \Delta z_u}\lambda_{\frac{1}{2}}^{j+\frac{1}{2}}T_{avg} \tag{A6.9}$$

Combination of Eq. [A6.9] and [A6.3] gives the following coefficients:

$$\beta_1 = C_1^{j+\frac{1}{2}} + \frac{\Delta t^j}{\Delta z_1 \Delta z_u}\lambda_{\frac{1}{2}}^{j+\frac{1}{2}} + \frac{\Delta t^j}{\Delta z_1 \Delta z_\ell}\lambda_{1\frac{1}{2}}^{j+\frac{1}{2}} \tag{A6.10}$$

$$\gamma_1 = -\frac{\Delta t^j}{\Delta z_1 \Delta z_\ell}\lambda_{1\frac{1}{2}}^{j+\frac{1}{2}} \tag{A6.11}$$

$$f_1 = C_1^{j+\frac{1}{2}}T_1^j + \frac{\Delta t^j}{\Delta z_1 \Delta z_u}\lambda_{\frac{1}{2}}^{j+\frac{1}{2}}T_{avg} \tag{A6.12}$$

Bottom node

SWAP adopts a heat flow rate qheat,bot (J cm^{-2} d^{-1}) at the bottom of the soil profile. At the bottom node, the general heat flow equation, Eq. [A6.1], transforms to:

$$C_n^{j+\frac{1}{2}}\left(T_n^{j+1}-T_n^j\right)=\frac{\Delta t^j}{\Delta z_n}\left[\lambda_{n-\frac{1}{2}}^{j+\frac{1}{2}}\frac{T_{n-1}^{j+1}-T_n^{j+1}}{\Delta z_u}-q_{\text{heat,bot}}\right]\tag{A6.13}$$

which can be written as:

$$-\frac{\Delta t^j}{\Delta z_n\Delta z_u}\lambda_{n-\frac{1}{2}}^{j+\frac{1}{2}}T_{n-1}^{j+1}+\left[C_n^{j+\frac{1}{2}}+\frac{\Delta t^j}{\Delta z_n\Delta z_u}\lambda_{n-\frac{1}{2}}^{j+\frac{1}{2}}\right]T_n^{j+1}=C_n^{j+\frac{1}{2}}T_n^j+\frac{\Delta t^j}{\Delta z_n}q_{\text{heat,bot}}\tag{A6.14}$$

Combination of Eq. [A6.14] and [A6.3] gives the following coefficients:

$$\alpha_n=-\frac{\Delta t^j}{\Delta z_n\Delta z_u}\lambda_{n-\frac{1}{2}}^{j+\frac{1}{2}}\tag{A6.15}$$

$$\beta_n=C_n^{j+\frac{1}{2}}+\frac{\Delta t^j}{\Delta z_n\Delta z_u}\lambda_{n-\frac{1}{2}}^{j+\frac{1}{2}}\tag{A6.16}$$

$$f_n=C_n^{j+\frac{1}{2}}T_n^j-\frac{\Delta t^j}{\Delta z_n}q_{\text{heat,bot}}\tag{A6.17}$$

In case of prescribed temperature Tbot at the soil profile bottom, Eq. [A6.1], transforms to:

$$C_n^{j+\frac{1}{2}}\left(T_n^{j+1}-T_n^j\right)=\frac{\Delta t^j}{\Delta z_n}\left[\lambda_{n-\frac{1}{2}}^{j+\frac{1}{2}}\frac{T_{n-1}^{j+1}-T_n^{j+1}}{\Delta z_u}-\lambda_{n+\frac{1}{2}}^{j+\frac{1}{2}}\frac{T_n^{j+1}-T_{bot}}{\Delta z_\ell}\right]\tag{A6.18}$$

which can be written as:

$$-\frac{\Delta t^j}{\Delta z_n\Delta z_u}\lambda_{n-\frac{1}{2}}^{j+\frac{1}{2}}T_{n-1}^{j+1}+\left[C_n^{j+\frac{1}{2}}+\frac{\Delta t^j}{\Delta z_n\Delta z_u}\lambda_{n-\frac{1}{2}}^{j+\frac{1}{2}}+\frac{\Delta t^j}{\Delta z_n\Delta z_\ell}\lambda_{n+\frac{1}{2}}^{j+\frac{1}{2}}\right]T_n^{j+1}=C_n^{j+\frac{1}{2}}T_n^j+\frac{\Delta t^j}{\Delta z_n\Delta z_\ell}\lambda_{n+\frac{1}{2}}^{j+\frac{1}{2}}T_{\text{bot}}\tag{A6.19}$$

Combination of Eq. [A6.19] and [A6.3] gives the following coefficients:

$$\alpha_n=-\frac{\Delta t^j}{\Delta z_n\Delta z_u}\lambda_{n-\frac{1}{2}}^{j+\frac{1}{2}}\tag{A6.20}$$

$$\beta_n=C_n^{j+\frac{1}{2}}+\frac{\Delta t^j}{\Delta z_n\Delta z_u}\lambda_{n-\frac{1}{2}}^{j+\frac{1}{2}}+\frac{\Delta t^j}{\Delta z_n\Delta z_\ell}\lambda_{n+\frac{1}{2}}^{j+\frac{1}{2}}\tag{A6.21}$$

$$f_n=C_n^{j+\frac{1}{2}}T_n^j+\frac{\Delta t^j}{\Delta z_n\Delta z_\ell}\lambda_{n+\frac{1}{2}}^{j+\frac{1}{2}}T_{\text{bot}}\tag{A6.12}$$

Appendix 7 Parameters of soil hydraulic functions: Staring series

After Wösten et al. (2001)

TOP-SOILS	Dutch nomenclature	Clay-Silt (50-µm) (%)	Clay (<2µm) (%)	Organic matter (%)	M50 (µm)	Dry bulk density (g cm⁻³)
Sand	*Zand*					
B1	Leemarm, zeer fijn tot matig fijn zand	4-10		1-4	140-170	1.4-1.7
B2	Sterk lemig, zeer fijn tot matig fijn zand	11-18		1-10	125-175	1.2-1.6
B3	Sterk lemig, zeer fijn tot matig fijn zand	18-29		3-13	105-165	1.1-1.5
B4	Zeer sterk lemig, zeer fijn tot matig fijn zand	30-50		2-5	118-160	1.1-1.5
B5	Grof zand			1-3	350-500	1.3-1.6
B6	Keileem	5-39		1-8	150-400	1.1-1.6
Loam	*Zavel*					
B7	Zeer lichte zavel		10-12	1-6		1.2-1.8
B8	Matig lichte zavel		12-16	0-4		1.2-1.6
B9	Zware zavel		18-25	1-8		1.2-1.6
Clay	*Klei*					
B10	Lichte klei		26-35	1-6		1.1-1.6
B11	Matig zware klei		35-50	3-15		0.9-1.7
B12	Zeer zware klei		51-77	3-5		0.9-1.3
Silt	*Leem*					
B13	Zandige leem	60-75		1-8		1.0-1.6
B14	Siltige leem	85-95		0-6		1.1-1.6
Peat	*Moerig*					
B15	Venig zand		2-6	15-22		1.0-1.3
B16	Zandig veen en veen		1-7	28-80		0.2-1.0
B17	Venige klei		30-80	20-30		0.9-1.2
B18	Kleiig veen		10-80	30-65		0.4-0.8

SUB-SOILS	Dutch nomenclature					
Sand	*Zand*					
O1	Leemarm, zeer fijn tot matig fijn zand	1-10		0-3	105-205	1.4-1.8
O2	Zwak lemig, zeer fijn tot matig fijn zand	10-16		1-3	105-175	1.4-1.7
O3	Sterk lemig, zeer fijn tot matig fijn zand	20-32		0-2	114-172	1.4-1.8
O4	Zeer sterk lemig, zeer fijn tot matig fijn zand	36-47		0-2	128-170	1.4-1.7
O5	Grof zand			0-2	220-400	1.5-1.7
O6	Keileem	5-40		1-7	150-400	1.1-1.6
O7	Beekleem	35-45		1-3	100-140	1.0-1.7
Loam	*Zavel*					
O8	Zeer lichte zavel		8-11	0-2		1.4-1.6
O9	Matig lichte zavel		12-17	0-2		1.3-1.7
O10	Zware zavel		18-22	0-3		1.3-1.5
Clay	*Klei*					
O11	Lichte klei		28-33	1-3		1.3-1.6
O12	Matig zware klei		35-48	0-3		1.0-1.5
O13	Zeer zware klei		50-77	0-3		1.0-1.4
Silt	*Leem*					
O14	Zandige leem	60-75		0-2		1.0-1.6
O15	Siltige leem	85-92		1-3		1.1-1.6
Peat	*Veen*					
O16	Oligotroof veen			40-96		0.1-0.7
O17	Mesotroof en eutroof veen			60-80		0.1-0.6
O18	Moerige tussenlaag			15-30		0.8-1.4

TOP-SOILS	θ_{res} (cm³ cm⁻³)	θ_{sat} (cm³ cm⁻³)	K_{sat} (cm d⁻¹)	α (cm⁻¹)	λ (-)	n[1] (-)
Sand						
B1	0.02	0.43	23.41	0.0234	-0.000	1.801
B2	0.02	0.42	12.52	0.0276	-1.060	1.491
B3	0.02	0.46	15.42	0.0144	-0.215	1.534
B4	0.02	0.46	29.22	0.0156	0.000	1.406
B5	0.01	0.36	52.91	0.0452	-0.359	1.933
B6	0.01	0.38	100.69	0.0222	-1.747	1.238
Loam						
B7	0.00	0.40	14.07	0.0194	-0.802	1.250
B8	0.01	0.43	2.36	0.0099	-2.244	1.288
B9	0.00	0.43	1.54	0.0065	-2.161	1.325
Clay						
B10	0.01	0.43	1.70	0.0064	-3.884	1.210
B11	0.01	0.59	4.53	0.0195	-5.901	1.109
B12	0.01	0.54	5.37	0.0239	-5.681	1.094
Silt						
B13	0.01	0.42	12.98	0.0084	-1.497	1.441
B14	0.01	0.42	0.80	0.0051	0.000	1.305
Peat						
B15	0.01	0.53	81.28	0.0242	-1.476	1.280
B16	0.01	0.80	6.79	0.0176	-2.259	1.293
B17	0.00	0.72	4.46	0.0180	-0.350	1.140
B18	0.00	0.77	6.67	0.0197	-1.845	1.154

SUB-SOILS	θ_{res} (cm³ cm⁻³)	θ_{sat} (cm³ cm⁻³)	K_{sat} (cm d⁻¹)	α (cm⁻¹)	λ (-)	n (-)
Sand						
O1	0.01	0.36	15.22	0.0224	0.000	2.286
O2	0.02	0.38	12.68	0.0213	0.168	1.951
O3	0.01	0.34	10.87	0.0170	0.000	1.717
O4	0.01	0.35	9.86	0.0155	0.000	1.525
O5	0.01	0.32	25.00	0.0521	0.000	2.374
O6	0.01	0.33	33.92	0.0162	-1.330	1.311
O7	0.01	0.51	39.10	0.0123	-2.023	1.152
Loam						
O8	0.00	0.47	9.08	0.0136	-0.803	1.342
O9	0.00	0.46	2.23	0.0094	-1.382	1.400
O10	0.01	0.48	2.12	0.0097	-1.879	1.257
Clay						
O11	0.00	0.42	13.79	0.0191	-1.384	1.152
O12	0.00	0.56	1.02	0.0095	-4.295	1.158
O13	0.00	0.57	4.37	0.0194	-5.955	1.089
Silt						
O14	0.01	0.38	1.51	0.0030	-0.292	1.728
O15	0.01	0.41	3.70	0.0071	0.912	1.298
Peat						
O16	0.00	0.89	1.07	0.0103	-1.411	1.376
O17	0.01	0.86	2.93	0.0123	-1.592	1.276
O18	0.01	0.57	43.45	0.0138	-1.204	1.323

[1] The parameters of the Mualem - van Genuchten model are explained in Chapter 2

Appendix 8 Critical pressure head values for root water extraction

After Taylor and Ashcroft (1972)

Crop	h_{3h}	h_{3l}	Crop	h_{3h}	h_{3l}
Vegetative crops			Deciduous fruit	-500	-800
Alfalfa	-1500	-1500	Avocadoes	-500	-500
Beans (snap and lima)	-750	-2000	Grapes		
Cabbage	-600	-700	early season	-400	-500
Canning peas	-300	-500	during maturity	-1000	-1000
Celery	-200	-300	Strawberries	-200	-300
Grass	-300	-1000	Cantaloupe	-350	-450
Lettuce	-400	-600	Tomatoes	-800	-1500
Tobacco	-300	-800	Bananas	-300	-1500
Sugar cane					
tensiometer	-150	-500	***Grain crops***		
blocks	-1000	-2000	Corn		
Sweet corn	-500	-1000	vegetative period	-500	-500
Turfgrass	-240	-360	during ripening	-8000	-12000
			Small grains		
Root crops			vegetative period	-400	-500
Onions			during ripening	-8000	-12000
early growth	-450	-550			
bulbing time	-550	-650	***Seed crops***		
Sugar beets	-400	-600	Alfalfa		
Potatoes	-300	-500	prior to bloom	-2000	-2000
Carrots	-550	-650	during bloom	-4000	-8000
Broccoli			during ripening	-8000	-15000
early	-450	-550	Carrots		
after budding	-600	-700	at 60 cm depth	-4000	-6000
Cauliflower	-600	-700	Onions		
			at 7 cm depth	-4000	-6000
Fruit crops			at 15 cm depth	-1500	-1500
Lemons	-400	-400	Lettuce		
Oranges	-200	-1000	during productive phase	-3000	-3000

Appendix 9 Salt tolerance data

After Maas (1990) [2]

Crop common name	Crop botanical name	ECmax [3] (dS m^{-1})	ECslope (% per dS m^{-1})	Rating [4]	Ref. [5]
Fiber and grain crops					
Barley [6]	Hordeum vulgare	8.0	5.0	T	1
Bean	Phaseolus vulgaris	1.0	19.0	S	1
Corn	Zea mays	1.7	12.0	MS	1
Cotton	Gossypium hirsutum	7.7	5.2	T	1
Peanut	Arachis hypogaea	3.2	29.0	MS	1
Rice (paddy)	Oryza sativa	3.0	12.0	S	1
Rye	Secale cereale	11.4	10.8	T	2
Sorghum	Sorghum bicolor	6.8	16.0	MT	2
Soybean	Glycine max	5.0	20.0	MT	1
Sugar beet [7]	Beta vulgaris	7.0	5.9	T	1
Sugar cane	Sacharum officinarum	1.7	5.9	MS	1
Wheat	Triticum aestivum	6.0	7.1	MT	1
Wheat, durum	Triticum turgidum	5.9	3.8	T	2
Grasses and forage crops					
Alfalfa	Medicago sativa	2.0	7.3	MS	1
Barley (forage) [e]	Hordeum vulgare	6.0	7.1	MT	1
Bermuda grass [8]	Cynodon dactylon	6.9	6.4	T	1
Clover, ladino	Trifolium repens	1.5	12.0	MS	1
Corn (forage)	Zea mays	1.8	7.4	MS	1
Cowpea (forage)	Vigna unguiculata	2.5	11.0	MS	3
Ryegrass, perennial	Lolium perenne	5.6	7.6	MT	1
Sundan grass	Sorghum sudanese	2.8	4.3	MT	1
Wheat (forage) [9]	Triticum aestivum	4.5	2.6	MT	2
Wheat, durum (forage)	Triticum turgidum	2.1	2.5	MT	2
Vegetables and fruit crops					
Bean	Phaseolus vulgaris	1.0	19.0	S	1
Beet, red [f]	Beta vulgaris	4.0	9.0	MT	1
Broccoli	Brassica oleracea botrytis	2.8	9.2	MS	1
Cabbage	Brassica oleracea capitata	1.8	9.7	MS	1
Carrot	Daucus carota	1.0	14.0	S	1
Corn, sweet	Zea mays	1.7	12.0	MS	1
Cucumber	Cucumis sativus	2.5	13.0	MS	1
Lettuce	Lactuca sativa	1.3	13.0	MS	1
Onion	Allium cepa	1.2	16.0	S	1
Potato	Solanum tuberosum	1.7	12.0	MS	1
Spinach	Spinacia oleracea	2.0	7.6	MS	1
Tomato	Lycopersicon lycopersicum	2.5	9.9	MS	1

---

[2] These data serve only as a guideline to relative tolerances among crops. Absolute tolerances vary, depending on climate, soil conditions and cultural practices

[3] In gypsiferous soils, plants will tolerate ECe values about 2 dS/m higher than indicated

[4] Ratings according to Maas (1990): S sensitive, MS moderately sensitive, MT moderately tolerant, and T tolerant

[5] References: 1 Maas and Hoffman (1977), 2 Francois et al. (1986), 3 West and Francois (1982)

[6] Less tolerant during seedling stage, ECe at this stage should not exceed 4 dS/m or 5 dS/m

[7] Sensitive during germination and emergence, ECe should not exceed 3 dS/m

[8] Average of several varieties. Suwannee and Coastal are about 20% more tolerant, and common and Greenfield are about 20% less tolerant than the average

[9] Data from one cultivar, 'Pobred'.

Appendix 10 Shrinkage characteristic data

After Bronswijk and Vermeer (1990)

Place [1]	Depth cm	Horizon -	ρ_s [2] g cm⁻³	CaCO$_3$	H [3]	<2	2-16	16-50	>50 µm	e_0 -	ν_1 -	ν_s -
				weight % of soil		weight % of mineral parts				Shrinkage par.		
1	0- 22	A11	2.52	0.0	10.3	39.9	20.9	33.4	5.8	0.45	1.0	0.0
	22-42	ACg	2.60	0.0	6.9	40.7	25.9	28.3	5.1	0.37	0.6	0.0
	42-78	C1g	2.66	2.5	4.5	58.1	24.7	16.2	1.1	0.43	0.7	0.0
	78-120	C2g	2.68	6.9	2.2	24.1	14.3	53.5	8.1	0.56	0.7	0.0
2	0- 26	Ap	2.64	1.4	4.8	45.4	27.8	16.6	10.2	0.52	0.8	0.2
	26-34	A12	2.61	0.8	3.9	45.9	27.4	18.9	6.8	0.46	0.9	0.0
	34-56	C11g	2.62	1.7	2.2	51.6	29.2	15.4	3.8	0.48	0.9	0.1
	56-75	C12g	2.68	3.3	1.9	39.1	24.1	32.8	4.0	0.50	0.9	0.1
	75-107	C13g	2.69	0.3	3.0	59.3	31.7	6.9	2.1	0.50	0.9	0.05
3	0- 29	Ap	2.65	9.0	3.3	52.0	24.2	20.4	3.4	0.49	0.7	0.2
	29-40	AC	2.67	10.6	2.9	62.9	17.0	17.7	2.4	0.50	0.8	0.2
	40-63	C21	2.69	11.3	2.7	52.4	25.3	18.3	4.0	0.55	0.8	0.1
	63-80	C22g	2.66	9.8	2.8	55.8	24.1	16.7	3.4	0.58	1.0	0.1
	80-100	C23g	2.69	11.6	2.2	59.6	26.4	12.2	1.8	0.57	1.0	0.1
4	0- 21	A11	2.59	11.7	5.9	34.8	17.9	27.9	19.5	0.52	1.0	0.0
	21-52	A12	2.61	11.1	6.2	42.9	22.1	26.5	8.5	0.53	0.9	0.0
	52-77	C21g	2.62	17.6	3.7	32.1	20.4	33.2	14.2	0.82	1.2	0.0
	77-100	C22g	2.63	18.8	3.1	16.2	10.1	37.8	36.0	0.79	1.0	0.0
5	0- 22	Ap1	2.66	9.9	2.6	36.8	22.2	27.5	13.5	0.48	0.8	0.0
	22-38	A12	2.66	8.1	2.2	45.6	27.2	22.9	4.3	0.56	0.8	0.0
	38-60	C22g	2.63	6.6	7.6	35.3	43.9	19.7	1.1	0.68	1.2	0.1
	60-90	C23g	2.59	5.8	7.0	15.9	23.9	58.2	2.0	1.10	2.0	0.0
	90-110	C24g	2.57	4.6	10.5	20.2	27.2	51.2	1.4	1.10	2.1	0.0
6	0- 18	A11	2.52	0.0	9.9	58.1	30.7	10.2	1.0	0.30	0.9	0.0
	18-30	A12	2.60	0.0	7.5	55.8	35.5	8.1	0.6	0.34	0.9	0.0
	30-58	C11g	2.64	0.0	3.7	59.6	29.5	10.1	0.8	0.37	0.5	0.0
	58-85	C12g	2.59	0.0	3.8	51.7	37.0	9.6	1.7	0.40	0.8	0.05
7	0- 35	Ap	2.67	10.2	2.1	30.8	15.7	30.2	23.3	0.43	1.0	0.0
	35-60	C21g	2.67	13.6	1.6	46.4	20.5	21.2	11.9	0.45	0.8	0.0
	60-80	C22g	2.70	15.7	1.3	41.9	18.3	23.3	15.5	0.40	1.3	0.0
	80-95	C23g	2.69	9.5	0.3	16.2	6.7	21.0	56.1	0.40	1.3	0.0

(1) Locations: 1-Oosterend, 2-Nieuw Beerta, 3-Nieuw Statenzijl, 4-Schermerhorn, 5-Dronten, 6-Bruchem and 7-Kats.
(2) Density of the solid phase
(3) Organic matter

Appendix 11 Examples of shrinkage characteristics of peat

Shrinkage characteristics of peat and peaty soils (after Hendriks, 2004). Black dots are measurements and lines are fits with Eq. (6.19). Parameter values concern parameters of Eq. (6.19).

Z-60

$\vartheta_s = 9.4$
$\vartheta_a = 8.4$
$e_0 = 2.2$
$\alpha = 0.60$
$\beta = 3.90$
$P = 0.79$

D-80

$\vartheta_s = 11.2$
$\vartheta_a = 10.8$
$e_0 = 2.2$
$\alpha = 0.50$
$\beta = 2.60$
$P = 0.48$

Z-80

$\vartheta_s = 12.0$
$\vartheta_a = 10.7$
$e_0 = 1.7$
$\alpha = 0.42$
$\beta = 3.13$
$P = 0.55$

N-80

$\vartheta_s = 13.5$
$\vartheta_a = 12.4$
$e_0 = 1.2$
$\alpha = 0.40$
$\beta = 2.50$
$P = 0.41$

A-45

$\vartheta_s = 12.6$
$\vartheta_a = 12.1$
$e_0 = 2.5$
$\alpha = 0.90$
$\beta = 4.50$
$P = 0.55$

A-25

$\vartheta_s = 7.3$
$\vartheta_a = 6.6$
$e_0 = 0.5$
$\alpha = 0.80$
$\beta = 1.78$
$P = 0.06$

Z-10

$\vartheta_s = 3.04$
$\vartheta_a = 2.67$
$e_0 = 0.36$
$\alpha = 0.90$
$\beta = 4.00$
$P = 0.29$

A-15

$\vartheta_s = 2.33$
$\vartheta_a = 2.21$
$e_0 = 0.52$
$\alpha = 0.70$
$\beta = 3.73$
$P = -0.13$

V-10

$\vartheta_s = 1.80$
$\vartheta_a = 1.62$
$e_0 = 1.10$
$\alpha = 1.00$
$\beta = 1.90$
$P = -0.07$
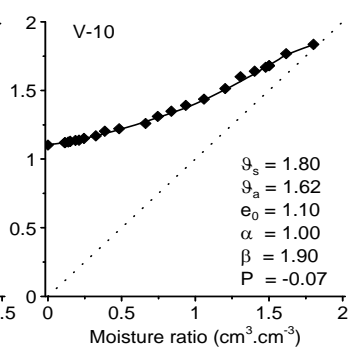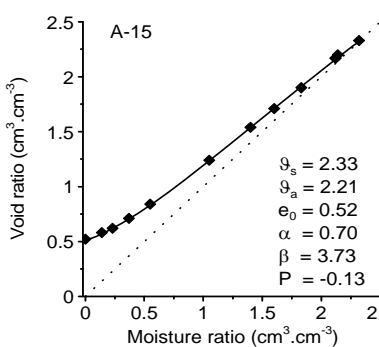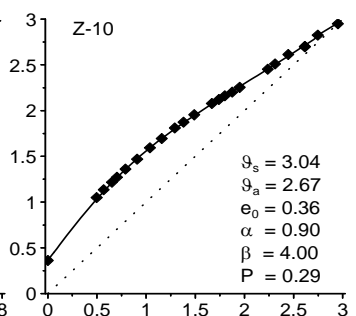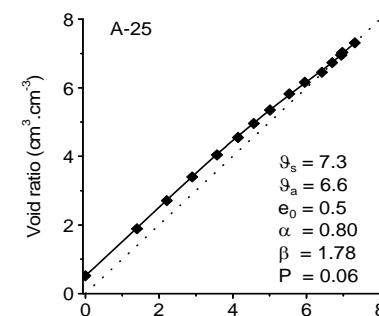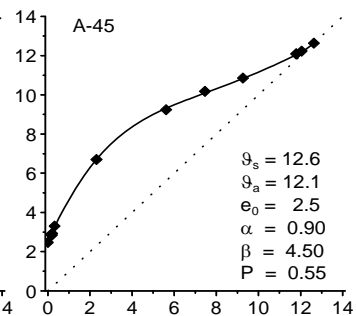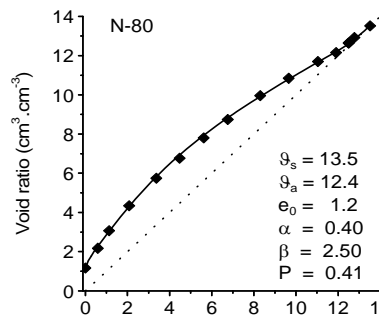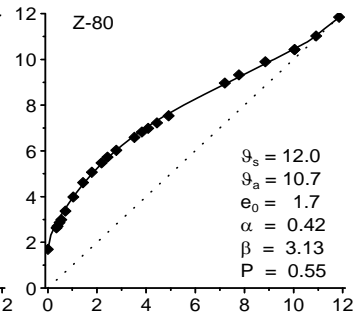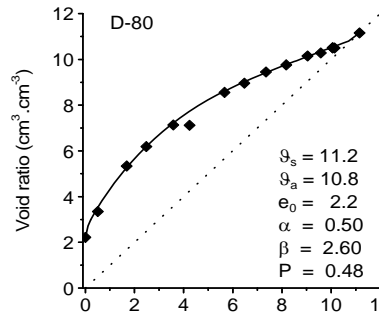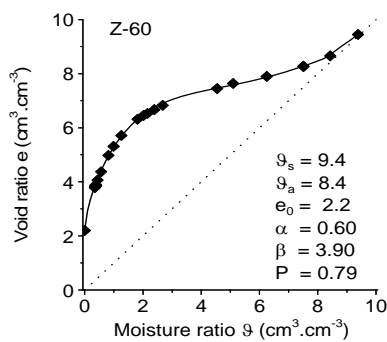
Description, organic matter and clay content (mass-%) of the peat soils. Figures in sample codes refer tot sample depths in cm.

Sample code	Soil description	Org. matter	Clay
A-15	peaty clay	33	40
A-25	clayey peat	62	21
A-45	sphagnum peat	93	1
D-80	wood peat	81	5
N-80	sphagnum peat	91	2
V-10	peaty, sandy clay	18	17
Z-10	clayey peat	48	36
Z-60	wood peat	82	4
Z-80	wood peat	83	4

Appendix 12 List of input array lengths

The array lengths of input data are defined as parameters in the Fortran file 'param.fi'. The array lengths can be enlarged by adjusting the values in 'param.fi' en recompilation of the Fortran code. In the internet version of WAP we did define the array lengths as listed in the Table below.

Code	Description	Array length
MAYRS	number of years in the simulation period	70
MAXDAT	number of days in the simulation period	MAYRS*366
MACROP	number of crops	200
MACP	number of compartments	500
MADR	number of drainage systems	5
MAHO	number of horizons	200
MABBC	number of time-dependent values for bottom boundary	10*366
MASCALE	number of scaling factors	100
MRAIN	number of rainfall records in case of detailed rainfall	40000
MAIRG	number of applied irrigations	10000
MAOUT	number of specified output dates	3000
MAOWL	number of open water levels (basic drainage routine)	10*366
MAWLP	number of open water levels in primary system	10*366
MAWLS	number of open water levels in secondary system	10*366
MAMP	number of surface water management periods	10*366
MADM	number of macropore domains	20
MASTEQ	number of static equilibrium relations	10000
NMETFILE	number of weather records in one year (48 per day)	17568

Appendix 13 List of main SWAP subroutines

Assim	gross CO2 assimilation rate of the crop
Bocodrb	calculate lateral drainage rate and state variables
Bocodre	calculate lateral drainage rate and state variables, including surface water system
Boundbottom	calculate lower boundary conditions
Boundtop	calculate top boundary conditions
CalcGwl	search for groundwater levels
CalcGrid	converts vertical discretization
CropFixed	prescribed crop growth
Drainage	lateral drainage
DeVries	calculate soil thermal properties
DivDra	divide drainage flux to compartments
Fluxes	calculate bottom and compartment fluxes
Grass	detailed grass growth routine
HConduc	calculate hydraulic conductivity from water content
HeadCalc	calculate pressure heads at next time
Hysteresis	check hysteretic reversal and update scanning curve
Integral	integrate intermediate and cumulative water fluxes
Irrigation	initialize and calculate irrigation
MacroPore	calculate crack shrinkage and swelling, including fluxes
MeteoInput	read meteorological data and return values of actual day
MoisCap	calculate moisture capacity from pressure head
NoCrop	specify crop characteristics for bare soil
OutAfo	formatted hydrological output for ANIMO/PESTLA (*.AFO)
OutAun	unformatted hydrological output for ANIMO/PESTLA (*.AUN)
OutBal	write overview balances (*.BAL)
OutBlc	write total water balances (*.BLC)
OutDrf	write drainage fluxes, runoff, etc. (*.DRF)
OutEnd	write final soil state variables for next initial condition
OutInc	write water balance increments (*.INC)
OutSba	write solute balance (*.SBA)
OutSwb	write surface water balance (*.SWB)
OutTem	write soil temperatures (*.TEM)
OutVap	write water and solute profile data (*.VAP)
OutWba	write water balance (*.WBA)
Penmon	calculate potential evaporation and transpiration rates
Ponding	calculation of runoff
PrHead	calculate pressure head from water content
Radiat	calculate fluxes of diffuse and PAR radiation
ReadSwap	read SWAP main input file
ReducEva	calculate actual soil evaporation
RootExtraction	calculate potential and actual water extraction by roots
Snow	snow submodel
SoilWater	calculate soil water rate/state variables
Solute	calculate solute transport
SurfaceWater	calculate rate/state variables of surface water system
Temperature	calculate soil temperatures
TimeControl	handles time variables, switches and flags
Totass	calculate daily total gross assimilation
Warn	output of warnings to screen and log file
WatCon	calculate water content from pressure head
WatStor	calculate water storage in soil profile and cracks

Wofost   detailed crop growth routine
WriteHead   write header with model version, project name, etc.

Appendix 14 Description of output files *.afo and *.aun

This annex describes the content of the output files with extension *.afo and *.aun. The content of both files is identic; they only differ in format: one file is binary and unformatted (*.aun) and the other file is formatted (*.afo). The description given in this annex uses the following symbols:

– Unit   = units as applied in these output files; units differ from those applied in Swap !
– R   = data are written to a new record;
– DT   = data type; R means Real*4, I means Integer*2;
– Mnemonic = the name of the variable as applied in the source code of Swap

Description of variable	Unit	Range	R	DT	Mnemonic
Time domain					
Year when hydrological simulation started	-	[1. .∞>	*	I	bruny
Year when hydrological simulation ended	-	[bruny..∞>	-	I	eruny
Time (Julian daynumber) when hydrological simulation started (Minimum); will be 0.0 when simulation started at 1st of January, 00.00 hour.	-	[0.0..366]	-	R	brund-1
Time (Julian daynumber) when hydrological simulation ended (Maximum)	-	[0.0..366]	-	R	erund
Step size of time-interval for dynamic hydrological data	d	[1.0..30.0]	-	R	period
Geometry of model system					
Number of model compartments	-	[1.numnod]	*	I	numnod
Number of horizons	-	[1 ..numlay	-	I	numlay
Number of drainage systems (value must be 0, 1, 2, 3, 4 or 5)	-	[0,1,2,3,4,5]	-	I	nrlevs
The following 4 variables (botcom – thetawp) are given for the horizons 1 – numlay:					
Compartment number of the deepest compartment (bottom) of each horizon/layer	-	[1..numnod]	*	I	botcom(numlay)
Volume fraction moisture at Saturation	m³ m⁻³	[0.0 .. 1.0]	*	R	thetas (numlay)
Volume fraction moisture at Field Capacity	m³ m⁻³	[0.0 .. 1.0]	*	R	thetafc(numlay)
Volume fraction moisture at Wilting point	m³ m⁻³	[0.0 .. 1.0]	*	R	thetawp(numlay)
The following variable dz is given for the compartments 1 – numnod Thickness of compartments	m	[0.001..100]	*	R	dz(numnod)

Description of variable	Unit	Range	R	DT	Mnemonic
Initial conditions					
The following variable theta is given for the compartments 1 – numnod					
Volume fraction moisture inItially present in compartments 1 – NUMNOD	m³ m⁻³	[0.0 .. 1.0]	*	R	theta(numnod)
InItial groundWAterlevel	m-surface	[0.0..∞>	*	R	gwl
Storage by inItial ponding (m+surface)	m+surface	[0.0..∞>	-	R	pond
Dynamic part					
Time (Julian daynumber) in hydrological model	-	[0.0..∞>	*	R	tcum
Precipitation (**incl. irrigation**) water flux	m d⁻¹	[0.0..∞>	-	R	iprec
Evaporation flux by interception	m d⁻¹	[0.0..∞>	-	R	iintc
Actual evaporation flux by bare soil	m d⁻¹	[0.0..∞>	-	R	ievap
Evaporation flux by ponding	m d⁻¹	[0.0]	-	R	0.0
Potential evaporation flux by soil	m d⁻¹	[0.0..∞>	-	R	ipeva
Potential transpiration flux	m d⁻¹	[0.0..∞>	-	R	iptra
Flux of surface RUnoff	m d⁻¹	[0.0..∞>	-	R	iruno
GroundwAter level at end of time-interval	m-surface	[0.0..∞>	-	R	gwl
Storage by ponding at soil surface at end of time-interval	m+surface	[0.0..∞>	-	R	pond

The variables h - inqdra are given for the compartments 1 - numnod, with one exception for inq, which is given for the compartments 1 – numnod+1

Description of variable	Unit	Range	R	DT	Mnemonic
Suction (pressure head) of soil moisture (negative when unsaturated)	cm	<-∞..+∞>	*	R	h(numnod)
Volume fraction of moisture at end of time-interval	m³ m⁻³	[0.0 .. 1.0]	*	R	theta(numnod)
Actual transpiration flux	m d⁻¹	[0.0..∞>	*	R	inqrot(numnod)
Flux incoming from above (compartments 1 – numnod+1, downward=positive)	m d⁻¹	[0.0..∞>	*	R	inq(numnod+1)

The presence of values for variables inqdra1-inqdra5 is determined by the variable nrlevs. The value of nrlevs determines the number of drainage systems for which flux densities must be given.

Description of variable	Unit	Range	R	DT	Mnemonic
Flux of drainage system of 1st order (e.g. canal)	m d⁻¹	[0.0..∞>	*	R	inqdra(1,numnod)
Flux of drainage system of 2nd order (e.g. ditch)	m d⁻¹	[0.0..∞>	*	R	inqdra(2,numnod)
Flux of drainage system of 3rd order (e.g. trench)	m d⁻¹	[0.0..∞>	*	R	inqdra(3,numnod)
Flux of drainage system of 4th order (e.g. tube drain)	m d⁻¹	[0.0..∞>	*	R	inqdra(4,numnod)
Flux of drainage system of 5th order (e.g. rapid drainage)	m d⁻¹	[0.0..∞>	*	R	inqdra(5,numnod)

Appendix 15 Description of output files *.bfo and *.bun

This annex describes the content of the output files with extension *.bfo and *.bun. The content of both files is identical; they only differ in format: one file is binary and unformatted (*.bun) and the other file is ascii and formatted (*.bfo). Differences between the (*.bfo, *.bun) and (*.aun, *.afo, 0) are indicated with a vertical line next to the text.

Part of the content of this file is optional and indicated with grey shading of the corresponding rows. The optional content is indiced with the switch SWOP (see section File Options).

The temperature parameter (Tsoil) has a value of "-99.9" when temperature processes were not simulated.

The snow-parameters (Ssnow, Igsnow, Isubl) have a value of "0", when snow processes were not simulated. This 0-value instead of -99.9-value is applied to facilitate uniformity of water balance calculations.

The description given in these pages uses the following symbols:
– Unit   = units as applied in these output files; units mostly differ from those applied in Swap
– Range   = upper and lower boundary of given data
– R   = an asterisk (*) indicates that data are written to a new record;
– DT   = data type; R means Real*4, I means Integer*2, C means CharacterString;
– Mnemonic = the name of the variable as applied in the source code of Swap

Description of variable	Unit	Range	R	DT	Mnemonic
Header of 5 records, each records with a fixed length of 80 characters					
Project Name (example: * Project: CranGras)	-	…	*	C80	Project
File Content (example: * File content: formatted hydrological data)	-	…	*	C80	FilText
File Name (example: * File name: Result.bfo)	-	…	*	C80	FilNam
Model Version (example: * Model version: SWAP3.0.0	-	…	*	C80	Model_ID
Date and time of file creation (example: * Generated at: 28-Mar-2003 13:59:31	-	…	*	C80	DTString
File Options					
SWitch for OPtions of content of this file (shaded parts in this table) SwOp = 1 : no data of macro pore flow SwOp = 2 : data of macro pore flow (in this table: shaded and red)	-	[1 ... 2]	*	I	swop
Time domain					
Year when hydrological simulation started	-	[1 ...]	*	I	bruny
Year when hydrological simulation ended	-	[bruny ...]	-	I	eruny
Time (Julian daynumber) when hydrological simulation started (Minimum); will be 0.0 when simulation started at 1st of January, 00.00 hour.	-	[0.0 ... 366.0]	-	R	brund-1
Time (Julian daynumber) when hydrological simulation ended (Maximum)	-	[0.0 ... 366.0]	-	R	erund

Geometry of model system

Number of model compartments	-	[1 ... numnod]	*	I	numnod
Number of horizons	-	[1 ... numlay]	-	I	numlay
Number of drainage systems (value must be 0, 1, 2, 3, 4 or 5)	-	[0 ... 5]	-	I	nrlevs

The following 4 variables (botcom … thetawp) are given for the horizons 1 ... numlay:

Compartment number of the deepest compartment (bottom) of each horizon/layer	-	[1 ... numnod]	*	I	botcom(numlay)
Volume fraction moisture at Saturation	$m^3 m^{-3}$	[0.0 ... 1.0]	*	R	thetas (numlay)
Volume fraction moisture at Field Capacity	$m^3 m^{-3}$	[0.0 ... 1.0]	*	R	thetafc(numlay)
Volume fraction moisture at Wilting point	$m^3 m^{-3}$	[0.0 ... 1.0]	*	R	thetawp(numlay)

The following variable dz is given for the compartments 1 ... numnod

Thickness of compartments	m	[0.001 ... 100.0]	*	R	dz(numnod)

Geometry of macropore system

Areic volume of static macropores in domain 1 (Main Bypass Flow domain) per compartment 1 … NUMNOD	$m^3 m^{-2}$	[0.0 ...]	*	R	VlMpStDm1(numnod)
Areic volume of static macropores in domain 2 (Internal Catchment domain) per compartment 1 … NUMNOD	$m^3 m^{-2}$	[0.0 ...]	*	R	VlMpStDm2(numnod)
Diameter of soil matrix polygones per compartment 1 … NUMNOD	m	[0.001 ... 10.0]	*	R	DiPoCp(numnod)

Initial conditions

The following variable theta and tempi are given for the compartments 1 … numnod

Volume fraction moisture initially present in compartments 1 … NUMNOD	$m^3 m^{-3}$	[0.0 ... 1.0]	*	R	Theta(numnod)
Initial groundwaterlevel (negative below soil surface, when positive use Pond)	m-surf.	[0.0 ...]	*	R	Gwl
Storage by initial ponding	m	[0.0 ...]	-	R	Pond
Storage by snow	m	[0.0 ...]	*	R	Ssnow
Soil temperature of compartments 1 ... NUMNOD	^{o}C	[-50.0 ... 50.0]	*	R	Tsoil(numnod)

Initial conditions for macropores, domain 1 (Main Bypass Flow domain)

Water level	m-surf.	[0.0 ...]	*	R	WaLevDm1
Areic volume	$m^3 m^{-2}$	[0.0 ...]	-	R	VlMpDm1
Areic volume of water stored	$m^3 m^{-2}$	[0.0 ...]	-	R	WaSrDm1

Initial conditions for macropores, domain 2 (Internal Catchment domain)

Areic volume	$m^3 m^{-2}$	[0.0 ...]	-	R	VlMpDm2
Areic volume of water stored	$m^3 m^{-2}$	[0.0 ...]	-	R	WaSrDm2

Description of variable	Unit	Range	R	DT	Mnemonic
Dynamic part					
Time (Julian daynumber) in hydrological model. (1.0 means: 1st of January, 24.00 hour)	-	[0.0 ...]	*	R	Daycum
Stepsize of time-interval for dynamic hydrological data	d	[1.0 ... 30.0]	-	R	period
Rainfall water flux	m d^{-1}	[0.0 ...]	-	R	Igrai
Snowfall water flux	m d-1	[0.0 ...]	-	R	Igsnow
Irrigation flux	m d^{-1}	[0.0 ...]	-	R	Igrid
Evaporation flux by interception of precipitation water	m d^{-1}	[0.0 ...]	-	R	Ierai
Evaporation flux by interception of irrigation water	m d^{-1}	[0.0 ...]	-	R	Ieirr
Sublimation of snow (Evaporation flux)	m d^{-1}	[0.0 ...]	-	R	ISubl
Actual evaporation flux by bare soil	m d^{-1}	[0.0 ...]	-	R	Ievap
Evaporation flux by ponding	m d^{-1}	[0.0]	-	R	Iepnd
Potential evaporation flux by soil	m d^{-1}	[0.0 ...]	-	R	Ipeva
Potential transpiration flux	m d^{-1}	[0.0 ...]	-	R	Iptra
Flux of surface Runon (originates from other source/field)	m d^{-1}	[0.0 ...]	-	R	Irunon
Flux of surface Runoff (negative value means inundation)	m d^{-1}	[...]	-	R	Iruno
Groundwater level at end of time-interval (negative below soil surface, when positive use Pond)	m-surf.	[0.0 ...]	-	R	Gwl
Storage by ponding at soil surface at end of time-interval	m	[0.0 ...]	-	R	Pond
Storage by snow at end of time-interval	m	[0.0 ...]	-	R	SSnow
Error in Water Balance	m	[...]	-	R	Wbalance

The variables h ... inqdra are given for the compartments 1 ... numnod, with one exception for inq, which is given for the compartments 1 ... numnod+1

Description of variable	Unit	Range	R	DT	Mnemonic
Suction (pressure head) of soil moisture (negative = unsaturated)	cm	[...]	*	R	h(numnod)
Volume fraction of moisture at end of time-interval	m^3 m^{-3}	[0.0 ... 1.0]	*	R	theta(numnod)
Actual transpiration flux	m d^{-1}	[0.0 ...]	*	R	inqrot(numnod)
Flux incoming from above (compartments 1 … numnod+1, positive = downward)	m d^{-1}	[...]	*	R	inq(numnod+1)

The presence of values for variables inqdra1…inqdra5 is determined by the variable nrlevs. The value of nrlevs determines the number of drainage systems for which flux densities must be given (postive: from soil to drainage system)

Description of variable	Unit	Range	R	DT	Mnemonic
Flux of drainage system of 1st order (e.g. canal)	m d^{-1}	[...]	*	R	inqdra(1,numnod)
Flux of drainage system of 2nd order (e.g. ditch)	m d^{-1}	[...]	*	R	inqdra(2,numnod)
Flux of drainage system of 3rd order (e.g. trench)	m d^{-1}	[...]	*	R	inqdra(3,numnod)
Flux of drainage system of 4th order (e.g. tube drain)	m d-1	[...]	*	R	inqdra(4,numnod)
Flux of drainage system of 5th order (e.g. rapid drainage)	m d-1	[...]	*	R	inqdra(5,numnod)
Soil cover	m^2 m^{-2}	[0.0 ... 1.0]	*	R	soco
LAI	m^2 m^{-2}	[0.0 ... 10.0]	-	R	lai
Rooting Depth	m	[0.0...numnnod]	-	R	drz

Crop Factor (or crop height)	- or cm	[0.0 ...]	-	R	cf
Average daily air temperature	^{o}C	[-50.0 ... 50.0]	*	R	tav
Average daily soil temperature of compartments 1... NUMNOD	^{o}C	[-50.0 ... 50.0]	*	R	tsoil(numnod)

Dynamic part for macropores, domain 1 (Main Bypass Flow domain)

Water level at end of time-interval	m-surf.	[0.0 ...]	*	R	WaLevDm1
Areic volume at end of time-interval	$m^3 m^{-2}$	[0.0 ...]	-	R	VlMpDm1
Areic volume of water stored at end of time-interval	$m^3 m^{-2}$	[0.0 ...]	-	R	WaSrDm1
Infiltration flux at soil surface directly by precipitation	m d^{-1}	[0.0 ...]	-	R	IQInTopPreDm1
Infiltration flux at soil surface indirectly by lateral overland flow (runoff)	m d^{-1}	[0.0 ...]	-	R	IQInTopLatDm1
Exchange flux with soil matrix per compartment 1-numnod (positive: from macropores into matrix)	m d-1	[...]	*	R	InQExcMtxDm1Cp(numnod)
Rapid drainage flux towards drain tube per compartment 1-numnod	m d^{-1}	[0.0 ...]	*	R	InQOutDrRapCp(numnod)
Average fraction of macropore wall in contact with macropore water during timestep per comp. 1-numnod	m d^{-1}	[0.0 ...]	*	R	FrMpWalWetDm1(numnod)

Dynamic part for macropores, domain 2 (Internal Catchment domain)

Areic volume at end of time-interval	$m^3 m^{-2}$	[0. 0 ...]	*	R	VlMpDm2
Areic volume of water stored at end of time-interval	$m^3 m^{-2}$	[0. 0 ...]	-	R	WaSrDm2
Infiltration flux at soil surface directly by precipitation	m d^{-1}	[0. 0 ...]	-	R	IQInTopPreDm2
Infiltration flux at soil surface indirectly by lateral overland flow (runoff)	m d^{-1}	[0. 0 ...]	-	R	IQInTopLatDm2
Exchange flux with soil matrix per compartment 1-numnod (positive: from macropores into matrix)	m d^{-1}	[...]	*	R	InQExcMtxDm2Cp(numnod)
Average fraction of macropore wall in contact with macropore water during timestep per comp. 1-numnod	m d^{-1}	[0.0 ...]	*	R	FrMpWalWetDm2(numnod)

Alterra
Postbus 47
6700 AA Wageningen
www.alterra.wur.nl